NTNU
Norwegian University of
Science and Technology

Stability Studies of an Offshore Wind Farms Cluster Connected with VSC-HVDC Transmission to the NORDEL Grid

Raphael Boinne

Master of Science in Electric Power Engineering
Submission date: April 2009
Supervisor: Terje Gjengedal, ELKRAFT
Co-supervisor: René Feuillet, INPG

Norwegian University of Science and Technology
Department of Electrical Power Engineering

Problem Description

According to the Kyoto Protocol ratified in 1998 by the European States, Norway should reduce its C02 emission. To reach this goal and to satisfy the rise of consumption, Norway, which has a large potential of wind power electricity, plans to build large wind farms up to 1000 MW in the North Sea. Furthermore, Norway is interconnected with the other Scandinavian countries and recently with the Netherlands and may supply them during peak consumption and thus have an important role on the stability of the Nordic grid. In this approach, STATKRAFT, the main Norwegian supplier of electricity studies the feasibility of large floating offshore wind farms linked with HVDC transmission to the shore.
The main work of the thesis is to simulate a large offshore wind farm connected with a VSC-HVDC transmission (Voltage Source Converter). Simulations shall be performed with the SIEMENS software PSS/E. Load flows on the entire NORDEL grid shall be done. The thesis will put emphasis on the stability of the system and the choice of the connection points. The feasibility of the connection of a wind farms cluster shall also be studied and investigated, as well as the mix of HVAC and HVDC connections inside the wind farms cluster.

Assignment given: 24. November 2008
Supervisor: Terje Gjengedal, ELKRAFT

PREFACE

This thesis has been written at the Department of Electrical Power Engineering at the Norwegian University of Science and Technology in cooperation with Statkraft. This thesis closes not only my Electrical Power Engineering International Master but also my two years spent in Norway as exchange student.

In the following, I would like to thank all the people who directly influenced my work and the progress of my master thesis.

Very special thanks go to Terje Gjengedal who was not only my supervisor but also the professor in charge of the wind power specialization course at NTNU which I followed last year. I have during this course acquired much new knowledge and I have also got the opportunity to visit wind turbine factories and climb up wind turbines. I would like to thank him for giving me the chance to write a master thesis on wind power and for all the advices and guidance he gave me during my work.

I would like to thank people from the SINTEF for their help and advice, especially the Professor Trond Toftevåg for his explanation.

I also want to thank Knut Sommerfelt for the time he took to help me with PSS/E.

I would like to thank all my Norwegian friends, especially my four housemates: Bjarte, Tarjei, Erik and Oyvind and also my officemate Sverre.

Special thank goes also to my Erasmus friends, especially Daniele and Luka with whom I have spent lot of my free time.

I would like to thank my French friends stayed in Norway, Maxime and Fabien, who have supported me during my thesis and with whom I have also spent lot of time.

Other thanks go to my girlfriend Sarah who let me go study abroad for so long.

Finally, I thank my family for supporting me throughout my studies and giving me the chance to study in Norway.

Raphael BOINNE
Trondheim, the 27th of April 2009

ABSTRACT

Offshore wind power has proven to be a renewable energy source with a high potential, especially in the North Sea, where an important development is going on. The location of the wind farms tends to move far from the coast to benefit stronger and more constant wind. In the same time, the power output of the wind farm is increasing to several hundreds of MW up to 1 GW. In the European liberalized electricity market, the interconnection of the countries become very important to facilitate the cross-border trade of electricity but also to improve the reliability of the grid. Combining this both aspects into one, a big offshore HVDC grid connecting countries and large wind farms spread allover the North Sea is currently being studied and developed. So in addition of the challenge given by a high penetration of the wind power production in the European power production scheme, new challenges are opened especially for the offshore transmission.

This master thesis presents the integration to grid of a single 1 GW or a cluster of wind farms connected to an oil rig with different connection scheme based on HVDC transmission using the Voltage Source Converter (VSC) technology. The connection of the offshore wind farms is done either with a single HVDC transmission or two HVDC transmissions connected to the main grid at two different Points of Common Connection situated in the south-west of Norway. The wind farms are not represented in detail but by a single generator. They are equipped for the simulation with Double Fed Induction Generators (DFIG) to be representative of the reality, almost half of the wind turbines are today equipped with DFIG technology.

Two disturbances are used to test the electrical stability of the system: a classical 150ms three fault phase in agreement with the grid code requirements on the ride fault through requirements and 100ms fault leading to the tripping of a line. The impact of using different types of generator is also investigated with the simulation of cluster wind farm where a wind farm is equipped with Fixed Speed Generator (FIG). The emphasis is put on the response of the VSC-converter and to a lesser extent on the behaviour of the wind turbine generator.

It is demonstrated the capacity of the VSC-converter to stabilize a small grid alone and to "isolate" a disturbance. The voltage and the frequency offshore are practically unaffected by a fault onshore and vice versa. As expected, it is demonstrated that the multiplication of the VSC-HVDC converter in a grid improves the stability of the system. Finally, it has been noticed that there maybe some interactions if several different types of generators are used. The replacement of a generator by another type inside the wind farm cluster may change completely the dynamic behaviour after a disturbance. Simulations are performed with PSS/E.

TABLE OF CONTENTS

TABLE OF FIGURES

TABLE OF TABLES

NOMENCLATURE

DFIG	: Double Fed Induction Generator
EWEA	: European Wind Energy Association
FACTS	: Flexible AC Transmission System
FIG	: Fixed Induction Generator
GWEC	: Global Wind Energy Council
HVDC	: High voltage direct current
IGBT	: Insulated Gate Bipolar Transistor
LCC	: Line Commutated Converter
NREL	: National Renewable Energy Laboratory
NVE	: Norwegian Water Resources and Energy Directorate (*Norges Vassdrags og Energidirektorat*)
PE	: PolyEthylene
PCC	: Point of Common connection
pu	: per unit
PWM	: Pulse Width Modulation
SCR	: Short Circuit Ratio
STATCOM	: Static synchronous Compensator
SVC	: Static Var Compensator
TSO	: Transmission System operator
UCTE	: Union for the Coordination of Transmission of Electricity
UKTSOA	: United Kingdom Transmission Operator
VSC	: Voltage Source Converter
XLPE	: Cross Linked PolyEthylene

INTRODUCTION

Europe is worried about its energy security, largely dependent and influenced by the political instability of areas exploiting oil and gas. The European Institutions have recognized and accepted the challenging environmental responsibilities linked to the climate change. So, new environmental and energetic policies emerged: new objectives are climate change mitigation by a reduction of CO_2 emission, the increase of the energy supply in a context of increasing import of energy and the deregulation of the energy sector. They can be resumed in the rules of the "3x20": 20% of the electrical production supply by renewable energies, a 20% decrease in the greenhouse gases emission and a reduction of 20% of the electrical consumption.

In addition of this geopolitical context, a huge development of the wind power occurs in Europe, especially in Germany, Spain, United Kingdom and to some extent in Denmark. The development of the wind power is commonly recognized as one of the most promising options in order to achieve these objectives. The principal reason is because wind power is a mature and competitive technology which allows producing power with a god yield and large power output, several dozens of MW for some wind farms compare to the photovoltaic for example.
In such development, the related opportunity to site the wind farm at sea in order to benefit from stronger and more constant wind become very important. An offshore development reduces the environmental and visual impact of wind turbine, now reaching 200m for the highest, which is one of the problems when situated on shore for the contestants.
The main impact of wind generation is due to its feature to be fluctuating and the possibility of electrical energy storage is very restricted, even with hydro pumped storage. So, to overcome this inconvenient, the development of a huge HVDC grid allover the North Sea, connecting the different countries and huge offshore wind farms is studied and some parts of it are already planned. Thus, wind farms spread allover large regions will reduce the variability of wind power generation.

In this project, Norway will have great role because the wind resources at its coasts are very high, interconnection will promote trade of electricity, petroleum sector will benefit of the connection of its oil rig to the grid and the national industries will be really involved: floating turbines development, submarine cables production, offshore constructions.
The wind power which has been until now mostly used to achieve a growth of electrical consumption in Europe will become part of the generation capacity with the hydro, coal, gas or nuclear plants. At the same time this new development creates news challenges in the electrical power transmission, for the grid regulation and for the power generation.

The purpose of this thesis is to study the dynamic behaviour of a small offshore grid comprising a single 1GW wind farm or a cluster of wind farm with an oil rig linked to the main Norwegian grid either with a single HVDC transmission or 2 HVDC transmissions. The technology Voltage Source Converter is used to model the HVDC transmission. The wind farms are not modeled in detail but the wind farm will be represented either equipped with DFIG generators or fixed speed generator. PSS/E will be used for all power system simulations.

1 PRESENTATION

1.1 STATE OF THE OFFSHORE WIND POWER IN THE NORTH SEA

The wind power has been until now mostly used to achieve a growth of electrical consumption in Europe. New environmental and energetic policies emerged because of the climate change and the security of energy supply. The development of the wind power is commonly recognized as one of the most promising options in order to achieve these objectives. Developed first on the shore owing to easier building conditions, the wind power is now going fast onto the sea with the new technologies. To place the wind farms to the sea allow to benefit of stronger and more constant wind and to reduce the visual impact. At the same time this new development creates news challenges in the electrical power transmission and in the power generation.

1.1.1 HISTORY

The story of the offshore wind power started in the Denmark in 1991. Vindeby was the first wind farm built and equipped with 11 Bonus 450kW. Until now, offshore wind farms have only been built in the North Sea and nowhere else. The development was slow during the first 10 years and started really in the beginning of this century. See Figure 1-1. Then, Denmark built several wind farms and was the first country to build one with an output over 100MW with Horns Rev, composed with 80 Vestas V90.

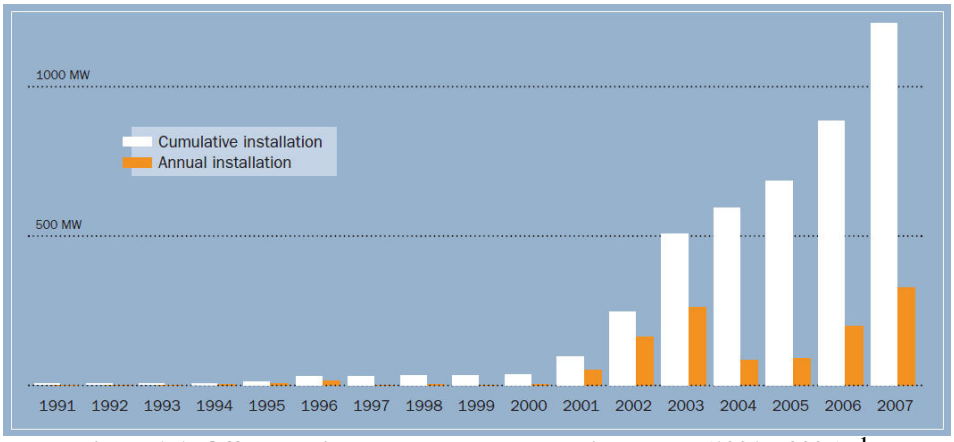

Figure 1-1: Offshore wind market development in Europe (1991 – 2007) [1]

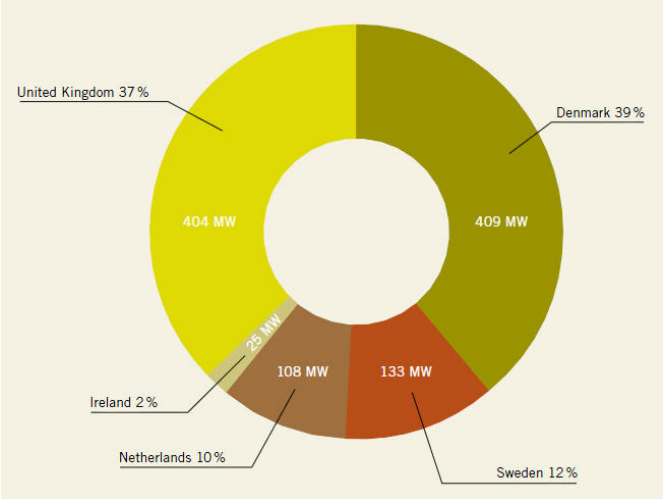

Figure 1-2: Repartition of the offshore wind power production in Europe (years 2007)

Location / Name	Country	Commissioning year	MW	No turbines	Turbines & power rating	Rotor diameter [m]	Spacing [D]
Vindeby	Denmark	1991	4.95	11	Bonus 450kW	37	9,1D/8,1D
Lely	Netherland	1994	2	4	NedWind 500kW	40	5D
Tunoe Knob	Denmark	1995	5	10	Vestas V39 500kW	39	10D/5D
Dronten	Netherland	1997	11.4	19	Nord Tank 600kW	43	
Bockstigen	Sweden	1998	2.5	5	Wind World 500kW	37	9,5D
Blyth	UK	2000	4	2	Vestas V66 2MW	66	
Middelgrunden	Denmark	2001	40	20	Bonus 2MW	76	2,4 D
Utgrunden I	Sweden	2001	10.5	7	GE 1,5MW	70.5	7D
Horn Rev	Denmark	2002	160	80	Vestas V80 2MW	80	7D/7D
Yttre Stengrund	Sweden	2002	10	5	Neg Micon 2MW	70	4D
Samsoe	Denmark	2003	23	10	Bonus 2,3MW	80	8D
Frederiskhavn	Denmark	2003	10.6	4	2x Vestas V66 2MW 1x Nordex 2,3MW 1x Bonus 2,3MW	66 90 80	#
North Hoyle	UK	2003	60	30	Vestas 2MW	80	10D/4D
Nysted	Denmark	2003	158	72	Bonus 2,3MW	80	8D/9D
Arklow Bank	Ireland	2004	25.2	7	GE 3,6 MW	106	6D
Kentish Flats	UK	2005	90	30	Vestas V90 3MW	90	7,7D/7,7D
Scroby Sands	UK	2005	76	38	Vestas V80 2MW	80	6,5D/5D
Barrow	UK	2006	90	30	Vestas V90 3MW	90	8,3D/5,5
Egmond/OWEZ	Netherland	2006	108	36	Vestas V90 3MW	90	11D/7D
Beatrice*	UK	2007	10	2	RePower 5MW	126.5	5,5D
Burbo bank	UK	2007	90	25	Bonus 3,6MW	107	6,7D/5D
Lillgrung	Sweden	2007	110	48	Bonus 2,3MW	93	
Inner Dousing	UK	2008	97	27	Bonus 3,6MW	107	
Lynn	UK	2008	97	27	Bonus 3,6MW	107	
Q7/Princess Amalia	Netherland	2008	120	60	Vestas V80 2MW	80	7D/7D
Gunfleet Sands I	UK	2009	108	30	Bonus 3,6MW	107	8,3D/4D
Gunfleet Sands II	UK	2009	64.8	18	Bonus 3,6MW	107	8,3D/4D
Rhyl flats	UK	2009	90	25	Bonus 3,6MW	107	
Robin Rigg A & B	UK	2009	180	60	Vestas V90 3MW	90	
C-Power**	Belgium	2009	300	36 (east) 24 (west)	RePower 5MW	126.5	7D/5D
Borkum west	Germany	2010	60	12	Multibrid & RePower 5MW	116	7D

No data found

#Test site for foundation

*Part of the Greater Gabbard project

**Only 30MW have been installed

Table 1-1: Features of the different offshore wind farms installed or under construction

The development Compared to the total wind power capacity installed in the world, the offshore wind power represents less than 2%, the global cumulative installed capacity of wind power was in 2008 around 94GW [2]. See Appendix A - 1. The cumulative installed capacity of offshore wind power in 2008 was reaching 1500MW.

Recently, as several wind farms have been commissioned in United Kingdom, this country become the top ranked country for the installed offshore wind power. This fast growing market in UK is due to an incentive policy thank to the high price of the electricity purchase. The total of offshore wind power is now up to 598 MW in UK. Netherlands have commissioned another offshore wind farm; Princess Amelia rated at 120 MW which gives a total amount of 228 MW installed for Netherland. In the same time, Belgium have started to build Thornton Bank with 30 MW already installed for the first round. The table 1-1 gives an overview of the offshore wind farm installed in Europe and their characteristics as the wind turbine type, the rotor diameter, the spacing between the turbines…

1.1.2 TECHNOLOGIES INVOLVED

A brief overview of the energy extracted from the wind will be now given. Depending on the wind speed the power output of the turbine varies, the cut-in wind speed is usually in a range of 3-4 m/s whereas the cut off wind speed in a range of 25-30m/s.
The power extracted from the wind for a wind turbine depends on the area swept by the rotor blades (A), the air density (ρ), the cube of wind velocity (v) and the efficient coefficient C_p. This coefficient cannot be higher than 0.59 according to Betz limit and depends on the pitch angle of the blade (β) and the tip speed ratio (λ). See the typical power curve in the next figure

$$P(v) = \frac{1}{2}.\rho.A.v^3.C_p(\lambda,\beta)$$
$$\lambda = \frac{R.\omega}{v} \qquad (1.1)$$

The companies Vestas, Re-Power, Siemens (Ex-Bonus), GE (general Electric) and recently Multibrid are sharing this growing market. These international engineering companies develop, produce and sell wind turbines with outputs ranging from 1.5 to 5 MW and rotor diameters of 70 to 126 m. The wind turbines are almost similar to the onshore wind turbines except systems to protect them from corrosion and salinity. The cooling system is often in closed circuit or with a system to remove the salt and impurities from the air.

The offshore wind farms are only set in shallow water, the depth does not exceed 50m, most of the time they are built on a sand bank. The deepest one is 44m in the "Beatrice Demonstrator Project" off Scotland. Two turbines rated at 5MW have been installed. Four different types of foundation have been used depending on the sea bed. The choice of the foundation depends principally of the sea bed. The monopole is widely used on sand sea bed and for very shallow water, less than 10 meters. Gravity and suction bucket foundations are used on sand sea bed whereas the tripod foundation might be used on rock sea bed. Lattice tower is used at "deep shallow" water.

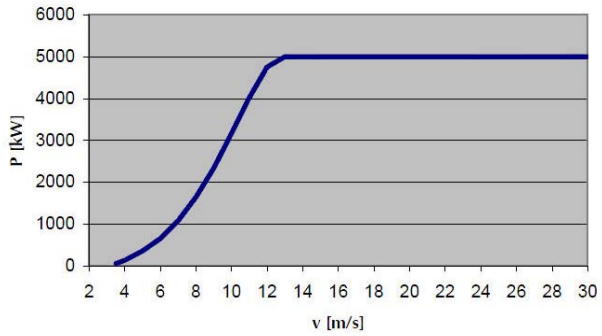

Figure 1-3: Power curve for the Repower 5MW

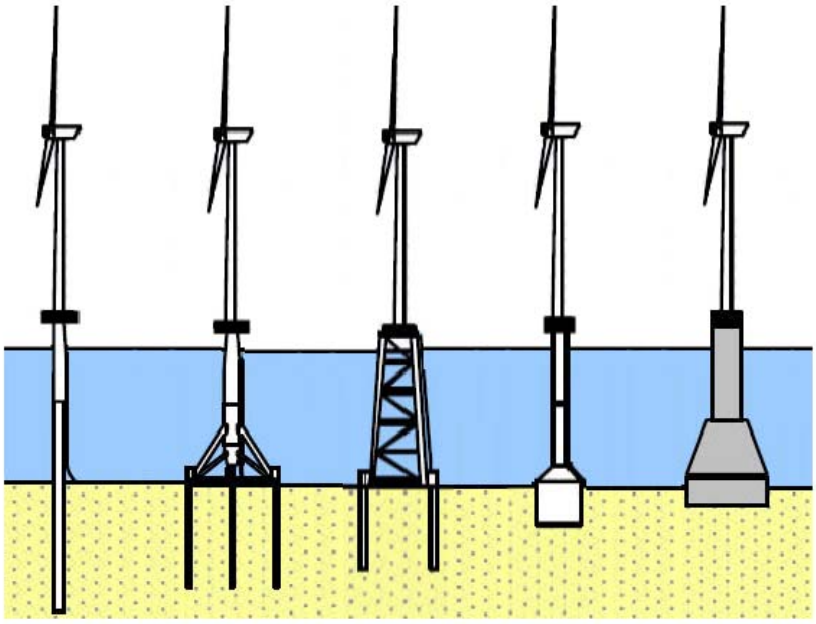

Figure 1-4: Different foundations: monopile, tripod, lattice tower, bucket (suction) and gravity.

Some of the offshore wind turbines have an access by helicopter for maintenance on the top of the nacelle. Otherwise maintenance is normally done by boat.

Several types of generator are used for the wind turbine lay onto the sea. The difference is coming from the choice of the constructor to develop such kind of generator. A gearless generator will be preferred because of the low maintenance required and the lower weight of the nacelle. More details about the wind turbine generators are given in the next paragraph 1.2.

Within the farm the connection between the wind turbines is done by submarine cables at a voltage comprises into 11kV and 33kV, most of the buried into the sea bed to prevent damage from anchor. Depending of the distance to the shore and the output power of the wind park, an offshore transformer might also be built close to the wind farm. Then a single AC tri-phase transmission connects the wind farm to the main grid at a voltage up to 420kV. Actually, only Nexans and ABB product those cables and share this market. They can provide cable up to 420kV rated at 1000MW. An example of such AC connection of an offshore wind farm is show in Figure 1-5 [3].

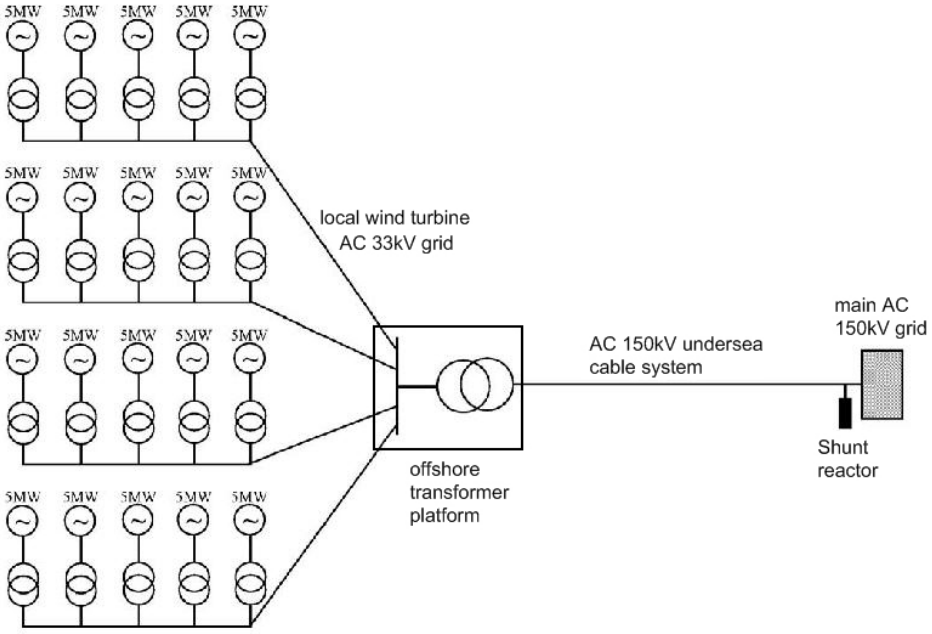

Figure 1-5: Typical electrical layout of an offshore wind farm with HVAC transmission.

The structure of an AC submarine cable is more complex than a classical underground cable. Other layers are added to withstand the harsher environment of the sea.Those AC submarine cables have different layers, each of them with a specific role. See the chapter 2.4. AC submarine cables with single or 3-core are shown in Figure 1-6.

Here is listed the different layers used in the submarine cable structure.

- The central conductor in steel or copper.
- A semi-conductor layer to prevent water trees, space charges or discharge in the insulating material. (Polyethylene with black carbon)
- The insulation in XLPE (Cross Linked Polyethylene)
- Another semiconductor layer.
- A metal sheath around (often lead alloy).
- Inner jacket (polyethylene).
- Tensile armour in galvanized steel (often 2 laid in counter helix).
- Outer cover in polypropylene yarn with asphalt.

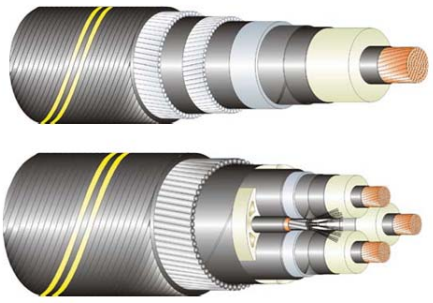

Figure 1-6: Single and three core cable with lead sheath, wire armour and fibbers optic for the 3-core.

1.1.3 TRENDS & MARKET

There is an incentive policy from the EU to promote the wind power in the North Sea. In 2006 the project *Trade Wind* has produced recommendations as well as technical and economic justifications for strategic decision making on the development of the power network, generation infrastructure and the power exchange market. [4] The conclusion of the work will be targeted at national public authorities, EU institutions, TSO's, regulators, wind farm developers and operators, turbine manufacturers, and other wind energy actors. The participants are expected to have a significant impact on future policies and developments of wind power integration in Europe, which will result in substantial economic benefits for the EU and the Member States.

Currently, the project *Norsewind* - for Northern Seas Wind Index Database - is supposed to build an offshore wind atlas above the North, Baltic and Irish Sea [5] by using several methods such as meteorological satellites, LIDAR (LIght Detection And Ranging) and met masts. This project involved several companies and university in all the countries around North Sea. Statoil in Norway is one of them.

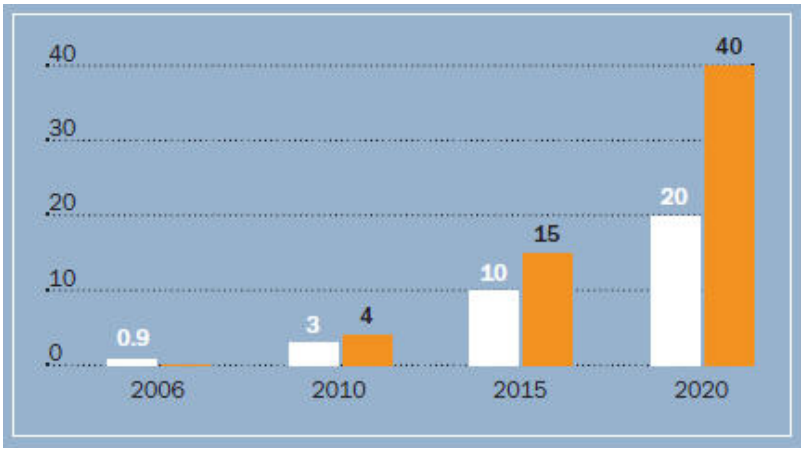

Figure 1-7: Installed offshore wind power in Europe in the next 10 years, low and high scenarios.

According to different scenarios, the market is expected to grow quickly in the next ten years. The installed power for the offshore wind power is in a range between 20 GW and up to 60 GW in 2030. The high scenario is given by the Trade Wind project. See Figure 1-7.

As example the German Energy Agency, the German Federal Maritime and Hydrographical Agency give a list containing projects with a total capacity of 26417 MW. Whereas in Great Britain, the British Department for Business Enterprise & Regulatory Reform (BERR) announced in 2007 a proposal to open up its seas to up to 33 GW offshore wind power by 2020. In addition to the currently realized and planned projects of Round 1 and Round 2 (about 10 GW of which 7.24 GW in the North Sea), there will be a Round 3 phase with projects up to 23 GW. [1]

By adding the offshore project announced or studied in the adjacent countries, the future total amount power installed is in line with the TradeWind high scenario for 2030. Such wind power generation capacity installed (60GW) would generate 230 TWH over one year with a capacity factor set at 45%. The capacity factor for an installation on shore is in the range 25- 35%. For comparison the energy generated by such grid is almost two times those consumed in Norway (in a range 110- 140 TWh depending on the year).Source NVE [6].

1.2 WIND TURBINE GENERATORS

There are currently four types of wind turbine generators. The technical information is mainly extracted from a report from EWEA [7]. The high voltage generator is not dealt with in this report.

1.2.1 FIXED SPEED WIND TURBINE

The first type of turbine is the fixed speed based on a squirrel cage asynchronous generator. Its rotor is driven by the turbine and its stator is directly connected to the grid. Due to consumption of reactive power for the induction machine those turbines are equipped with a capacitor bank. Its rotation speed can only vary slightly (between 1% and 2%), which is almost "fixed speed" in comparison with the other wind turbine concepts. The concept exists also in double speed version which gives an improved performance and lower noise production at low wind speeds. Aerodynamic control combined with this concept is mostly passive stall, and as a consequence there are few active control options, besides connecting and disconnecting, especially if there is no blade pitch change mechanism.

The concept has been continuously further developed, for example in the so-called active stall designs, where the blade pitch angle can be changed towards stall by the control system. A fixed speed turbine generator is presented Figure 1-8.

The European market share is around 30% and the manufacturers providing this technology are Suzlon, Nordex, Siemens Bonus and Ecotècnia.

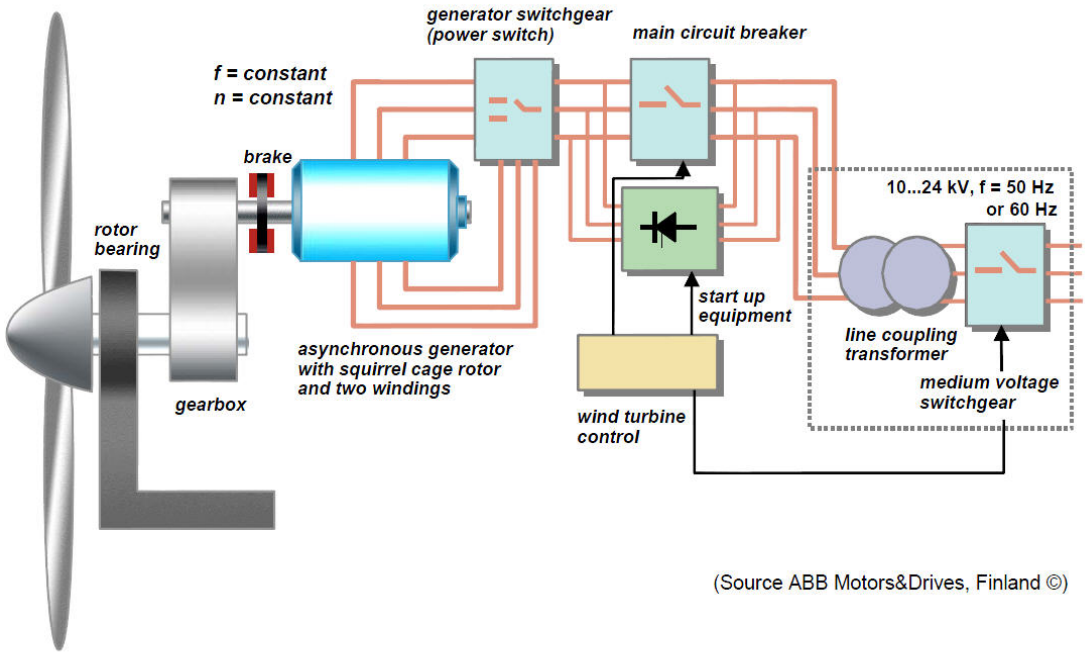

Figure 1-8: Fixed speed concept base on squirrel cage induction generator.

1.2.2 LIMITED VARIABLE SPEED WIND TURBINE

The concept is similar to the previous but a wound rotor induction generator is used instead of a squirrel cage generator. Power electronics are applied to control the rotor electrical resistance and allows the rotor to vary its speed up and down ±10%. This system improves the power quality and reduces the mechanical load on the different components. Those turbines are usually equipped with an active blade pitch control.

The concept has been development by Vestas and the European share market is around 10% for this kind of turbine.

1.2.3 VARIABLE SPEED WIND TURBINE WITH DFIG

The induction generator has a wound rotor, which is connected to the grid through a back-to-back voltage source converter that controls the excitation system in order to decouple the mechanical and electrical rotor frequency and to match the grid and rotor frequency. The application of power electronics provides control of active and reactive power, enabling active voltage control. In this type of systems, approximately up to 40% of the power output is going through the inverter to the grid and the other part is directly going to the grid. The range of the variation speed is approximately 40% up and down from the synchronous speed.
Those turbines have ride fault through and reactive power capabilities.

All the type of aerodynamic control can be used with those turbines, either active blade pitch control or active/passive stall control.

This concept is the most popular and the European share market for this concept is around 45%. Almost all the manufacturers provide this technology: General Electric, Re-power, Vestas, Nordex, Gamesa, Ecotecnia, Ingetur and Suzlon.

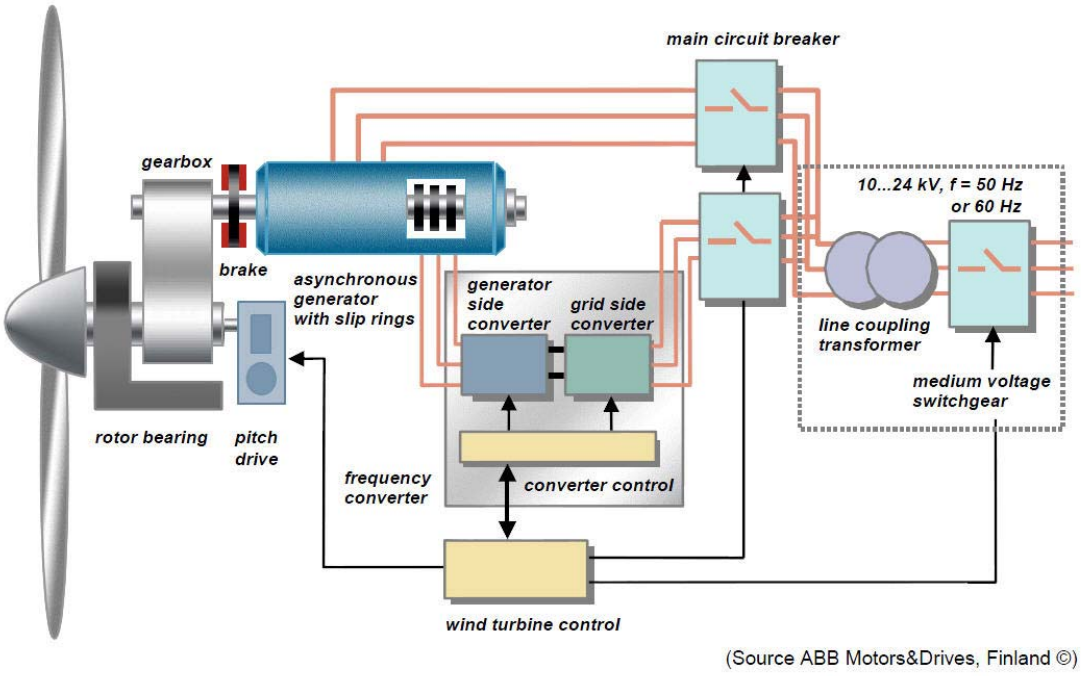

Figure 1-9: Double-fed induction generator for variable speed turbine.

1.2.4 VARIABLE SPEED WIND TURBINE WITH FULL SCALE FREQUENCY CONVERTER

This concept can be the classical drive train (with gearbox) or direct drive train (gearless). The stator is connected to the grid through a full power electronic converter. The voltage source controller (VSC) technology is used, explained later. The rotor has excitation windings or permanent magnet. All the types of generator can be used: synchronous generator with wound rotor, permanent magnet generator or squirrel cage induction generator.
According to the concept chosen, with or without gear box or hybrid (a low step gear box will be used with medium speed generator) the generator will be different. A slow running generator in a gearless concept will have a large diameter due to the higher number of pole pairs. The E-112 from Enercom has 86 poles pairs instead of 6 for the 5-M Repower at almost same power rating.

Those turbines can provide a larger range of speed and have better reactive and voltage control, in addition of a better ride fault through capability due to its VSC controller. Active and reactive power can be controlled separately.

The gearless design avoids the mechanical complexity of gears and hydraulics and maintenance going with.

This concept has been widely introduced by Enercon but now other manufacturers provide it: Multibrid, General Electric, Winvind, Jeumont, Zephyros… This technology represents now around 15% of the European share market but 60% for the German market.

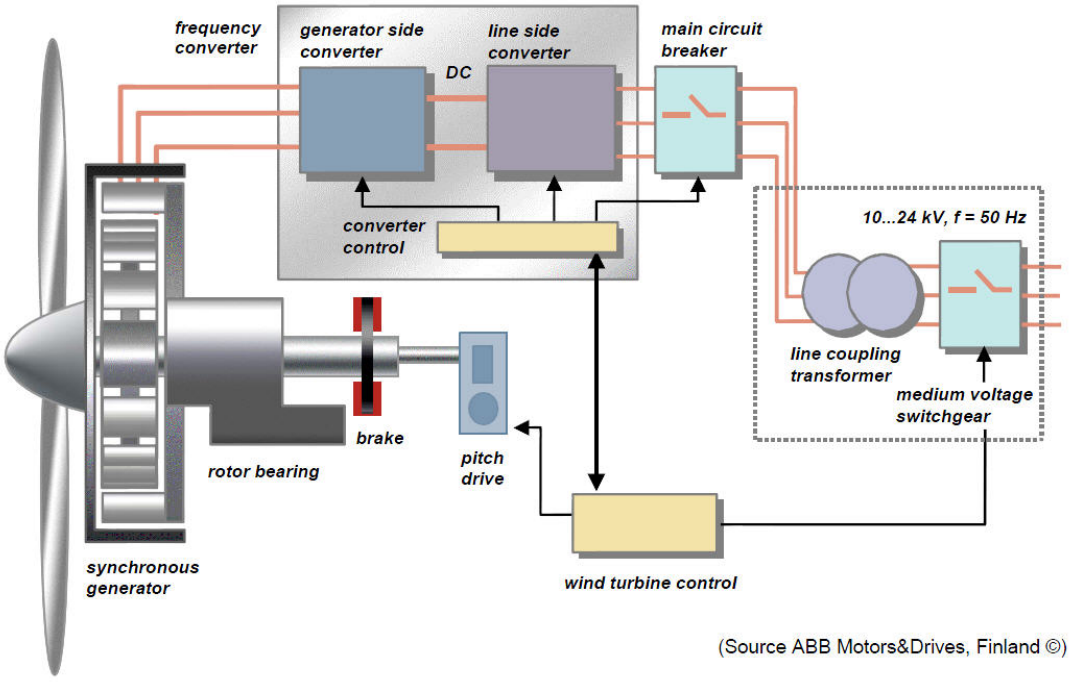

Figure 1-10: Gearless design with permanent magnet generator for variable speed turbine with converter.

1.3 FUTURE OF THE WIND POWER

An important development of offshore wind power, at least in Europe is predictable and will be a chance for the industries involved in this technology and for Europe, which are at the state-of-the-art on this field.
The location of the offshore wind farm will change and will go further from the shore and in deep water. In the same time the output power of a wind farm will increase with the number of machine installed and the rated output power of single turbine. Directly connected to these changing, new types of foundation and transmission are needed. This will be dealt with in below.

1.3.1 CHALLENGE OF A HIGH PENETRATION OF WIND POWER

The offshore wind power will play an important role in the penetration of the wind power into the grid and the electrical generation scheme in Europe. New control, new way of management in the power generation and the dispatching will be necessary.

Traditionally, wind energy generation has been connected to the network grid assuming that its size and influence are small and therefore the connection requirements have been less stringent. This is changing with the projected penetration of wind power in the order of several dozens of GW. Furthermore, the size of the wind farm increasing on shore and offshore, it will have significant influence. For example, the 24th of November 2008, the production coming from wind power in Spain had reached 41% of the power production for a capacity of 9900MW. [8]
Typically wind farms do not contribute to the stabilization or the regulation of the AC grid. At present, none of the wind farms, including the large Horns Rev offshore installation, can contribute to the AC system control or stability enhancement and they simply disconnect in case of AC faults. As the power share from wind farms increase, it is necessary that wind farms should take more active role in the AC systems regulation and support.

The network operators have raised many issues with wind power generation, especially for large-scale generation, in order to enable secure and reliable system operation. Similarly as with conventional generators, wind farms are now required to comply with stringent connection requirements including: reactive power support, transient recovery, system stability and voltage/frequency regulation, power quality, as well as scheduling and reserve availability are also considered. The conventional wind generation concepts based on fixed speed generator have difficulties in meeting all the above interconnection requirements, in a less important way the doubly fed induction generators. The emergence of the variable speed wind turbine with full scale converter will help to contribute to the stabilization and the regulation of the network in a process of high penetration of wind power.
In a certain way, the use of HVDC transmission and the interconnection will help this high predictable penetration of wind power into the electrical power production in Europe. This report will go onto it.

1.3.2 HVDC NETWORK IN THE NORTH SEA, INTERCONNECTION

All the countries in Europe are now interconnected. It contributes to secure and improve the supply of electricity. According to the geography, the Baltic and Scandinavian countries are linked thanks to HVDC to be able to cross the seas in between them. So, Norway is interconnected with Denmark (Skagerrak - 1GW) and recently with the Netherlands (Norned – 700 MW), whereas Sweden is interconnected with Germany (Baltic – 600MW) and Poland (Swepol – 600MW) and Finland with Estonia (Eastlink – 350MW). Great Britain is also interconnected with France with the Crosslink (2GW) and with Ireland with the Mohle Interconnector (500MW). Another link is planned between Germany and Norway. So, an HVDC network already exits in the North, Irish and Baltic seas.

The Nordel grid is presented next page, the HVDC link for the interconnection between the Scandinavian countries and the European countries are in purple.

Figure 1-11: Nordic grid in the Nordel system: the HVDC transmissions crossing the seas are in blue

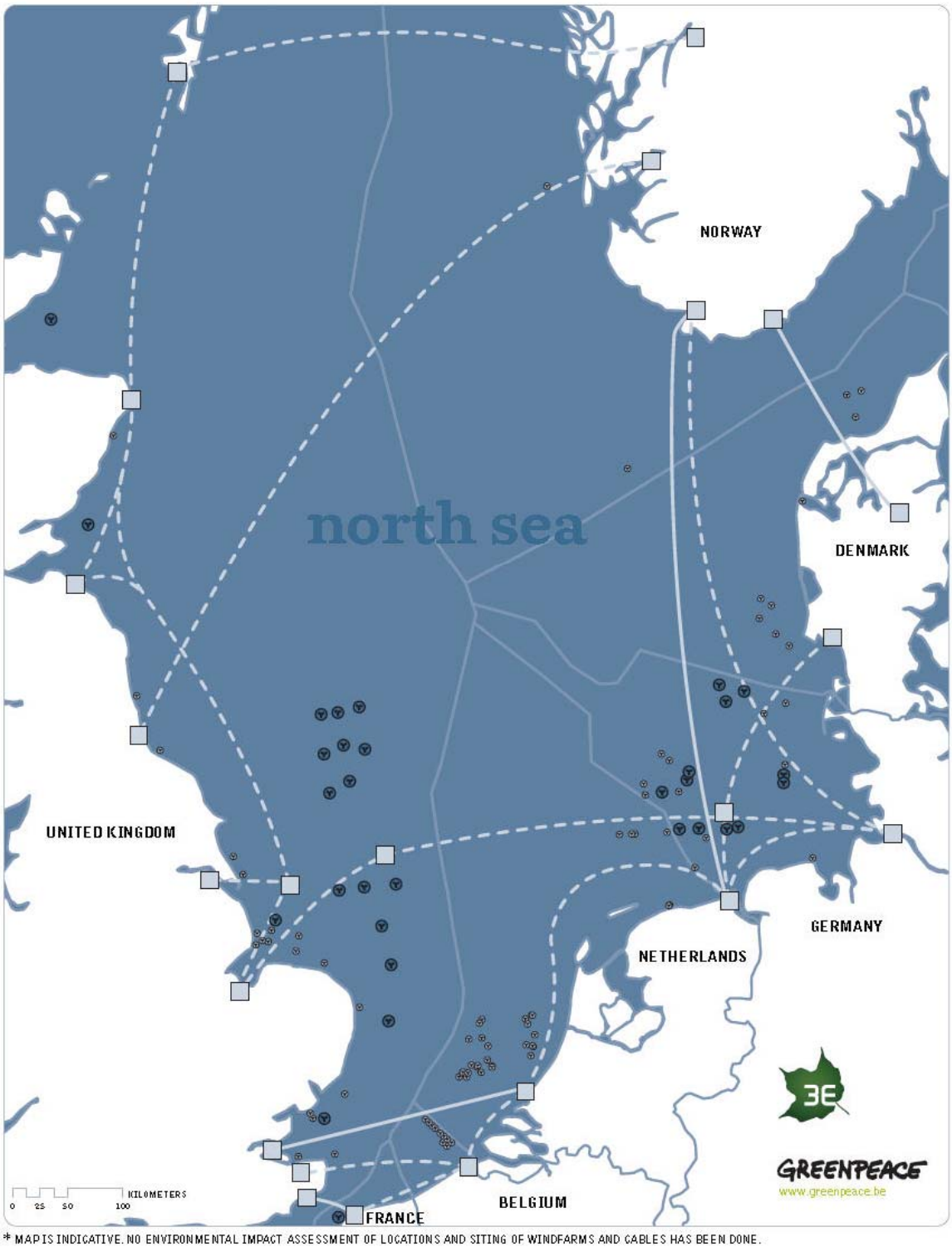

Figure 1-12: Example of an HVDC offshore grid with offshore wind farm spread allover the North Sea

Legend: Blue squares represent HVDC converter station, full grey line the HVDC links already operating, dotted grey line proposal HVDC links and offshore wind farms are represented by blue circle.

An idea will be to use and develop this network according to the development of the offshore wind power. Thus, with offshore wind farms set over large regions, at least spread allover North Sea, the accumulation of the generated power will contribute to reduce the period of full load and very low load but smoothing this generated power. By using the spatial spread of offshore wind power, medium level power is obtained a larger fraction of time but the periods of full production are reduced. It will also contribute to reduce the variability of wind power in the range of hours.

In a report [9] on such grid, it has been calculated that variations up to ±5% occur of all hourly samples whereas it could be ±20% for a single wind farm. Furthermore by using short term prediction of the generated power, the occurrence of variations beyond 10 % appears to be negligible. Situations of full and no load occur during a negligible fraction of time. So, such grid associated with a large amount of offshore wind power capacity could be able to replace thermal base load plants and thus to decrease CO2 emission, but also increase the supply security and the reliability during peak load.

An offshore grid in the North Sea by increasing the interconnection will encourage electricity trade and offer a better flexibility and security of supply. So the offshore generated power could be dispatched to the areas with high demand. Moreover, an offshore grid in the North Sea allows the import of electricity from hydro power from Norway to the British (UKTSOA) and the UCTE system. Thus, Norway will have a special and import role in this offshore HVDC grid.

An example of this offshore HVDC grid connecting countries and offshore wind farms is represented Figure 1-12 page 14.

1.3.3 FLOATING OFFSHORE WIND TURBINE

The continental plateau stops very close to the Norwegian coast, so the water become very deep and the classical foundation for offshore turbine are not suitable and cannot be used. So the Norwegian industries started to develop several concepts of floating wind turbine to solve this problem. Two projects have now been kicked off and are supported by huge companies such as Statoil, Hydro, Shell, Statkraft…

Both concepts are floating turbines using ballast instead of a floating platform. A ballast is fixed at the bottom of the tower of the wind turbine. The ballast permits to put the wind turbine gravity centre below the floating point of the structure then the tower is anchored to the sea bed either with tensile anchor or with several leech anchors. Thus the stability is ensured. The hulls of the floating turbine will not be larger than regular tug-boats can tow. Those floating turbine are suitable for deep water offshore locations in 100-700m water depths.

The HYWIND® supported by Hydro used a floating concrete structure [10]. It allows to build it on land and then to tow the tower to sea. Same process has been used for many decades with offshore oil platforms. A regular offshore wind turbine is set atop a 120 meter high floating concrete cylinder with ballast and which will be moored to the sea floor with three sturdy anchor lines which are not tensed. The motions at the top of the tower are sufficiently small to allow the wind turbine to function efficiently. The concept is call spar-buoy.

The concept has been tested and validated with a reduced scale prototype at Marintek's Ocean Basin laboratory in Trondheim. Statoil plans to install the wind turbine in autumn 2009 in the south east of Norway.

The HYWIND® concept is presented in Figure 1-13.

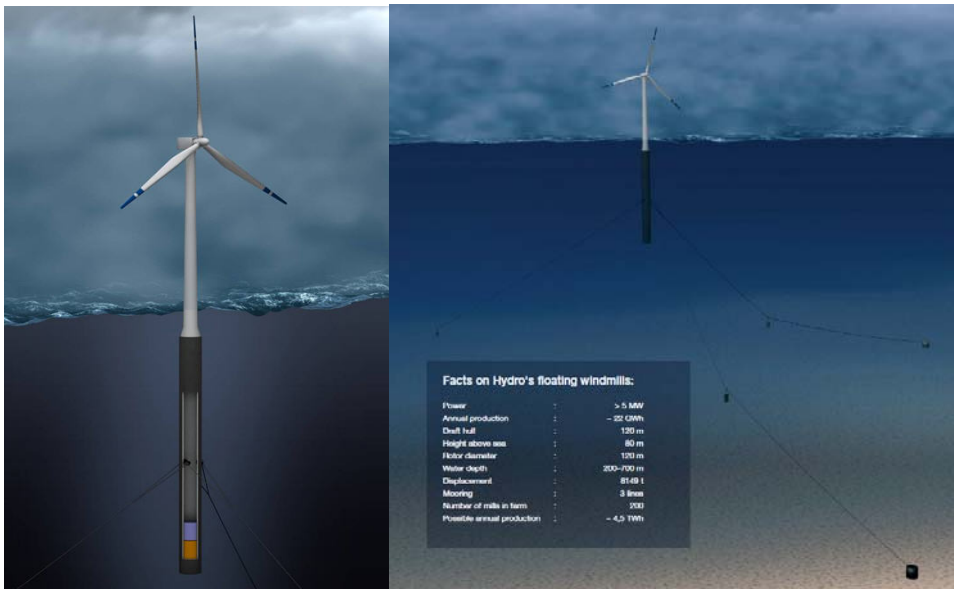

Figure 1-13: HYWIND project, detailed view on the ballast (left) and view on the mooring system (right)

Figure 1-14: SWAY project, tow of a floating turbine (left) and view on the mooring tensed leg (right).

The SWAY® concept supported by Statoil has the same floating ballast concept but differ on the mooring concept and particularly on the turbine type. [11] This floating tower is anchored to the seabed by a tension leg and suction anchor. The system uses a downwind rotor contrary to most conventional wind turbine. The design reduces the load on the system and allows the structure, under normal operating conditions, to tip approx. 10 degrees with the wind. The nacelle and tower are aerodynamically designed to limit the turbulence. See figure above.

A pilot phase of the Utsira offshore wind farm is to build a 5 MW prototype floating wind turbine this year and then install it off the coast in 2010. The goal is to build a 280MW wind farm located approx. 17 km west of Utsira island, the possible start up of the construction is set in 2016.

In the world other concepts are studied such the Blue H project in Netherland based on a floating platform. Some projects plan to put several turbines on a same triangular platform at each tip. The National Renewable Energy Laboratory (NREL) in USA is also working on such projects.

1.4 SPECIFIC ROLE FOR NORWAY

The Nordic electrical generation system is a mix of production resources. Nordel is the collaboration organization of the Transmission System Operators (TSOs) of Denmark, Finland, Iceland, Norway, and Sweden.

The Nordic power exchange stock is the Nord Pool, established in 1993 as an exchange for the Norwegian electricity market. It has been extended progressively to the other countries. Since 2002, all those countries are part of this market. Two markets are available. The Elspot market which offer trade for day-ahead. Prices are determined through auction with supply and demand participation for each hour in the day. The Elbas market is a short term market for physical power trading. Norway contrary to the other countries is separated into several price areas.

Sweden and Finland have mix of hydropower, nuclear and other thermal plants, whereas Denmark is dominated by thermal power plant with a large contribution from wind power. Iceland gets electricity mainly from hydro and geothermal plants. The total electricity consumption and production is around 410 TWh for the entire area.

		Nordel	Denmark	Finland	Iceland	Norway	Sweden
Population	Mill.	25	5.5	5.3	0.3	4.7	9.2
Total consumption	TWh	412.6	36.4	90.4	12	127.4	146.4
Maximum load	GW	61.1	6.1	12.5	1.3	18.6	22.7
Electricity generation	TWh	409.2	37	77.8	12	137.4	145.1
Breakdown of electricity generation							
Hydropower	%	55	0	18	70	98	45
Nuclear power	%	21	-	29	-	-	44
Other thermal power	%	21	81	53	0	1	10
Wind power	%	3	19	0	-	1	1
Geothermal power	%	-	-	-	30	-	-

Table 1-2: Presentation of the Nordel countries, power generation type, load, consumption…

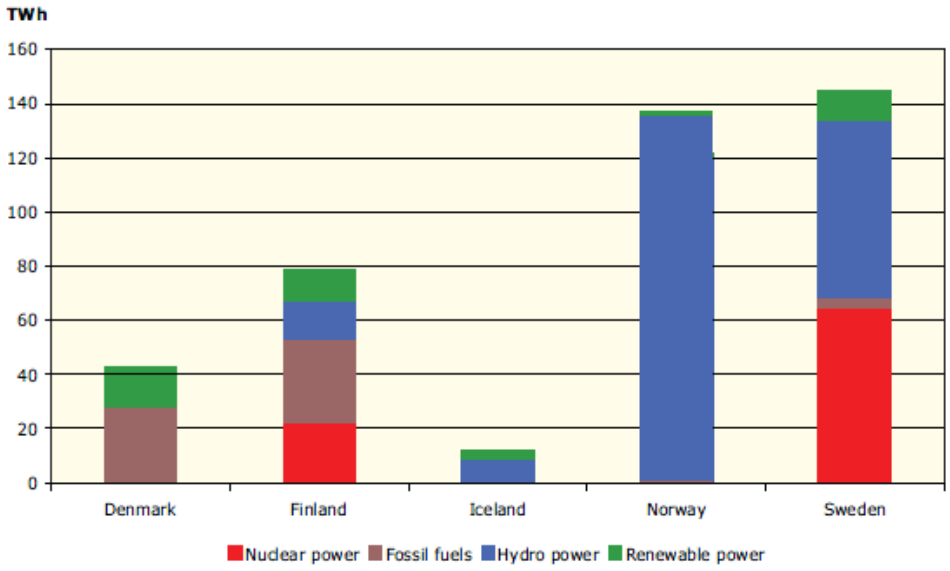

Figure 1-15: Total electricity generation in the NORDEL countries in 2007.

1.4.1 HIGH WIND RESOURCES

Norway will have an important role in such energy system. Norway has a very large wind resource, not only in the North Sea but also on shore and along the entire coast, from south Norway up to the North above the Polar Circle. Even if the climatic conditions are not easier in the north, some wind farms are already functioning in this area. The Norwegian atlas states that wind farms set on coastal area may theoretically produce 1000 TWh per year and up to 800TWh per year may come from offshore wind power based on shallow water. A common ambition of 20 TWh produced by wind power in 2020 has been "fixed" by the government and all the actors of this development. Such energy represents around 6 or 7 GW of installed capacity. The forecast of NVE (Norwegian Water Resources and Energy Directorate) is to have 3-4 TWh produced by wind power in 2010 and increase it to reach the goal. Today, up to 380 MW have been installed and produces more than 1 TWh per year. Even if the interest for wind power is currently growing in Norway, there is still a lack of a real fixed national goal and a good economic subsidy scheme to ensure a quick and strong wind power development. Therefore, due to the high wind resources the original goal can still be reached and overstepped.

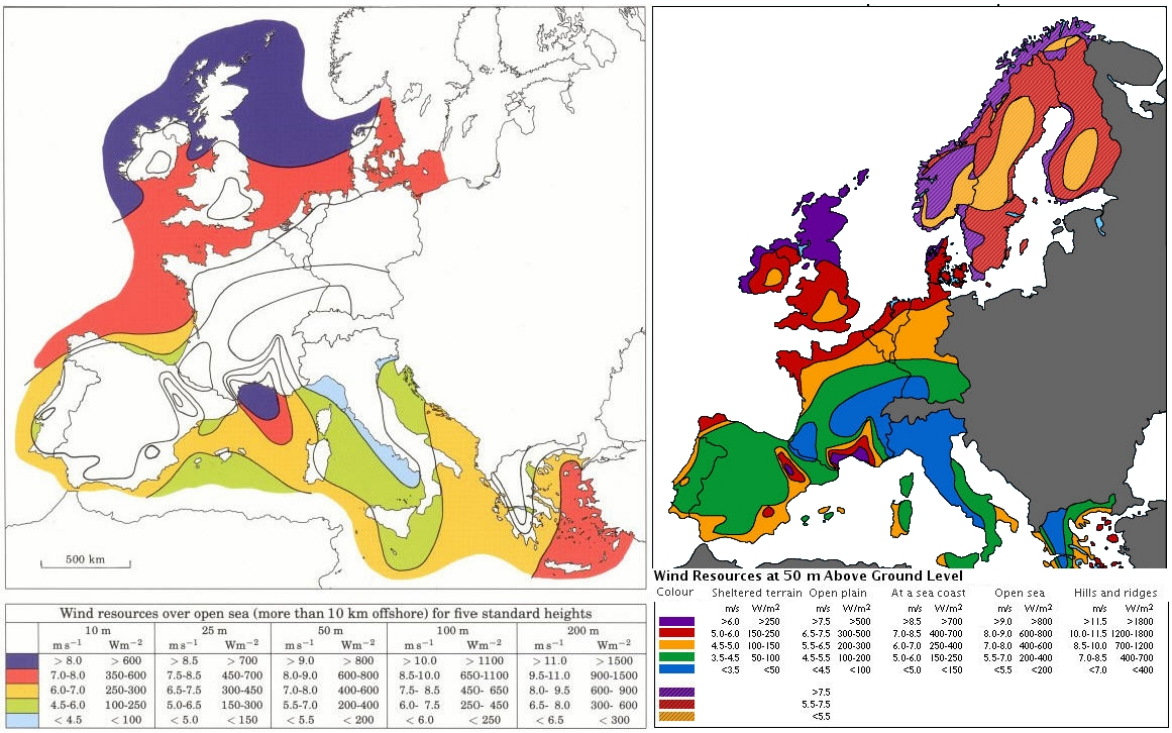

Wind resources over open sea (more than 10 km offshore) for five standard heights

	10 m		25 m		50 m		100 m		200 m	
	ms^{-1}	Wm^{-2}	ms^{-1}	Wm^{-2}	ms^{-1}	Wm^{-2}	ms^{-1}	Wm^{-2}	ms^{-1}	Wm^{-2}
	> 8.0	> 600	> 8.5	> 700	> 9.0	> 800	> 10.0	> 1100	> 11.0	> 1500
	7.0-8.0	350-600	7.5-8.5	450-700	8.0-9.0	600-800	8.5-10.0	650-1100	9.5-11.0	900-1500
	6.0-7.0	250-300	6.5-7.5	300-450	7.0-8.0	400-600	7.5- 8.5	450- 650	8.0- 9.5	600- 900
	4.5-6.0	100-250	5.0-6.5	150-300	5.5-7.0	200-400	6.0- 7.5	250- 450	6.5- 8.0	300- 600
	< 4.5	< 100	< 5.0	< 150	< 5.5	< 200	< 6.0	< 250	< 6.5	< 300

Figure 1-16: European wind atlas offshore and onshore, source RISØ

Statkraft ambition is to produce 3 TWh in 2015 and they owns today 3 wind farms for an output power capacity of 245MW (Lebesby, Smøla and Hitra). In addition, a unique offshore or cluster wind farm rated at 1 GW is studied in the North Sea.

1.4.2 ELECTRICITY PRODUCTION BASED ON HYDROPOWER

The national production of electricity per year is in a range 110-140 TWh, this energy comes mainly from hydropower, 99%. The last percent comes from biomass, wind power and gas power station. The hydro power is principally situated in the south of Norway. See above Figure 1-11:Nordel grid, the blue rectangles within a yellow triangle represent large hydro plant.

Although the water is a natural resource and consequently free, it has a value while retaining by the dams called water value. It depends of several parameters as the level of water in the reservoir, the quantity of snow in the surrounding mountains, the weather forecasts or if another reservoir is set above. By comparing this water value with the spot price, it is possible to optimize the production of a hydro power plant to get the best benefit. For a hydro power plant with reservoir level at its maximum, the water value become null if a water income is planned, and the production of the plant will be push to its maximum in order to increase its water value. This is the case with small hydro or run-of-river hydro plants.

1.4.3 BALANCE WIND POWER WITH HYDRO POWER

The introduction of wind power (shore and offshore) in the Norwegian system is easier than in a thermal or nuclear based power system. The penetration of wind power can be very high.

Firstly, the correlation between wind and hydro generation is weak which leads to a stable system. Secondly the wind power generation is normally more important in winter than in summer, whereas water inflows are essentially in summer. The seasonal wind power variations will on average fit well the consumption and is opposite to the average seasonal hydro inflow. Thus, there is a good balance between the two generation types over one year. Finally, wind generation varies less than hydro generation over years. The standard deviation is higher for hydro production than for wind generation (10% versus 14% for Norway). Studies show that the variations of the mean power of wind over 20 years are around 10% while variations for hydro power are around 20%. Wind power generation over long period is then more predictable and constant than water inflows in large area, so generation plans can be more accurate.

Wind is a free resource, but in the opposite of water, wind has no value because it can not be stocked and used when spot price is high. Wind is an "instantaneous" resource. A wind farm can produce power as long as the wind blows, and if a wind farm does not produce at its maximum, the resource is lost. Thus a wind farm will always have priority on the hydro power plant. One exception is when the reservoir is full then the hydro power plant will produce. It is also possible to use wind power generation during low consumption for a pump-storage systems. Energy produced by the wind power generation will be used to pump the water in upper reservoirs. So, flexibility is increased for a production based on hydro by adding wind power.

Consequently, the combination of wind power and hydropower is very good and useful to control the electricity production in Norway and in the surrounding of the North Sea but also to manage the water value of the hydro power plants.

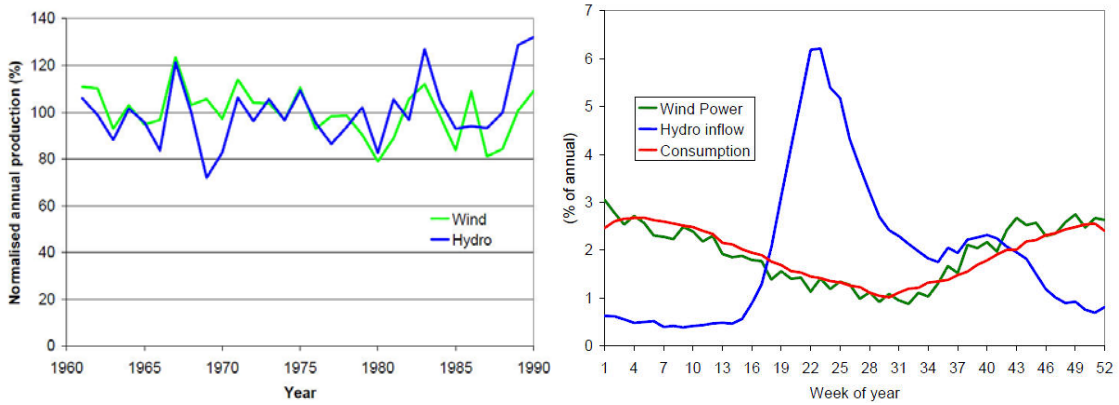

Figure 1-17: Normalized annual production of wind and hydro generation and week by week variation in wind power production compared with consumption and hydro inflow over one year.

1.4.4 ECONOMIC BENEFIT

Norway could earn a lot with a development of such offshore grid and offshore wind power development. The national industries are at the state-of-the-art in offshore field due to the oil and gas exploitation in the North Sea started for 40 years. Its industry has large knowledge on offshore construction such as oil rig, offshore platform, submarine modules… Norway produces a large part of all the submarine cables for AC and DC transmission. The main factory owned by Nexans is set in the Oslo fjord at Halden. The ABB factory is set in Sweden at Karlskrona. Both supply the world for high power transmission subsea cables. These two firms will be really involved in such development. Furthermore, companies as Aker Solution are involved on the construction of offshore foundations due to the experience on petroleum sector.

As said previously, offshore (in general) wind power may permit to add flexibility in the hydro based power generation and the management of the water value of the hydro reservoir.

Another way for Norway to take advantage of such grid will be to use the oil rig as transformer or converter station to reduce the cost of such installation. Thus the offshore oil rigs could be supplied by offshore wind farms or by hydropower plant based on the shore when the wind speed is too low. This grid will open up the potential to electrify the offshore petroleum installations in the North Sea; 60-70% by wind power. It will reduce the emission of CO_2 from the offshore platform large contributor of the Norwegian CO_2 emission. Oil rigs are normally supplied by power gas station installed on board and so emits greenhouse gases. An example is the connection of the oil rig of the Ekofiks field with a VSC- HVDC link between Germany and Norway, which will also link large wind farms off the German and the Norwegian coasts.[12] See map below.

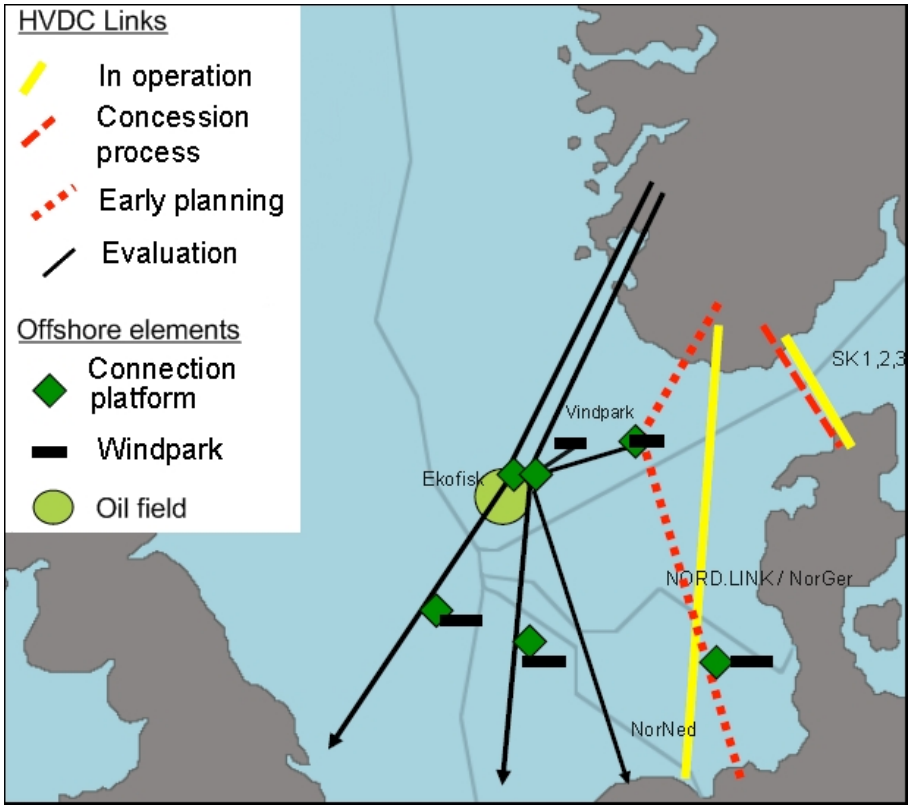

Figure 1-18: Example of interconnection of existing oil rig, offshore wind farms and countries

2 HVDC TECHNOLOGY

2.1 HISTORY

Alternating current (AC) advocated by Westinghouse and Nikola Tesla is emerged victorious from the Current War for electric power distribution in the late 1880s at the hands of direct current (DC) promoted by Thomas Edison. Since that time the AC transmission is used and is still dominant due to an easier transformation in higher voltage thanks to the transformer and thus a higher efficiency in the transmission. The first Three-Phase transmission was introduced in 1893. But engineers had still never given up on DC.

The first way to produce DC current was to use DC generator (rotating DC machines). A first 50 km long line was built in Germany between Munich and Miesband, at 2kV. Then, few systems have been installed. For example, one in 1889 in Italy by the Acquedotto de Ferrari-Galliera Company, which transmitted 630 kW at 14 kV DC over a distance of 120 km. Another system was built in France; the Moutiers-Lyon system worked from 1903 until 1936 with a transmitted power of 8.6 MW. But the rotating machinery required high maintenance and had high energy losses. So, the HVAC did not have any competitor until the 50s.

Practical manipulation of DC voltages only became possible with the development of "power electronic devices" such as mercury arc valves and later semiconductor devices, such as thyristors, IGBTs, MOSFETs. In an HVDC system, electric power is taken from one point in a three-phase AC network, converted to DC in a converter station (rectifier), then transmitted to the receiving point by cables (often) or by power lines, finally converted back to AC in another converter station (inverter) in order to be injected into the receiving AC network.
Currently, there are mainly two types of converter. [13] The conventional HVDC transmission employs Line-Commutated current source Converter. LCC-HVDC system is a mature technology today. New HVDC transmission uses VSC (Self-Commutated Voltage Source Converter) with pulse-width modulation. The main difference between the two technologies is the converter valves. Conventional HVDC transmission employs thyristor valves instead of IGBT valves for the VSC-HVDC.

2.1.1 MERCURY ARC VALVES

Research into mercury arc valves and static converters for voltages up to 1000 V began at the end of the 1920s and continued until the building of a test station for trials at higher powers in Sweden in 1945 by the company ASEA.

The Elbe-Projekt was the name of the first commercial HVDC transmission system in the world, based on mercury arc valves. Some experimental installations were demonstrated between 1933 and 1942. Contracts were signed with AEG (Allgemeine Elektrizitäts-Gesellschaft, General Electricity Company) and Siemens in 1941, and construction began of a bipolar direct current line from the Elbe hydro power station near Dessau, to Berlin, in 1943. The line was designed to transmit 60 MW using a symmetrical bipolar operating voltage of 200 kV and a rated current150A. Two single-core earth cables were used. The nominal justification for the project was that, during wartime, a buried cable would be less conspicuous as a bombing target. The system was never put into service due to the war chaos in Germany. The situation in post-war Germany allowed the Soviets to dismantle the system. The equipment was moved to the Soviet Union and was reused in the building of a 100 kilometers long 200 kV monopolar high voltage direct current line with a maximum transmission rating of 30 MW between Moscow and Kashira, in 1951. In the same time the Gotland project in Sweden is achieved in 1954 based on mercury arc valves as well. The introduction of the fully-static mercury arc valve to commercial service marked the beginning of the modern era of HVDC transmission. Mercury arc valves were common in systems designed up to 1975.

2.2 THYRISTOR AND CLASSICAL HVDC

2.2.1 THYRISTOR

In the 1960s, the thyristor arrived and the first commercial thyristor converter station operated in 1970 in Gotland.

The thyristor is a solid-state semiconductor device similar to the diode, but with an extra control terminal that is used to switch the device on at a particular instant during the AC cycle. The current can only flow from the anode to the cathode as soon as a positive voltage is applied at these terminal and a current flows through the gate. The thyristor become conductive. As soon as the current is null or negative, it stops to conduct according to its diode property. Nowadays, the state of the art for thyristors available on the market is called Light Triggered Thyristor, the light is used in the gate instead of a current and photons replace the electrons. Such thyristors have a blocking voltage up to 8kV and may carry a current up to 4kA.

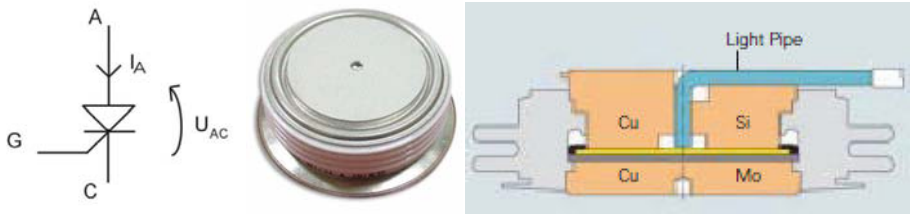

Figure 2-1: Symbol, picture and scheme of a thyristor wafer (Light Triggered Thyristor).

Because the voltages in HVDC systems, up to 800 kV in some cases, exceed the breakdown voltages of the semiconductor devices, the thyristors are put into series and parallel to withstand to the voltage and the current, in a system called valves. It comprises also the cooling system, command elements and all the fire protection. The thyristor valves allow good flexibility for the constructor to build the converter station.

2.2.2 LCC-HVDC CONVERTER

Such kind of HVDC transmissions is called conventional HVDC or HVDC LCC for *Line Commutated Converters*. The converter station (rectifier and inverter) comprises [14]:

- Transformers
- Thyristor valves
- AC and DC filters
- DC current filtering reactance
- Capacitors or STATCOM
- DC cable(s)

A scheme with the components of a LCC converter is shown in Figure 2-2. Pictures of a converter station and of a thyristor valve are also presented.

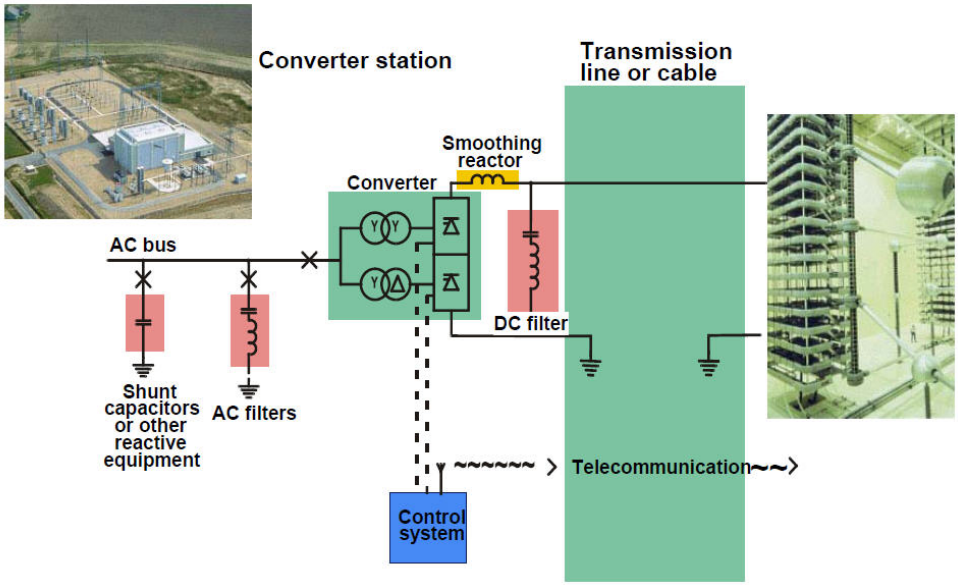

Figure 2-2: Scheme of an entire converter station, pictures of converter station and thyristor valve

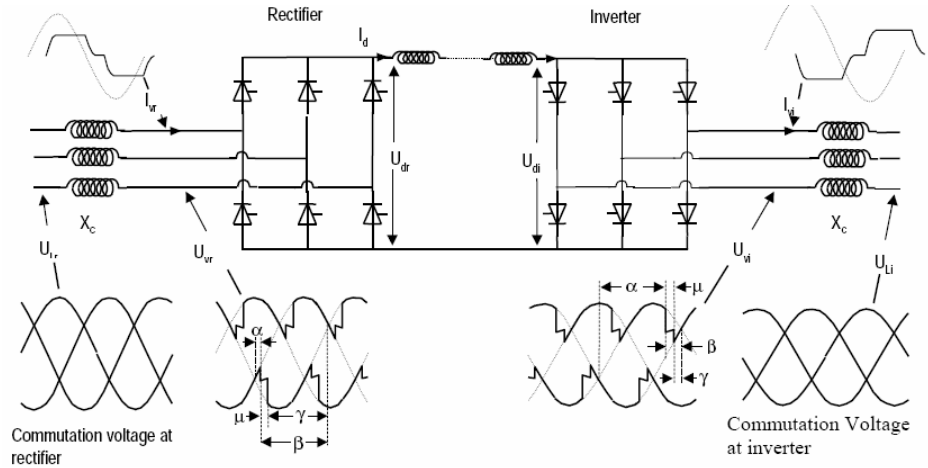

Figure 2-3: Scheme of basic 6-thyristor valves

The converter transformers are specially design for this application. With respect to the ground potentials the LCC converter cannot generate zero voltage, so the insulation requirements across the transformer are higher than with a normal one. The transformer receives also some harmonic currents leading to stresses and losses.

The output of these transformers is then connected to AC filters and then to a bridge rectifier formed by a defined number of valves. The basic configuration uses six valves, connecting each of the three phases to each of the DC lines. However, with a phase change only every sixty degrees, considerable harmonics remain on the DC line. An improvement of this configuration uses 12 valves (often known as a twelve-pulse system).It is the typical HVDC transmission system nowadays. The AC is split into two separate three phase supplies before transformation. One of the sets of supplies is then configured to have a star secondary (Y-Y), the other a delta secondary (Δ-Y), establishing a 30 degree phase difference between the two sets of three phases. With twelve valves connecting each of the two sets of three phases to the two DC rails, there is a phase change every 30 degrees, and harmonics are considerably reduced. In addition to the conversion transformers and valve-sets, various passive resistive and reactive components help to filter harmonics out of the DC line such as STACOM or capacitances. DC filters are also needed to avoid current interruption with minimum load, to limit DC fault currents and reduce current harmonic in the cable.

2.2.3 FUNCTIONING OF LCC-HVDC CONVERTER

The mechanism of the converter is the following. There must be a positive voltage on the valve and a firing pulse on the thyristor to allow the current to flow. The instant when current begins to flow through a valve or to another can be delayed by displacing the firing pulse. The current in the DC line is the sum of the current coming from each branch. This method permits the average DC voltage to be modified. The natural firing point is the point where two phase voltages intersect. So, the values of the firing angle determine the direction of the active power transmission. The converter in rectifier mode will have firing angle comprise within 0 and 90 and in inverter mode the angle will be within 90 and 180. It is easier to reverse the direction of energy flow only by changing the firing angle. Notice that a communication between the rectifier and the inverter is needed. This communication might be done by using optic fibers within the DC cable. For a 90 firing angle, none active power is transmitted. See next Figure 2-4.

By ignoring the AC-side inductance, the direct voltage U_d is proportional to the AC voltage U_{ll} and the cosinus of the firing angle α. The equation is given below.

$$U_d = \frac{3.\sqrt{2}}{\pi}.V_{ll}.\cos\alpha \tag{2.1}$$

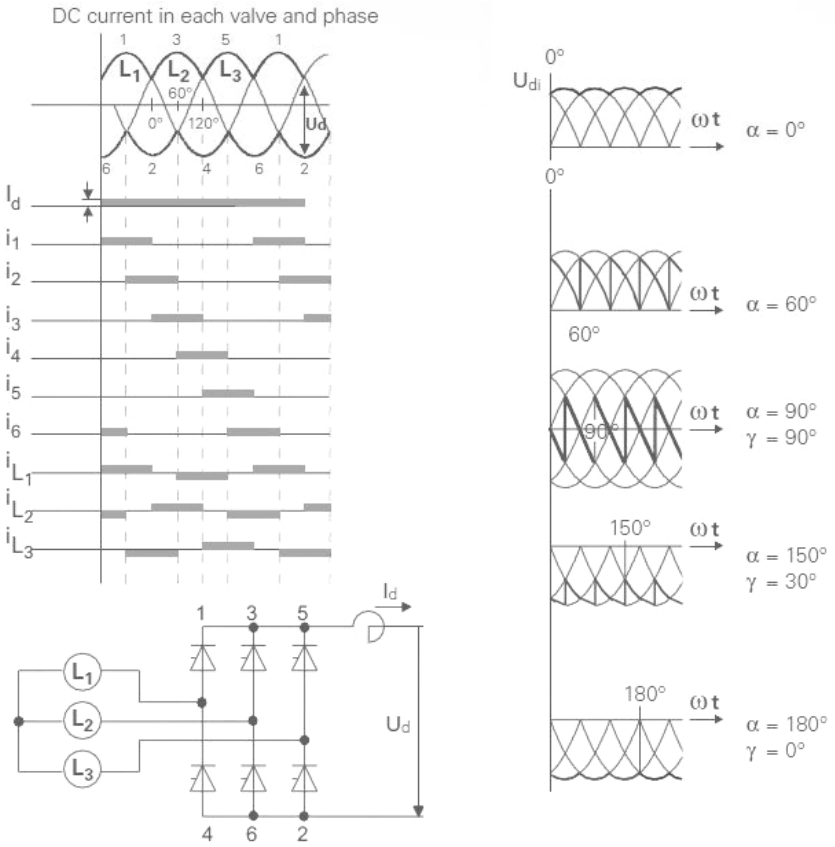

Figure 2-4: Principle of functioning of LCC-HVDC

2.2.4 THE NEED TO BALANCE THE REACTIVE POWER

However, the converter consumes lot of reactive power, which is an inconvenient for the stability of the network. The converter operates at a lagging power factor and such draw reactive power from the AC network. The reactive power demand is depending on the load and on the way the converter is working: constant voltage on the line, constant DC current. Active and reactive powers are calculated as follow:

$$P = 1,35.V_{ll}.I_d \cos\alpha$$
$$Q = 1,35.V_{ll}.I_d \sin\alpha \quad (2.2)$$

The reactive power can be expressed with the active power.

$$Q = P.\tan\alpha \quad (2.3)$$

The power factor of such installation can be calculated with some assumption by the relation[15]:

$$PF = \frac{3}{\pi}.\cos\alpha \quad (2.4)$$

As said previously, the converter needs a capacitor bank and AC filter in order to be connected to the grid. The reactive power consumption should always be under a certain value, which is done thank to the shunt bank and harmonic filter set after the converter on the AC side. Without a reactive compensation for the converter, the grid will be destabilized. The reactive power balance is given below.

$$Q_{net} = +Q_{conv} - Q_{fk}.U^2 - Qc.U^2 \quad (2.5)$$

Furthermore classical HVDC need synchronous voltage sources in order to operate and at least to start. Such systems don't have a black start capability according to this inconvenient.

In the late of the 1990s the IGBT (Insulated Gated Bipolar Transistor) appeared in the power converter station using the Voltage Source Converter (VSC). See next chapter

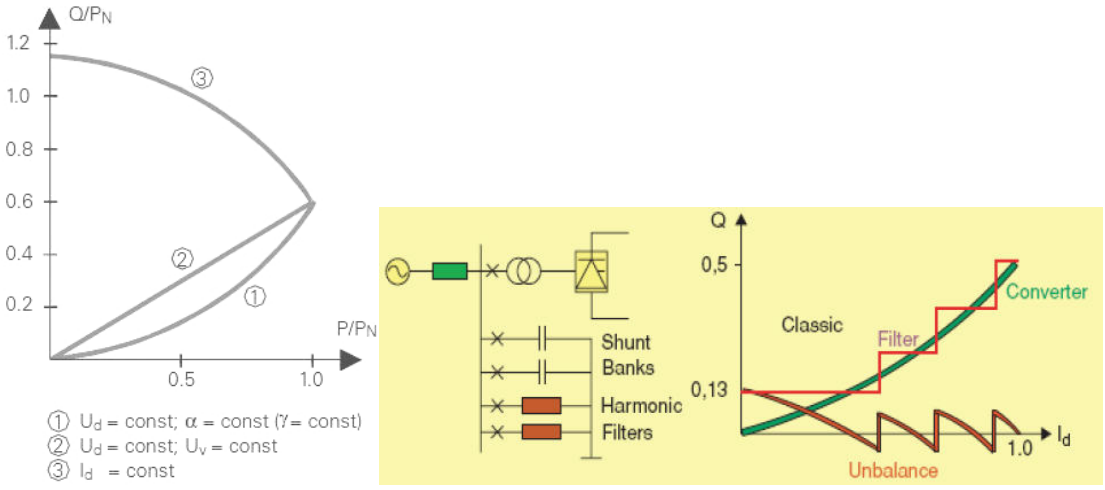

Figure 2-5: Functioning way of classical HVDC and reactive power created with and without filter (green)

2.3 IGBT AND HVDC BASED ON VSC TECHNOLOGY

2.3.1 IGBT (INSULATED GATE BIPOLAR TRANSISTOR)

The HVDC using VSC transmission uses Insulated-Gate Bipolar Transistor (IGBT) valves such are self-commutated. First-generation of IGBT was used in the 1980s but was slow and presented problems in operation. A second generation, appeared in the 1990s, resolved these problems and permits a faster switching time than the first-generation. In the 2000s, new IGBTs appeared with very good performance for high current and voltage. An IGBT is the combination of a Bipolar Junction Transistor *PNP* (BJT) and a MOSFET. Thus it takes the advantages of both devices: low conduction losses for the BJT and fast commutation for the MOSFET.

IGBT cells have a small size (around $1cm^2$). Thus many IGBT cells are connected in parallel in IGBT chips and then in modules capable to handle current up to 2.4kA with blocking voltage up to 6.5kV. As for the thyristors, many modules are connected in series into valves to withstand to the high-voltage levels. So, a valve may comprise up to 20 billions of IGBT cells. See below Figure 2-6

Innovations in IGBT and capacitor technology open up for a concept in the VSC technology called the multilevel VSC, which is used for the second generation of HVDC PLUS. See paragraph 2.3.4.

2.3.2 VSC-HVDC CONVERTER

As for the conventional HVDC transmission system, HVDC-VSC comprises:

- Transformers
- IGBT valves
- Converters reactors
- AC filters
- DC current filtering reactance
- DC cable(s)

The scheme of a VSC-HVDC converter is shown Figure 2-7. A picture of a converter station can be observed later in report in Figure 2-21.

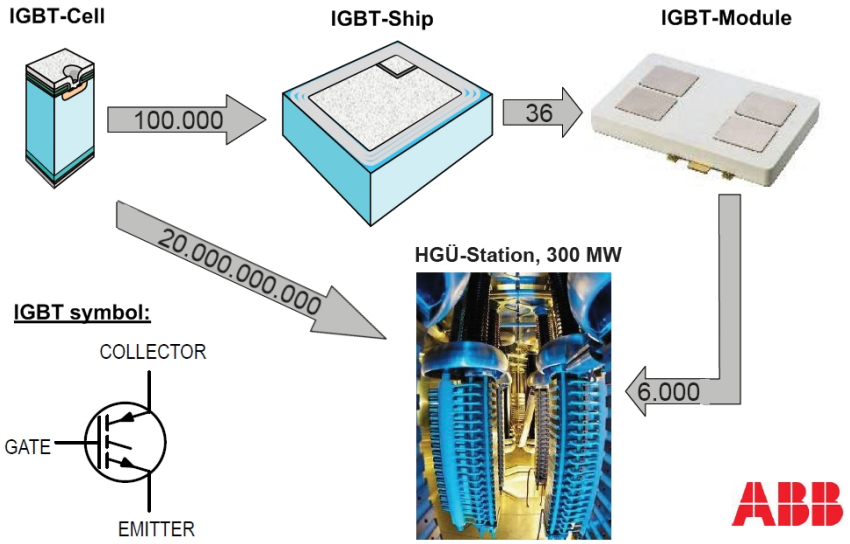

Figure 2-6: IGBT symbol and representation of a valve from IGBT cells. (Source ABB)

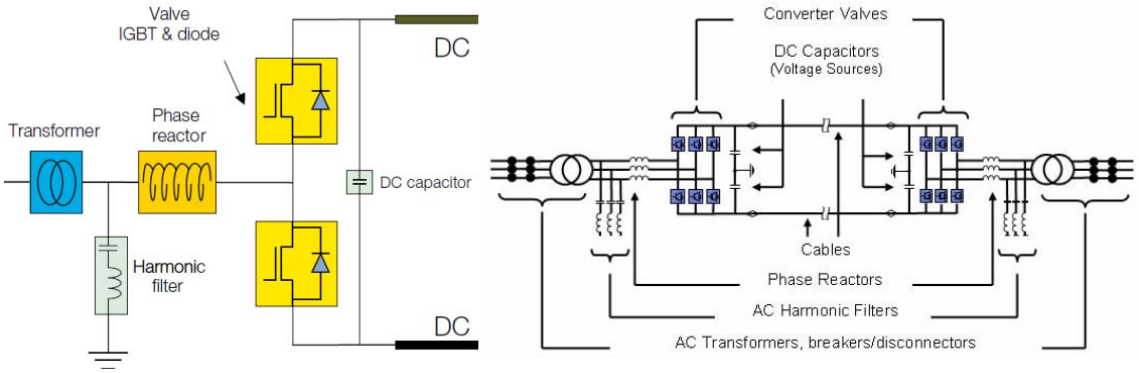

Figure 2-7: Scheme of VSC-HVDC, left one phase (or leg) and right complete transmission

Series-connected IGBTs with anti-parallel diodes form the valve of the VSC converter and snubber capacitors are connected in parallel to each of the semi conductor devices to avoid overvoltage in the IGBT valves.

The converter reactor is one of the key components in a voltage source converter to permit continuous and independent control of active and reactive power. The main purposes of the converter reactor are to limit the short circuit current at the IGBT valves and to provide a low-pass filter of the PWM pattern (Explained in the following paragraph 2.3.3).
The harmonic currents related to the switching frequency and generated by the converter are blocked by the converter reactor. There is one converter reactor per phase. They consist of vertical coils, standing on insulators. They are several meters tall and several meters in diameter

The harmonics content on the AC bus voltage are reduced by an AC filter between the converter reactor and the transformer, which is a classical one as opposed to the special converter transformer needed for conventional HVDC.

Losses come from two main contributors: conduction and switching. Conduction losses can be reduced by using larger semiconductor area. Switching losses depend on the switching time and the voltage and current at the switching instant. The switching frequency then determines the average switching losses. The switching losses can be reduced by using a soft switching commutation scheme. The switching frequency is several kHz, 2kHz is the operating frequency for the HVDC Light®.

2.3.3 FUNCTIONING OF A VSC-HVDC CONVERTER

HVDC-VSC uses Pulse Width Modulation (PWM) control to give the desired fundamental frequency voltage. The principle will be now explained in inverter mode (similar control is done in rectifier mode):

A control signal is needed to achieve the control of the switching of the IGBT valves. A sinusoidal control signal $V_{control}$ is compared with a triangular signal V_{tri} to decide which valve should be conducting. The comparison between both signals is the following for a bipolar transmission.

$$\begin{aligned} V_{control} > V_{tri} &\rightarrow T_{A+} on \rightarrow V_{A0} = \frac{V_d}{2} \\ V_{control} < V_{tri} &\rightarrow T_{A-} on \rightarrow V_{A0} = -\frac{V_d}{2} \end{aligned} \tag{2.6}$$

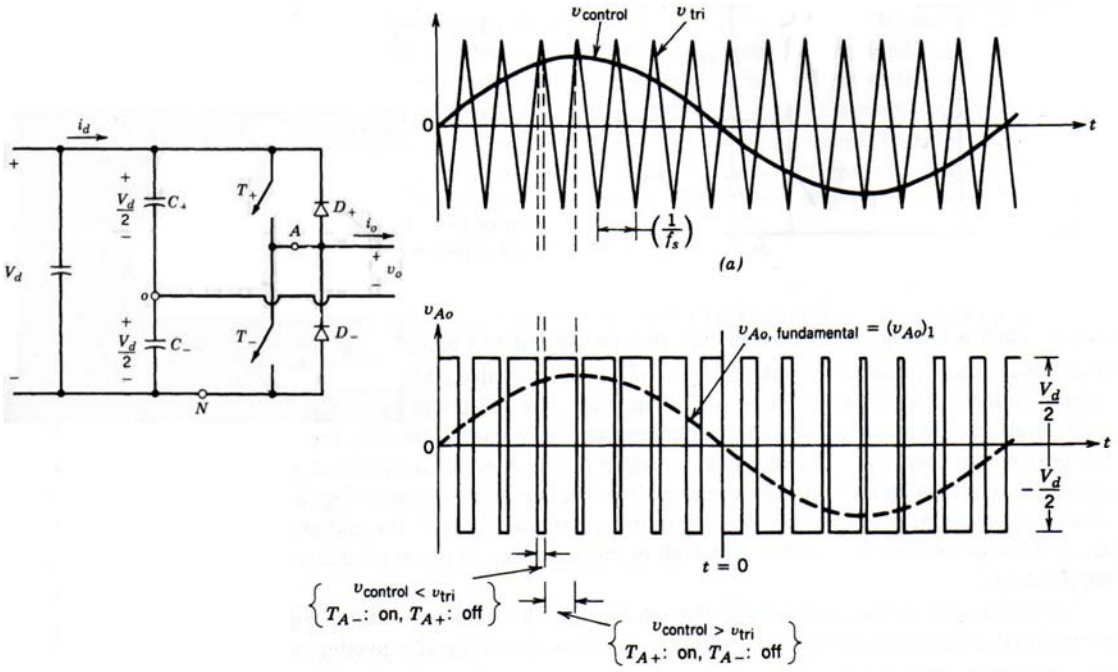

Figure 2-8: Scheme of one leg inverter and pulse width modulation principle.

The triangular wave form V_{tri} is at a switching frequency fs. The control signal $V_{control}$ is used to modulate the switch duty ratio at a frequency f_1 (also called modulating frequency).

The inverter output is not a perfect sine wave and contains voltage components at harmonic frequency f_1, so higher harmonics are created at higher frequencies. So, the fundamental component $(V_{A0})_1$ has to be filtered out. As the harmonics have high frequencies, they are "easily" filtered by small filters.
A frequency modulation ratio m_f is defined

$$m_f = \frac{f_s}{f_1} \tag{2.7}$$

As long as the amplitude of V_{tri} is higher than the amplitude of $V_{control}$, the amplitude of the output voltage is proportional with the amplitude of the modulation ration m_a defined with the peak values as:

$$m_a = \frac{\hat{V}_{control}}{\hat{V}_{tri}} \tag{2.8}$$

The fundamental component is calculated as follow

$$\begin{aligned} \left(V_{A0}\right)_1 &= m_a . \frac{V_d}{2} . \sin \omega_1 t \\ \left(\hat{V}_{A0}\right)_1 &= m_a . \frac{V_d}{2} \end{aligned} \tag{2.9}$$

As long as ma is smaller than 1, the scheme is a linear modulation. As soon as the amplitude of $V_{control}$ is higher than V_{tri}, the output voltage is no longer proportional and the modulation scheme enter in an over-modulation functioning (m_a>1). But this configuration will not be dealt with in this report.

In a 3-phase transmission, each "leg" of the converter is controlled separately from the 2 others.

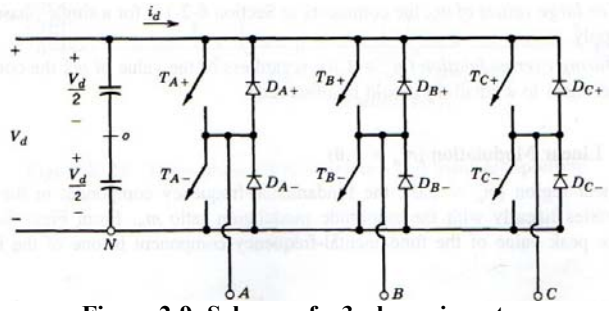

Figure 2-9: Scheme of a 3-phases inverter

The voltage V_{AN} is given with the relation.

$$V_{AN} = V_{A0} + V_{0N} = V_{A0} + \frac{1}{2}.V_d \tag{2.10}$$

Output voltages are similar than with one leg. Due to the 120°phase shift between phase voltage, the line-to-line rms voltage at the fundamental frequency is given by the relation below:

$$\begin{aligned} (V_{ll})_1 &= (V_{AN})_1 - (V_{BN})_1 = \frac{\sqrt{3}}{\sqrt{2}}.(\hat{V}_{AN})_1 \\ (V_{ll})_1 &\simeq 0.612.m_a.V_d \end{aligned} \tag{2.11}$$

Only the bipolar PWM is studied, in the unipolar scheme 2 sinusoidal control signals are compared with the triangular signal.

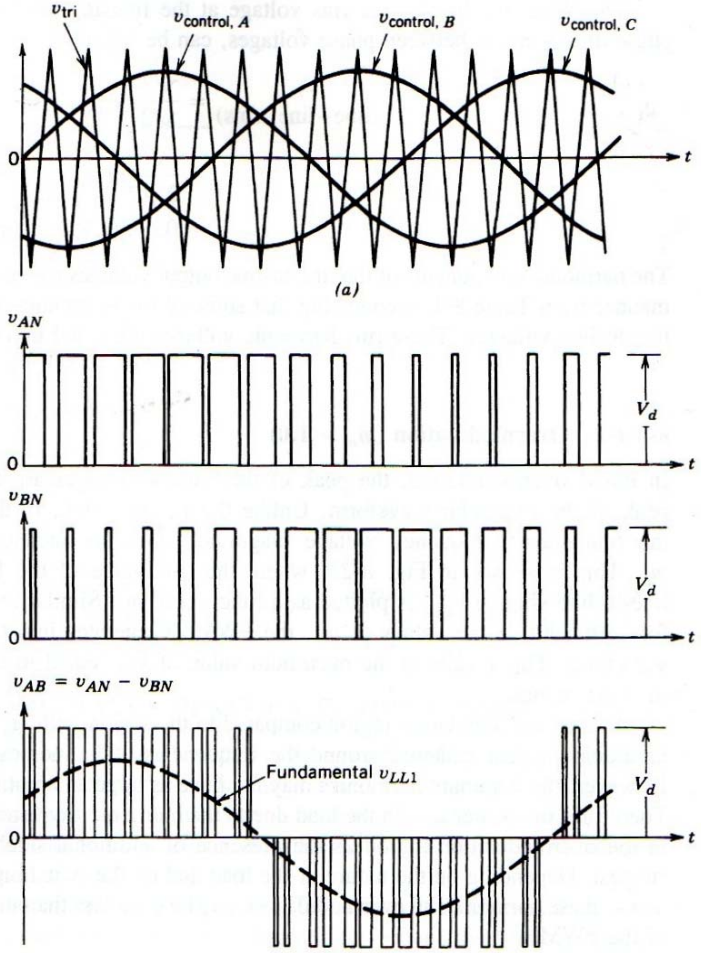

Figure 2-10: Principle of Pulse Width Modulation in a 3-phases inverter.

2.3.4 HVDC PLUS® & HVDC LIGHT®

Both concepts are very similar in lot of point. ABB developing the HVDC Light® and Siemens the HVDC Plus® have solutions for up to 1000 MW.[16] [17]

The design of the substation is very close to each other, a module concept is used to provide flexibility in the building. The size (volume and weight) is very small for both, but the HVDC Light® concept has a lower weight whereas the HVDC Plus® concept can have a smaller volume by using SF_6 insulated device to shrink the converter down as minimum as possible. Those criteria are very important for offshore construction.
The converter stations require little maintenance. The stations are designed to be unmanned, and can be operated remotely.

Before being commissioned, both concepts are tested as much as possible in the factory before equipment is sent offshore. The majority of equipment for HVDC Light® is delivered in enclosures, and is tested at the factory before shipment. The HVDC Plus® module is completely assembled and pre-tested in a shipyard

The electrical concept is similar. Pulse Width Modulation is used. Standard transformer can be used; giving lower price and better availability. The cables are laid in pair with DC current in opposite directions with the advantages that it eliminates the magnetic fields which may harm the fauna.

The main difference between HVDC Plus® and Light® is on the number of level in the converter. The HVDC Plus® from Siemens uses a new multi-level approach, individual module capacitors are uniformly distributed throughout the topology, and each level is individually controlled to generate a small voltage step. In this way, each module within the multi-level converter is a discrete voltage source in itself, with a local capacitor to define its voltage step without creating ripple voltage distortion across the converter's other phases. By incrementally controlling each step, an almost sinusoidal voltage is generated at the AC outputs of the multi-valves. To allow the use of modular IGBTs, Siemens has developed an economical and fail-safe short-circuit mechanism within the multilevel module.

The HVDC Light® concept uses the existing two- or three level converters using Pulse Width Modulation (PWM) which have to switch the full DC voltage in large steps. This causes harmonic distortion and high transient stresses resulting in HF noise but being easily filtered down.

2.4 HVDC SUBMARINE CABLES

In this section, the information about the different types of submarine cables is extracted from a previous work done as pre-master thesis.[1]

The design of HVDC cables is complex and difficult; a great deal of experience and research work is required to develop a cable. Thermal, dynamic pressure and protection against the corrosion are of great importance. It exists three different types of cable with as main difference the insulating materials:

- Low Pressure Oil Filled cables (LPOF)
- Mass-impregnated cable (MI)
- Polymeric insulation (LDPE and XLPE)

Until now, the cables used for HVDC transmission and distribution, have been paper insulated cables: LPOF or MI. The LPOF cable is constructed with an impregnated paper insulation in which the paper tapes are impregnated after lapping by oil from a pipe in the core of the cable. It won't be deal with on this report because the technology become obsolete and has too much drawback.

Most of the cables installed until now are MI cable.The first reason is that the adoption of XLPE for DC is not possible by simple translation of the AC technology. Last reason is economic. The demand for using HVDC cables has in the past been very low, mostly in underwater installations, so that the use of polyethylene in HVDC became attractive to cable manufacturers only when the number of HVDC projects increased sufficiently to make the development costs recoverable. Therefore for one decade the HVDC cables with polymeric insulation are appeared and become more and more interesting economically.

In the appendix a table gives some significant data about HVDC cables used in HVDC schemes all over the world. [18] The next table indicates clearly that the HVDC cables installed are mostly the paper-impregnated or oil-filled cables. [19] Although the paper-impregnated cables continue to be used currently for high power transmission, the place of the polymeric insulation cable is growing up with the improvement of the technology.

The laying operations of a cable into the sea are complex. Several ships are needed, a cable laying ship and some barges or transport vessels with the length of cable. The cable laying operations can only start with an adequate period of favorable weather is predicted. The cable is laid by a vessel where a part of the cables are stocked. The handling vessel have also all the tools to transfer the cable from its storage area to its planned position in the sea bed. A big wheel is used to put the cable into the water and a turn table to unroll it. Some control system are use to accelerate or brake the drums or the turntable to prevent any mechanical stress. The speed of a cable laying vessel is often about 5km/h with a maximum of 10 km/h if the cable is not buried. Now, satellites are used to control the exact route of the cable and the cable laying process is facilitated. Nowadays a trench can be cut and simultaneously the cable can be introduced into thanks to the new submarine machines.

The MI and the XLPE cable will be now studied.

[1] Pre-master thesis: HVDC submarine cables – Supervisors: Marta MOULINAS and Tore UNDELAND

	Name	year	Voltage (kV)	Power per cable (MW)	No Cables	Conductor size (mm^2)	Type	Length (km)
1	Gotland	1954	100	20	1	90	MI	100
2	Cross Channel	1961	100	80	2	390	MI	51
3	SA. CO. I	1965	200	100	[2]	420	MI	119
4	Cook Strait1	1965/92	250	300	2	520	GF	39
5	Konti Skan Sweden	1965	285	300	1	625	MI	64
	Konti Skan Læsoe	1965	285	250	1	310	OF	23
6	Vancouver1	1969	300	156	2	400	MI	31
7	Kingnorth	1971	266	320	2	800	OF	84
8	Mallorca	1974	200	100	4	500	OF	44
9	Skagerrak	1976	262	250	2	800	MI	125
10	Vancouver2	1976	300	185	2	400	OF	35
11	Hokaido Honshu	1980/93	250	300	2	600	OF	43
12	Gotland 2/3	1983	150	160	2	800	MI	100
13	IFA 2000	1986	275	250	8	900	MI	50
14	Konti Skan 2/3	1988/91	285	300	2	1200	MI	64
15	Fenno Skan	1989	400	500	1	1200	MI	200
16	Cook Strait2	1991	350	500	2	1400	MI	40
17	St Lawrence	1993	500	625	6	1400	OF	5
18	Hawai	Failure	300	250	2	1600	OF	67+154
19	Skagerrak 3	1993	350	500	1	1400	MI	125
20	Sheju	1993	180	150	2	800	MI	95
21	Baltic Cable	1994	450	600	1	1600	MI	250
22	Kontek	1995	400	600	1	800	OF	55
23	Leyte	1997	350	440	1	No data	MI	21
24	Gotland	1999	80	25	2	No data	Polymeric	70
25	Tjæreborg	2000	9	8	2	No data	Polymeric	5
26	Swepol	2000	450	600	1	2100	MI	250
27	Moyhle	2000	250	250	2	1000	MI+IRC	55
28	Cross sound	2002	150	175	2	1300	Polymeric	42
29	Greece Italy	2001	400	500	1	1250	MI	160
30	Troll A	2004	80	20	4	300	Polymeric	68
31	East Link	2006	150	175	2	1000	Polymeric	74
32	NordNed	2008	450	350	[2] / 2	790 / 700	MI	420 / 150
33	Saipei	2009	500	500	2	No data	MI	420
34	Valhall	2009	150	78	1	No data	MI+IRC	292
35	Nord E ON 1	2010	150	200	2	No data	Polymeric	128

MI= mass impregnated cable; OF=oil filled cable; GF=gas filled cable; IRC= integrated return conductor; Yellow=link out of service - Blue=link which have been upgraded *commissioning year / upgraded* - In [ ] the two cores flat cable

Table 2-1: Significant DC cable data of submarine HVDC transmission in the world

2.4.1 MASS IMPREGNATED CABLES

The mass impregnated cables are composed from the centre of: the conductor, a semiconductor screen or layers, then the insulation made with impregnated paper. Another semiconductor screen is put before the shield made with lead and all the mechanical and corrosion protections. By increasing the load, the insulation will expand and try to break out the exterior sheathing. A deformation on it will occur, even very thin. The impregnant of the paper is not fluid at the maximum continuous operating temperature. So it prevents the cable to increase its size and also mechanical stress during high loading.

The paper is applied to the cable as ribbons with a thickness of about 1mm and a width of about 20 mm. The paper is wound with a pitch angle that is slightly higher than the width of the ribbon. The winding is performed so that the gaps, called butt gap, are displaced by about 30% of the ribbon width for each layer. Thus it does not create continuous oil filled canals where partial discharge might occur. There are necessary to prevent pile up of layers. Butt gaps prevent as well mechanical damage on the pressure side when the cable is bent during the installation. Furthermore, the paper ribbons must be able to slide to each other; else a break in the paper could occur. Thus, the process of fabrication must be accurate and the tension in the paper ribbon must be carefully chosen. The paper employed must be of high purity without ions, a low humidity to prevent discharges.

The aim of the lead sheath is to tight the cable according to the chemical property of the metal, but also to take the opportunity of its ductility for the laying operation. The semiconductor screen or layer must prevent discharges and transfer of charge from the conductor to the insulation. It avoids also the irregularities and the protusions to reduce space charge accumulation.

As the entire length of a HVDC link cannot be laid and produced in one time, some joints have to done. This work is long and should be accomplished with accuracy. All the layers are put on each other, from the centre to the exterior; the metal parts are brazed or welded each other, the paper ribbons are wound by the same way (can be applied by hand) etc… The flexibility is often reduced on this part of the cable. The joint are always a point of weakness and vulnerability. On the rout of a cable, the joint cannot often be laid very deep, the maximum depth allowed is 500m, whereas the cable can be laid up to 1000m of depth.

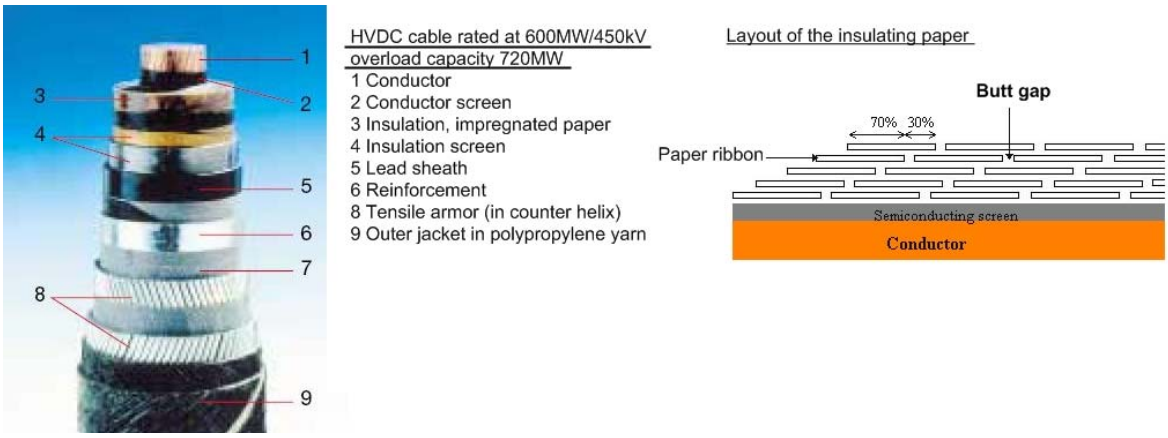

Figure 2-11: Picture of the SwePol link power cable and layout of the ribbon paper.

2.4.2 POLYMERIC CABLES

The polymeric insulating cable uses the XLPE (cross linked polyethylene), the same used for the AC cable but which has been modified with addition of additives and other polymers. The reason is that the electrical field has not the same behaviour in the DC insulation than in the AC insulation.

The structure of the cable is similar than the structure of mass impregnated cable. In the core of the cable, there is the conductor, often copper. The insulation made with an XLPE base is in between two semiconductor screens or layers. Then, a lead sheath surrounded with an inner jacket (often in polyethylene) prevents water penetration in the insulation. Finally, all the mechanical and corrosion protections composed by the armouring and an outer jacket in polypropylene yarn impregnated with asphalt are wrapped onto. For deep submarine cables, the armouring is doubled to resist of the water pressure and eventual damages. The mechanical strength of the cable is provided by steel tape and two layers of steel-wire armour. The steel wires are applied in opposite directions to form a counter-helix, which eliminates any torsional stress.

Due to the property of the insulation (low density of PE), the polymeric cable is lighter as a paper insulated cable. The good insulating properties allow less insulation, thus the radius of the cable is smaller and less mechanical protection is needed. HVDC polymer cables are more flexible because of the robust and flexible insulation material. Those cables have smaller bending radius compared to paper insulated cables which are handicapped by the paper layers. This property allows better flexibility in the laying process and the choice of the cable rout. For example, the smaller bending radius make possible to go around obstacles such as rocks, etc…

The working temperature is high and it makes it possible to use it in the tropical area without big changes. HVDC polymer cables are possible to handle at lower temperatures compared to paper insulated cables. It might be an advantage for transmission link in cold area like Scandinavia or the supply of oil rig in Norway or Russia.

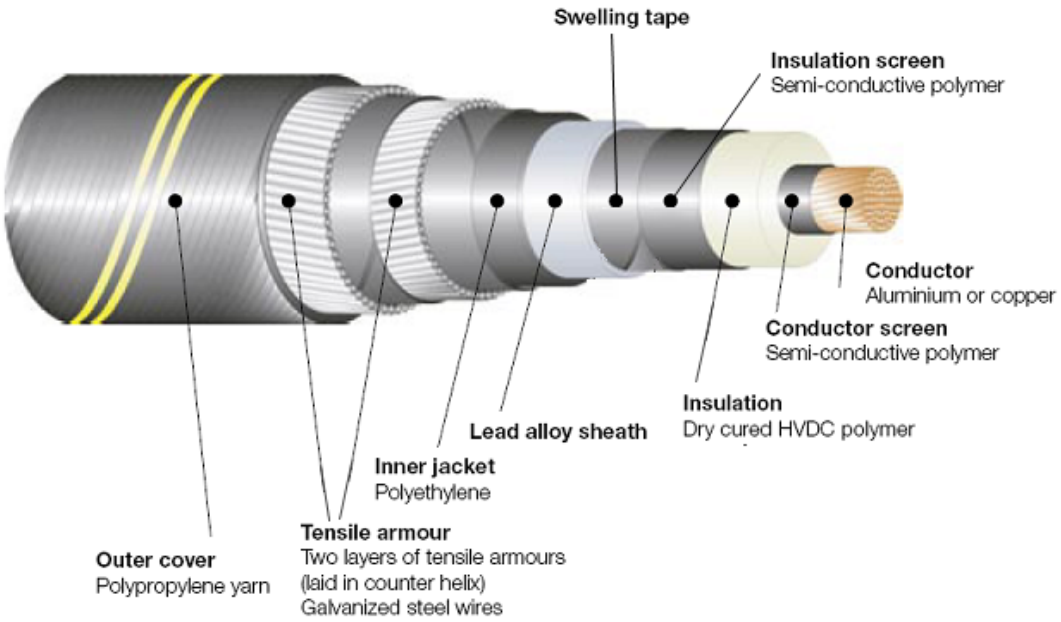

Figure 2-12: Deep submarine cable with polymeric insulation for DC transmission.

Pre-fabricated joint can be used for polymeric cable. The mechanical, thermal and electrical properties of the flexible joint have to match the cable. The conductor joint is therefore welded. The insulation system is restored by lapping and successively vulcanizing semi-conductive and insulating tapes around the cable. Then the lead-sheath, PE sheath and armoring are restored. The water tightness is achieved by swaging down a lead sheath over the joint. To maintain and ensure the continuity of the PE-sheath, a heat shrinkable tube is employed over the lead tube. Joining of polymer cables is become simpler and requires less skill. The process is also faster, so is an advantage during the installation in the sea.

It has to be noticed that actually only ABB manufactured this type of cable and use an extruded process to made it. The insulation system is triple extruded, i.e. the conductor screen, the insulation and the insulation screen are extruded simultaneously. ABB calls its new cable technology HVDC Light® according to its properties.

2.4.3 CONCLUSION

It is now widely believed that extruded polymeric HVDC cables offer significant advantages over the traditional paper insulated cable types. A higher conductor temperature can be used, giving a more compact cable for the same power rating. Lighter moisture barriers can be used, giving a lighter cable. Joining of extruded cables is much simpler and requires less skill. The use of extruded cables avoids the significant long-term environmental hazards associated with oil leaks. The mass impregnated technology is suitable only for the high power range.

2.5 HVDC SYSTEM CONFIGURATIONS

HVDC power transmission cable schemes can be variously configured. Depending upon the function and location of the converter stations, various configurations of HVDC systems can be identified. The ones drawn in this section involve LCC-HVDC configurations but similar types of configurations exist for VSC-HVDC with or without transformers depending upon the project.

The basic HVDC cable transmission scheme is a monopolar installation that uses the earth and sea to return the current. The sea return reduces the cost of the interconnection since only one cable is necessary between the two converter stations. Losses are also kept to a minimum as the return path has a huge cross section, which makes the resistance negligible. The only losses are due to the voltage drops at the anode and the cathode. The good conductivity of the earth and seawater makes it easy to design the electrodes, and it can be said that field experience with monopolar transmissions is excellent. This kind of system has also disadvantages and environmental restrictions. The electrodes have to be located well away from the converter stations and the main HVDC cable to avoid corrosion of pipelines or other metallic structures in the vicinity as well as direct current pick-up in transformer neutrals. In a monopolar metallic return system, return current flows through a conductor in the form of a medium-voltage cable, thus avoiding potential problems associated with ground return current.

A further development of the monopolar transmission scheme is the bipolar configuration. It is actually two monopolar systems combined, one at positive and one at negative polarity with respect to ground. Each monopolar side can operate on its own with ground return; however, if the current at the two poles is equal, each pole's ground current is cancelled to zero. In such cases, the ground path is used for short-term emergency operation when one pole is out of service. This configuration is mainly used with VSC technology.

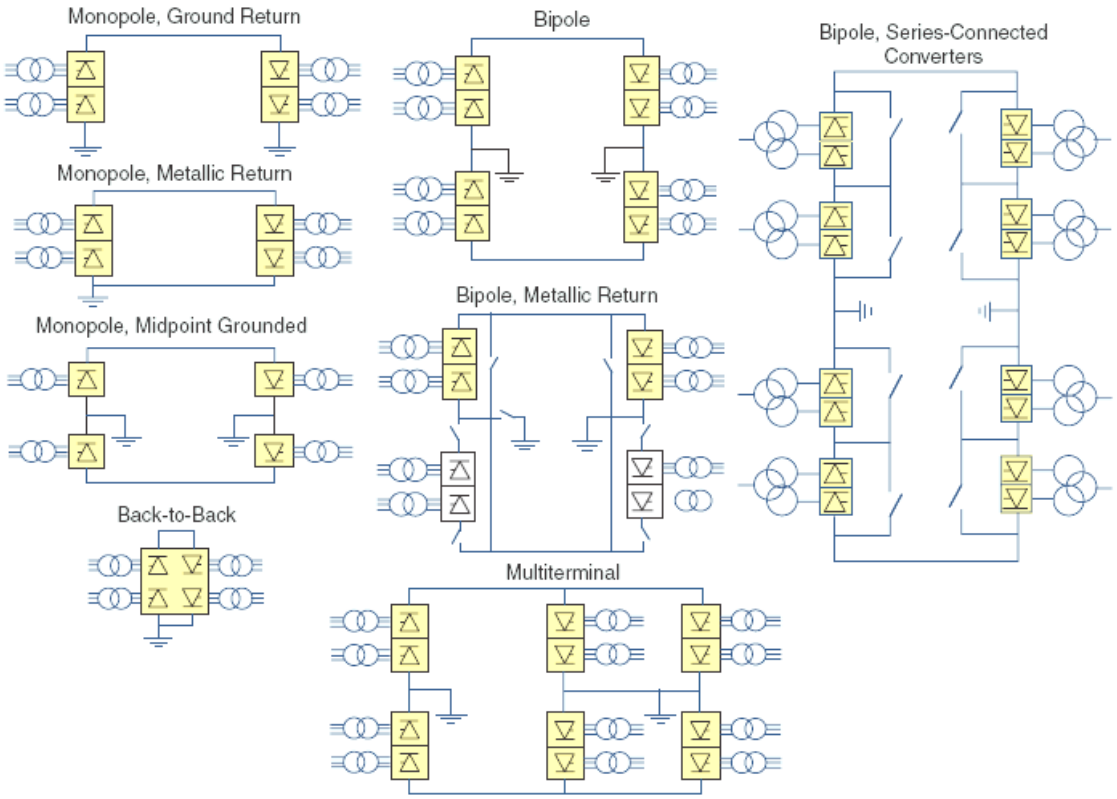

Figure 2-13: HVDC configurations and operating modes

2.5.1 BACK TO BACK HVDC SYSTEM

In this case, the two converter stations are located at the same site and there is no transmission of power with a DC link over a long distance. A block diagram of a back-to-back LCC-HVDC system with 12-pulse converters is shown in Figure 2-14. The two AC systems interconnected may have the same or different frequency (asynchronous interconnection).

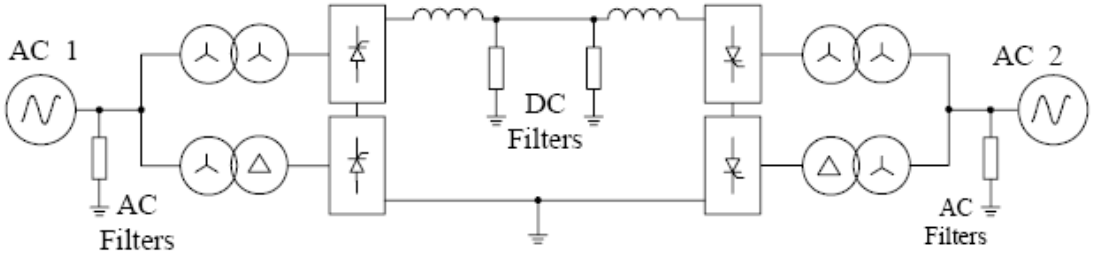

Figure 2-14: Back-to-back LCC-HVDC system with 12-pulse converters

2.5.2 MONOPOLAR CONFIGURATION

In this configuration, two converters are used which are separated by a single pole line and a positive or a negative DC voltage is used. Many of the cable transmissions with submarine connections use monopolar system. The ground is used to return current. Figure 2-15 shows a block diagram of a monopolar LCC-HVDC system with 12-pulse converters.

To reduce cable costs and cable losses it is possible to use two insulated DC cables in spite that it is a monopolar link. This makes the current small and the cable losses low but requires a higher converter voltage. This technology has been used for the NordNed connection between Norway and Netherlands. A scheme of such monopolar configuration with two cables is shown Figure 2-16.

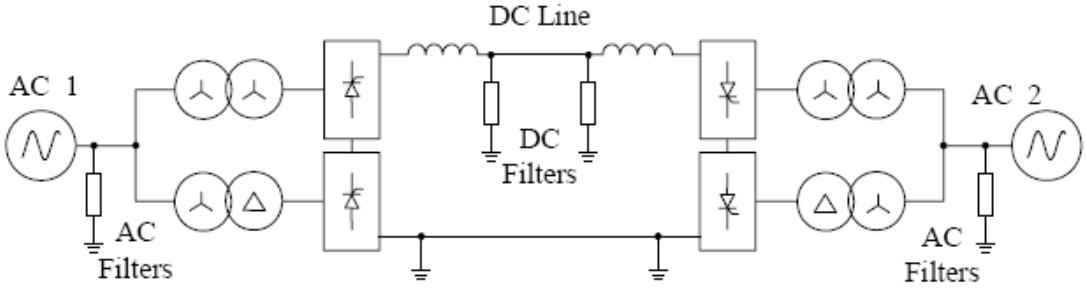

Figure 2-15: Monopolar LCC-HVDC system with 12-pulse converters and metallic return conductor.

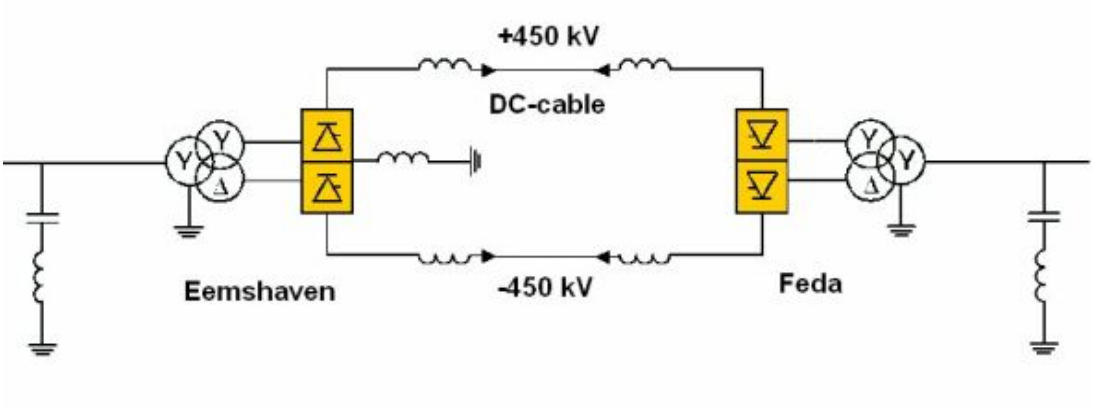

Figure 2-16: Monopolar LCC system with two cables (Norned link)

2.5.3 BIPOLAR CONFIGURATION

This is the most commonly used configuration of a VSC-HVDC system in applications. It utilizes a bipolar configuration with two independent poles, one at the positive voltage and the second at the negative voltage. In fact, the bipolar system is two monopolar systems.

The advantage of such system is that one pole can continue to transmit power in the case that the other one is out of service for whatever reason. In other words, each system can operate on its own as an independent system with the earth return. Since one is positive and one is negative, in case that both poles have equal currents. The ground reference is made at the midpoint in the DC link. The ground current is zero theoretically, or in practice within a 1% difference. The 12-pulse based bipolar LCC-HVDC system is depicted in Figure 2-17 .

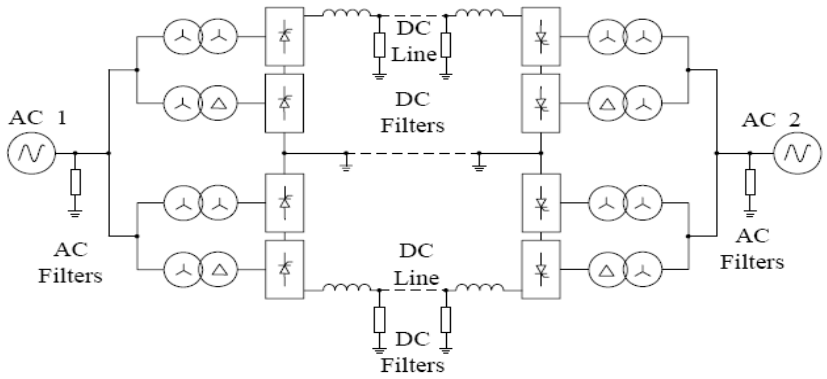

Figure 2-17: Bipolar LCC-HVDC system with one 12-pulse converter per pole

2.6 MULTITERMINAL HVDC

The multiterminal HVDC can use either conventional HVDC technology either the VSC technology. Currently, the largest multiterminal HVDC in service is set in Canada and USA.[20] The power is generated at the La Grande II hydro power station in the James Bay area (Quebec), converted into DC at the Radisson Converter Station, and transmitted over the multi-terminal system to load centers in Montreal and Boston. This line has 5 converter stations using conventional technology and DC power lines instead of cable. The power rating of each station is in a range of 1850-2250MW. The distance between the furthest stations is 1500km.

2.6.1 PRINCIPLE

There are two approaches for building this kind of system, either in parallel connection or either in series connection [21].In case of parallel connection the switching elements in the halfway tapping station(s) must be able to withstand the full line voltage and then the current that will flow through the tap will be proportional to the rated capacity of the line. In contrary for a series connection, the converter must be able to pass trough the full current.

The control approach for multiterminal HVDC will be slightly different from the two-terminal scheme where two type of control are possible. Either the DC voltage is kept constant whereas the current varies with power or the contrary; current is kept constant and the voltage varies with the drawback of line losses even at low load.

For the parallel scheme the constant voltage approach is the best suitable and can be implemented by VSC. For a tapping station with small power rating, it will be preferable to use a series connection because of the capability of the switching device to withstand the current.

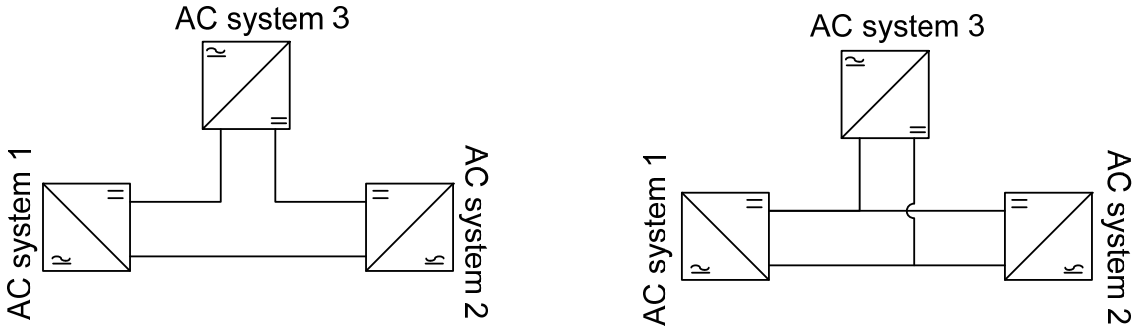

Figure 2-18: Multiterminal scheme with 3 converter stations in series (left) and in parallel (right)

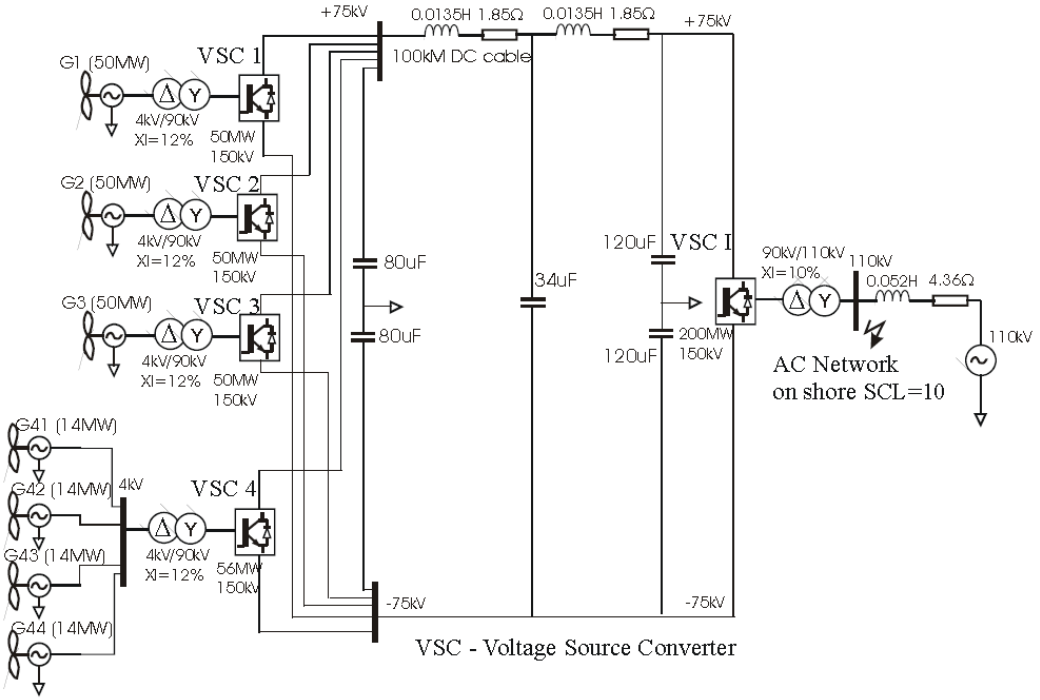

Figure 2-19: Example of connection of wind farm thanks to multiterminal HVDC.

The use of the multiterminal will be very useful in case of an offshore DC grid and for the interconnection of several offshore wind farms. An example of a system built for simulation of the connection of 200MW wind farm is represented next figure. Four 50 MW wind farms are connected in parallel, but the output power of a real system will be higher.

The major challenge for the multiterminal HVDC systems is the treatment of fault in the DC system. There is currently no DC circuit breaker available for high power rating. The usual protection strategy to de-energized the line is based on the use of the AC breaker and a fast control strategy of the converter. A point of concern is the energy stored in the DC cables, especially the case for VSC system where a large DC smoothing capacitor is applied. Some improvement has to be made on the fault treatment for DC line.

2.7 ADVANTAGE AND DRAWBACK OF EACH TECHNOLOGY

2.7.1 FOOTPRINT OF THE CONVERTER STATION

The size (volume, footprint) of VSC converter station is smaller than for LCC converter station. For example a 600MW LCC converter station requires about 14000 m^2 whereas a VSC HVDC needs only 3000m^2. This advantage opens new application for the HVDC transmission such as the supply of oil platform or the connection of large offshore wind farms to the main grid.
Such offshore converter will be very similar to another transformer platform or can be added to another existing offshore oil rig. Since 2004, the Troll A plat form in North Sea has been connected to the Norwegian main grid with this technology. The footprint of the converter station, housed in a pre-fabricate module is only 300m^2 for a rating power of 2x 40 MW.

Furthermore, converter transformers are significant parts in a converter station especially for the weight. The size of the converter may also be shrunk down by using gas insulating station (GIS). The converter reactors take a large volume inside the converter station. A picture of the future 400MW offshore station of Borkum (Germany) is shown next page [22].

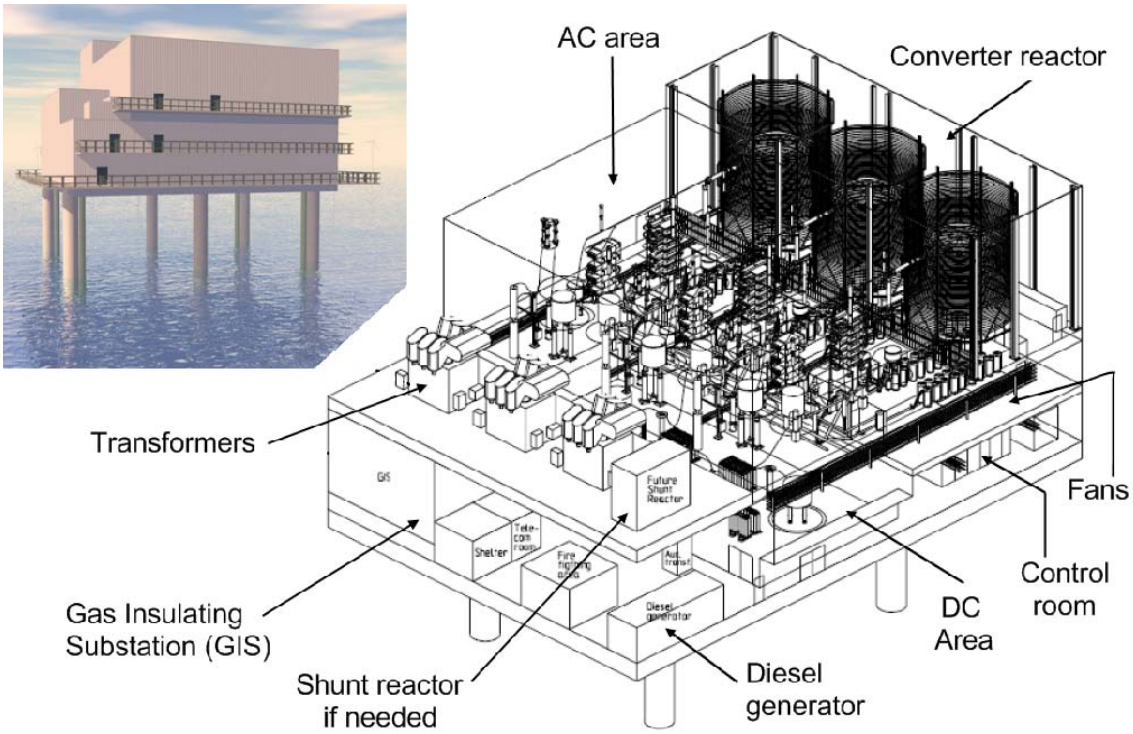

Figure 2-20: Picture and layout of the future offshore converter platform Nord E.ON1.

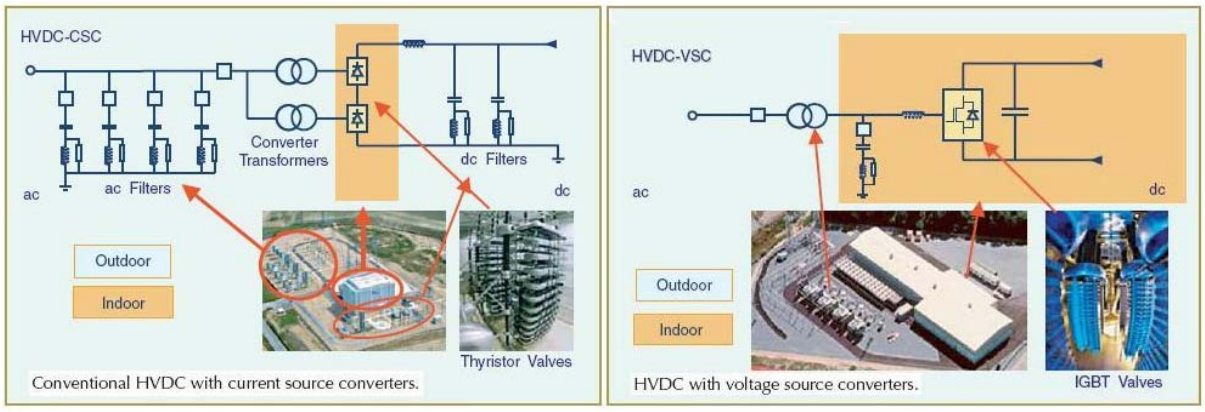

Figure 2-21: Conventional HVDC with LCC technology and VSC-HVDC

2.7.2 TRANSFORMERS

The VSC controller allows the use of normal transformer and thus it gives more flexibility to build and design the offshore station. Standard two-winding transformer design can be used.

2.7.3 REACTIVE POWER CONTROL & STABILITY

The VSC controller can control the reactive power and the voltage. So, it gives a serious advantage to the VSC technology in fault through capability and black start capability. The reactive control for the classical technology is done by capacitor bank (slow switching scheme), thus the flexibility is not good and a continuous control can not be done.

Voltage stability problems may also be experienced at the terminals of HVDC links used for either long distance or back-to-back applications. They are usually associated with the unfavorable reactive power "load" characteristics of the converters. The HVDC link control strategies have a very significant influence on such problems, since the active and reactive power at the AC/DC junction are determined by the controls.

Recent developments in HVDC technology (Voltage Source Converters) have significantly increased the limits for stable operation of HVDC links in weak systems as compared with the limits for conventional HVDC converter.

2.7.4 SUMMARY

The next table is a summary of the two main different technologies, LCC and VSC. It is shown the pros and the cons of each technology.[23]

	Conventional LCC HVDC	**VSC-HVDC type HVDC Ligth® or Plus®**
Size single range converter	150 - 1500MW	50 – 1100MW
Semiconductor technology	Thyristor	IGBT
Converter technology	Line commutated	Self commutated
Relative volume	4-6	1
Type of cable	Mass impregnated	Polymeric / Mass impregnated
Control of active power	Yes	Yes
Control of reactive power	No, only switching regulation	yes, continuous control
Voltage control	Limited	Extensive
Fault ride through	No	Yes
Black start capability	No	Yes
Minimum short circuit capability in AC grid	> 2x rated power	No required
Power reversal without interruption	No	Yes
Minimum DC power flow	5-10% of rated power	No minimum required
Typical losses per convertor	0,80 %	2%
Operating experience	>20 years	8 years
Operating experience offshore	No	Yes (Troll A)

Table 2-2: Properties of VSC and LCC technologies.

2.8 APPLICATIONS AND FUTURE

The area of application for the HVDC technology is very wide now:

- Long distance power transmission
- Underground and submarine transmission
- Interconnection between asynchronous networks
- Offshore transmission and power supply
- Power supply for large cities by underground cables
- Stabilization and reliability of a weak grid.

Power system reliability in the region is increased by adding new HVDC cable links. In the event of grid disruptions, the rapid power balancing ability of these links can be used to compensate for fluctuations in frequency and voltage. For example, it is technically feasible to reverse the entire 600 MW power throughput of the SwePol Link in just 1.3 seconds, although this is not a feature that will be used in practice.[24]

However the improvement of the HVDC technology is driven by the improvement in power electronics especially for the valves. The increase of the voltage and power transmitted by the power station is directly due to the improvement of the semi-conductor. The voltage and current ratings of thyristor and IGBT are increasing and the valve too. Finally the providers of HVDC converter try to reduce the losses in each type of valves. They also try to improve the IGBT technology in order to be equal in power and voltage rates with the thyristor technology. It is interesting to notice that the use of IGBT become more and more interesting. See Figure 2-22, the red curve. ABB with the *HVDC Light*® and Siemens with the *HVDC Plus*® try to improve the VSC technology up to 1500MW.

Recent developments in three other major fields: cable system, system design and HVDC control has opened the possibility to the increase the power rating of VSC based HVDC and greatly expand the area of application. To reduce the cost is also a challenge in order to be more competitive with AC transmission.[25]

The main promising application of the HVDC technology is the long distance bulk power transmission for remote resources such as large-scale wind farms or the supply of offshore platforms. An example of power transmission for offshore wind farm resources is shown Figure 3-6. Recently, in September 2007, the German utility E.ON Netz has awarded a contract to ABB to supply the power equipment that will integrate the world's largest offshore wind farm into the German grid. The Borkum2 wind farm consist of 80 wind generators of 5 MW located about 130 km from the coast in the North Sea. ABB is responsible for system engineering including design, supply and installation of the offshore converter, sea and land cable systems and the onshore converter. HVDC Light® will be used and the commissioning year of the whole system should be in 2010 [26].

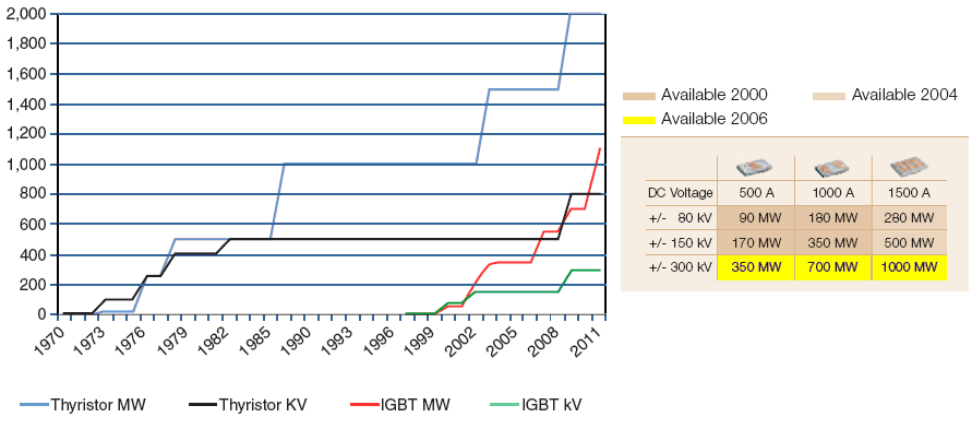

Figure 2-22: Voltage trend for the semi-conductors and improvement of IGBT module for HVDC Light®

3 HVDC TRANSMISSION & OFFSHORE WIND POWER

3.1 HVDC VERSUS HVAC

Two technology options are available for the transmission system for offshore: high-voltage AC (HVAC) and high-voltage DC (HVDC). The current consensus is that HVAC is the most economical option for distances shorter than 60 km. Between 60 and 80 km, HVAC and HVDC are expected to be similar in cost. The specificities of the project make the difference. Longer than 80 km, HVDC systems will likely be least costly, mainly because the capacity of a given HVAC cable drops off with distance due to the capacitive characteristics of the cable and their associated losses. The cost to balance the reactive power production by shunt reactor or other devices increases with the distance. DC transmission avoids these losses entirely, so it is the preferred technology for longer distances. However we can easily assume that in the next future this critical length will decrease with the improvement of the DC technology.

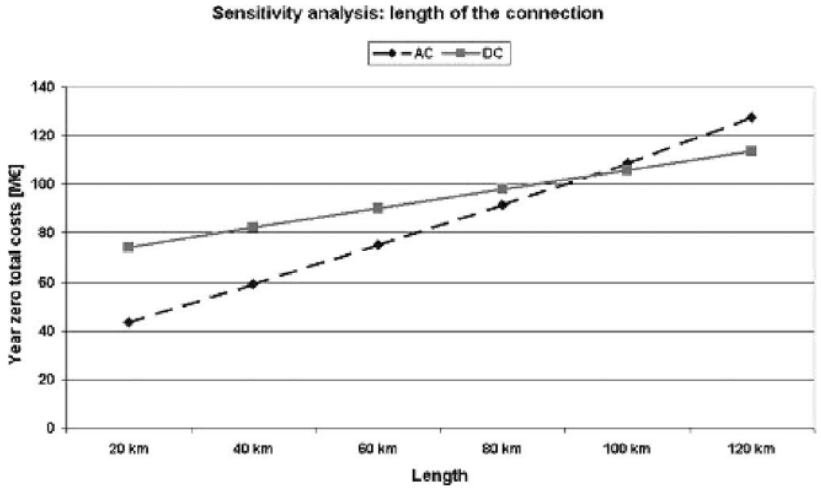

Figure 3-1: Break-even economic point of AC versus DC undersea transmission

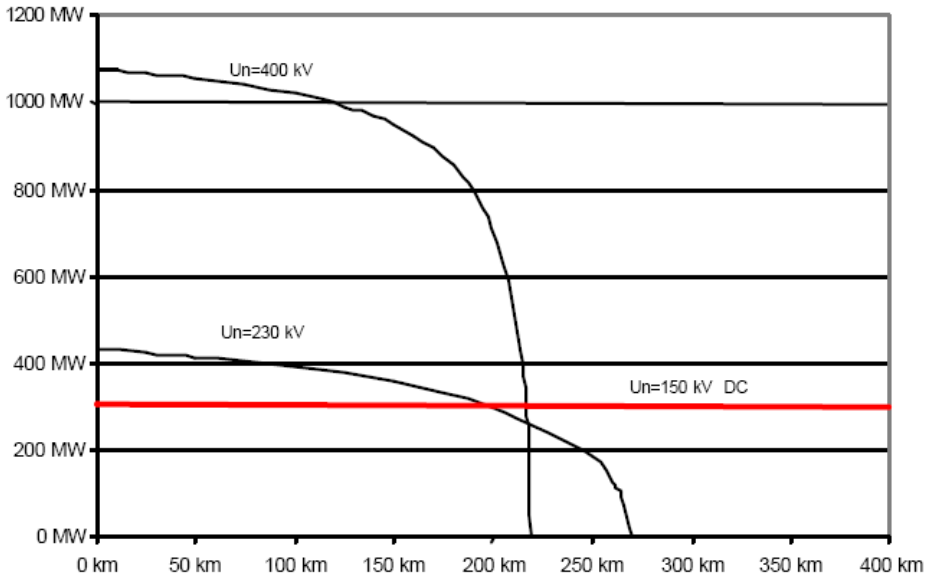

Figure 3-2: Critical length for AC and DC cable and for different voltages

For example the results of the sensitivity analyses for the 100-MW wind farm are presented in the chart above. It shows that when varying the length of the connection, a break-even point of costs for ac and dc transmission appears (at a distance of about 90 km from offshore wind farm to onshore substation).The following chart shows the power transfer capacity of AC cable and DC cable in red versus the length. Even if the AC cable can transfer more energy than a DC cable, the connection length is limited by the capacitive effect of the cable. There is no limited distance for a DC transmission in opposition to the AC cable because of no capacitive effect.

Up to 100km the AC transmission had too much losses and HVDC become better. The main inconvenient in the HVDC transmission is the price of the converter stations.

As said previously, with the cost of the converter station, the main problem is the treatment of the fault in high voltage DC system. Nowadays, the DC circuit breakers have very low rating power compare to the AC circuit breaker. Clearing a fault in a DC line is difficult because the current and the voltage never cross 0, so a strategy based on a fast control of the converter and using in the same time the AC circuit breaker.

3.2 GRID REQUIREMENTS FOR WIND POWER IN NORWAY

The grid code requirements specifies some issues such as the fault ride through, the frequency range, the reactive range capability and voltage control, etc… These rules are technical requirements that a plant must satisfy in order to be connected to the transmission system and to ensure the security of operation in the power system.

3.2.1 FREQUENCY AND OPERATION TIME

The Norwegian grid code [27] requires that the power plants (hydro, gas…) should be able to operate continuously between 49Hz and 52Hz. The more the frequency goes above or below certain limit the more the operation time decreases. Limits of operation time are between 45Hz and 47.5Hz for at least 20s and between 55Hz and 57Hz for at least 10s. For wind power, the frequency requirement is less strict; wind farms can operate continuously between 47.5Hz and 52Hz. The voltage should be between 0.9pu and 1.05pu. All the frequency and voltage requirements are summed up in the next table and chart.

Frequency [Hz]	Maximum operation time	
	Power plants	Wind farms
45 – 47.5	20s	20s
47.5 – 49	30 min	Continuously
49 – 52	Continuously	Continuously
52 – 53	30 min	30 min
53 – 55	20s	20s
55 – 57	10s	10s

Table 3-1: Operation time at different frequencies for power plants and wind farms.

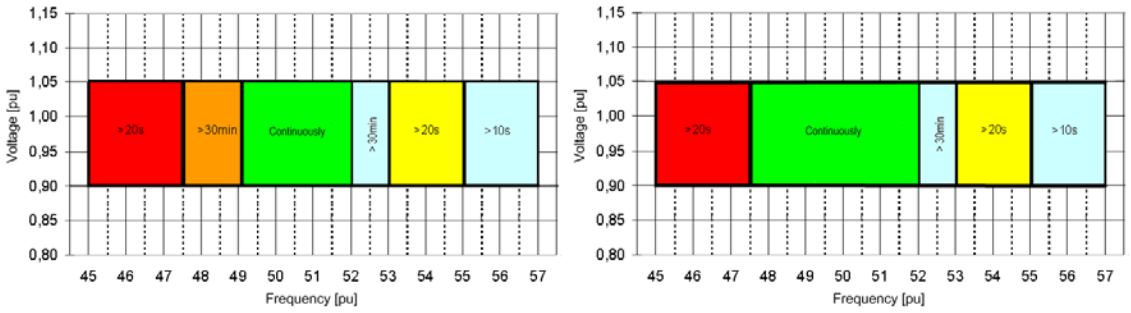

Figure 3-3: Frequency and voltage requirement for hydro and gas plants (left) and wind farms (right).

3.2.2 REACTIVE POWER CAPABILITY

For the active control of the wind farm, in normal operating conditions the wind turbine's current production is not limited to create a frequency reserve in the case of low frequency on the grid. The reactive power control and reactive capability are also different for wind power than for the other power plants. The reactive power capability of 0.95 power factor lagging to 0.95 power factor leading should be available at the output of the wind farm, instead of 0.91 power factor leading and lagging for the other power plants.

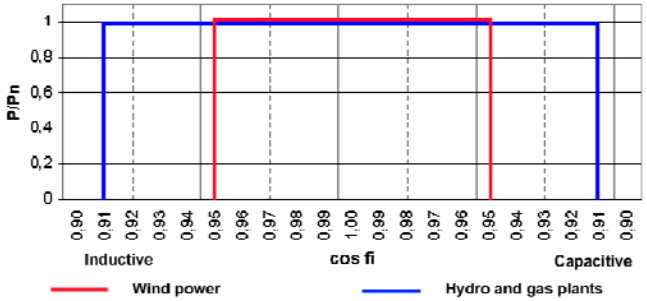

Figure 3-4: Reactive power capability for wind power and for other generation plants.

3.2.3 FAULT-RIDE-THROUGH REQUIREMENT

All the power plants should stay connected during the fault and contribute to the short circuit current. The plant must be able to deliver power and stay connected when the voltage is above a certain profile of the voltage at its connection point. It's the principle of the fault through capability.
The requirement for the fault through capability in Norway for power plants connected to the grid with a voltage superior of 200kV is the following:

- Voltage reduction to 0% during 150ms
- Voltage increase to 25%
- Linear voltage increase from 25% to 90% during 750 ms
- Constant voltage at 90%

For power plant connected at a voltage below 220kV the requirement is the following:

- Voltage reduction to 15% during 400ms
- Linear voltage increase from 15% to 85% during 600s
- Constant voltage at 85% until 10s
- Recovery voltage above 90% after

The fault-ride-through requirements are shown graphically.

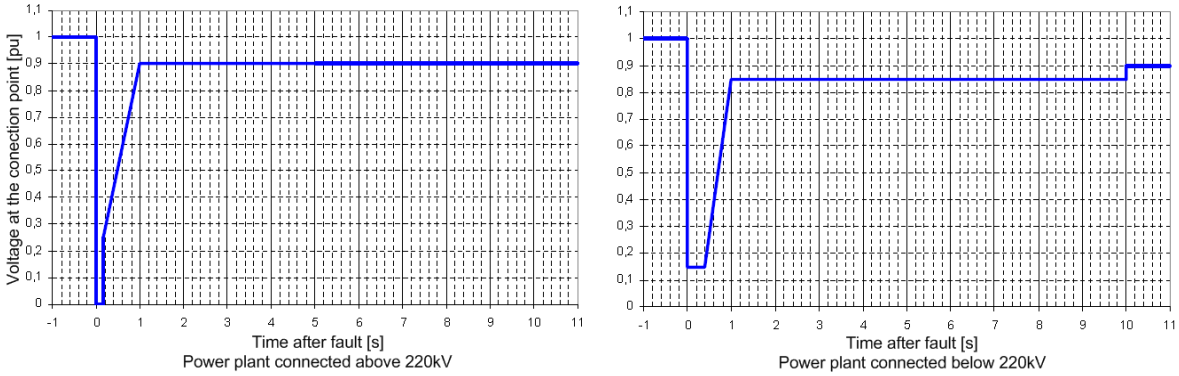

Figure 3-5: Fault-ride-through requirement for power plant above and below 220kV.

In our simulations, the reference will be the fault ride though requirement for plant connected above 220kV even if the wind farm are generally connected below this voltage. Furthermore, the voltage recovery will be more requiring; a wind farm able to success the test for connection above 220kV will able to success those for connection below 220kV.

3.3 VSC-HVDC FOR LARGE OFFSHORE WIND FARM OR CLUSTER

As said previously, a VSC-HVDC transmission is suitable and very efficient for the long distance bulk power transmission and for offshore connection. First, the footprint of the VSC converter and the solutions offered by the manufacturers (Siemens or ABB) with module pre-tested and in enclosure are real advantages. Secondly, the use of polymeric submarine cables will give more flexibility for the choice of the cable rout. Such transmission may transfer more than 1000MW. Then, the electrical properties of those converters allow the reinforcement of a weak grid by controlling the voltage and reactive power, to increase the electrical stability by playing the role of SVC when no power flows through. Thank to and the black start capability of the converter, such large offshore wind farm will be used as classical power plant in case of black out. So, in case of large wind farms or set in the high sea far from the coast, this solution will be the best.

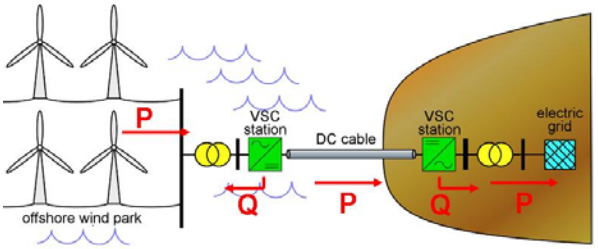

Figure 3-6: Example of connection of an offshore wind farm with HVDC-VSC technology.

3.3.1 ELECTRICAL LAYOUT

In the future, the wind turbines for such large offshore wind farm will be rated at 5MW. Only Re-power and Multibrid are currently selling such turbines on the offshore market. The Norwegian projects of floating turbine plan to use turbine rated at 5MW. So, the wind farm will comprise 200 turbines, several transformers to collect the power coming from the different row of turbines, all the protection devices and some emergency generators to supply the offshore platform in case of failure or problem. It is very important to have a redundancy of transformers and buses to ensure a better reliability of the entire wind farm.

According to the manufacturers and experience, even tough a failure is rare for a transformer, it can occur and the repair time is very long, several months. At the Nysted offshore wind farm, with only one main transformer, a major transformer failure led to an approximate 4.5 months outage of the entire wind farm. Even though they had a spare transformer winding and luck with available cranes, vessels, weather and personnel to fix the transformer, the outage time was as long as 4.5 months.
So for a wind farm rated at 1GW, 5 transformers rated at 200 or 250MVA might be used. Thus, in case of failure of one it might be possible to use the other trough connecting buses. It will result in a 25 % outage of the potential in the wind farm for several months or if over capacity had been chosen no outage will occur. The overcapacity of the transformer will lead to a better life of the transformer because loaded only at 80%. Those will be forced oil cooled transformers due to the large MVA rated.
In addition, the collecting bus must withstand an extra amount of power during failure and must also be oversized. Each transformer will collect power from 5 rows collecting each 40 MW with 8 turbines per row. The collecting cable inside the row will be rated in a range of 33kV to 72 kV depending of the power that should be collected. The connection between each end row might be studied to increase reliability in case of failure inside a turbine or on the collecting cable. So, if a fault occurs inside a row, it can be isolated and the power could flow through another row by connecting the rest of the turbine to it. A proposal electrical layout with redundancy is shown Figure 3-7.

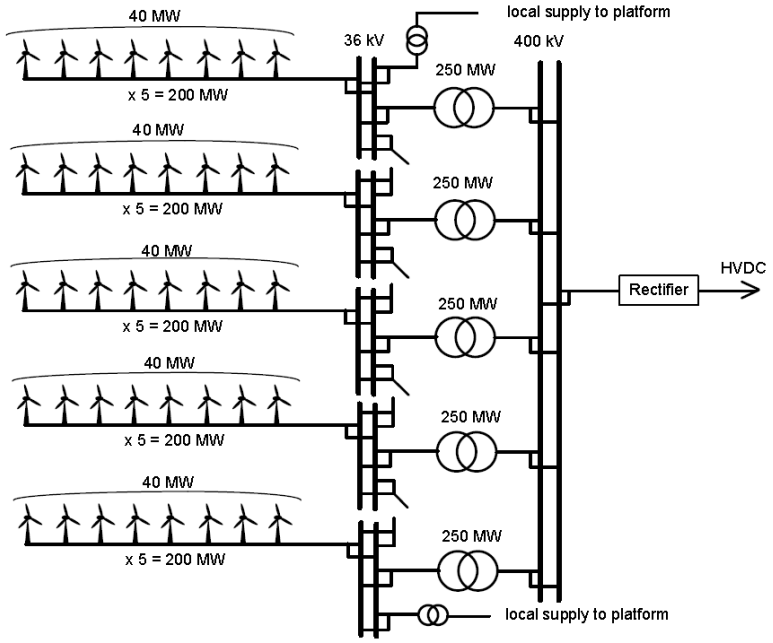

Figure 3-7: Proposal layout for large offshore wind farm with redundancy. Source Statkraft.

The rest of the substation in the offshore platform must be set in a gas insulated station (GIS) to shrink down the substation in order to gain maximum place and avoid salinity problem. The SF_6 is often used as the insulating gas due to its electrical properties. The drawback of using this technology is the risk of gas leak because of environmental concerns, especially on the greenhouse effect. The technology is now well known and the tightness of the enclosure is well achieved.

In case of cluster of wind farm, the links between each can be achieved either with HVAC if the distance is not long or by VSC-HVDC if the distance is superior to 60 km. An HVAC connection will lead to a creation of reactive power due to the capacitive effect of the submarine cables and shunt reactors have to be used to compensate and draw it. The reactive capability of the wind turbine may also be used if variable speed turbines are chosen.
The multiterminal HVDC technology can also be used to avoid problem with reactive power due to AC cable. It will be particulary suitable to link several will farm or in case of an offshore HVDC grid in the North Sea, which will link main grid and offshore wind farms.

During fault, whatever the HVDC scheme use, bipolar or multiterminal, the VSC converter may supply reactive power and during normal operation it can control the voltage and the offshore grid frequency. They will be part of the control and of the regulation of the AC grid inside the offshore wind farms and at the PCCs at the main grid.

3.3.2 GEOGRAPHIC LAYOUT OF AN OFFSHORE WIND FARM

The geographic layout of the large offshore wind farm had to give significant space between each of the 200 turbines to avoid wake turbulences but also to minimize the length of cables. If the turbines were spread over too wide an area to increase the efficiency of the farm, the cost of cabling would be very large. Generally, the spacing between each turbine is around 5-8 diameters. See in Table 1-1 presented in paragraph 1.1.1, the spacing between the turbines inside the constructed wind farms. Therefore, only a fairly concentrated group of turbines was considered. Ideally, all the wind turbines should be as close as possible to the transformer offshore platform in order to reduce the length of cables. This could be achieved simply by encircling the platform with a ring of turbines. The area of such wind farms is approximately 100km^2.

However, as the offshore platform must be accessible for supply vessels it would be impractical to completely surround the rig and increase the risk of a ship collision into a turbine. In case of prevailing wind direction only three sides of the platform can be arranged. The sea bed, rout of other cables or pipeline, strong streams must also be taken into account in the layout and can become constraint. Two examples of geographical layout are shown: Beatrice wind farm layout with prevailing wind direction, constraint and restriction on the placement of turbine, the second free of restriction with no prevailing wind.

Some economical studies have to be made in order to validate the benefit of the overcapacity of transformers and buses, the redundancy of bus and the oversizing of the collecting cables to allow connection to another row.

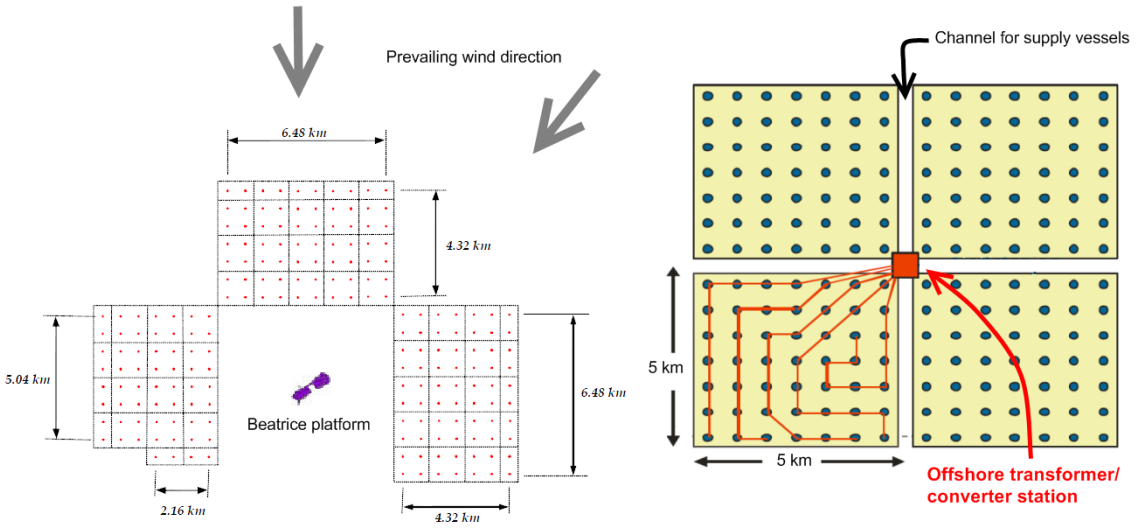

Figure 3-8: Proposal geographical layouts for 1 GW offshore wind farm.

4 CASES STUDIED & POWER SYSTEM STABILITY

4.1 CASES STUDIED

In this report, four cases will be studied and modeled. Static and dynamic simulation will be performed on them. For each case, a figure with the main data has been drawn to represent the offshore system modeled. The voltage is written in red whereas the bus numbers are in grey. Some data about the cable are also given.

- A connection to a unique 1GW wind farm by one VSC HVDC transmission rated at 1 GW. The MVA capacity of the DC transmission is 1140MVA with a DC cable length of 100km.

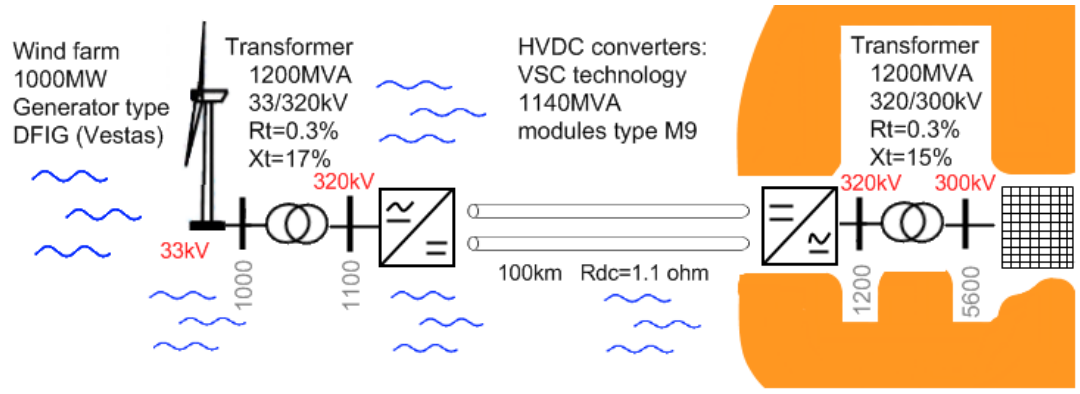

Figure 4-1: Case 1 studied, one 1GW wind farm and one HVDC transmission

- A cluster wind farm and oil rig is connected to the shore with a unique VSC-HVDC transmission. The offshore comprises wind farms rated at 500MW (1) and 400MW (2) and one of them supply an oil rig represented by a load (150MW and 50MVar). Wind farms are connected together with an AC grid with submarine cables.

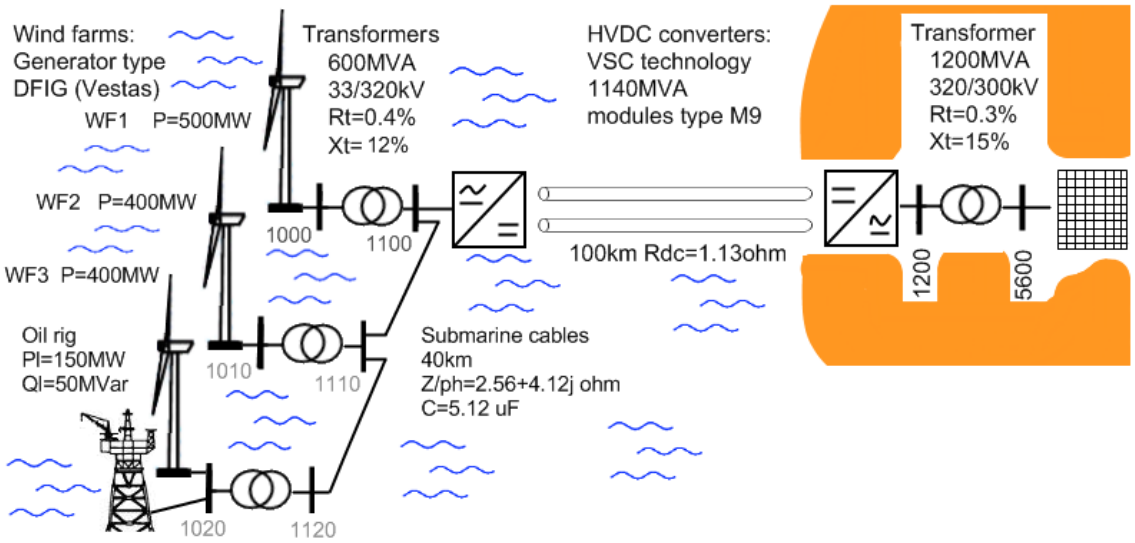

Figure 4-2: Case 2 studied, cluster of 3 wind farms and one HVDC transmission

- A unique wind farm connected to 2 VSC-HVDC transmissions rated at 500MW each with 2 PCC in the shore. The length of the transmissions are different, one is 100km whereas the second is 200km.

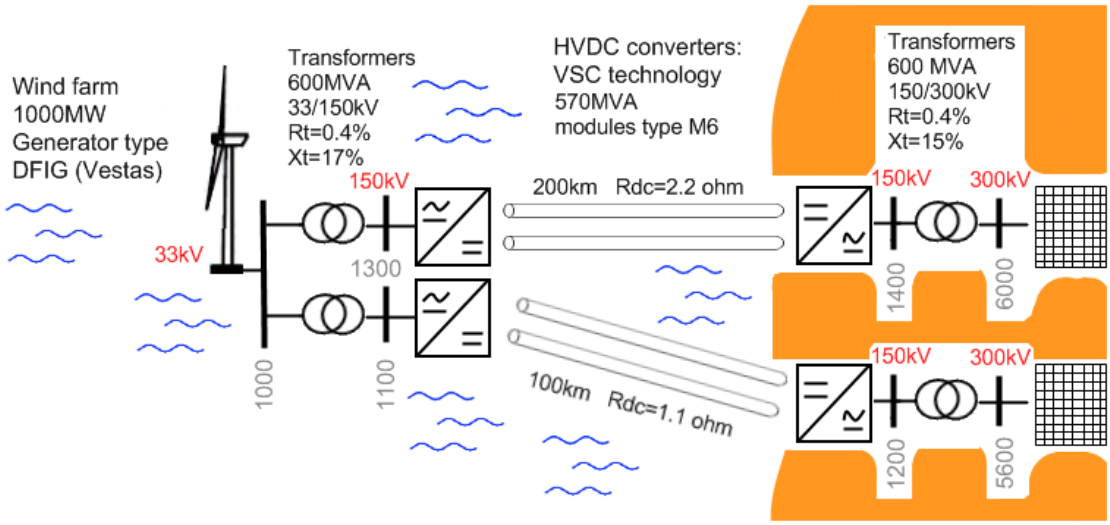

Figure 4-3: Case 3 studied, one 1 GW wind farm and 2 HVDC transmissions

- The same cluster wind farm as previous is connected to the shore with 2 VSC-HVDC transmissions rated at 500MW each. This could represent the HVDC links to the petroleum installation at the Ekofisk oil field and the wind farm planned in the surrounding. See above Figure 1-18.

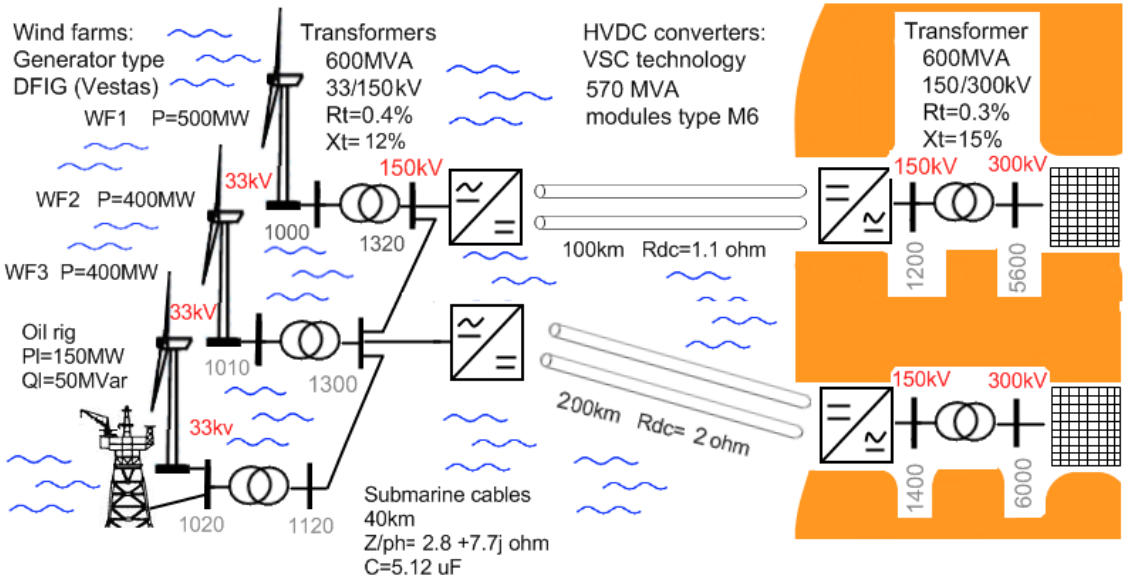

Figure 4-4: Case 4 studied, cluster of 3 wind farms and 2 HVDC transmissions.

Another option to link the wind farm would have been to link them with a multiterminal VSC-HVDC but no models were currently available in PSS/E. So, this project has been given up.

4.2 POWER SYSTEM STABILITY

The definition given by IEEE and the CIGRE is the following [28]:
"Power system stability is the ability of an electric power system, for a given initial operating condition, to regain a state of operating equilibrium after being subjected to a physical disturbance, with most system variables bounded so that practically the entire system remains intact."

Then, different kind of stability can be studied:
- The rotor angle stability
- The voltage stability
- The frequency stability

The rotor and the voltage stability can be analyzed according to large or small disturbances.
In this report the rotor angle stability will be not dealt with, but might be used for some explanations.

The definitions given by the CIGRE and IEEE are the followings:
- *Frequency stability refers to the ability of a power system to maintain steady frequency following a severe system upset resulting in a significant imbalance between generation and load. It depends on the ability to maintain/restore equilibrium between system generation and load.*
- *Voltage stability refers to the ability of a power system to maintain steady voltages at all buses in the system after being subjected to a disturbance from a given initial operating condition. It depends on the ability to maintain/restore equilibrium between load demand and load supply from the power system.*

The large or small disturbances on the voltage stability may lead to short or long-term phenomenon. Short-term voltage stability involves dynamics of fast acting components such as induction motors, HVDC converters or electronically controlled loads…The study period of interest is in the order of several seconds. Long-term voltage stability involves slower acting equipment such as tap-changing transformers, thermostatically controlled loads. The study period of interest may extend to several minutes. Thus, long-term simulations are required for analysis of system dynamic performance.

The term voltage collapse is used if an event or a sequence of events accompanying voltage instability leads to a blackout or abnormally low voltages in a significant part of the power system.

The power system stability will be analyzed in the next chapters. For each case, a load flow will be presented, only the voltage and the angle in the surrounding of the PCC will be analyzed. In addition, the voltage and the power given by the swing buses in Sweden will be given. Then some fault will be performed on the system: onshore faults, offshore faults in the bus or on the line between the wind farms. Comments on the plots will be also made.

All the faults performed are three phase faults with zero impedance.

4.3 POINT OF COMMON CONNECTION

There are some restrictions on the implantation of HVDC transmission to the main grid. The choice of the point of common connection must be studied. The AC grid must be strong enough to receive the power from the HVDC transmission and the mechanical inertia of the AC system has to be large enough to maintain the required voltage and frequency. Those recommendations are given by IEEE [29]

A normal parameter for measuring the strength at a busbar in an AC network is short-circuit power SC_{MVA}. This parameter depends on the fault current I_{Fault} [A], the nominal voltage at the bus V_{AC} [V] and the Thevenin impedance seen from the bus Z_{Th} [Ω]. The equation is given below:

$$SC_{MVA} = I_{Fault}.V_{AC} = \frac{V_{AC}^2}{Z_{Th}} \tag{4.1}$$

In our simulation, the choice of short circuit with zero impedance has been made. However, it does not imply that the Thevenin impedance is zero because it depends also from the AC system around: line, generator, transformer, etc… The closer a generator is located to a busbar, the more will it contribute to reducing the Thevenin impedance seen from the busbar. More lines connected to the busbar will also contribute to reducing the Thevenin impedance; hence also increase the short-circuit power.

In order to connect a HVDC link based on thyristor technology to an AC system, two requirements have to be fulfilled [9]. The short-circuit power has to be large enough compared to the power from the HVDC link. The short-circuit ratio (SCR) is calculated simply by doing the ratio between the short-circuit power at the connection point SC_{MVA} [MVA] and the rating of the HVDC link P_{HVDC} [MW]. The equation is given above:

$$SCR = \frac{SC_{MVA}}{P_{HVDC}} = \frac{V_{AC}^2}{Z_{Th}.P_{HVDC}} \tag{4.2}$$

In addition to a sufficient large SCR, the mechanical inertia of the AC system has to be large enough in order to maintain the required voltage and frequency. An effective inertia constant H_{dc} is defined as presented in .The inertia constant has to be above 3 for a HVDC transmission.

$$H_{DC} = \frac{Inertia\_AC\_sytem\_[MW.s]}{MW\_rating\_AC\_system} \tag{4.3}$$

This report doesn't deal with this value.

In Norway, there are 2 PCCs available for 1GW HVDC connection. It is situated in South West Norway at Feda and Kåstø. [30] The PCCs correspond to the bus 5600 (South west Norway) and 6000 (West Norway) in our grid model. See the following paragraphs.

The SCR has been calculated with PSS/E. See Appendix C - 1. The SC_{MVA} is 18000MWA at bus 5600 whereas at bus 6000 the SC_{MVA} is 26000MWA. Then the SCR can be deduced easily with a 1000MW HVDC transmission. The best PCC in the grid is the bus 6000. However in our simulations with a single HVDC transmission the PCC chosen is the bus 5600 because the south coast of Norway is the area where the integration of offshore wind power is the more probable due to the depth sea.

5 PSS/E MODELS

This chapter present the models used in the simulations. Several programs should have been used to perform the stationary and dynamical simulations of an electrical power system, such as Simpow, Eurostag and DIgSilent.

The choice of PSS/E (owned by Siemens) is simple. All the models needed for this work were available in the library of the software. It was also this used by the SINTEF, Statnett (the Norwegian TSO) and to a lesser extent Statkraft. So, it was an easiest way to be helped if any problem occurred or to get models. Some grid models for Norway or Nordic countries are available from the SINTEF, whereas an HVDC Light model is available from ABB. But this model was commercial available only for companies with confidential agreement.

First, a load flow analysis is done on the entire system and thus, the load flow data provides the initial conditions for the dynamic simulation of the model. Then, generators and load have to be converted as Norton equivalents. See Appendix D - 1. The conversion is based on recommendations from the SINTEF. Finally, the dynamic simulation can be performed after the conversion of load and generator.

5.1 IMPROVEMENT OF THE NORDIC MODEL

The electrical Nordic model has been given by the SINTEF. In this non detailed model of the NORDEL grid, Norway, Sweden, Denmark and Finland are represented by 37 buses. The model comprised 300kV and 420kV buses and one swing bus set in Sweden. A SVC (Static Var Compensator) to control the voltage during fault or dynamic simulation is set in Norway with a 22,5kV bus. The model is a 1000MVA system base. It has been decided to improve and change some characteristics of the model.

5.1.1 REPRESENTATION OF SKAGERRAK AND NORNED HVDC LINKS

Firstly, 2 links to represent the Norned and Skagerrak links has been added. According to the characteristic of classical HVDC compensated, the links were imitated by a simple HVAC link with any reactance and capacitance. A load is put at the end, the sign of the load representing the transfer of active power. Two new buses (8600 Denmark, 9100 Netherlands) and 2 branches (Norned from 9100 to 5600, Skaggerak from 5603 to 8600) have been added.

5.1.2 CREATION OF AREAS

Secondly, 4 areas have been created to obtain a better control of the production and the load within the system. The areas are the followings:

- Norway
- Sweden & Finland
- Netherlands & Denmark
- Offshore wind farm(s).

5.1.3 EXPORT SCENARIO FOR NORWAY

The load and production of the entire model have been changed to be in an export scenario for Norway, to be representative of peak consumption were Norway supply Sweden, Denmark and Netherland. More specifications are given in the Table 5-1. The transfer of active and reactive power is presented Figure 5-1.

	Initial model		Improved model	
	Production [MW]	**Load [MW]**	**Production [MW]**	**Load [MW]**
Norway	19214	14190	17500	14190
Sweden – Finland	24723	28137	26500	28137
Denmark - Netherland	1038	1526	1038	1526
Offshore wind farm(s)			0*	0**
* Power capacity may change with the simulation ≈1000MW ** For the last configuration, oil rig is modeled as load 150MW				

Table 5-1: Production and load per area in the model.

5.1.4 ORIGINAL LOAD FLOW CASE

The Nordel grid used is shown in the Appendix D - 2 in a large scale. Only the load flow case in the surrounding of the PCC will be analyzed. All the report from PSS/E can be found in the Appendix D - 3 4 5. From those reports the entire voltage and phase angle at each buses of the system fulfill the grid requirements. All the generators are in their reactive capabilities ($\cos \varphi < 0.9$) except the swing bus which has a power factor of 0.86. A low flow from the South-west of Norway is shown next page. The next table gives the bus voltage and the angle.

Bus number	Name	Voltage [pu]	Angle [°]	Pgen [MW]	Qgen [Mvar]
3300	SV-SW	1.000	0	4255	2558
5400	CNTR3 A	1.007	28.4	1679	109
5401	CNTR4 A	0.998	25.8		
5600	SOUTH 3A	1.010	22.2	2769	571
5601	SOUTH 4A	0.992	22.4		
5602	SOUTH 4B	0.969	17.1		
5603	SOUTH 3B	0.936	15.9		
6000	WEST 3	1.005	28.1	1194	-171
6001	WEST 4	1.000	27.3		
6100	NWEST 3	1.000	28.1	2481	742

Table 5-2: Original load flow in the surrounding of the PCC

A map with color gradient shows the voltage in the grid system. See Figure 5-3. The north of Norway gets a highest voltage whereas 2 areas in South East of Norway and Central Sweden have low voltage.

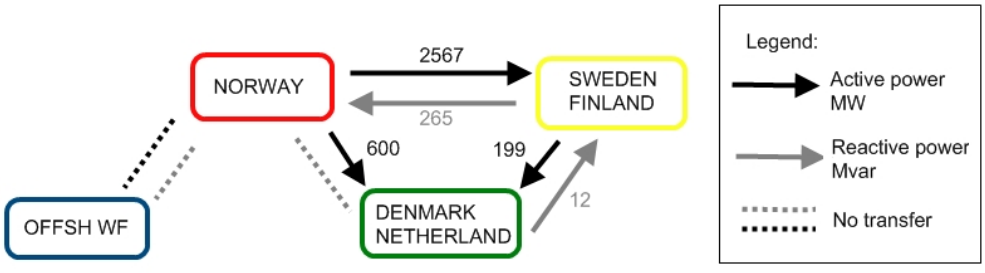

Figure 5-1: Transfer of active and reactive power between the areas

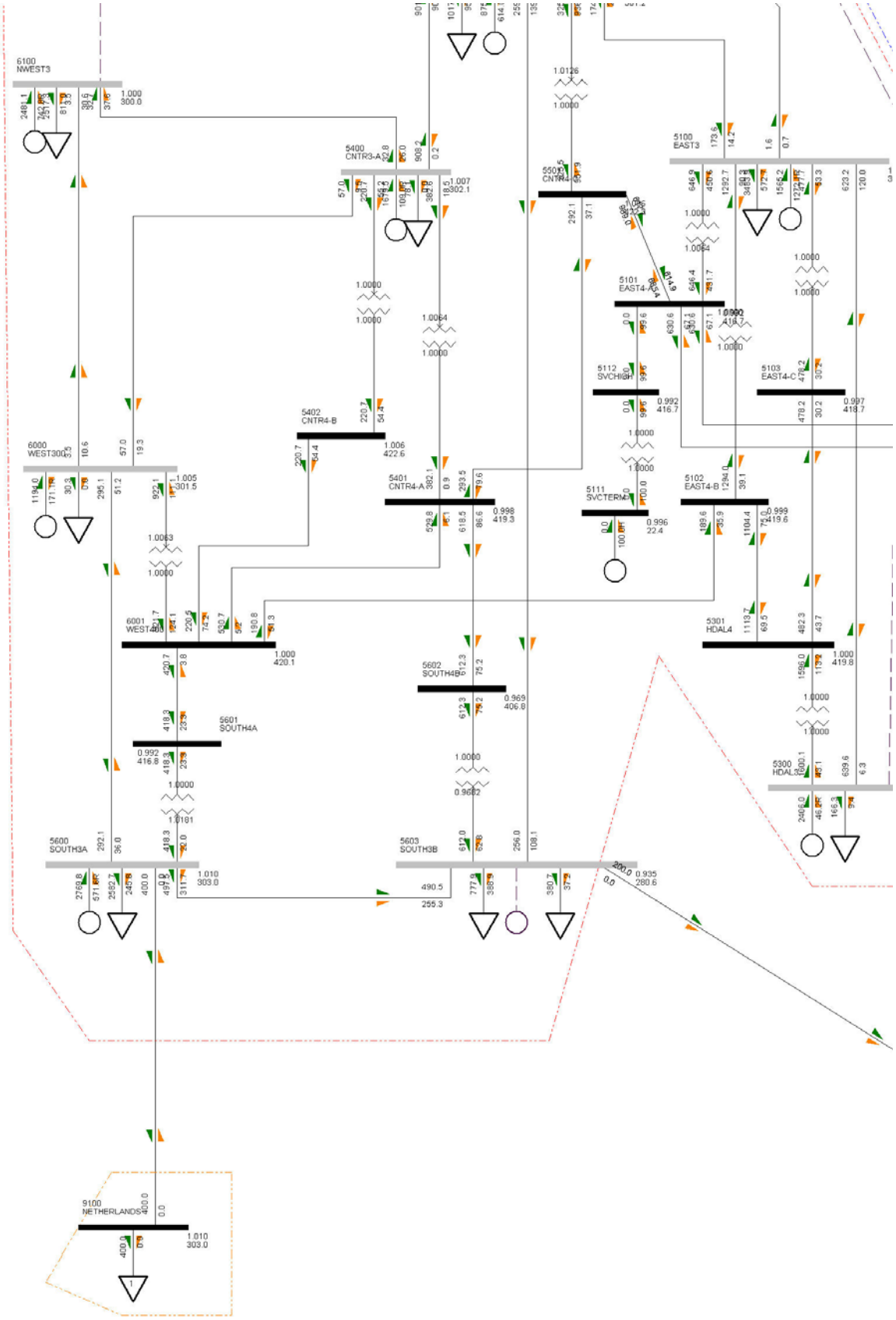

Figure 5-2: Picture of the load flow in south Norway

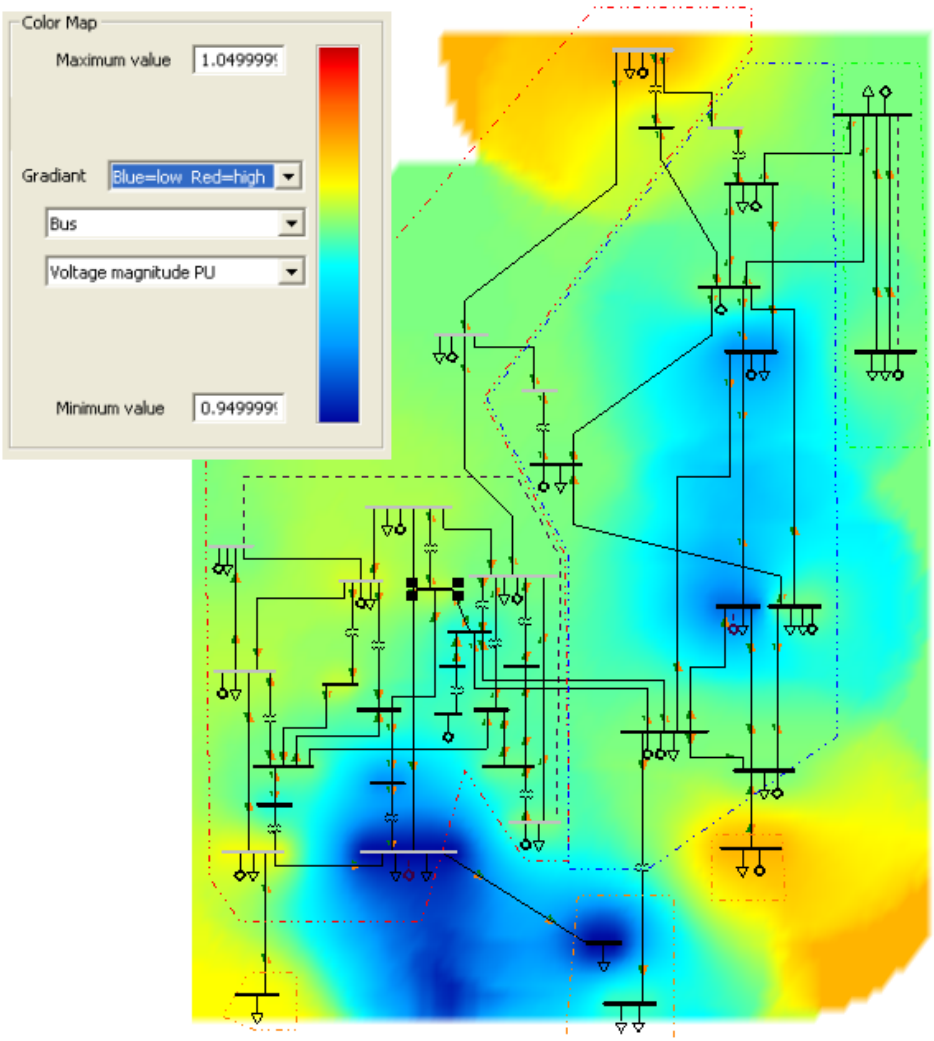

Figure 5-3: Gradient color map of the buses voltage, blue = low and red = high

5.1.5 DYNAMIC RESPONSE OF THE SYSTEM

The dynamic response of the system during a fault has been quickly analyzed. It has been observed that small oscillations in the active and reactive power produced by the generator occurred after clearing a fault. The similar phenomena occurred also for the rotor speed of the generators and the frequency of the system. They swung around the pre-fault value. Oscillations were undamped and sustained.

This problem has been investigated. By looking at the generator parameters, it appeared that one key parameter was missing in the dynamic parameter of each machine: The speed damping D. It gives an approximate representation of the damping effect contributed by the speed sensitivity of system loads. The value of D could range from near zero for systems with predominantly resistive load to approximately two for systems with a large percentage of loads with large inertia such as industrial load. [31] It has been assumed a mix of resistive and inertia load. The parameter has been put in a range from 0.8 to 1.2 for each generator. The SVC parameters have also been changed to improve the response of the system.

The different simulations and trials can be found from the Appendix D - 6 to the Appendix D - 11.

5.2 VSC-HVDC MODEL USED

Due to restriction on the access to the ABB model, this option has been given up. The files out from the Statkraft's server were automatically corrupted to avoid any exterior use. Although the VSC-HVDC model given in the PSS/E library has not the same control system for the converter than the HVDC Light model supply by ABB, it has been decided to use it. A comparison between the two models had already been done in Sweden by KTH (Royal Institute of Technologies) with the Gotland HVDC link. The study concluded that both models are similar for the load flow calculation, but their dynamic responses are slightly different, especially in the production of reactive and active power during a fault [32]. The analysis of the dynamic simulation should be done by taking into account this inconvenient and be treated with critical eyes.

5.2.1 HVDC LIGHT®

The configuration of the VSC-HVDC models has been made from the data given by ABB on their converters. For the simulation, 2 different converters have been used to model 1000MW and 500MW HVDC transmissions. According to the existing technologies, converters types M6 with a DC voltage set at 150kV and M9 with a DC voltage set at 300kV has been modeled. The data are given by the table extracted in the ABB documentation on the HVDC Light® technology.

HVDC Light® modules		Currents [A]		
		627 (2 sub)	1233 (4 sub)	1881 (6 sub)
Voltage [kV]	±80	M1 = 101MVA	M2 =199MVA	M3 = 304MVA
	±150	M4 = 190MVA	M5 = 373MVA	M6 = 570MVA
	±320	M7 = 380MVA	M8 = 747MVA	M9 = 1140MVA

Modules	DC voltage	DC current	Base power**	Sending power	Receiving power [MW]					
Types	kV	A	MVA	MW	B-to-B*	50km	100km	200km	400km	800km
M6	150	1881	570	574	555	552	549	544	533	
M9	320	1881	1140	1224	1184	1181	1178	1172	1161	1137
* Back-to-Back configuration										
** Used to calculate the data given in pu, P/Q diagram explains why base power > sending power										

Table 5-3: HVDC Light® modules with their characteristics: voltage, current and based power.

According to ABB, the converter can be modeled in power flow as a simple generator with capacitor representing all filters [33]. The limits of converter are set according to the limit of the VSC converter. The operating area is given in Figure 5-4.

In the literature, the common losses for a VSC converter are around 3-5% of the rated power. Converter losses have also been calculated from the data given by ABB. Two parameters must be filled in the PSS/E model, a fixed loss and one depending on the current.

The sending power and the power at the receiving end are given for each module. By using the back-to-back configuration, the loss for 2 converters can be found by subtraction.

$$P_{Loss/conv} = P_{Sending} - P_{Back-to-Back} \tag{5.1}$$

The loss parameter depending on the ampacity is found by using the 3 different modules rated at same voltage but with a different ampacity. Here is presented the method to calculate the losses for the 320KV DC transmission. The losses in function of the ampacity are plotted on Figure 5-5 for the module M7, M8 and M9. The steepness will give the losses depending on the current for 2 converters and the fixed losses for 2 converters in given at the intersection of the linear trend line and the vertical axis.

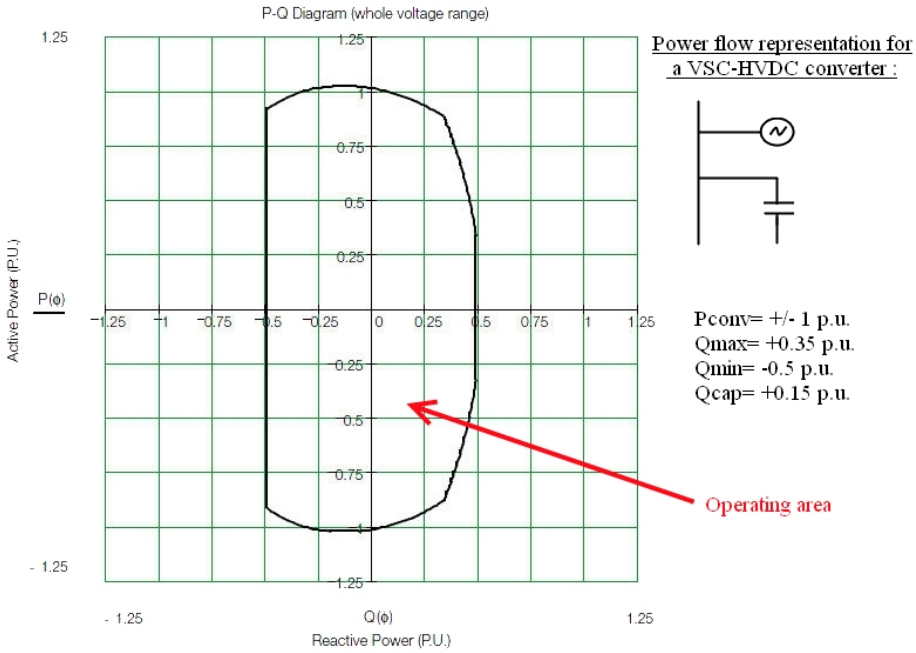

Figure 5-4: Typical P/G diagram for an HVDC Light converter.

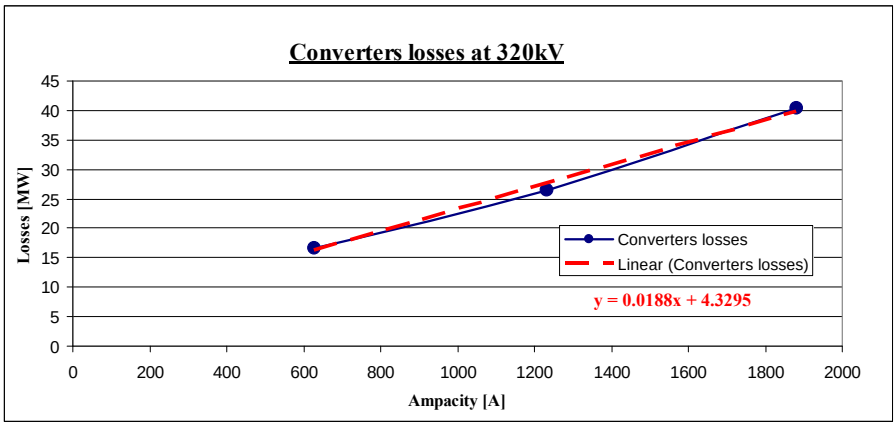

Figure 5-5: Plot of the converter losses at 320kV, modules M7, M8 and M9

So, from the plot and the linear trendline equation, the value for the fixed losses are 4,33MW for 2 converters and 18kW/A for both converter. So, for a single converter, the fixed losses are 2150kW and the losses depending on the current are 9kW/A. Similar process has been used to find the losses for the DC line rated at 150kV. However, the real values have been found and were very close to those found but they have not been used[2]. Differences are mainly for the parameter B, because the current at the receiving end is lower than at the sending end. Assumption that current was the same has been made with this method. A table presents the experimental and the real value of the loss parameters.

Parameter	Transmission rated at 320kV		Transmission rated at 150kV	
	Found	Real	Found	Real
A [kW]	2150	2280	1090	1140
B [kW/A]	9	7.5	5	3.7

Table 5-4: Loss parameters for the VSC-HVDC converter in load flow analysis

[2] They have been found at the end of the thesis and could not have been used because of missing time to do the simulations again.

5.2.2 CONSTRUCTION OF THE HVDC LIGHT MODEL

A VSC-HVDC Light is given in the PSS/E library but some of the parameter are not in agreement with the module chosen and thus have been changed. The load flow model can be easily modeled and parameters easy to fill according to the data given by ABB.

A capacitor bank is put at each converter bus to represent all the filters and the snubber capacitors in the converter as said above (Q_{cap}=0.15p.u.). In the user manual, it is explicitly written that the filter has to be modeled. "*AC filters corresponding to a VSC can be modeled as fixed or switched capacitive shunt at the ac bus to which the VSC is connected*"[34] The choice of fixed capacitive shunt has been made because no dynamic models were needed afterwards.

The transformer is not included in the model and has to be modeled. "*Any transformer associated with the VSC DC line should be modeled by an explicit transformer record in the PSS™E power flow data*". The transformer parameters are given below.

The next figure shows a VSC HVDC line on PSS/E. The converters are connected at bus 1100 and 1200. They are represented by the "black diode" on the line; the filters are represented by the fixed capacitors. The arrows show the transfer of active power in green and reactive power in orange. The transformers are also visible to link the converter to the wind farm or to the grid.

The DC line comprises 2 converters; one has to control the active power flowing at one end whereas the second must control the voltage. In steady state, the user can chose either a voltage control of the bus or a power factor control. Simulations have been made with both controls. In voltage control mode, the user can chose the percent Mvar required to hold the voltage at the controlled bus that has to be contributed by the VSC converter.

Then, the total DC resistance must also be filled, as well as the converter losses (fixed and dependent of the current flowing).

Finally the MVA capacity must be filled. For the simulations, 2 types of converter have been used rated at 570MVA and 1140MVA.

In dynamic mode, the parameters used were given by the user's manual. [35] Some of them have been changed because not in agreement with the grid or the system. Thus, the reactive power limits of the converter have been changed according to the MVA rating. The reactance (converter reactor) and the voltage maximal have also been slightly changed.

A table with the parameter is given in Appendix D - 12.

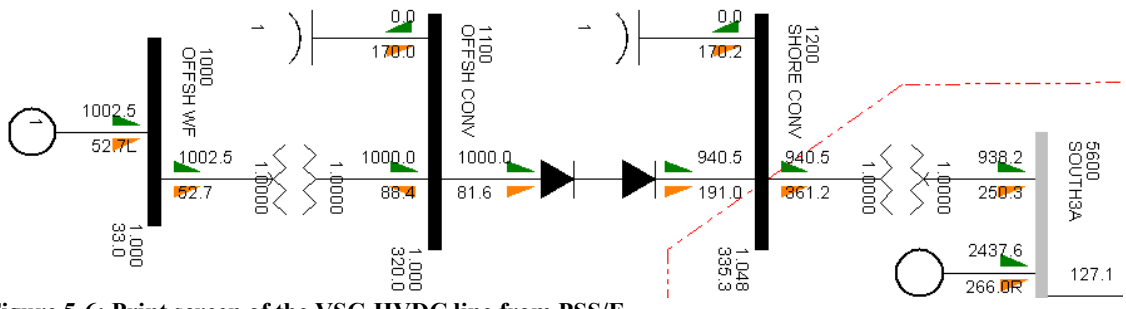

Figure 5-6: Print screen of the VSC-HVDC line from PSS/E

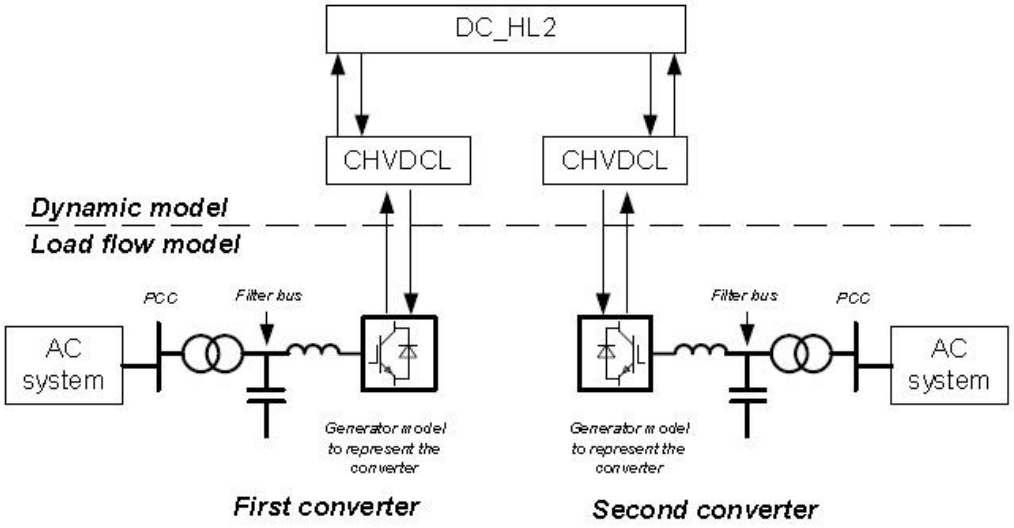

Figure 5-7: HVDC Light model in PSS/E library

5.3 WIND TURBINES MODEL USED

For short circuit studies, the representation of a wind turbine generator depends on the specific generator technology. Generally the turbine representation must include all parts that will contribute to the short circuit current for a fault in the vicinity of a wind turbine generator. For fixed speed induction generators the machine itself can be modeled to represent a wind turbine generator. For variable speed DFIG, the machine must be modeled and the smaller partial load converters can generally be neglected. For variable speed induction generator with full load converter, the wind turbine generator is decoupled from the AC network therefore only the converter can be modeled to simulate the short circuit behavior of the wind turbine generator. But this configuration will not be studied in this report:

The wind turbines in the simulation are modeled by a unique conventional induction generator. The PSS/E modeled is called CIMTR3. This model is suitable for shared use in regional models such as that used. CIMTR3 represent a single-cage or double-cage induction generator with rotor flux transients. This model is more accurate for large frequency deviation. It can also represent a DFIG by assuming that the control on the rotor introduces inertia in the response of the machine during disturbance [36].

The dynamic data for the generator are those used to simulate a turbine Vestas V-82 [37] or a Bonus 2.3MW (Source SINTEF). Although those turbines are rated around 2MW, it will be representative of the dynamic behavior of a wind turbine even rated at 5MW. The dynamic data are given in Appendix D - 13. The Bonus is a fixed speed turbine (classical asynchronous induction generator) whereas the Vestas is a variable speed turbine (DFIG). So, the main difference between both is the value of the inertia H is set at 2 for the Bonus and 5.3 for the Vestas.

The induction generator operates at rotational speed given (proportional) by the grid frequency. They also consume reactive power to magnetize the stator and the reactor. In the simulation, the power factor will close to 1 by assuming all the reactive power created in the wind farm by the subsea cable is compensated. To fill the Norwegian grid code and requirement (cos φ = 0.95), the minimum and reactive power supplied or absorbed by the farm is calculated by the relation below.

$$Q_{Min/Max} = \pm P.\tan(arc\cos(0.95)) \quad (5.2)$$

For the case of a unique 1 GW wind farm, it will be assumed that all the reactive power created inside the wind farm by the submarine cable is compensated by shunt reactors or by other devices. So, cos(φ) will be equal to 1.

The reactive capability of the turbines will be used to balance a part of the reactive power created by the submarine cables. Thus, the model of turbine used in such kind of cluster has to be chosen carefully: variable speed with DFIG or variable speed with full-scale frequency converter. Otherwise some compensated devices have to be used if another turbine type is chosen (fixed speed turbine) or if the turbines don't have enough reactive power capability.

5.4 MISCELLANEOUS

Other electrical systems have been used and have also necessitated some calculations of parameters.

5.4.1 AC SUBMARINE CABLES

Different types of cable have been modeled depending on the purpose. In the cluster wind farm, a cable rated at 320kV and able to transmit 550 MW is used for the connection between the offshore platforms. For the cluster connected with 2 HVDC transmissions, a cable rated at 150kV has been chosen because less power was transmit into the submarine cables. All the data are given per phase and per km in the table below [38].The length of the cable will determine the value of each parameter.

Voltage [kV]	Power [MW]	1/3 core	R [Ω/km]	X [Ω/km]	C [μF/km]
320	550	1	0.064	0.103	0.13
150	300	1	0.070	0.110	0.13

Table 5-5: Data cable used inside the cluster wind farm. Source ABB and Nexans.

5.4.2 STATIC VAR COMPENSATOR

Flexible AC Transmission System (FACTS) can provide voltage and reactive power control. Several types of FACTS exist but the Static Var Compensator is the most widely installed FACTS equipment in the grid. It mimics a variable shunt susceptance and uses fast thyristor controller. It adjusts its value automatically in response to changes in the network. Thus, it has the ability to draw either capacitive or inductive current from the network.

Only the SVC has been used for the dynamic simulation. A SVC model is available in the PSS/E library: CSVGN5. This model is used to control the main grid voltage during dynamic simulation. It has also been used to solve stability problem on the offshore grid with fixed speed generator. See Appendix D - 6 for the dynamic parameter of the SVC.

Another FACTS could also have been used, the STATCOM which consist of two-level VSC with a DC energy storage device, a coupling transformer connected in a shunt with the AC system and the associated control circuit. In contrary to the SVC, the STATCOM can provide both active and reactive power. It was available in the PSS/E library.

The operating mode of the devices to control the voltage at a wind farm is shown. A wind farm and a load are represented with a line to transmit power to a transformer link at a PCC. The voltage at the PCC can be adjusted thanks to the SVC or the STACOM. The equation is shown below each scheme.

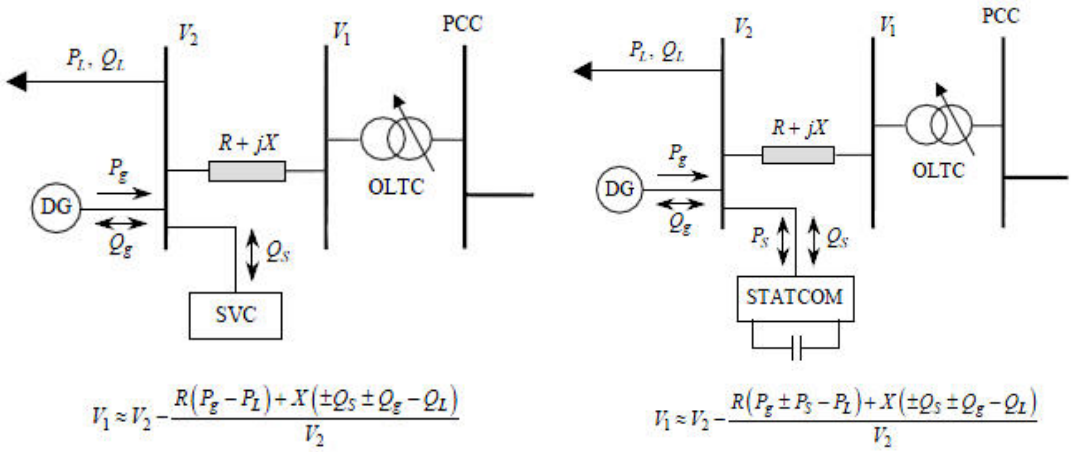

Figure 5-8: Operating mode of a SVC and a STACOM for wind power application.

5.4.3 TRANSFORMERS

As said previously, in case of large wind farms several transformers with a rated capacity in a range of 200 and 300MVA will be put in parallel for reliability and feasibility reason. It is explained in the paragraph 3.3.1. In our simulation this has been represented by a single transformer because fault applied on transformers was not the purpose of this report. Two types of offshore transformers have been added to the model rated at 1200 MVA or rated at 600MVA. The choice of two-winding transformer with a voltage control on one bus has been made. The resistance and reactance are in pu on system MVA base and winding voltage based. For this size of transformer, the rated voltage impedance was assumed to be in a range of 12-17%.

MVA rated	Low/high voltage [kV]	Rt [%]	Rated Voltage impedance Xt [%]	Place	R [pu] Based 1GVA	X [pu] Based 1GVA
600	150/300	0.4	15	Shore	0.0066	0.25
600	33/320	0.4	12	Offshore	0.0066	0.20
600	33/150	0.4	12	Offshore	0.0066	0.20
1200	33/320	0.3	17	Offshore	0.0025	0.14
1200	300/320	0.3	15	Shore	0.0025	0.12

Table 5-6: Parameter for two windings transformer used

.

6 SIMULATION: CONNECTION OF LARGE WIND FARM WITH A SINGLE HVDC TRANSMISSION

A large wind farm is connected with VSC HVDC transmission to the bus 5600 in south-west Norway. The length of the transmission is 100 km. The generators of the wind farm are DFIG type and thus the parameter of the Vestas turbine is used. According to the balance between wind power and hydro, the connection of the wind farm while producing will reduce the consumption in Norway, especially in the PCC. So, production of the generator at bus 5600 is reduced of 350MW and the rest of the wind. Then, the rest of the production in Norway is reduced by 400MW, distributed to the other Norwegian generator. So, an amount of 250MW is added to the system which is compensated by the SWING bus. Thus the swing buses in Sweden must only supply 4000MW instead of 4250 MW. The locations of the fault are shown in Figure 6-2 with a red lightning

6.1 LOAD FLOW CASE

Three new buses are added to the system, buses 1100 and 1200 represent the converter offshore and onshore whereas the bus 1000 represent the offshore wind farm. The voltage in the system is unchanged, only the bus angles are changed. The power factor of the generator at the swing bus is still the same with a power factor of 0.86 corresponding to an angle of 30°.

Bus number	Name	Voltage [pu]	Angle [°]	Δ Angle [°]	Pgen [MW]	Qgen [Mvar]
3300	SV-SW	1.000	0	0	3988.5	2333.8
5400	CNTR3 A	1.007	33.3	4.9	1637.5	122.94
5401	CNTR4 A	0.998	30.9	5.1		
5600	SOUTH 3A	1.010	30.9	8.7	2437.6	266.0
5601	SOUTH 4A	0.992	31	8.6		
5602	SOUTH 4B	0.969	23.3	6.2		
5603	SOUTH 3B	0.936	22.3	6.4		
6000	WEST 3	1.005	33.5	5.4	1164.2	-182.8
6001	WEST 4	1.000	32.7	5.4		
6100	NWEST 3	1.000	32.8	4.7	2419.2	749.0
1000	OFFSH WF	1.000	0			
1100	OFFSH CONV	1.000	-8.1			
1200	SHORE CONV	1.048	37		1002.5	52.7

Table 6-1: Load flow in the surrounding of the PCC and at the offshore wind farm.

All the bus and machine data are given in Appendix E - 1 and Appendix E - 2.The exchange of power between the areas is also changed and is presented in the next figure. The south grid of Norway with the HVDC transmission and the wind farm are shown in the next page. All the flows of power in the system are shown with the arrows (green for active power and orange for reactive power).

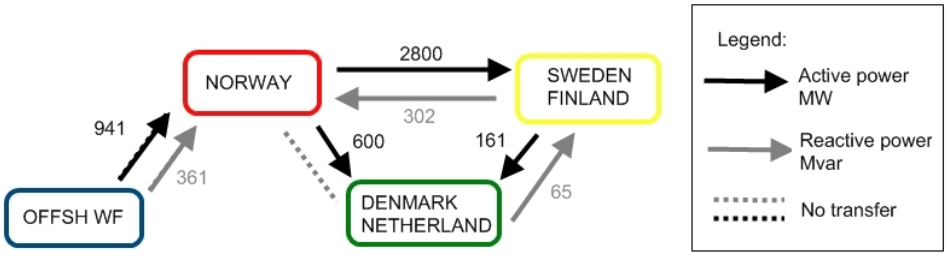

Figure 6-1: Exchange of active and reactive power between the areas

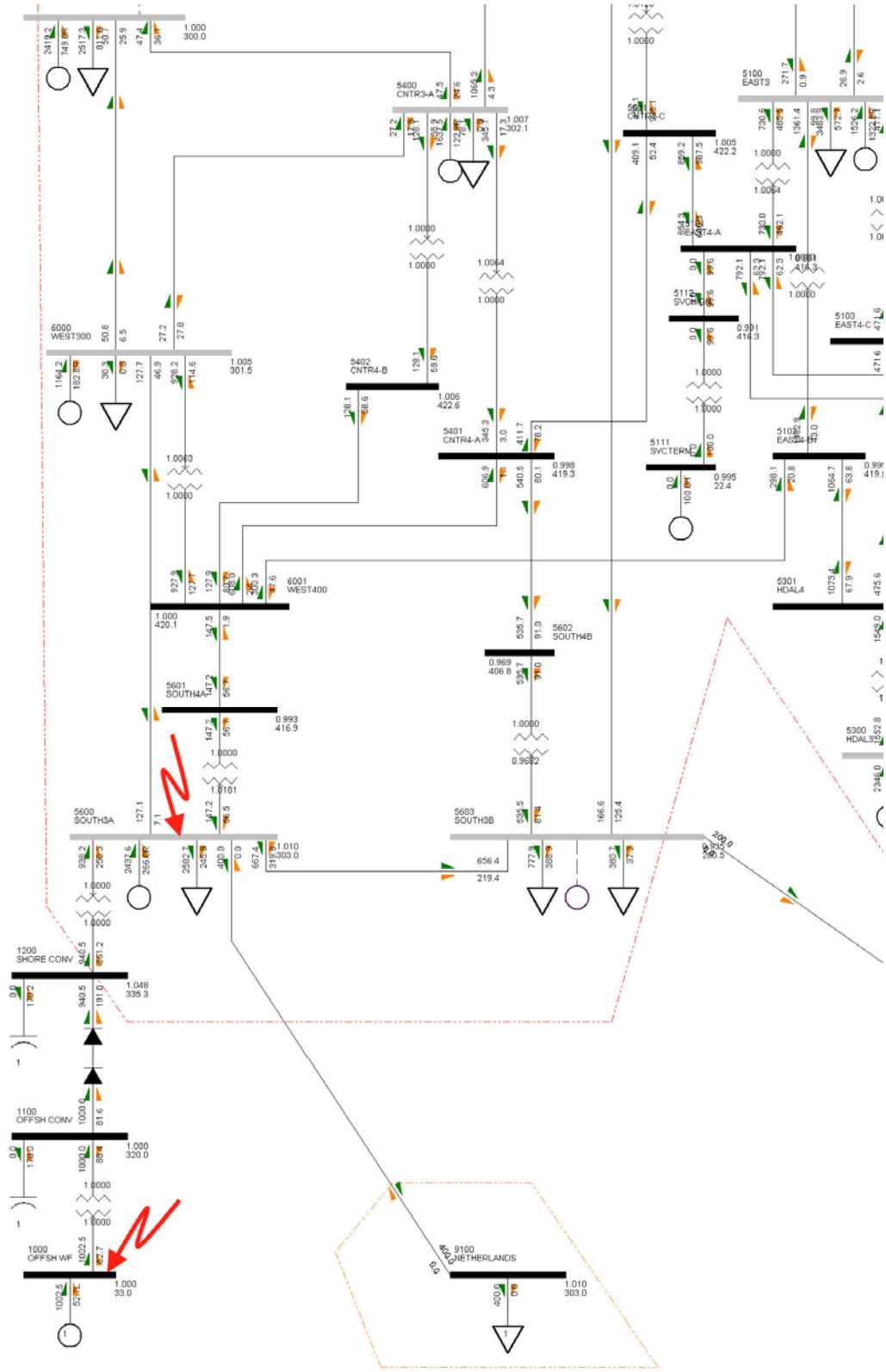

Figure 6-2: Load flow in South Norway, VSC HVDC transmission is set at the bottom, left side

6.2 ONSHORE FAULT ON PCC & VSC IN PF CONTROL

A fault has been performed at the PCC on the bus 5600. The consequences of the disturbance are shown on the next plots.

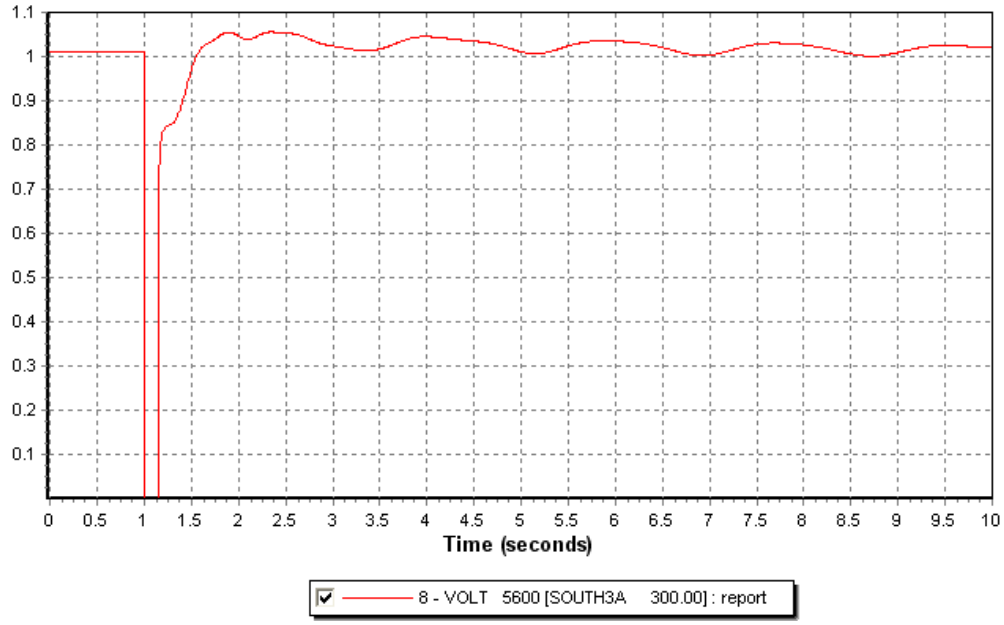

Figure 6-3: Voltage at the PCC, bus 5600 in pu

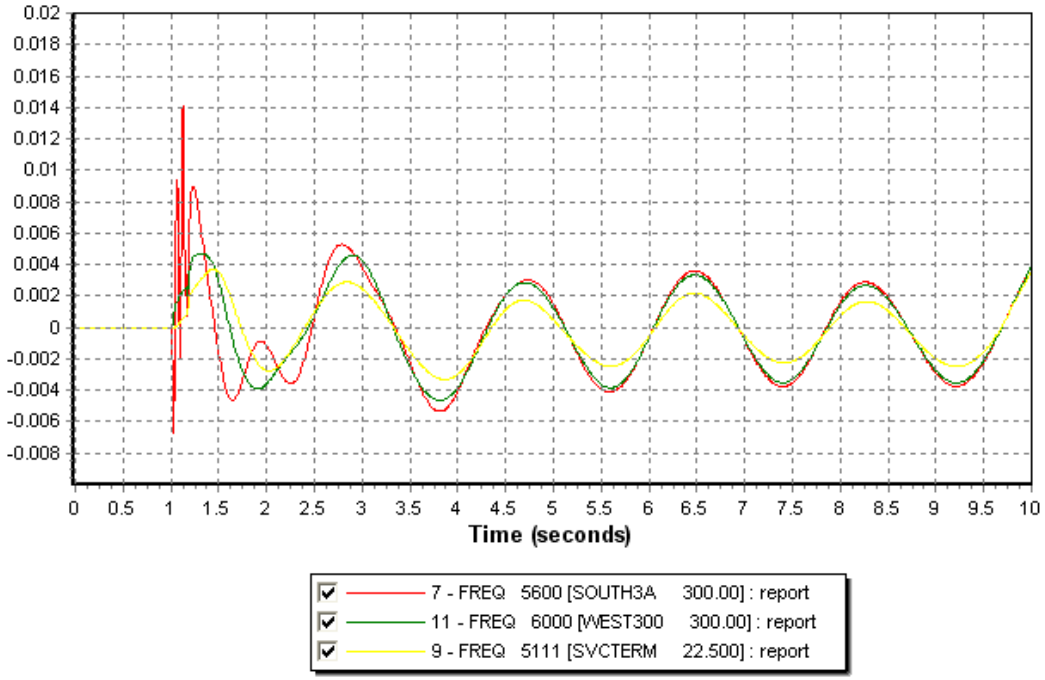

Figure 6-4: Frequency variation onshore at the PCC,at bus 6000 and at the SVC (5111), 0.02pu=1Hz

The voltage recovers 300 ms after the fault is cleared but some damped oscillations continue after. The maximum oscillation amplitude observed is 0.03pu. The voltage is still in the range of 0.9-1.1 pu. Same oscillations are observed in the entire grid. See Appendix E - 3. The frequency is also oscillating with an amplitude of 0.3 – 0.4 Hz. The period of those oscillations is 2s (0.5Hz).

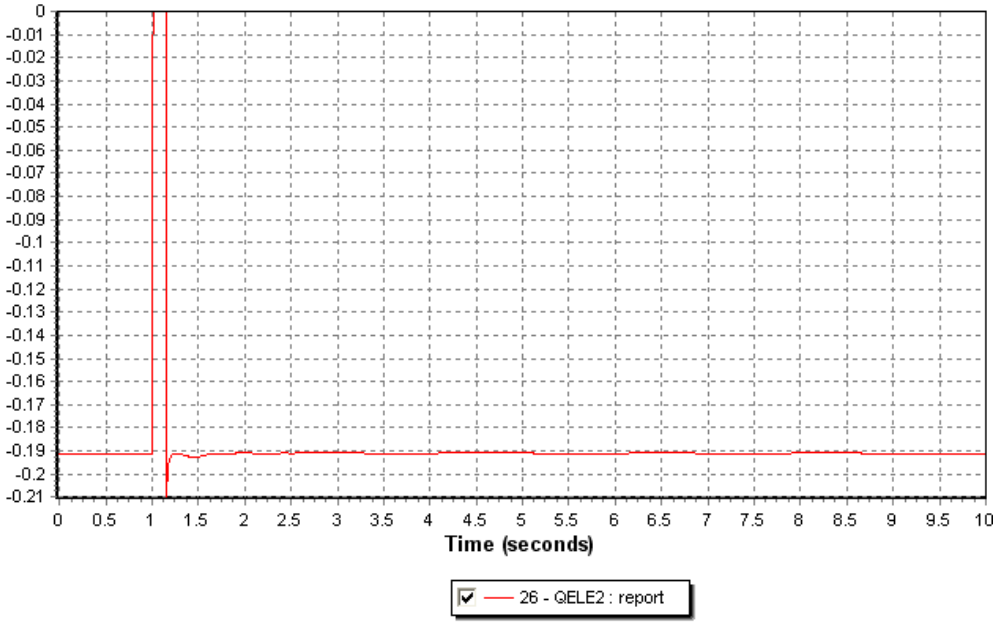

Figure 6-5: Reactive power supply by the VSC-HVDC converter, in pu on system base, reversed axis.

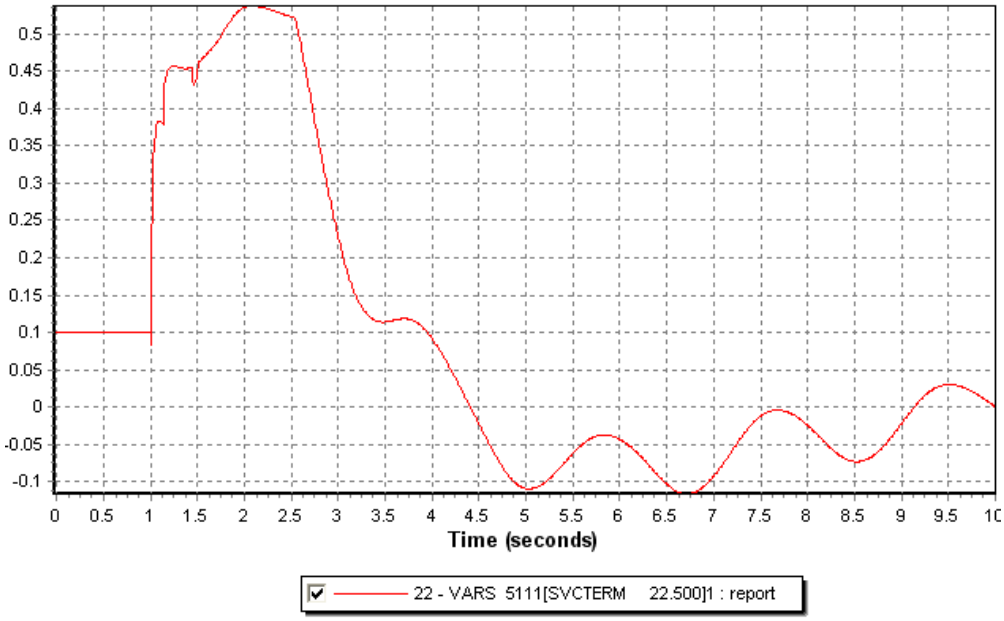

Figure 6-6: Reactive power from the SVC in pu on system base.

With the power factor control, the SVC does not response very well to the fault. Only 20Mvar are supplied by the converter when the fault is cleared. The stability is assured mainly by the SVC which supplies 400Mvar to the system to go through the fault. The SVC produces as much as reactive power as possible to raise the voltage. After 4s the reactive power is quickly regulated down to maintain the voltage at 1 pu. Then, the SVC tries to regulate the voltage oscillation by supplying and absorbing 50 Mvar.

The behaviour of the generator can be observed in the Appendix E - 4. After a peak during the fault, deviations from the synchronous speed of the generator are observed, as consequence, a variation in the active power production. When clearing the fault the generator absorbs reactive power (700Mvar) and then recovers slowly its normal functioning: supply the grid with reactive power (250Mvar).

The wind farm offshore is "isolated" of the fault thank to the HVDC connection. Small variation on voltage and frequency during the fault occur, but disappears rapidly thank to the offshore converter (voltage control). A variation of 0.7 Hz is observed, then the frequency regain progressively its original state. A variation of 0.02 pu is observed on the voltage but 500ms after the fault, the voltage recovers.

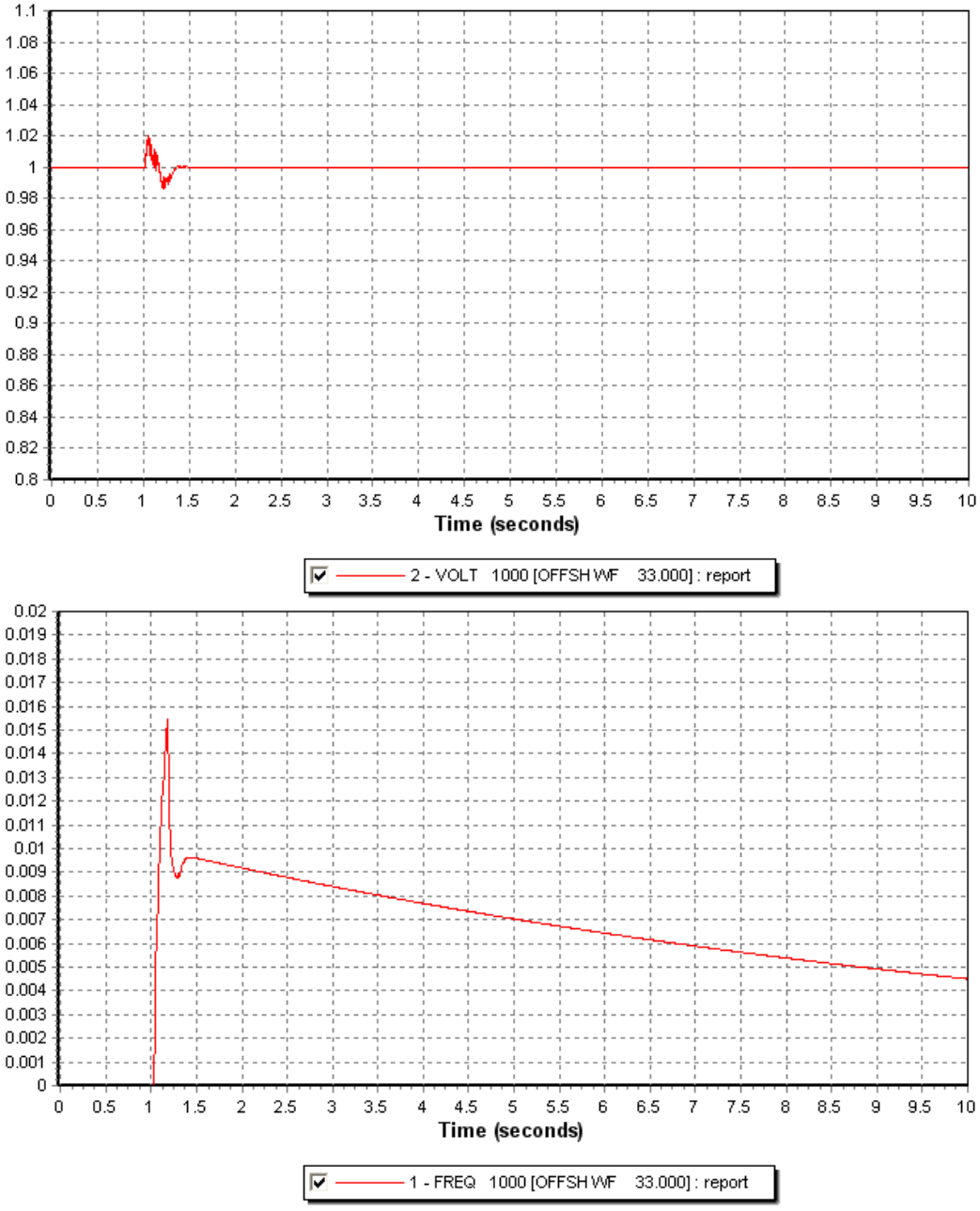

Figure 6-7: voltage and variation frequency (0.02pu=1Hz) in pu at the offshore wind farm.

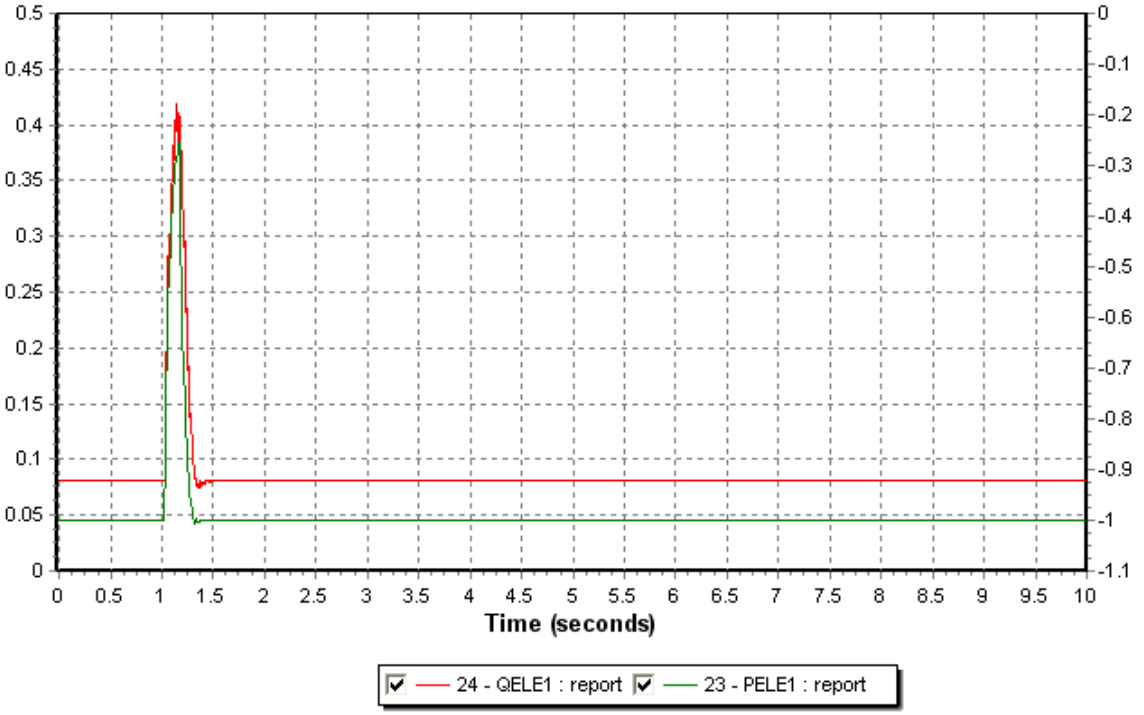

Figure 6-8: Reactive (reversed axis) and active power from the offshore converter, in pu on system base.

During the fault, the flow of active power decreases quickly in the HVDC transmission without reaching 0. Approximately 250MW continue to flow in the offshore converter when fault is cleared. The converter during the fault absorbs reactive power.

Longer simulation (30 sec) has been performed to confirm the stability of the system. The voltage is shown below. This plot confirms the damped oscillations.

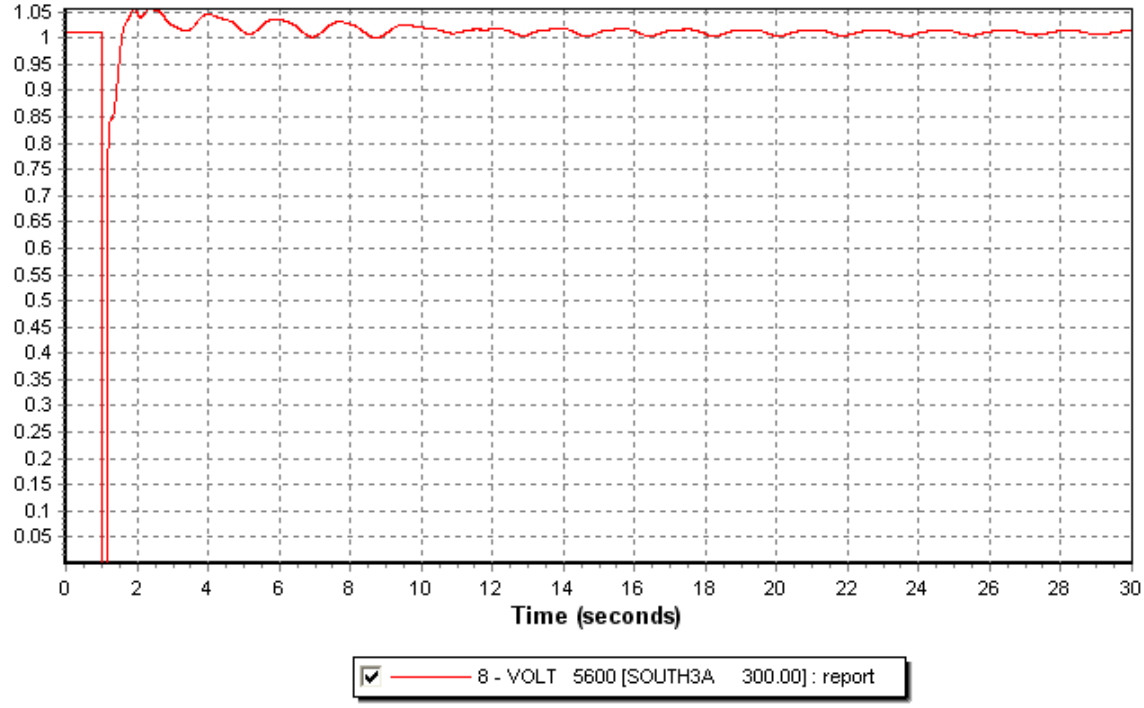

Figure 6-9: 30 seconds simulation, voltage at bus 5600.

6.3 ONSHORE FAULT AT PCC & VOLTAGE CONTROL

Now, the same fault has been performed but the VSC-HVDC converter is put in voltage control mode.

Voltage recovers 300ms after cleared the fault, then really small damped oscillations occurs. They disappear quickly, 6 seconds after the fault. The maximum amplitude of oscillation is 0.02pu. The frequency is also slightly oscillating after the fault occured, maximum deviation is 0.1Hz.

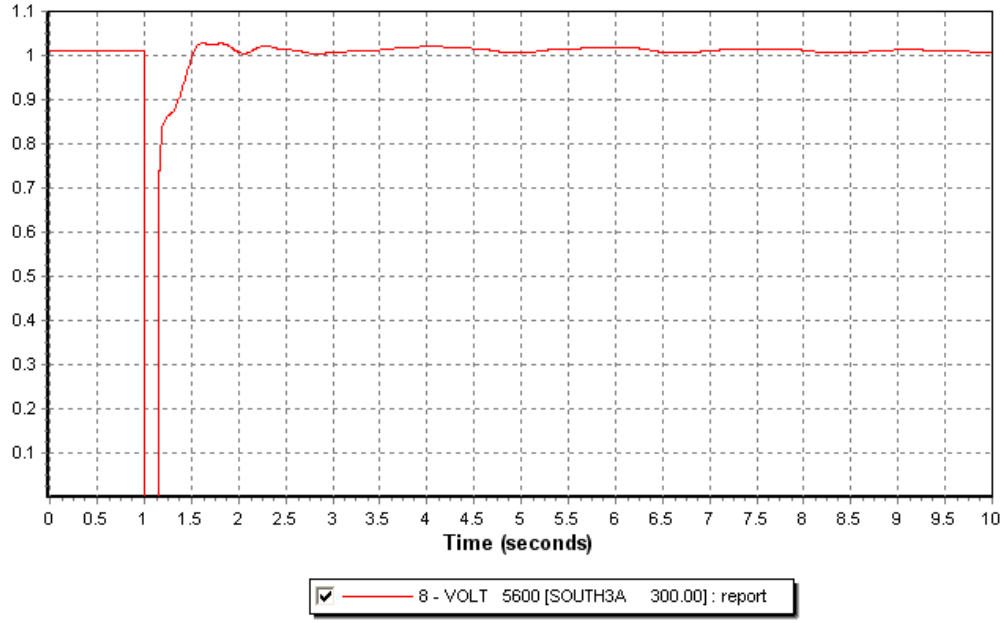

Figure 6-10: Voltage at PCC bus 5600 in pu.

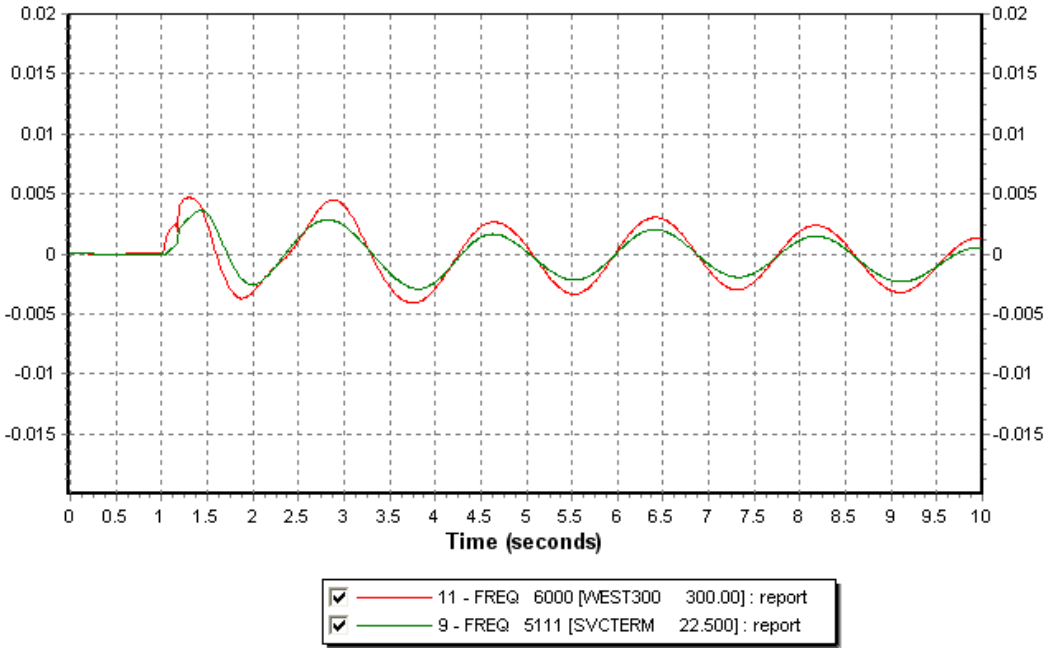

Figure 6-11: Variation frequency on shore at bus 6000 and at the SVC.

The onshore converter in voltage control responds very well to the fault. Before the fault, it supplies reactive power to the grid. During the fault it stops to supply reactive power and absorbs 200Mvar while clearing the fault. This peak has to be investigated. Then, the converter supplies a peak of 450Mvar to rise up the voltage to 1pu. Finally the converter regulates the flow of reactive power down to maintain the voltage around 1pu. It can be observed during this state it reaches its limit down (-570Mvar). See Figure 6-12.

As previous, the flow of active power decreases quickly in the HVDC transmission during the fault. Approximately 170MW continue to flow in the onshore converter when fault is cleared, less than with PF control by taking into account the losses in the DC line. The recovery of the pre-fault transmission is almost instantaneous (100ms). See Figure 6-13.

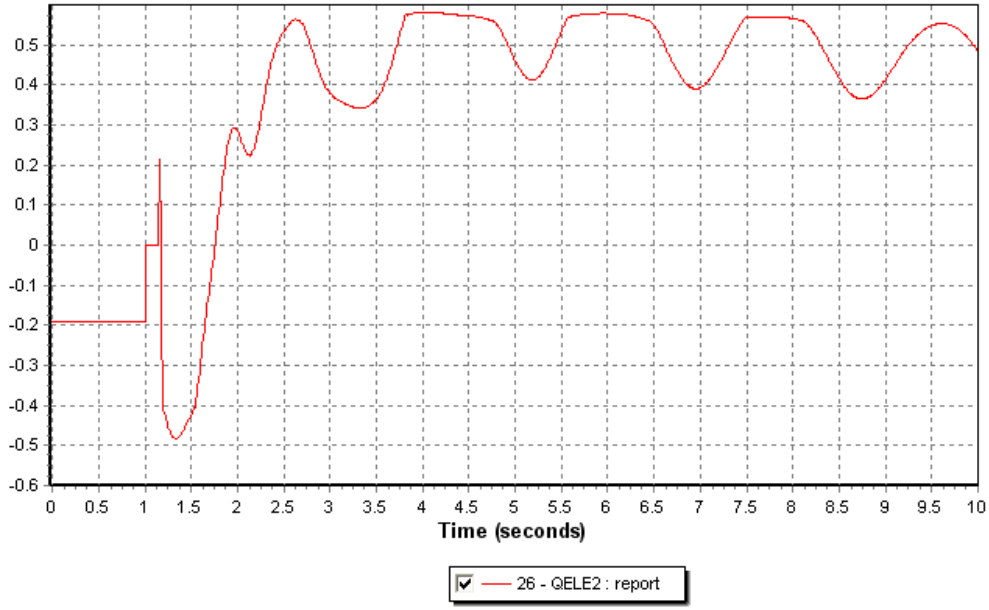

Figure 6-12: Reactive power from the onshore VSC-converter in pu on system base, reverse axis.

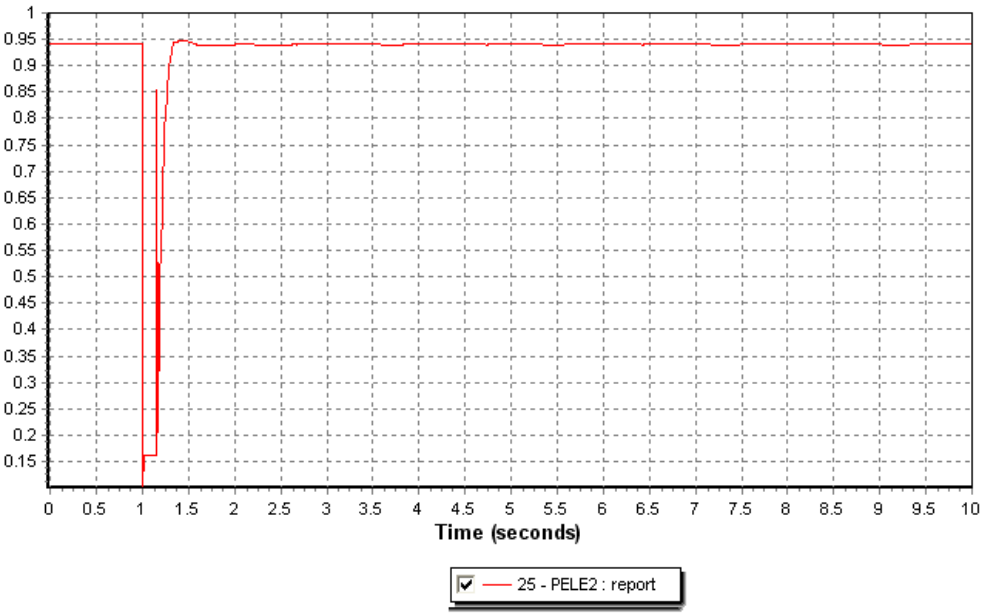

Figure 6-13: Active power from the onshore VSC-converter, in pu on system base

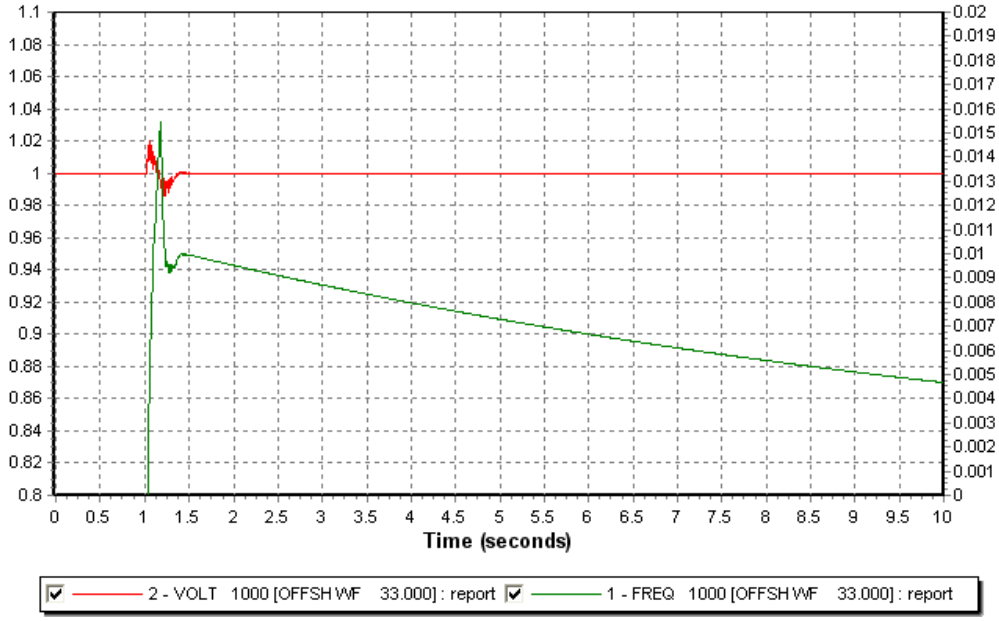

Figure 6-14: Voltage and frequency variation offshore at the wind farm (bus 1000) in pu.

The fault on the offshore side is almost invisible. Small variations occur on the voltage over 500ms during the fault. Maximum variation is 0.02pu. A frequency peak of 50.75Hz is observed and then the frequency goes down to its original value. See figure above.

6.3.1 ESTABLISHMENT OF A NEW STABLE STEADY STATE

Longer simulation has been performed after the fault to see the long stability of the system. It seems that the system recovers another state of stability.

The voltage definitely recovers its original value, but the frequency changes little, a raise of 0.15Hz on the system is observed. At 15s, a change in the state of the system for an unknown reason occurs. See Figure 6-16 next page.

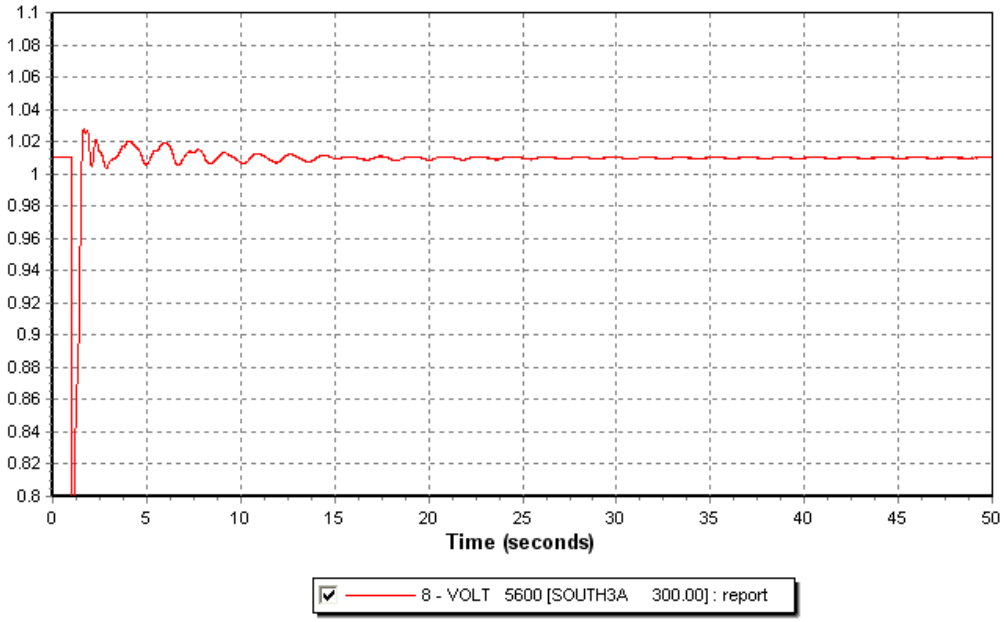

Figure 6-15: 50s simulation, voltage at bus 5600 in pu

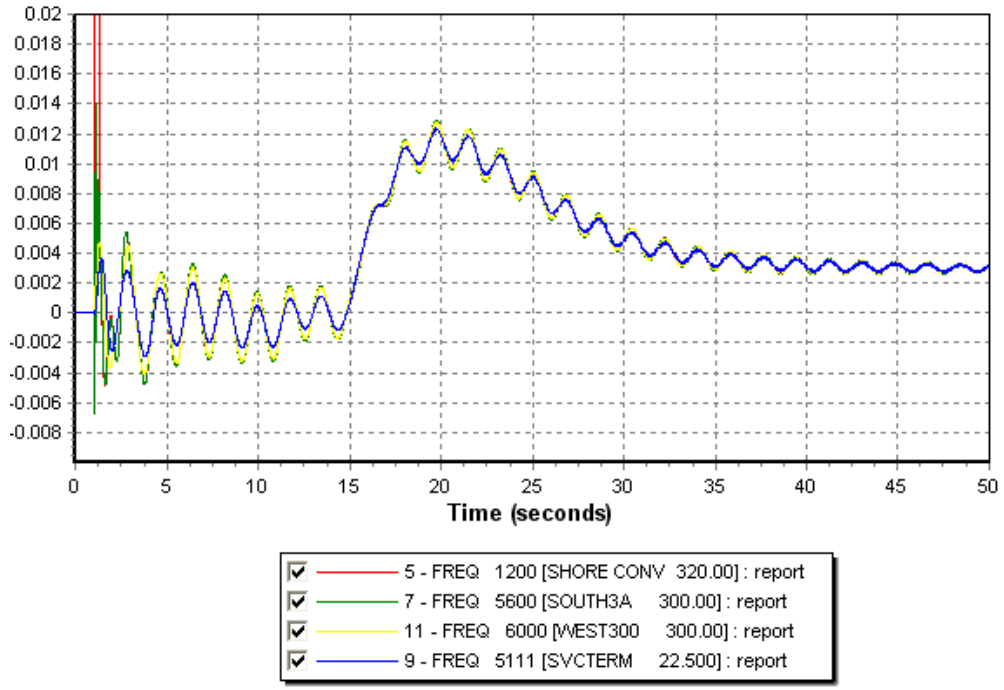

Figure 6-16: 50s simulation, frequency variation onshore at different buses in pu, 0.02pu=1Hz

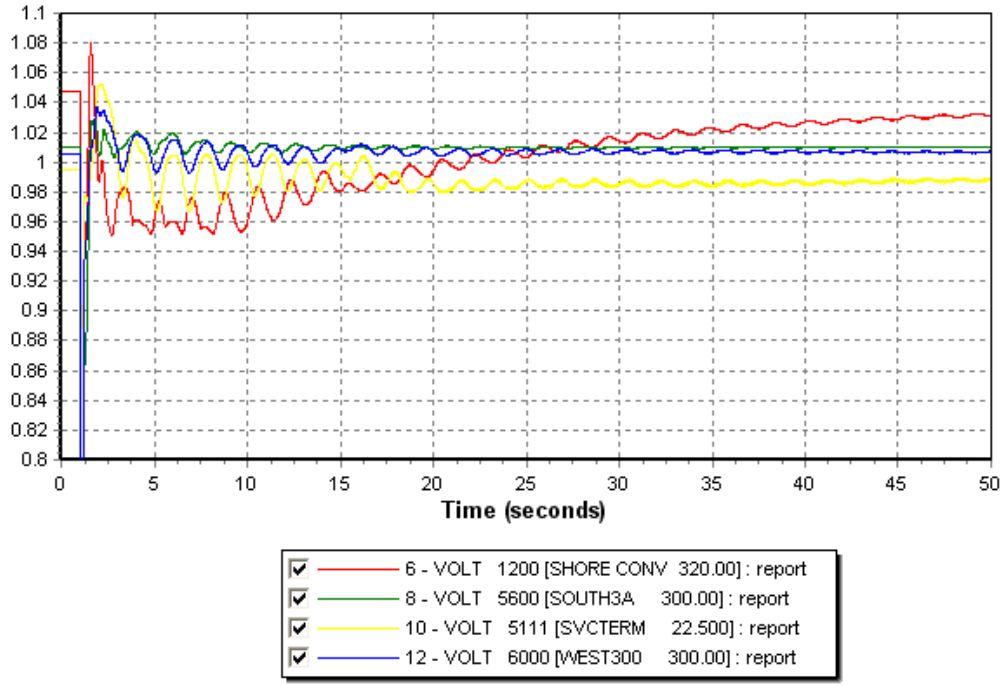

Figure 6-17: 50s simulation; voltage in pu at different buses.

The voltage at the converter and the SVC are very affected by the regulating of the voltage and take long time to reach their original states. The voltage at the onshore VSC-converter falls down to 0.95pu during the recovery. See red curve in the figure above. Same behaviour can be observed at the bus of the SVC, see yellow curve. The parameter of the SVC and the HVDC converter might be the reason.

This changing of state is visible in the reactive power from the SVC and the HVDC converter. After the voltage recovery, the VSC-converter is regulating down and reactive power swing with middle oscillation. Suddenly, at 15s these oscillations become smaller but the converter continues to regulate down in the same way, only the amplitude of the oscillation are changed. See Figure 6-18.

For the SVC, at 15s while the reactive power is being regulated down and is slowly being regained its pre-fault state, the reactive power is regulated down once again and the SVC starts to absorb reactive power. It has to be notice that the voltage at its bus goes down from 0.02pu in the same time. Finally, it regulates to a new state. See Figure 6-19.

This establishment of a new state with a new frequency will be discussed in the next paragraph.

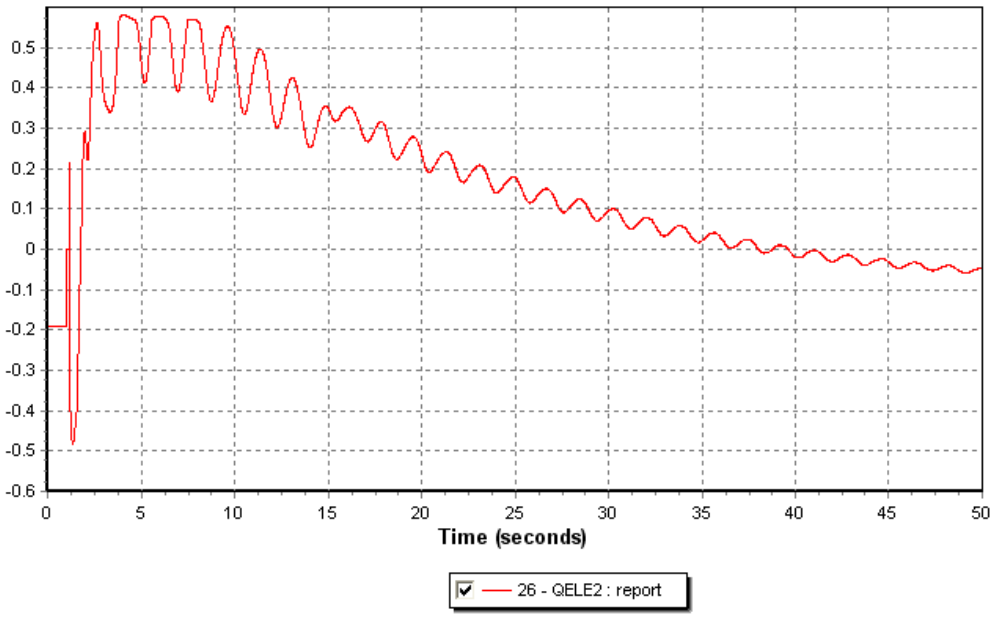

Figure 6-18: 50s simulation; reactive power from the HVDC converter in pu on system base

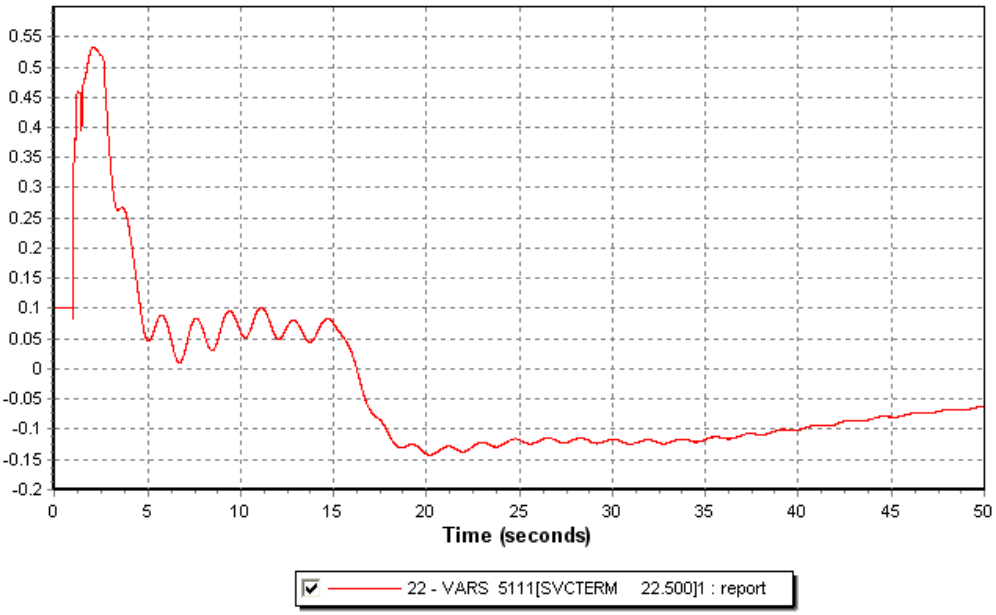

Figure 6-19:50s simulation, reactive power from the SVC in pu on system base

6.3.2 DISCUSSION

A voltage drop at the bus of the regulator (SVC and VSC) can be observed. It has to be linked with the regulation of reactive power coming from the device.

The establishment of a new state will be now tried to be explained. Three reasons might explain that phenomenon.

- The first one is that the simulation has been started with power flow control on the HVDC converter. As soon as the fault has been cleared, the control of the converter is set in voltage control mode. This has been done by taking into account the initial condition, to regain the same pre-fault voltage. So a different a state may occur, but it doesn't explain why it occurs at 15 seconds.
- The second reason might be in the control of the SVC which first tries to do like a coarse regulation the first 15 seconds and then do an accurate regulated voltage.
- The last reason might be that the voltage at the regulated bus 5600 reaches a stable voltage, so the HVDC controller "stop" the control and the SVC must compensate the amount of reactive power unabsorbed and lead to a new regulated control more accurate.

The increase of frequency can only be explained by a increase of the rotor speed of the generator in the main grid, which lead to a change in a reactive power production of the generator. It could then explain why the SVC and the HVDC converter change their regulation at 15s.

6.4 OFFSHORE FAULT

A fault has been performed at the offshore wind farm bus. The consequences of the disturbance will be presented in the next figures and plots.

A high peak occurs while clearing the fault, the amplitude of the peak is 1.7pu (56kV instead of 33kV). This voltage peak is brief (few ms). 250ms after the fault has occurred; the voltage regains this original value. The amplitude of the peak, although it is brief might be a problem for the system especially for the transformer insulation and the electronic valve in the converter. The phenomena will be discussed later.

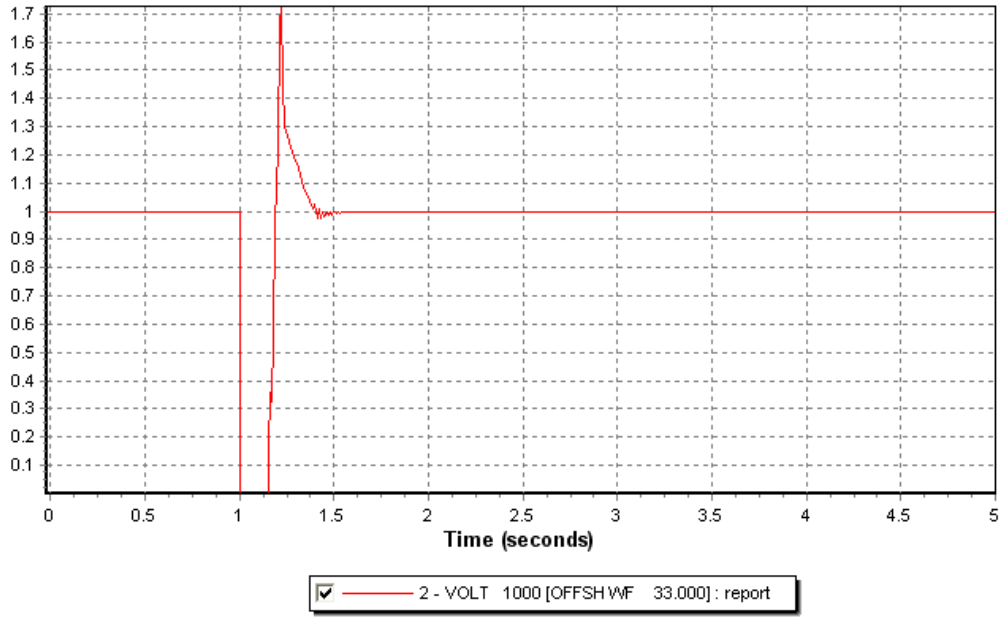

Figure 6-20: Voltage at offshore wind farm bus where fault occurs in pu

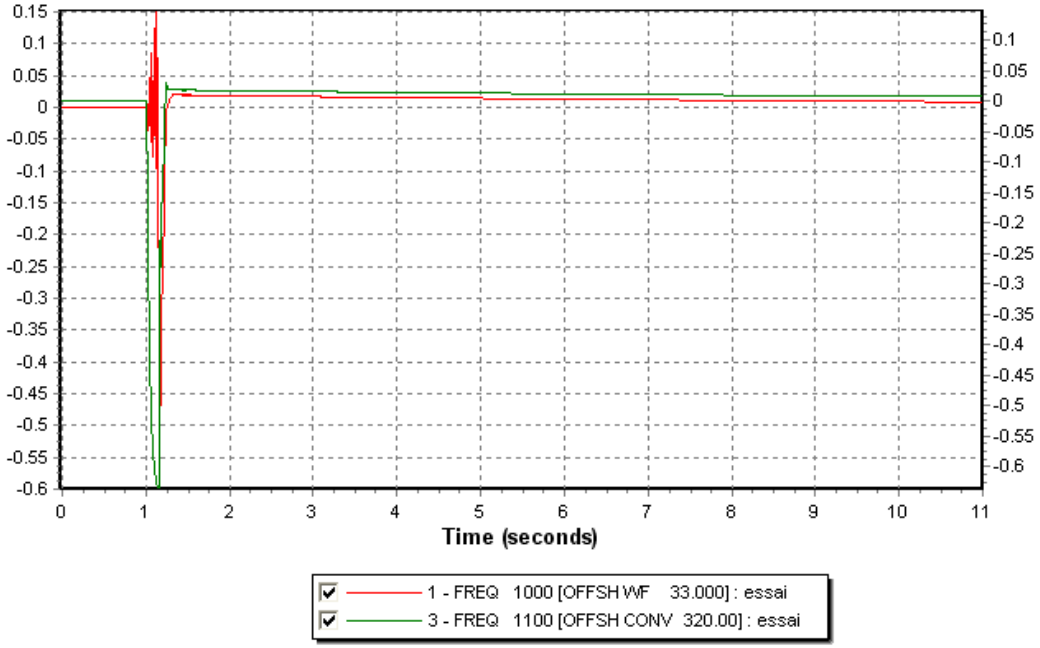

Figure 6-21: Frequency variation at the offshore buses 1000 and 1100, 0.02pu=1Hz.

Those frequencies during the fault fall briefly down to 20Hz at the bus fault and to 30Hz at the offshore converter. After clearing the fault the frequency regain progressively this original value. The maximum frequency displacement out of the fault is 2Hz. The offshore system fulfills the Statnett requirement for frequency. See Figure 6-21.

The generator representing the offshore wind farm will be now studied. The rotor speed increases during the fault and as soon as the fault is cleared, it stops to accelerate and slow down progressively.

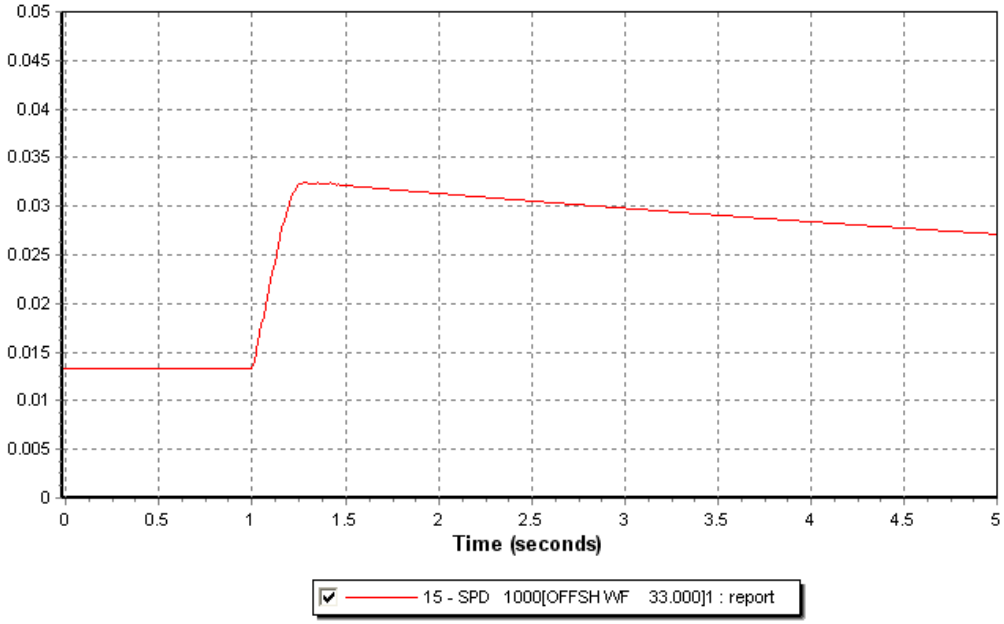

Figure 6-22: Rotor speed from the generator representing the wind farm in pu

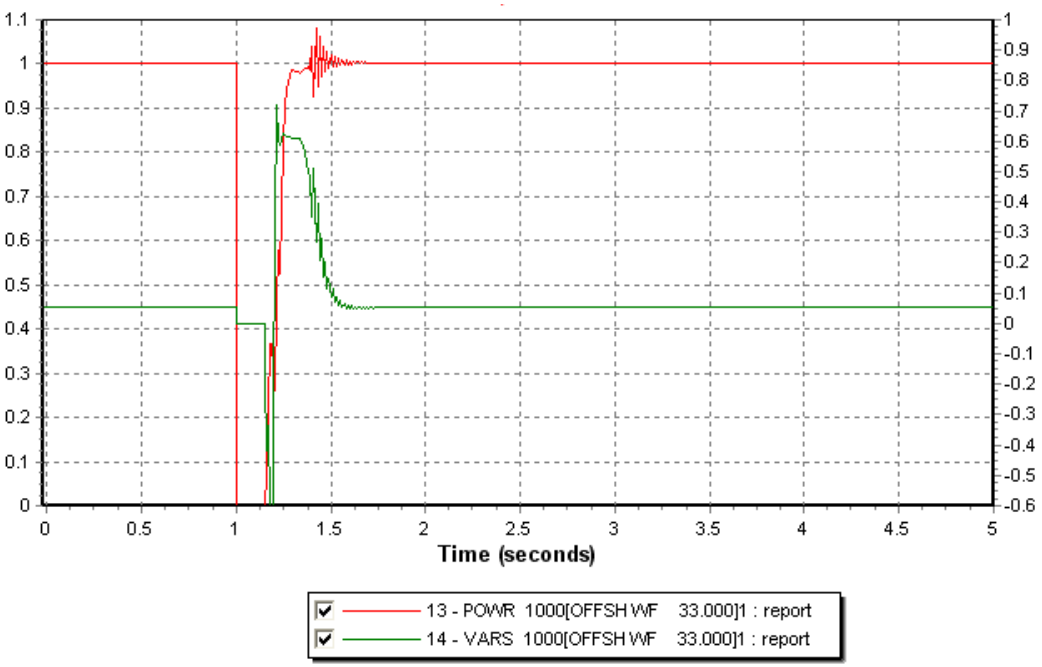

Figure 6-23: Active and reactive power generated by the generator, in pu on system base

The generator at the wind farm buses where the fault occurs is representative of the dynamic behaviour of the generators of the wind turbines. During the fault the wind farm stops to produce power, but recovery is very fast. The generator produces lot of reactive power in order to increase the generation of active power. Some oscillations are observable when it reaches its pre-fault power production. It might be linked when the high voltage peak goes back to 1pu. See Figure 6-23.

The consequences on shore are now investigated. Voltage, frequency and response of the SVC are given below. Few frequency and voltage variations occur following the fault. But this variation amplitude are very small (0.01pu for the voltage and 0.2 Hz for the frequency). The consequences on shore can be considered as negligible.

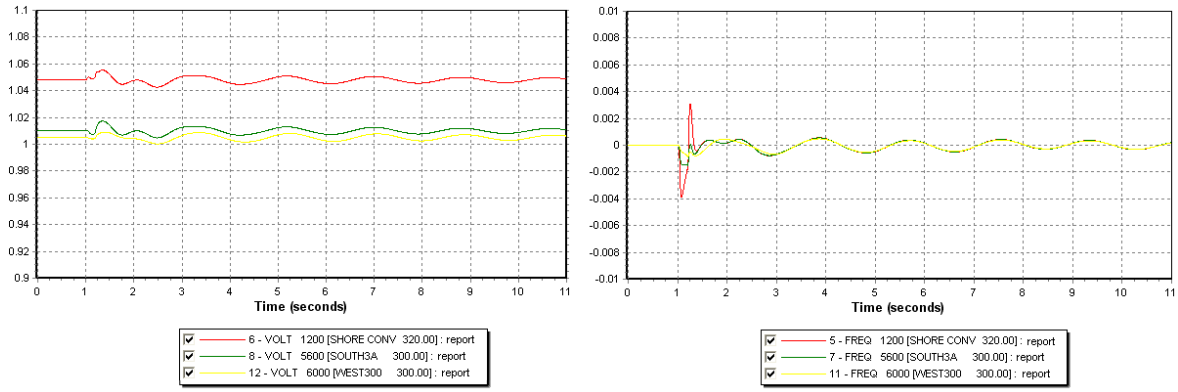

Figure 6-24: Frequency and voltage on shore at buses 1200, 5600 and 6000 in pu.

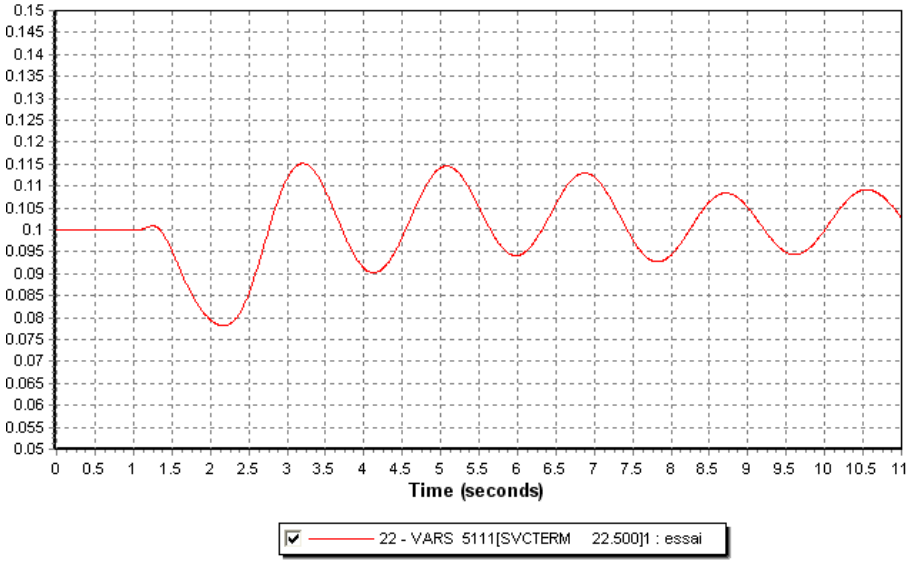

Figure 6-25: Response of the SVC, reactive power in pu on system base

The SVC which regulates the entire grid reacts to the small voltage disturbance and supplies around 20Mvar of reactive power to the system. See Figure 6-25 above.

Regarding the HVDC transmission and the converters, each converter reacts independently for the other. There is no correlation between both converters for the reactive power generation due to the voltage control. The offshore converter supplies little reactive power (200 Mvar) to recover the voltage. Then the converter regulates down and absorbs reactive power to reduce the voltage peak.
The active power flowing is similar to the power given by the generator. See Figure 6-26.
The onshore converter must regulate the oscillating voltage at the main grid. Its can be observed that its regulation is very accurate, few Kvar are generated. See Figure 6-27 green curve.

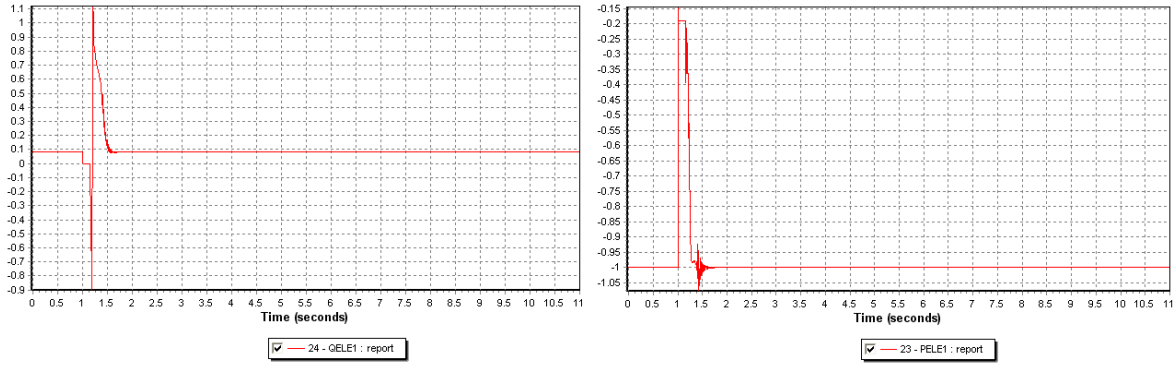

Figure 6-26: Reactive (reverse axis) and active power from the offshore converter in pu on system base

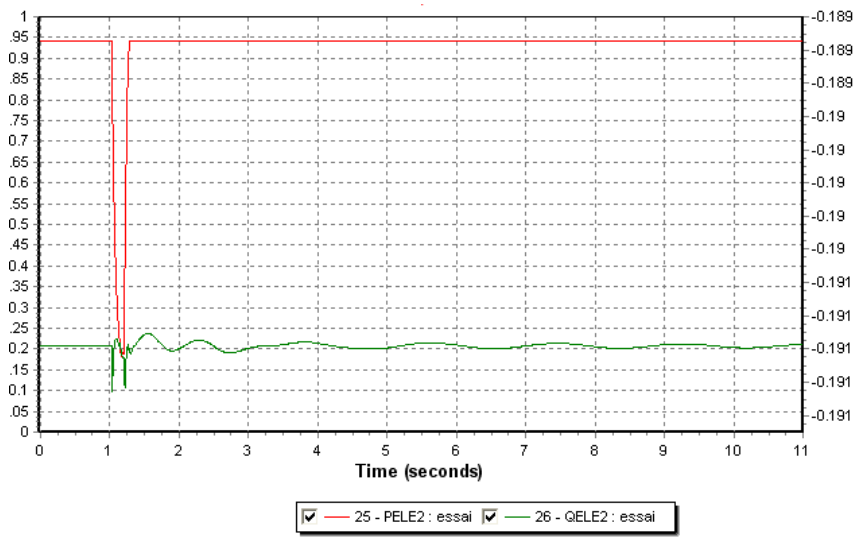

Figure 6-27: Active and reactive power supplied by the shore converter in pu on system base

6.4.1 DISCUSSION

The system is able to ride through the fault but the amplitude of the voltage peak; although it is brief might be a problem for the system especially for the transformer insulation and the electronic valve in the converter. The reason of this peak is unclear; an explanation might be that the rotor stocks a lot of energy by increasing its speed during the fault as soon as the fault is cleared; this energy has to be evacuated. By looking at the power produced, the peak voltage is high when the generated power is low so the current is also low. So the rotating energy is transfer into electrical energy when the rotor speed decreases, as the power is still low a peak of voltage occurs. But the shape of the rotor speed normally should have been more shaped during the deceleration.

Another possibility is that the HVDC converter was not able to prevent this peak, because of wrong dynamic parameters.

In any case, a voltage peak of this amplitude will damage electrical equipment in the offshore wind farm grid: transformers, submarines cable or the IGBT modules inside the VSC-converter.
So, this fault must be analyzed further or devices to prevent such overvoltage must be installed into the offshore grid.

7 SIMULATION: CONNECTION OF WIND FARM CLUSTER WITH A SINGLE HVDC TRANSMISSION

In this section, the emphasis will be put on the offshore grid; the onshore grid is expected to response with a similar way as in the previous section. A fault will be performed onshore at the PCC to validate it. Then, a fault will be performed at the main wind farm and after at the "transmission bus" close to the wind farm. Finally, the same fault will be performed but with the replacement of one DFIG generator by a fixed speed generator. See in Figure 7-1, the faults are represented by a red lightning and the generator replacement by a red arrowed circle.

7.1 LOAD FLOW CASE

The load flow is unchanged to the shore. The same scheme of generation as in the previous configuration is used. The power generation is reduced at the PCC. Same amount of active and reactive are sent to the shore through the HVDC transmission. The transfer of power between the area is stayed the same. Four new buses have been added to the model as indicated above in paragraph **Error! Reference source not found.**. The wind farms are not working at their rated power output (500MW and 2x 400MW). It has been assumed that the wind was not strong enough in order the turbines were able to reach the nominal power output, so the wind farm generates 461MW and 350MW, as presented in the table below.

Bus number	Name	Voltage [pu]	Angle [°]	Δ Angle [°]	Pgen [MW]	Qgen [Mvar]
3300	SV-SW	1.000	0	0	3988.5	2333.8
5400	CNTR3 A	1.007	33.3	4.9	1637.5	122.94
5401	CNTR4 A	0.998	30.9	5.1		
5600	SOUTH 3A	1.010	30.9	8.7	2437.6	266.0
5601	SOUTH 4A	0.992	31	8.6		
5602	SOUTH 4B	0.969	23.3	6.2		
5603	SOUTH 3B	0.936	22.3	6.4		
6000	WEST 3	1.005	33.5	5.4	1164.2	-182.8
6001	WEST 4	1.000	32.7	5.4		
6100	NWEST 3	1.000	32.8	4.7	2419.2	749.0
1000	OFFSH WF	1.000	0		461.2186	2.9
1100	OFFSH CONV	1.00	-5.3			
1010	OFFSH WF B	1.000	-0.8		350.0000	-29.5
1020	OFFSH WF & RIG	1.000	-1.7		350.0000	-1.6
1110	OFF TRANS B	1.014	-4.1			
1120	OFF TRANS C	1.018	-3.6			
1200	SHORE CONV	1.054	37.2			

Table 7-1: Load flow in the surrounding of the PCC and in the wind farm cluster.

The detail of all the load flow can be found in Appendix F - 1 and in Appendix F- 2. The next figure show the load flow in the offshore grid. Two shunt reactors of 60Mvar have been used to absorb a part of the reactive power created by the submarine cables, the rest being absorbed by the reactive capability of the wind farm.

In this section, the emphasis will be put on the offshore grid; the onshore is expected to response with a similar way as in the previous section.

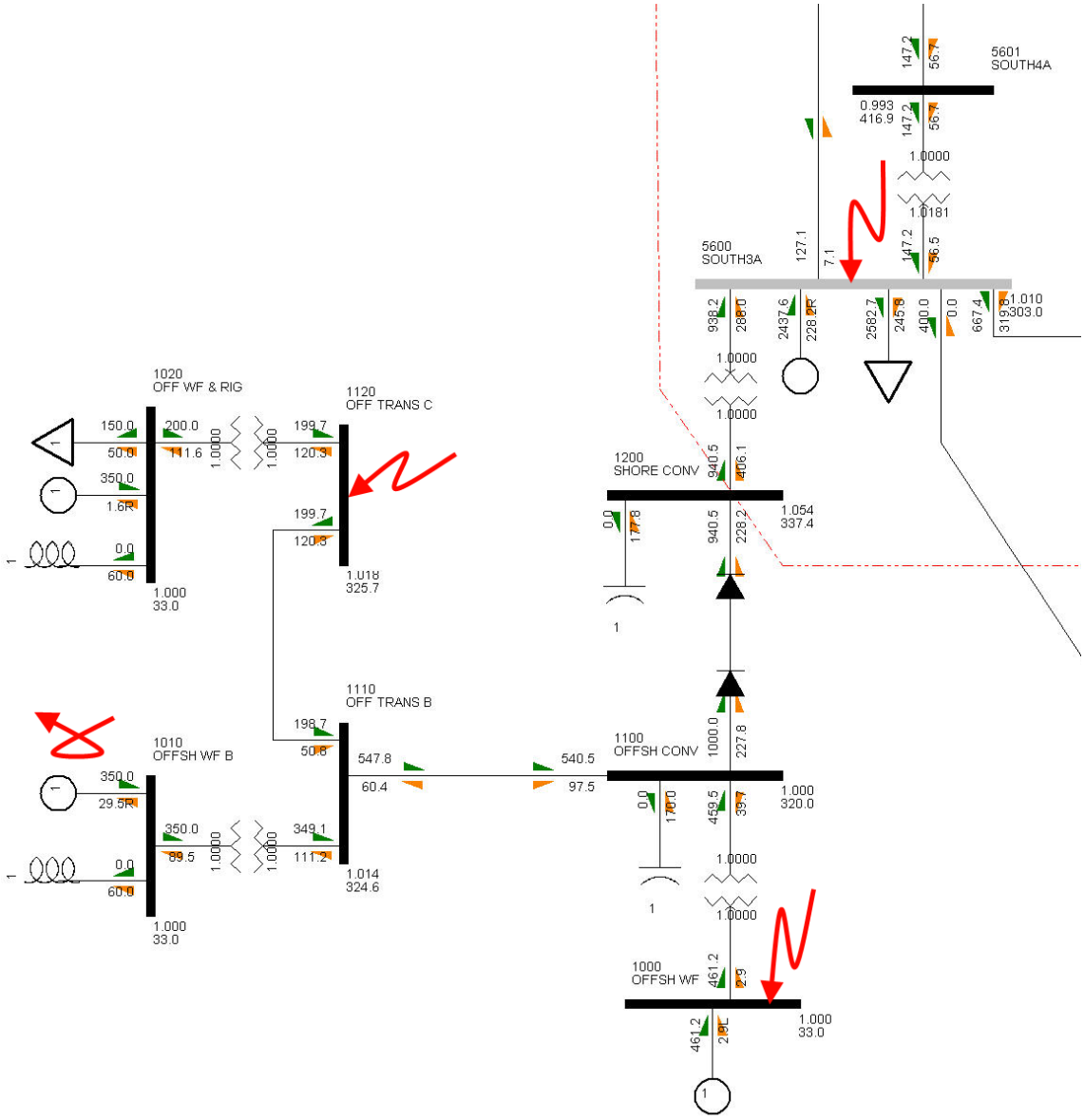

Figure 7-1: Picture of the offshore wind farm cluster and the HVDC transmission.

7.2 FAULT ONSHORE AT PCC

As the load flow is the same and the dynamic parameters are the same as before, the dynamic response to a fault is the same as previously. It has been shown that the consequences of a fault at the PCC are small on the other side of the HVDC transmission. Thus, the consequence of a fault onshore will not be analyzed in this part but a simulation has still been done to confirm this assumption.

Only the offshore frequency, the voltage and the reactive power from the HVDC converter are shown next page. One second after the fault the system regains its original state and it is not very affected by this fault thank to the voltage control of the HVDC converter.

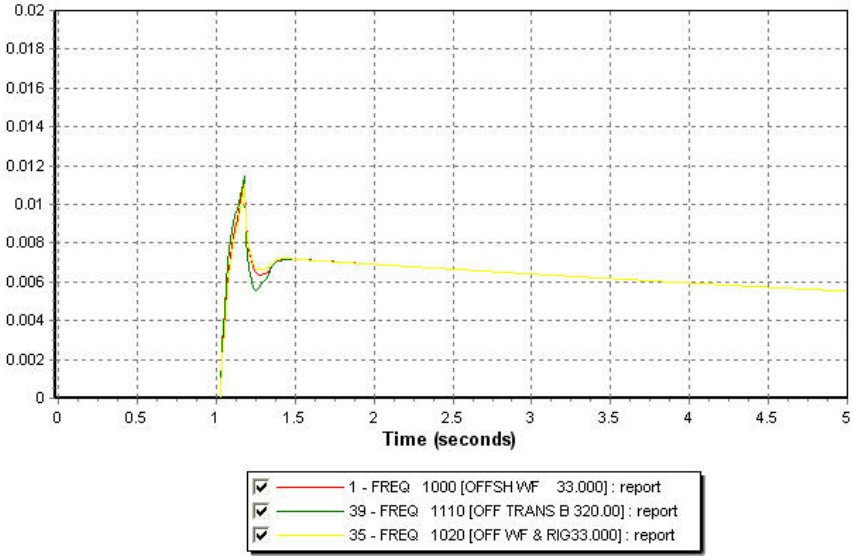

Figure 7-2: Frequency variation at different buses offshore, 0.02pu=1Hz.

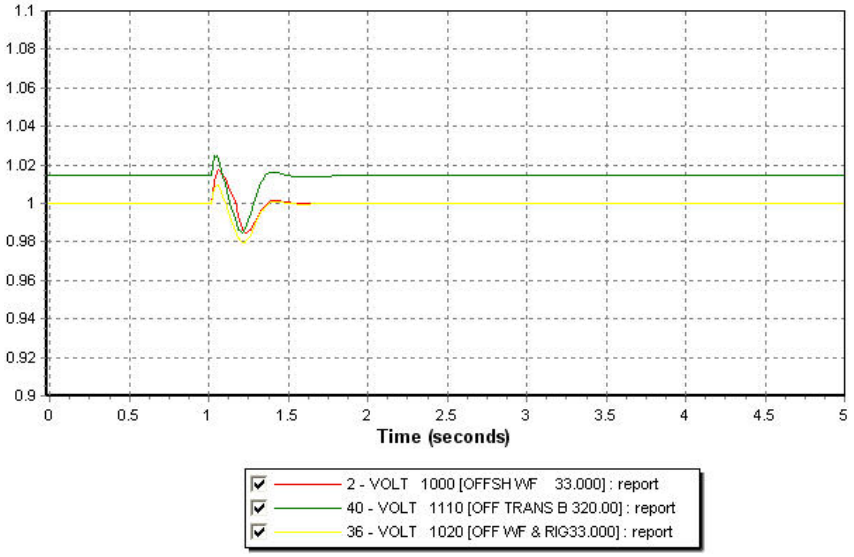

Figure 7-3: Voltage in pu at different buses offshore in pu

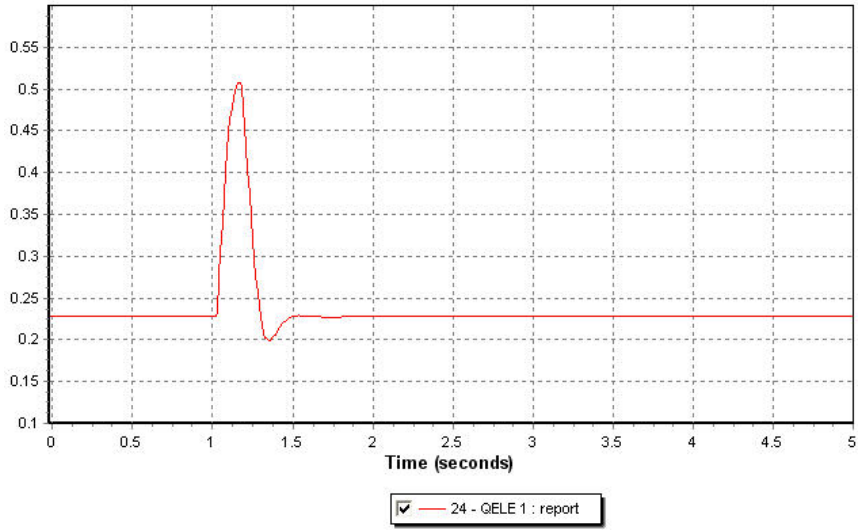

Figure 7-4: Reactive power from the offshore HVDC converter in pu on system bse

7.3 FAULT OFFSHORE AT THE MAIN WIND FARM

A three phase fault has been performed at the bus of the 500MW wind farm close to the offshore converter. The result of the simulation is presented below.

The voltage is recovered quickly, 1 second after cleared the fault it regains its original value. A small overvoltage before recovery can be observed at 1.7s. See Figure 7-5
The same result is obtained in the other buses of the offshore grid. Due to the distance to the fault and to the contribution from the generator, the voltage doesn't reach 0. See Figure 7-6. The voltage at the transmission buses (1110 and 1120) is show in Appendix F - 3.

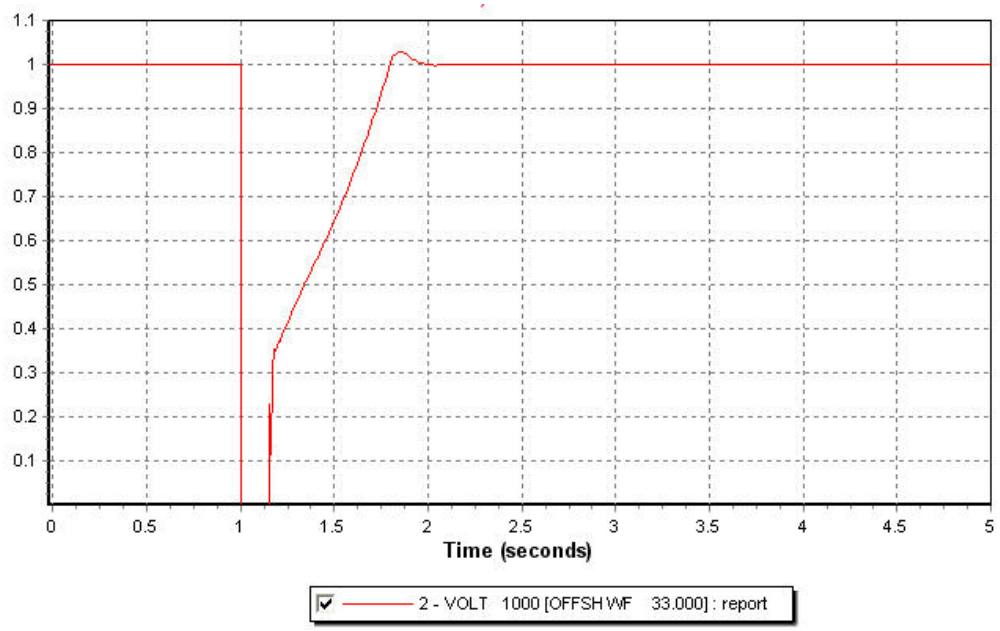

Figure 7-5: voltage at the wind farm during fault in pu

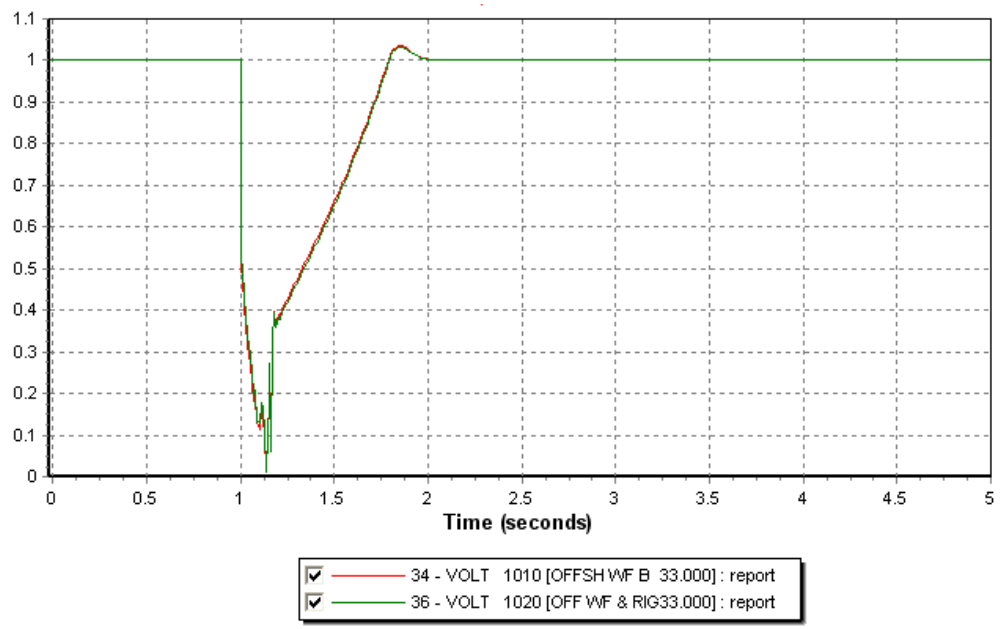

Figure 7-6: Voltage at the other wind farms in pu

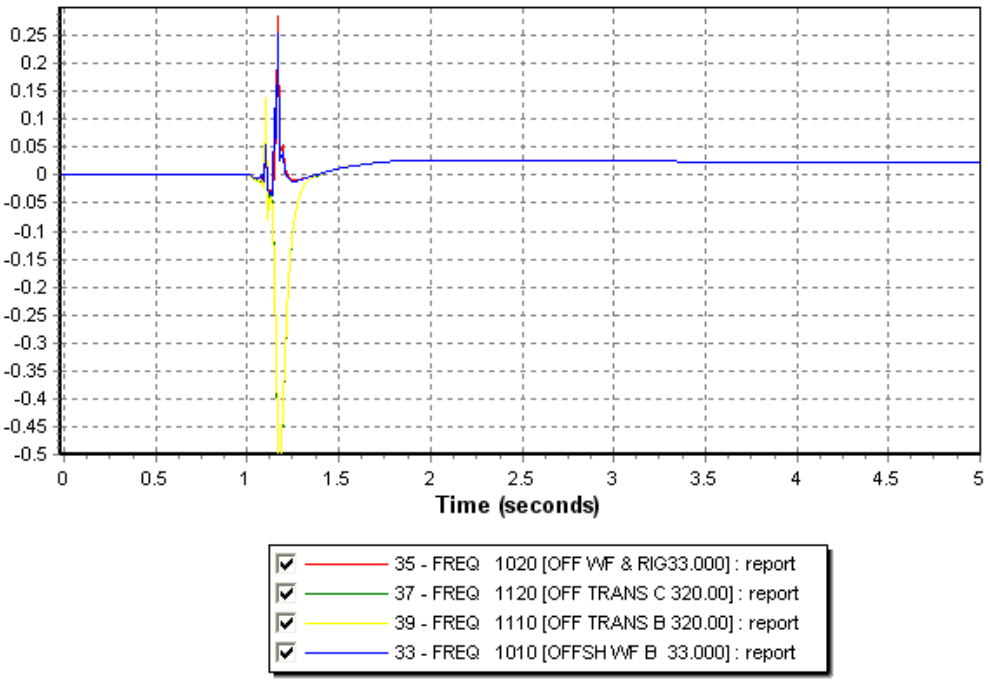

Figure 7-7: Frequency at the other bus. Green curve is over written by the yellow one and red by the blue.

At the transmission buses (1110 and 1120) after a peak frequency during the fault a drop of frequency is observed when the fault is cleared. Frequency falls during 100ms under 40 Hz. Contrary occurs at the wind farm buses where frequency increases quickly to 55Hz. Finally, the system regains a normal frequency when voltage is around 1pu.

At clearing time active power from the main wind farm goes from 0 to 100MW instantaneously and then increases progressively. It recovers its pre-fault generation state 1s after the fault. See in the next figure the green curve. The generator absorbs a peak of reactive power to stop the acceleration of the rotor. The same dynamic is observed for the 2 other wind farms.
See Appendix F - 5.

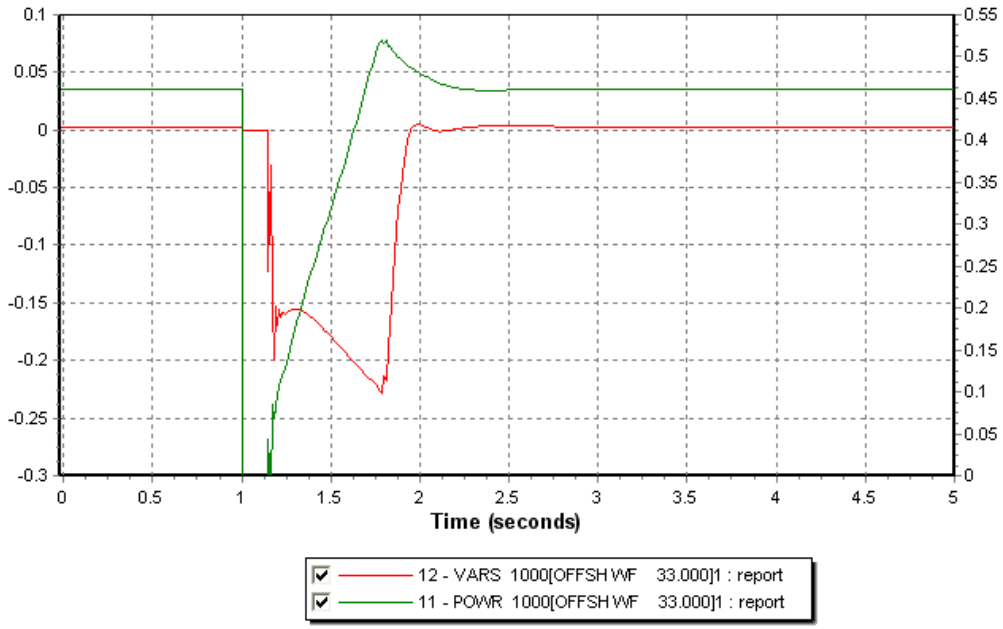

Figure 7-8: Behaviour of the generator in the main wind farm.

The HVDC controller stops during the fault to absorb the reactive power created in the system. After the fault has been cleared, it produces as much at possible reactive power to raise the voltage and then when voltage is recovered, it controls down and regains its original state absorbing 240Mvar. During the fault, the active power through the DC transmission stops progressively. The power flows normally at 1.8s.

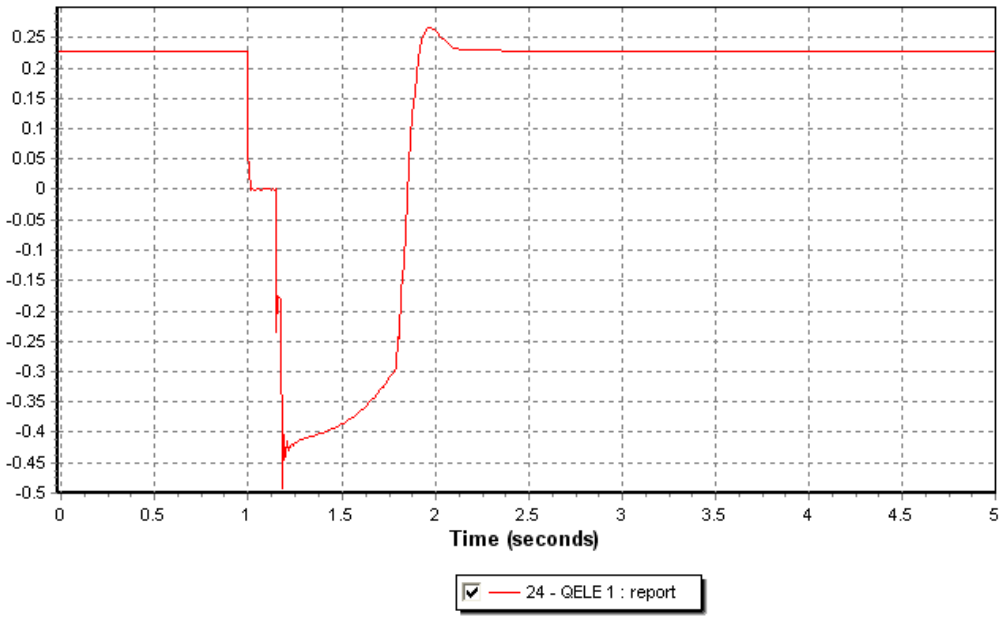

Figure 7-9: Reactive power from the HVDC converter, reversed axis, in pu on system base

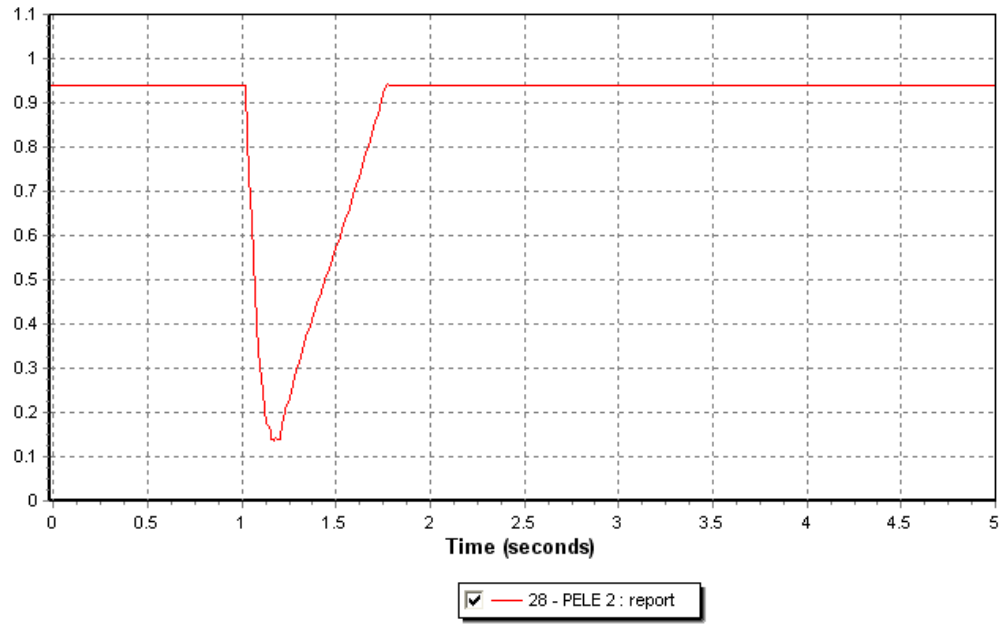

Figure 7-10: Active power flowing in the offshore HVDC converter in pu on system base

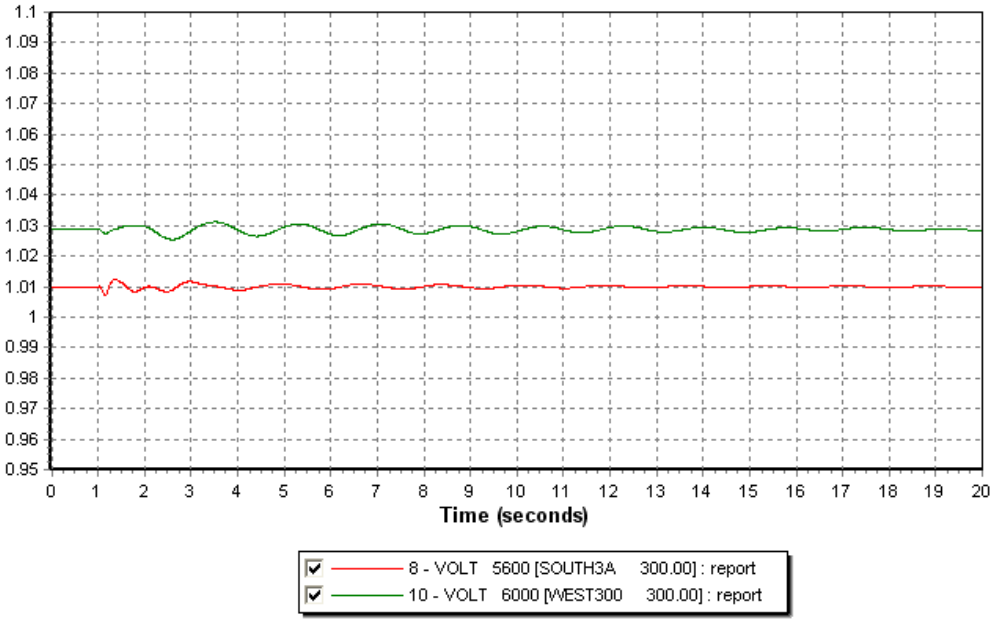

Figure 7-11: Voltage at the PCC at bus 6000 in pu

Voltage and frequency variation on shore due to the fault are small and are corrected by the SVC and the shore HVDC controller. It can be notice that the voltage regains a stable value earlier at the PCC due to the control of the VSC controller. See Figure 7-11. The frequency variation and the response of the SVC are shown in Appendix F - 6 and Appendix F - 7.

7.4 FAULT CLOSE TO THE OIL RIG AT TRANSMISSION BUS 1120

A three phase fault has been performed at the transmission bus 1120 close to the oil rig. The voltage is recovered quickly, 1 second after cleared the fault it regains its original value. A small overvoltage before recovery can be observed at 1.7s. See Figure 7-12. The other voltages in the grid have the same shape. Voltage close to offshore converter is shown below Figure 7-13 whereas the voltage at bus 1010 and 1110 can be found in Appendix F - 8.

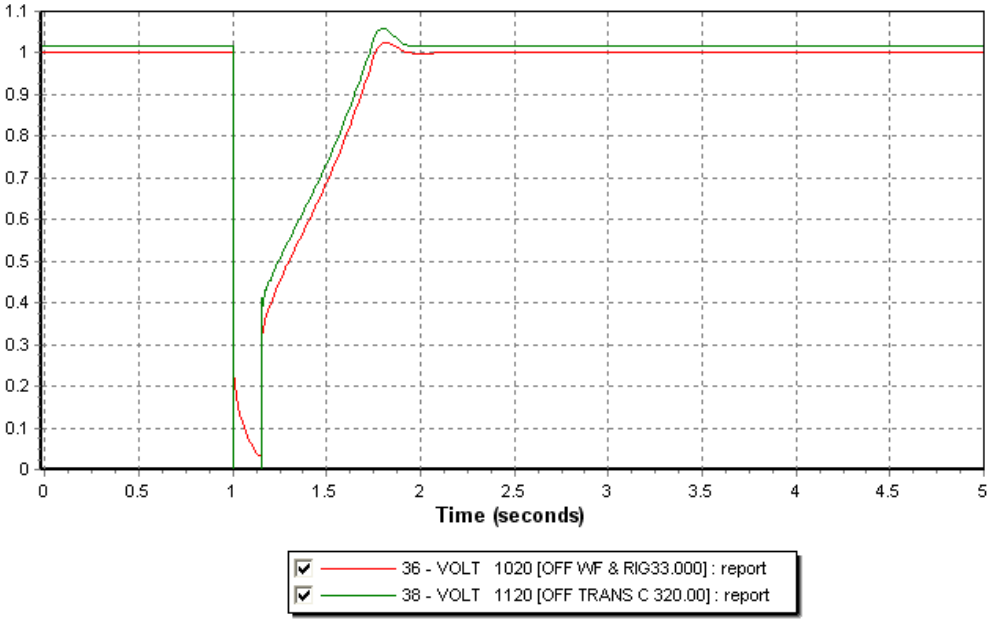

Figure 7-12: Voltage at the oil rig (bus 1020) and at transmission bus 1120 in pu

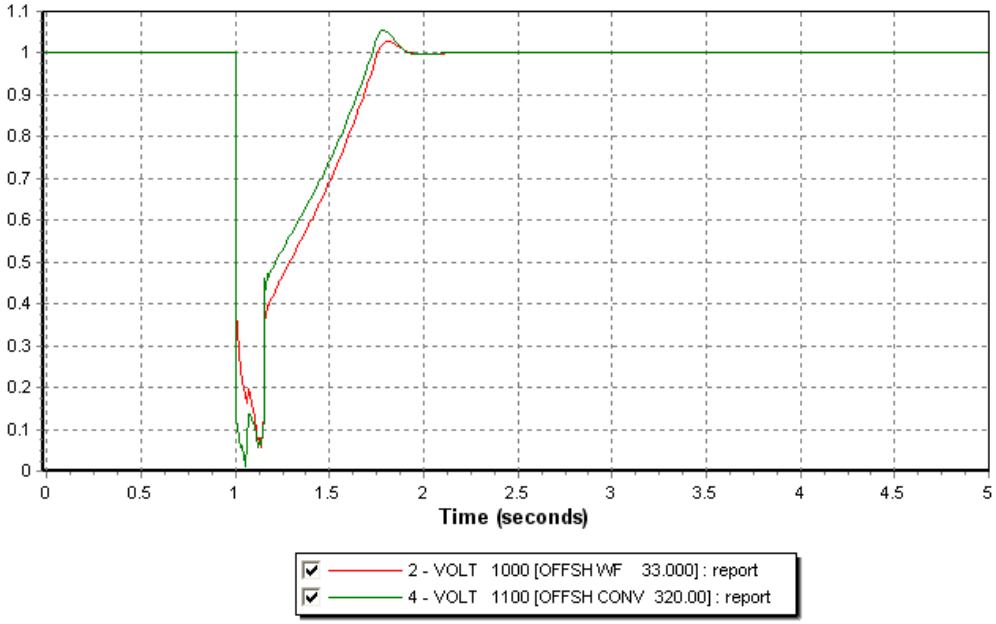

Figure 7-13: Voltage at the connection point with the offshore converter and the main wind farm in pu

The overvoltage before voltage recovering is slightly higher for the transmission bus and the offshore converter. Same observation can be done at the oil rig (buses 1020 and 1120) and at the collecting point of the HVDC (buses 1000 and 1100). The frequency is lower at the transmission buses and the voltage higher.

The HVDC controller stops during the fault to absorb the reactive power created in the system. Then, after the fault has been cleared it produces as much as possible reactive power to raise the voltage up (supplies 400Mvar) and then when voltage is recovered it controls down and regains its original state absorbing 240Mvar. During the fault, the active power through the DC transmission stops progressively. The power flows normally at 1.8s. See next figure.

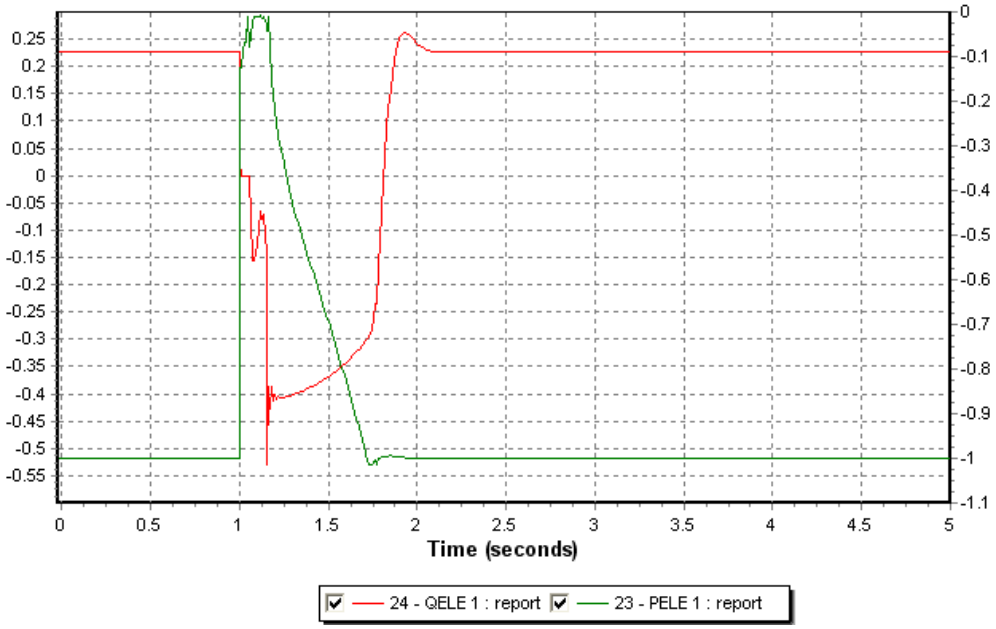

Figure 7-14: Response of the offshore HVDC converter, reactive (reversed axis) and active power

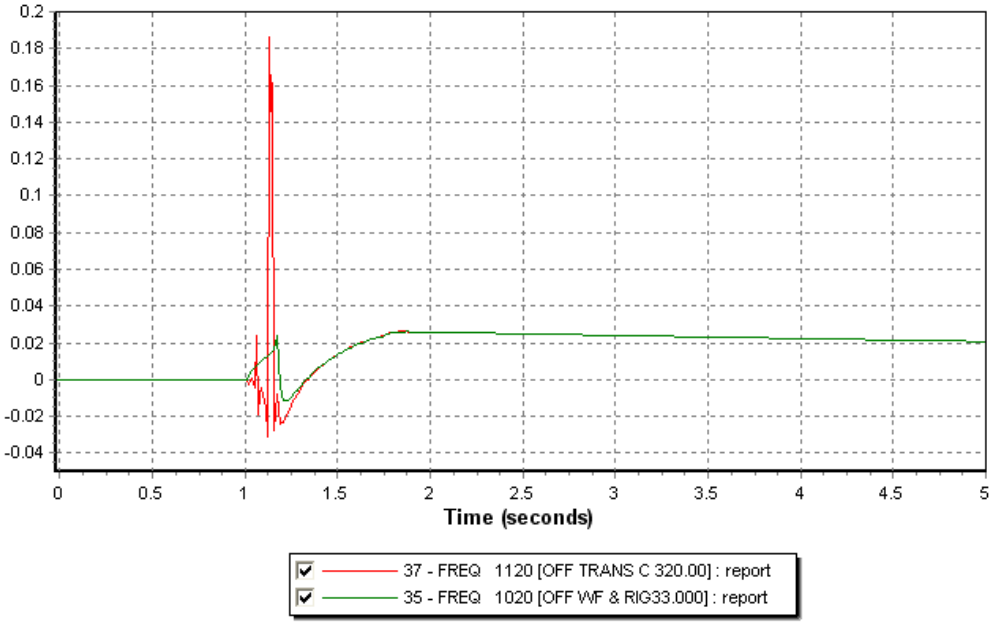

Figure 7-15: Frequency variation at the oil rig (bus 1020) and at transmission (bus 1120) in pu

The frequency close to the fault location oscillates during the fault at the transmission bus whereas it rises for the generator bus. A high peak in the frequency variation can be observed on the transmission bus when the fault is cleared. Rapidly after clearing, frequencies join them and rise until voltage recovery to decrease slightly to the original value. See above Figure 7-15

Low peak of frequency during voltage recovery is observed at the converter bus. This can be explained by the fact that the converter absorbs and need active power. In the same time to ensure the voltage recovery a large amount of reactive power is given by the converter. See below Figure 7-16. There is exactly the same shape for frequency variation for the middle buses 1010 and 1110. Plots are shown in Appendix F - 9. A detailed frequency variation and voltage at the bus fault is given in Appendix F - 11.

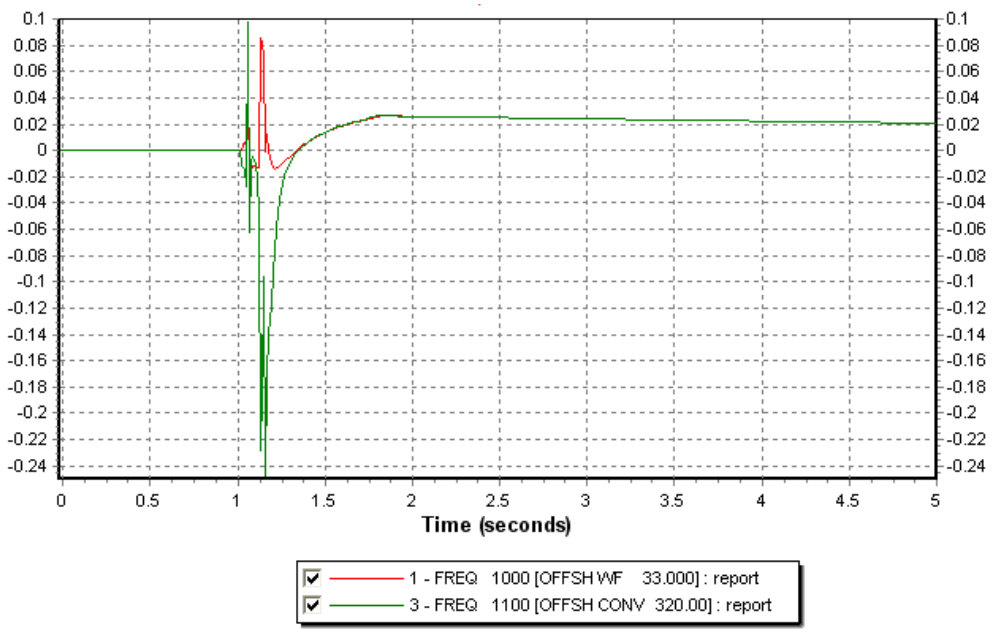

Figure 7-16: Frequency variation at the offshore converter (1100) and the main wind farm (1000) in pu

The dynamic behaviour of the generators during the fault is more or less the same. During the fault the generators stop to supply active power and the speed of the rotor increase (with the frequency). The generators must supply a large amount of reactive power during the fault and then it absorbs reactive power during recovery voltage. Next figures show their dynamic behaviour, Figure 7-17 and Figure 7-18. Detailed dynamic behaviour of generator at the fault can be found in Appendix F - 10.

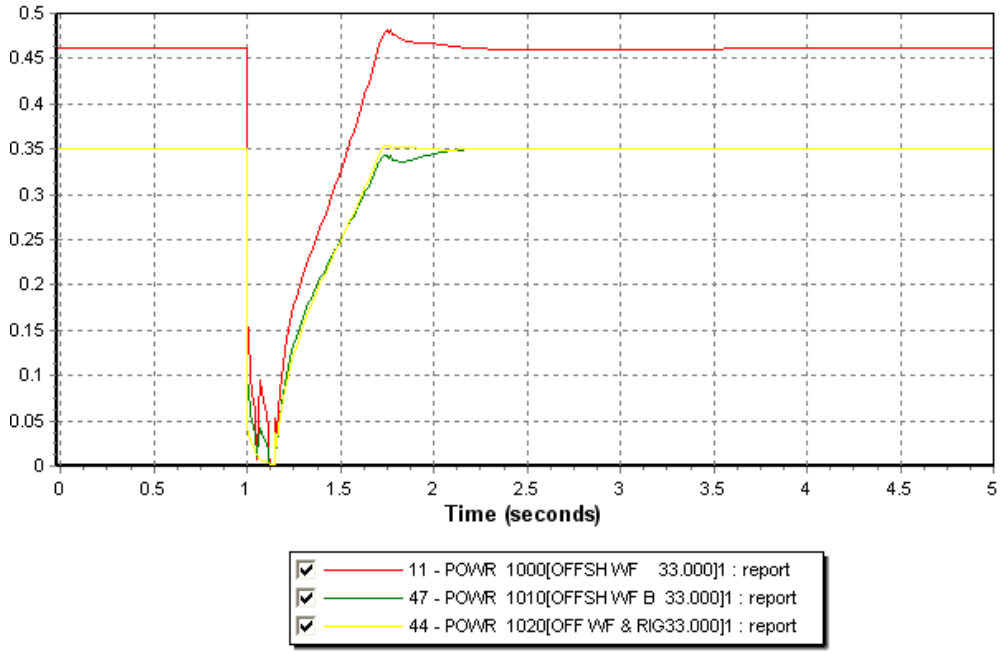

Figure 7-17: Active power supply by the generators in the offshore grid, in pu on system base

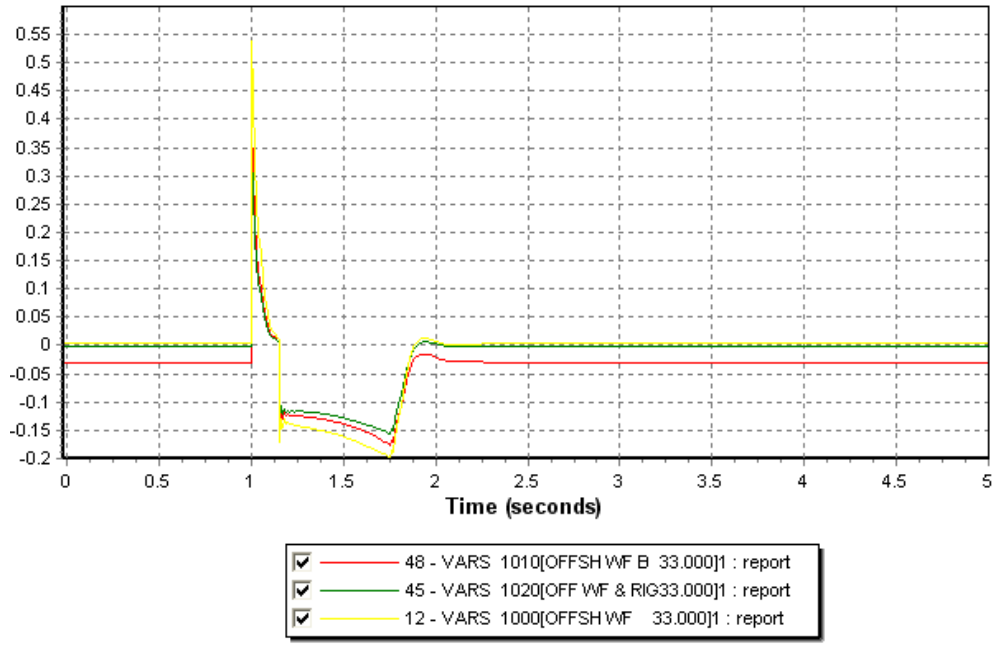

Figure 7-18: Reactive power supply by the generators in the offshore grid in pu on system base

The flow of active and reactive inside the wind farm cluster is represented here. The active power flow is shown in red (left axis) and the reactive power flow inside the cable in green (right axis). The reactive power supplied by the VSC-converter during the recovery is clearly observable, green curve the peak between 1.2 and 2s. The stop of the active power flow inside the cable is also observable. See Figure 7-19.

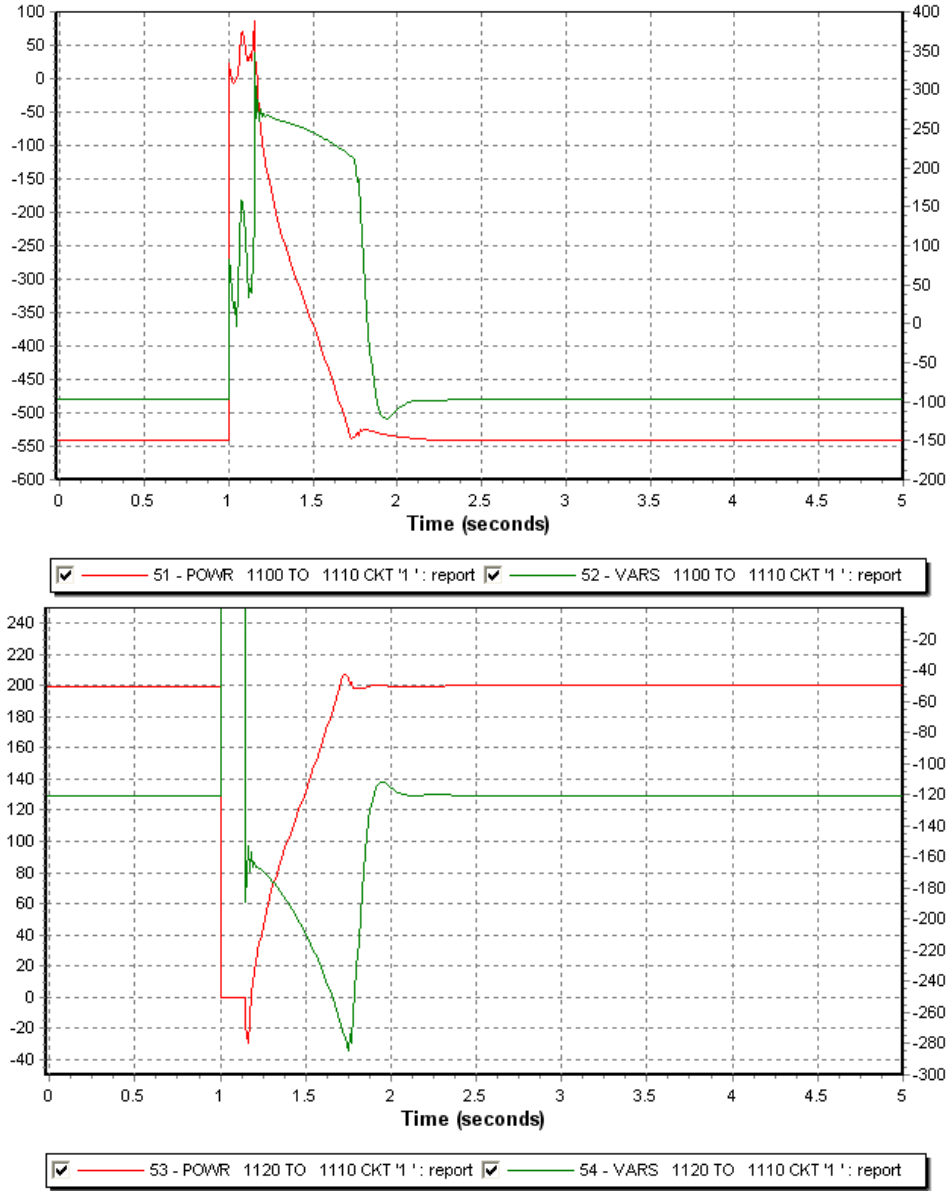

Figure 7-19: Flow of active and reactive power in the submarine cables in MW and Mvar.

7.5 REPLACEMENT OF A DFIG BY A FIG AT BUS 1010

The stability will be now analyzed regarding the type of the generator. A mix of the both generator has been used. Two wind farms (at the oil rig and at the HVDC converter) are equipped with DFIG machine by using the Vestas model whereas the central wind farm is modeled by using fixed speed wind turbine generator by using the Bonus model. As said before the fixed speed model has been tested and had given good result while using alone.

7.5.1 INSTABILITY ON THE OFFSHORE GRID

The same fault as previous has been performed at bus 1120 close to the wind farm. The expected result was not the expected one. The system is become unstable as shown below. The possible reasons will be explained later.

The voltage goes down during the fault and then thanks to the reactive power given by the HVDC converter, the voltage tries to recover 1 pu but is only able to reach 0.5pu and finally the system crashes 400ms later. It is interesting to see that the voltage goes down first at the bus with the fixed speed generator, see blue curve in Figure 7-20.

During the steady state the converter absorbs 250Mvar, stops during the fault and after the clearing time the converter reaches its limit (400Mvar), but the first peak was reaching 480Mvar. Thus, it seems that reactive power is missing in order the system goes through the fault. See next page.

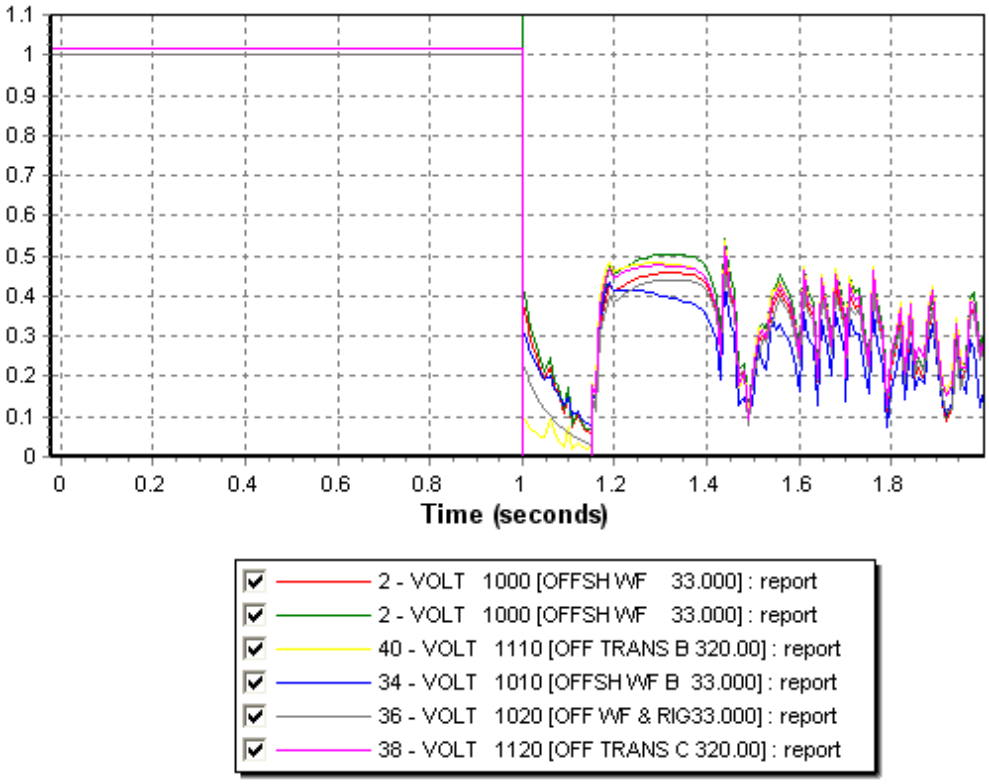

Figure 7-20: Offshore voltage at different buses in pu

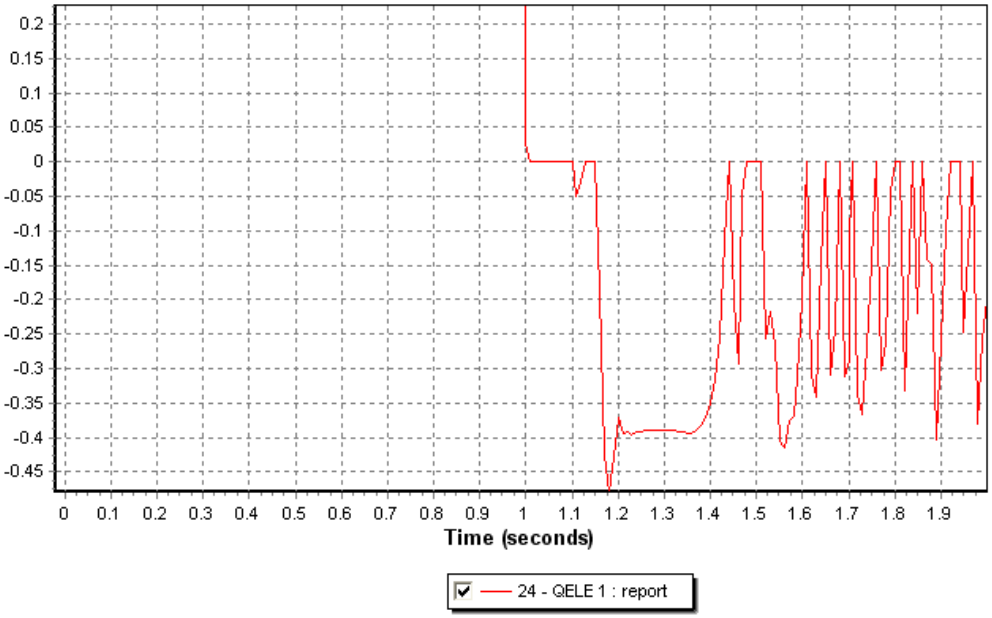

Figure 7-21: Reactive power from the HVDC converter in pu on system base

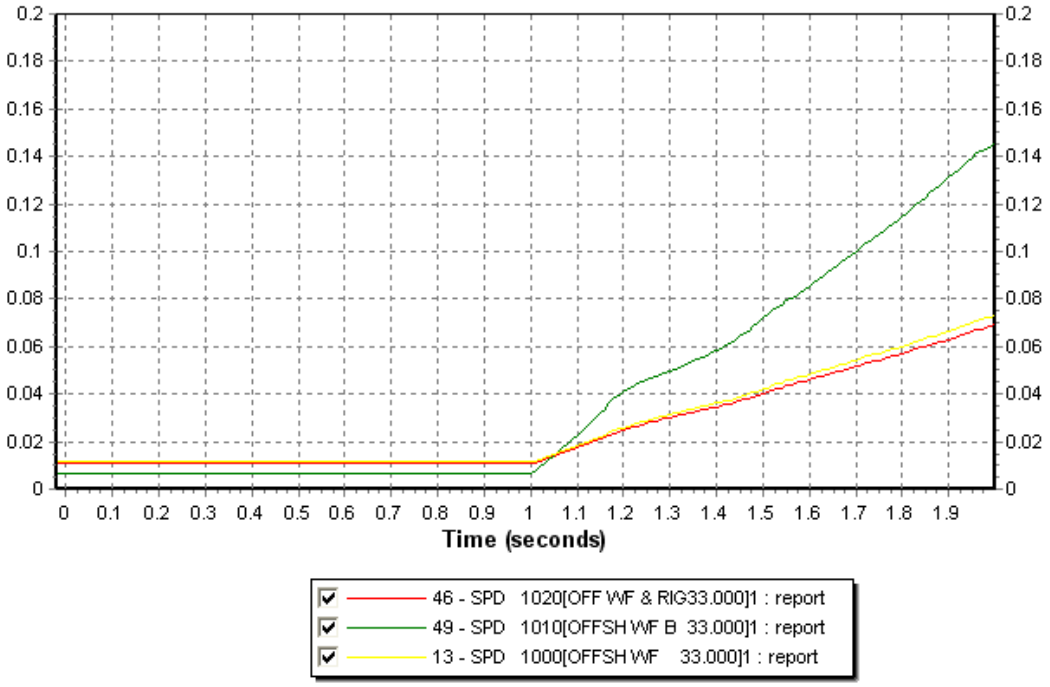

Figure 7-22: Rotor speed for each wind turbine generator in pu, FIG in green

The difference between both technologies can be here clearly observed. The speed increases faster for the fixed speed machine (green curve) than for the DFIG machine because of the control of the second. The consequence of the response of the HVDC converter is observable on the rise of the rotor speed which slows during the contribution of reactive power. See figure above.

Each types of generator don't use the reactive power with the same way, the DFIG technology will absorb a peak of reactive power at clearing time and then slowly decrease this consumption whereas the fixed speed generator will absorb it progressively more and more reactive power, explained by the fact that the voltage is going down in the same time. See Figure 7-23.

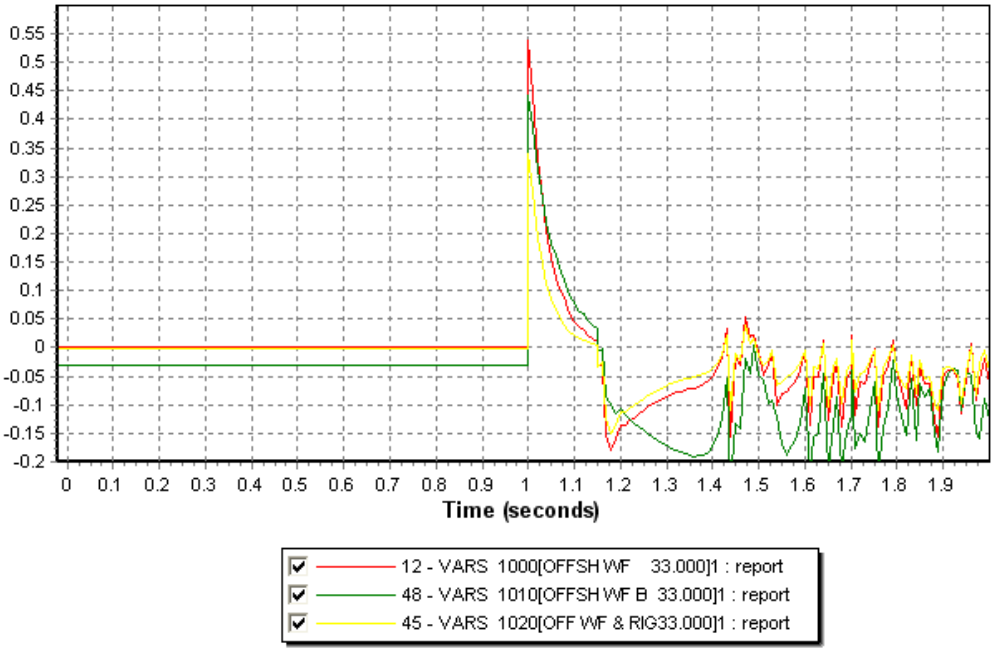

Figure 7-23: Reactive power from the generator, DFIG in red and yellow, FIG in green in pu on system base

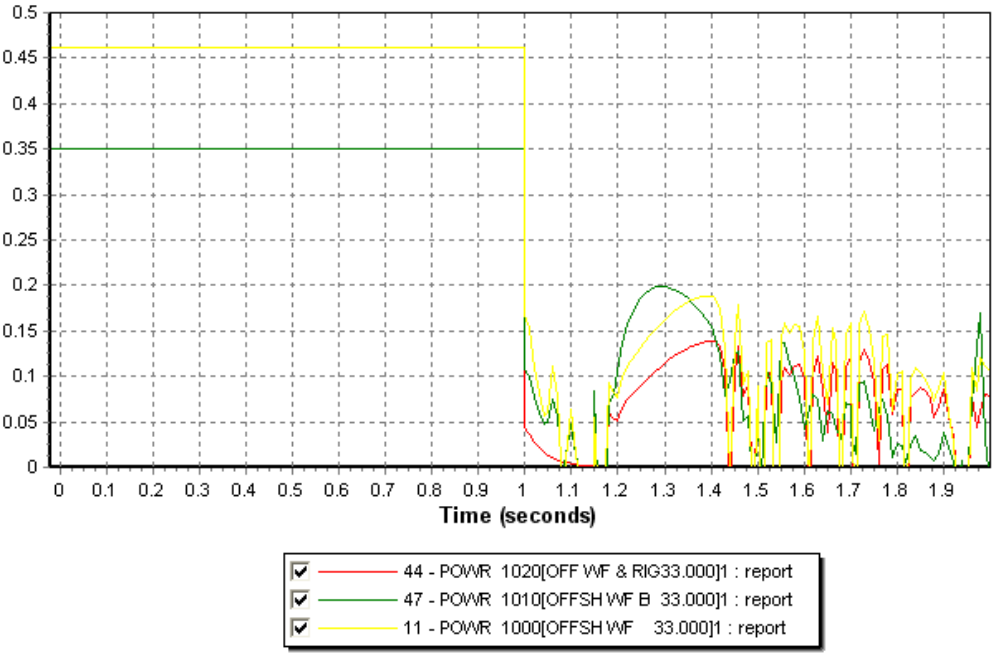

Figure 7-24: Power from the offshore generator, DFIG in red and yellow, FIG in green in pu on system base

Strangely, the fixed speed generator supplies faster more active power (tip around 1.3s) but stops earlier. The active power created by the DFIGs increases progressively until the fixed speed generator stop to supply (1.45s). The rise of generated active power by the DFIG is more progressive. See figure above

Then the system collapses and will lead to a blackout in the offshore grid but thank to the HVDC connection the consequence on shore are very small. Very small frequency and current variations occur. See Appendix F - 12:On shore voltage at bus 5600 and 6000 in pu and Appendix F - 13: Frequency variation at buses 5600 and 6000 in pu on system base.
In the reality all the wind farms would have been disconnected.

7.5.2 BEHAVIOUR OF AN INDUCTION MACHINE

A quick overview of the dynamic behaviour of the machine will be now given to understand why the rotor speed cannot stop to increase. This speed rise leads to destabilize the system.

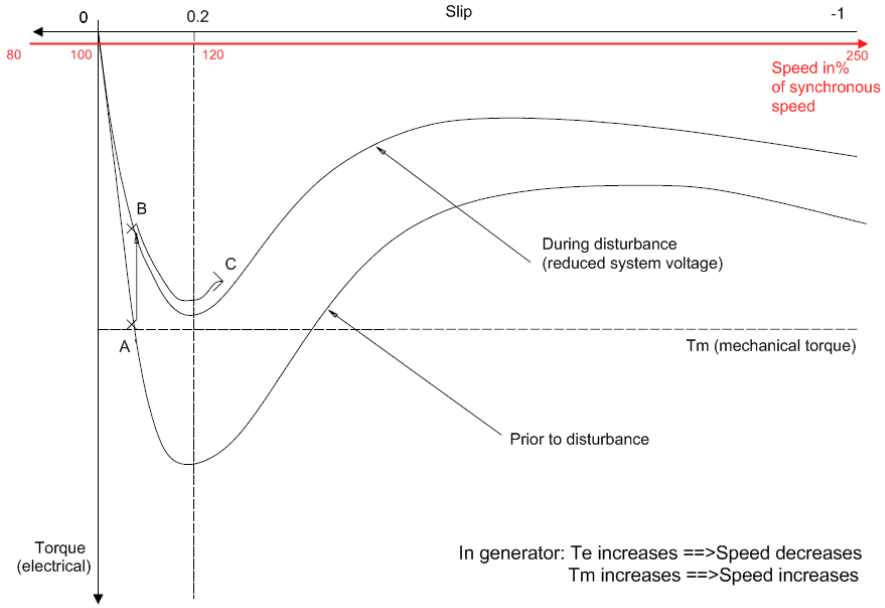

Figure 7-25: Behaviour of an induction machine in generator mode

During the fault the electrical power falls to a low value. So, the electrical torque speed curve changes because of the voltage changing down. On the figure, from the steady state (point A) we move to point B. Because the mechanical torque Tm is greater than the electrical torque Te, the generator accelerates. On the graph it follows the torque speed curve to a point C. If the electrical torque at fault clearing is less than the turbine's mechanical torque and if it had reached a point beyond the breakdown torque it is in unstable position and the rotor speed will run away. It may lead to the destruction of the generator. If the breakdown point is not overpass the system will go to a stable equilibrium between electrical torque and mechanical torque.
The second Law of Newton may also explain the phenomena. For a generator, it is written as follow:

$$J.\frac{d\omega}{dt} = T_m - T_e \tag{5.3}$$

As show on the figure, when Te increases and Tm is constant, the speed decreases, but when Tm increases and Te is constant, the speed increases. In addition it has to be said that the rotor speed is directly connected to the frequency of the grid in case of induction machine.

This paragraph explains why the first wind turbine generation is often disconnected during a fault on the network. Now, some voltage protection can be used to ride through this low voltage and avoid uncontrolled acceleration.

The options to solve this problem are either to get the possibility to have a high reserve of reactive power, either to have a control of the rotor speed or to avoid a very low voltage.
A reserve of reactive power can be achieved by increasing the capability of the VSC-HVDC converter (hard to do in the reality) or by switched capacitor bank. Then, some control can be added on the rotor of the fixed speed, in our case it can be achieved by increasing the inertia of the machine. Finally, the addition of SVC to control the voltage at the bus with fixed speed generator is also a feasible option.

The stability problem will now be tried to be solved.

7.5.3 TEST BY INCREASING THE REACTIVE POWER DURING RECOVERY

The first idea by looking at the response of the HVDC converter is that there is not enough reactive power and the voltage is long to recover. The low voltage leads to the acceleration of the rotor speed. A test with a super HVDC converter which can supply 200Mvar more has been used.

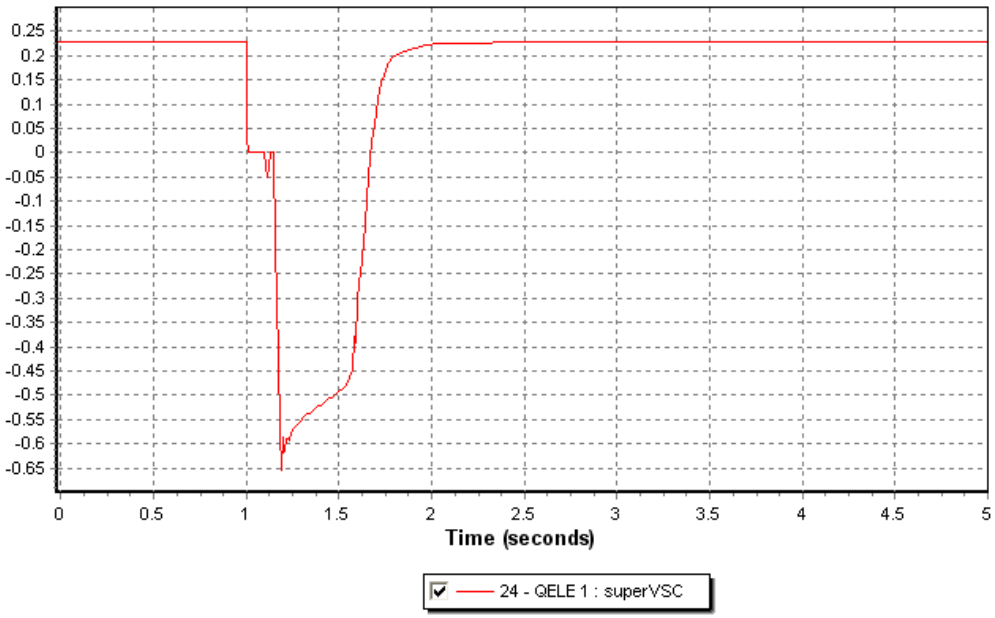

Figure 7-26: Reactive power from the "super" HVDC converter in pu on system base.

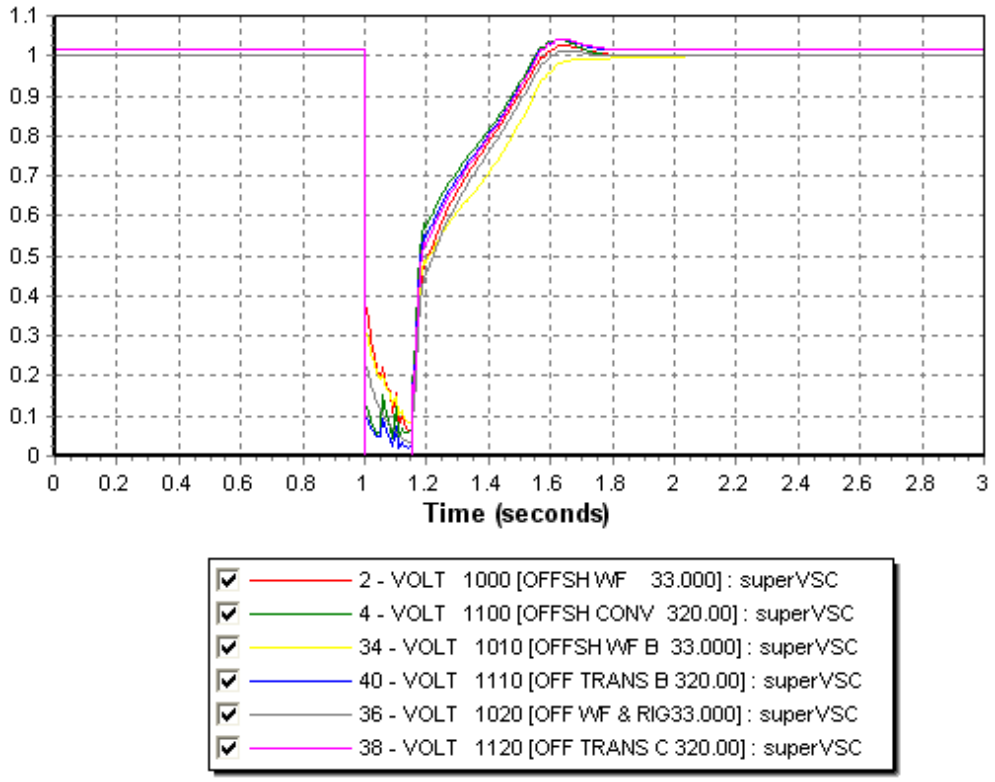

Figure 7-27: Voltage of the offshore grid in pu

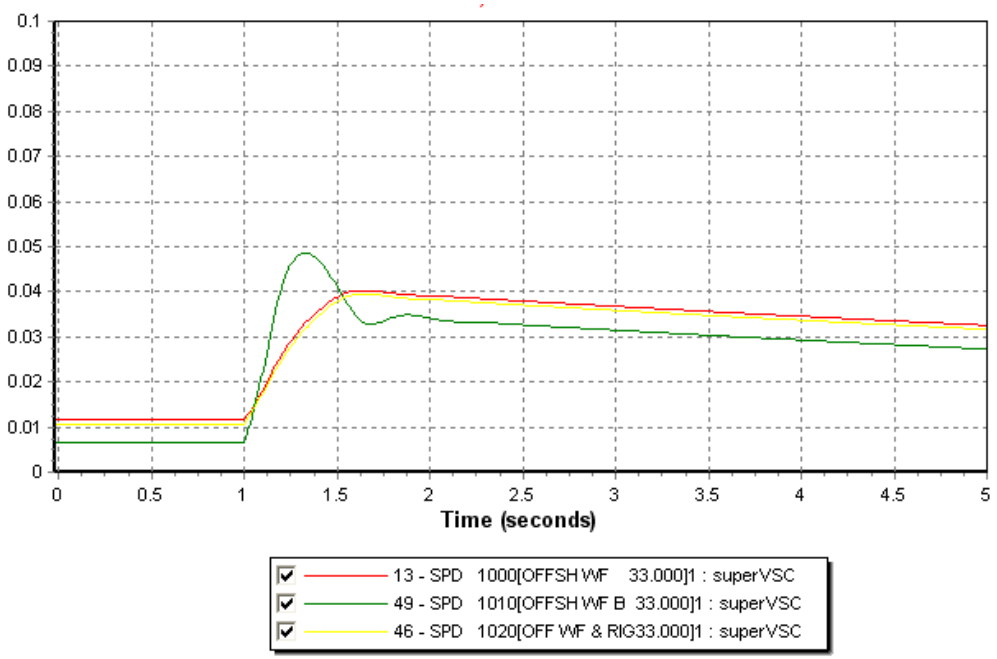

Figure 7-28: Rotor speed of the different generators, FIG in green and DFIG in red and yellow

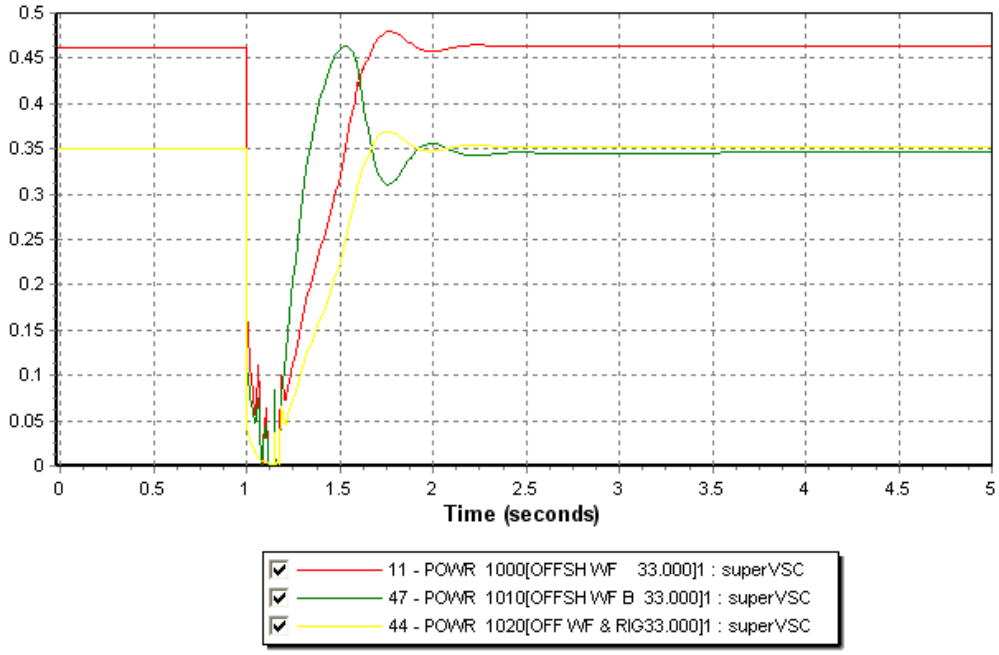

Figure 7-29: Active power from the generator, FIG, in pu system base

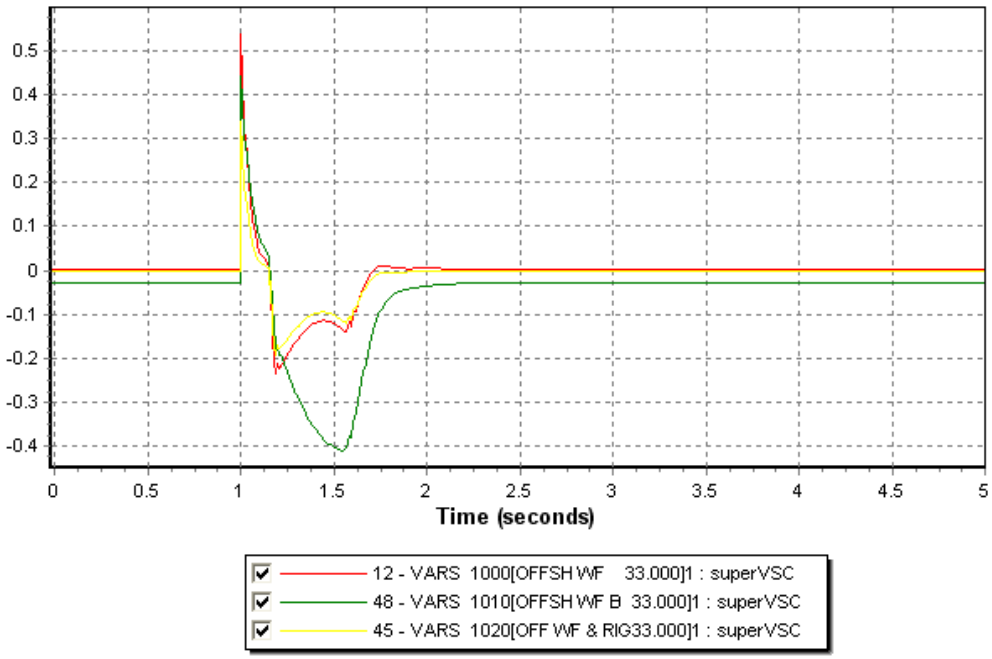

Figure 7-30: Reactive power from the generator, FIG in green, in pu system base

The new super VSC converter is able to supply 600Mvar during the recovery. As shown in the figure above the system is able to go through the fault. It can be observed that a lot of reactive power is needed to stop the acceleration and reverse the rotor speed of the fixed speed generator. This variation can also be linked with the variation of active power during recovery. The voltage recovers and the frequency stabilizes. Increasing the reactive power capability of the VSC-HVDC converter will be an option but this is not feasible in the reality.

7.5.4 TEST BY INCREASING THE INERTIA OF THE FIXED SPEED GENERATOR

To increase the inertia of the machine is also an option. As for the DFIG, a higher inertia will represent a machine with some automatic control. It could be a limited variable speed generator with variable rotor resistance to adjust the torque speed curve of the machine.

Several simulations have been performed to find which value of the inertia will keep the system stable. The characteristic of the VSC converter were unchanged for the simulation (limit in a range of -570Mvar and 400Mvar). The first value that keeps the system stable is H=2.5. A dichotomy process has been used to find it. The simulation is presented below. The system is pretty long to regain its steady state, more than 1.5s. So, it does not fulfill the grid requirements.

The lowest voltage during the recovery is set at the fixed speed generator; it is almost 0.1pu below the others. See Figure 7-31for the voltage inside the wind farm cluster, curve yellow represent the voltage at the fixed speed generator.

The VSC converter doesn't reach its limit during recovery; it supplies less than 400 Mvar. See Figure 7-32 for the HVDC converter response.

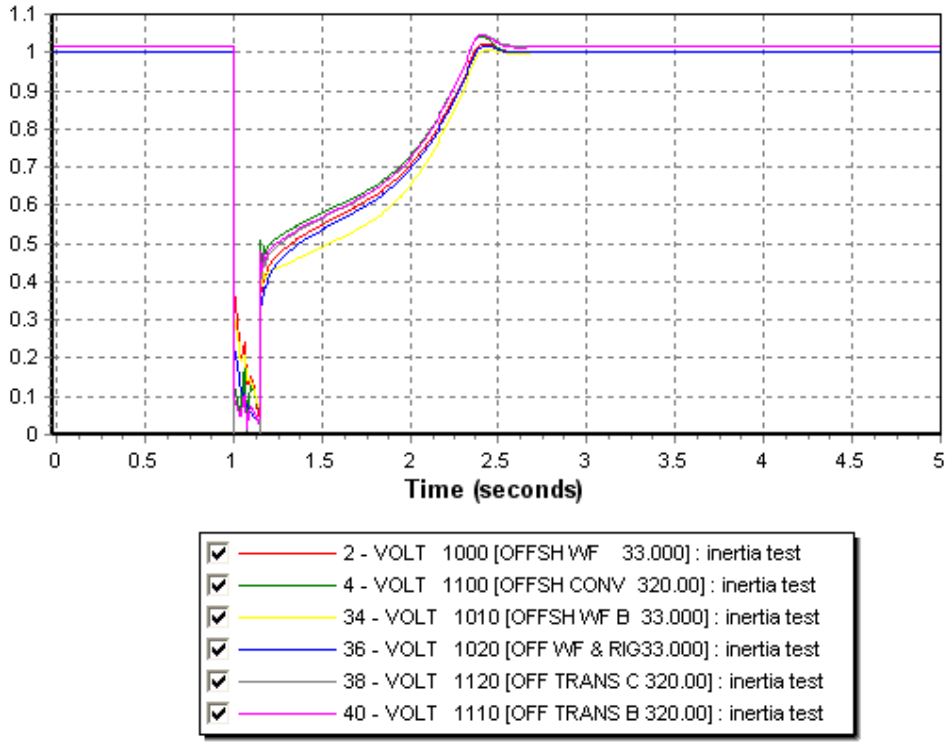

Figure 7-31: Voltage at the offshore buses, fixed speed generator voltage in yellow in pu

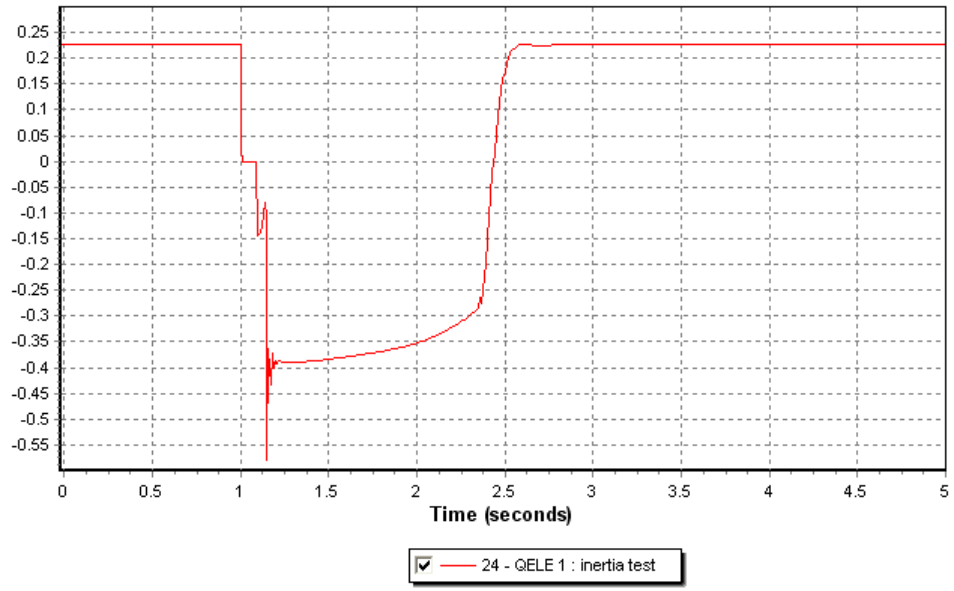

Figure 7-32: Response of the HVDC converter, reverse axis, in pu on system base

The dynamic responses of the generators are also different especially for the reactive power. The fixed speed induction generator need less reactive power than previously almost 200Mvar less. However the fixed speed generator regains its generating state earlier than the 2 other generators. The speed of the generator increase until 0.06pu whereas in the previous simulation in was increasing 0.05pu. This is due to the fact that the system is longer to response, so the rotor speed has more time to accelerate.
The dynamic behaviour of the generators is show next figures. See Figure 7-33: Rotor speed, active power and reactive power generated, FIG in green.

The response of the system doesn't fill the grid requirement, especially about the time of response.

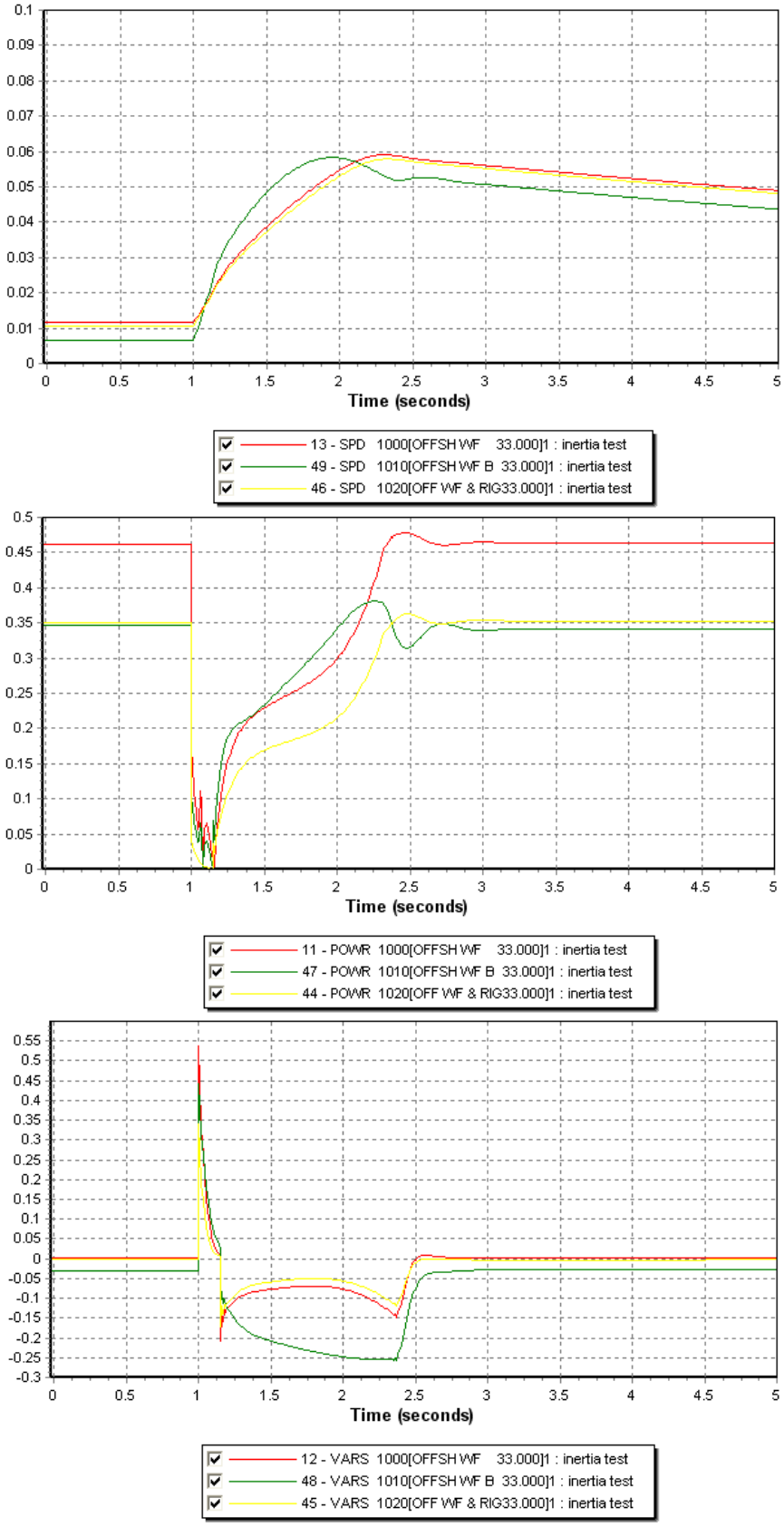

Figure 7-33: Rotor speed, active power and reactive power generated, FIG in green

7.5.5 TEST WITH SVC TO KEEP THE VOLTAGE HIGHER

Another option is to use an SVC to control the voltage at the same bus as the fixed speed generator. As 200Mvar were missing during the recovery, a 250MVA SVC is added at the same bus as the fixed speed generator (bus 1010). A new load flow has been performed and any changes have been observed. The SVC does not generate any reactive power during steady state. On the next figure the SVC is show with the red arrow. The SVC is the same type as those used to regulate the onshore grid (library CSVGN5) and the same dynamic parameters have been used except the MVA rating.

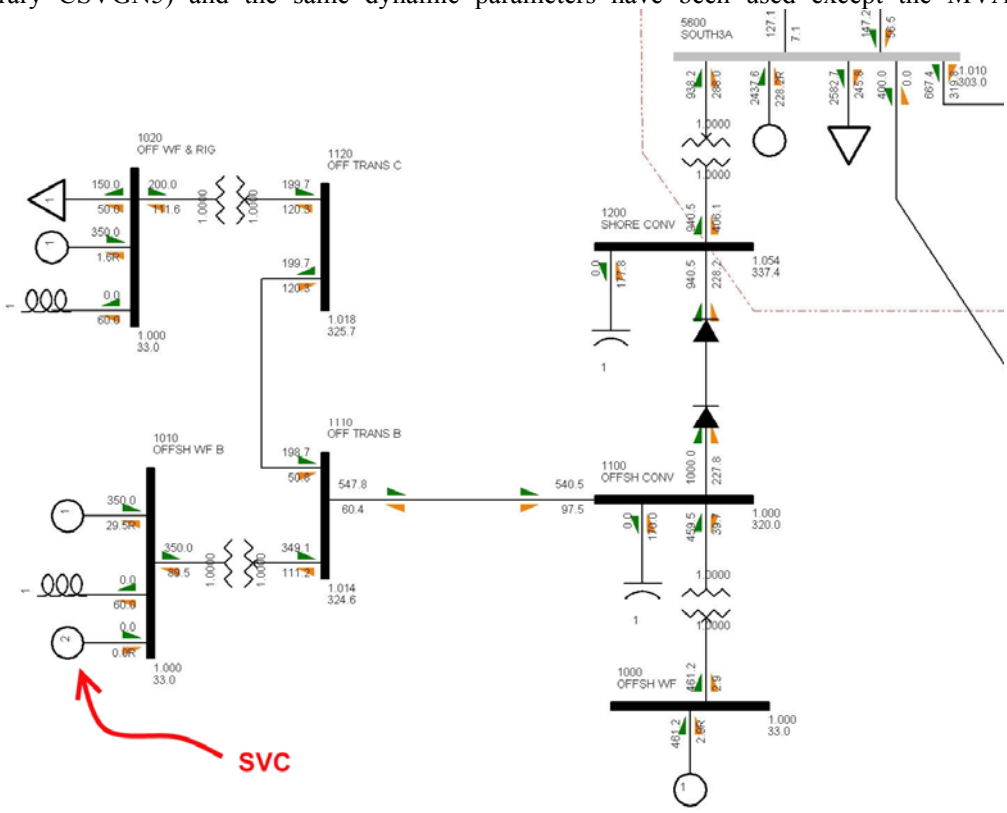

Figure 7-34: Load flow with the 250Mvar offshore SVC at the bus 1010.

The result of the dynamic simulation is presented below. The new system is able to go through the fault thank to the addition of the SVC.

The voltages recover slowly but not as slow as previously; recovering time is approximately 1s. One second is the necessary time to recover a voltage close to 1 pu. According the response of the SVC, the voltage becomes higher than 1pu at bus 1010 for 2s after recovery and then it goes down to 1pu. See the blue curve at Figure 7-35.

The response of the VSC converter is similar as before. It supplies in reactive power the offshore grid during recovery (400Mvar). Afterward it regulates down around 2.5s and absorbs the excess to stop the rise of the voltage and to stabilize it. See next page Figure 7-36.

The SVC get the same kind of dynamic behaviour, but it supplies longer in reactive power to maintain the voltage above 1pu at bus 1010 and then regulates it down around 5s. Just after the fault has been cleared the voltage is low so the SVC is not able to supply at its maximum but it increases progressively its contribution with the increase of the voltage (from 1.15 to 2.2s). See below Figure 7-37.

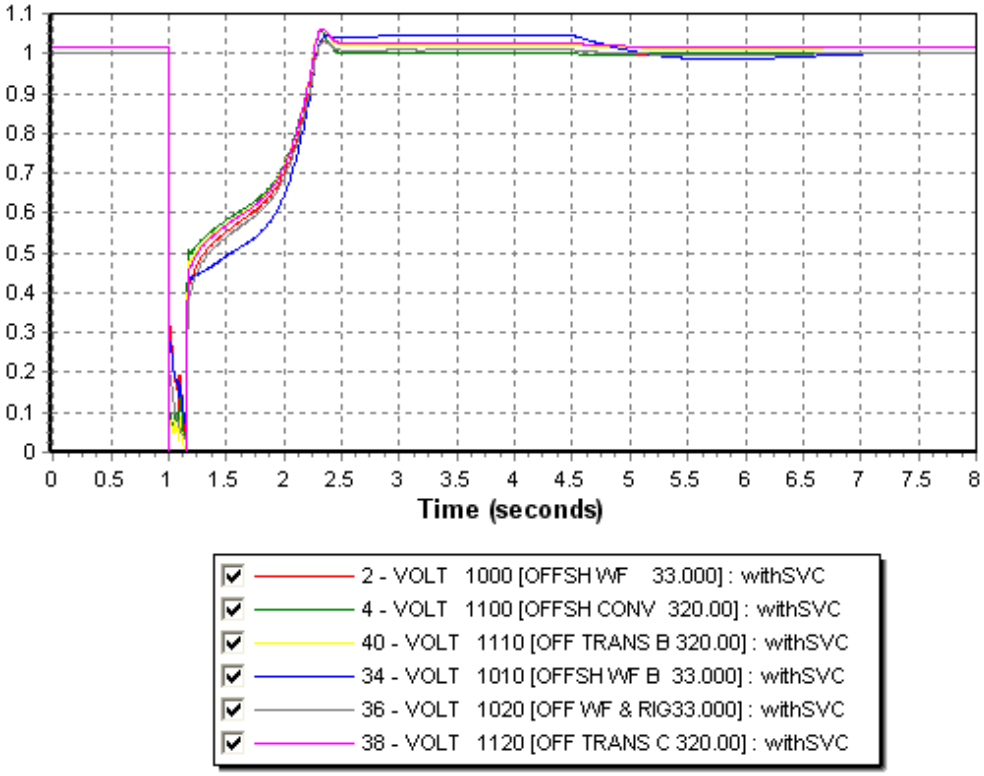

Figure 7-35: Offshore voltage at different buses in pu

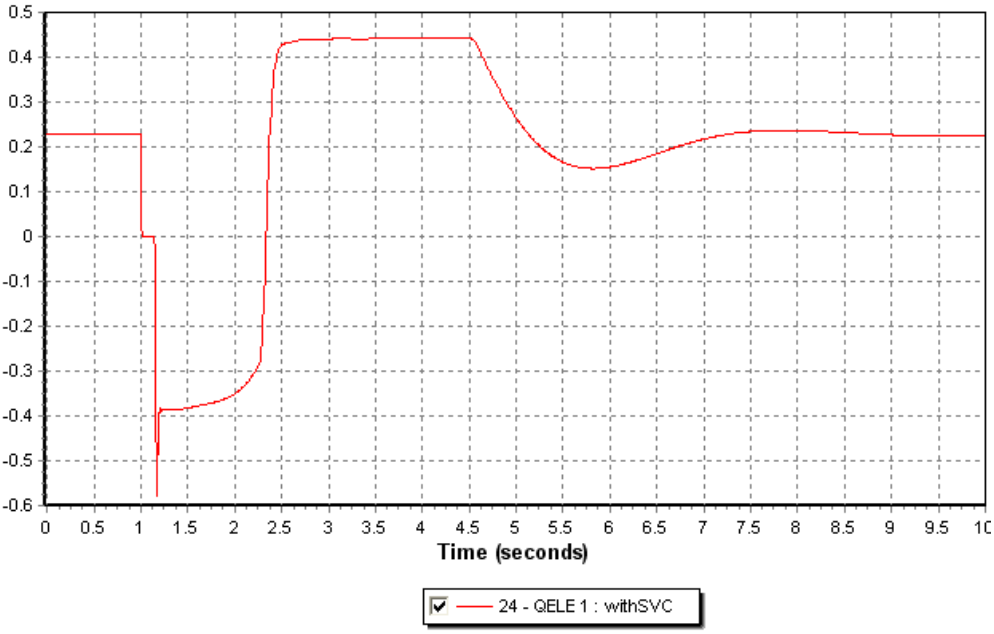

Figure 7-36: Reactive power from the HVDC converter in pu on system base, reverse axis

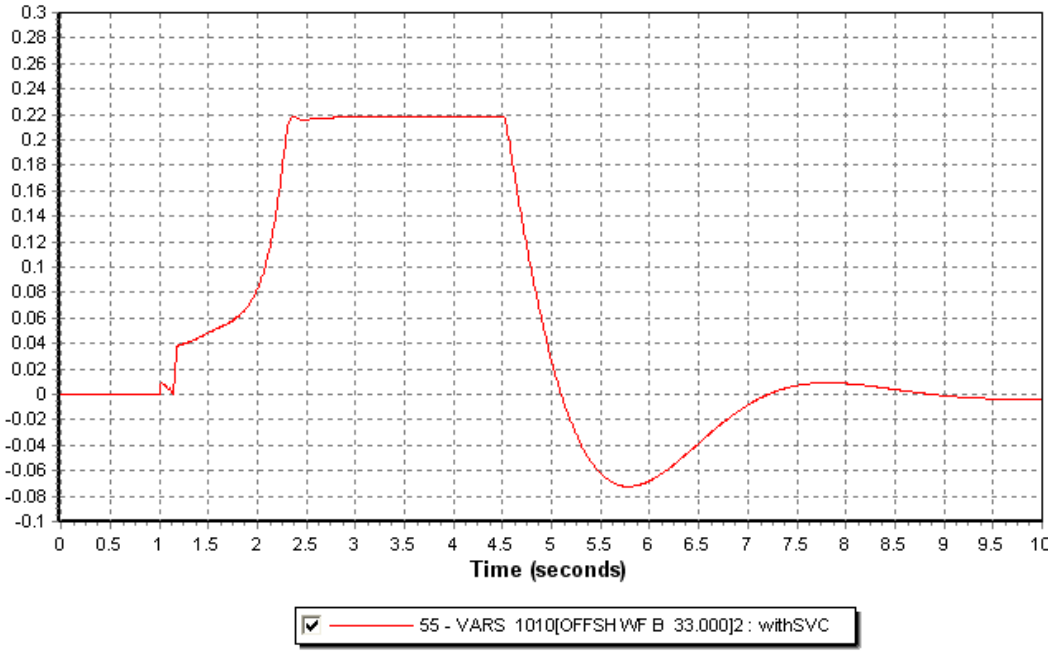

Figure 7-37: Reactive power from the SVC at bus 1010 in pu on system base

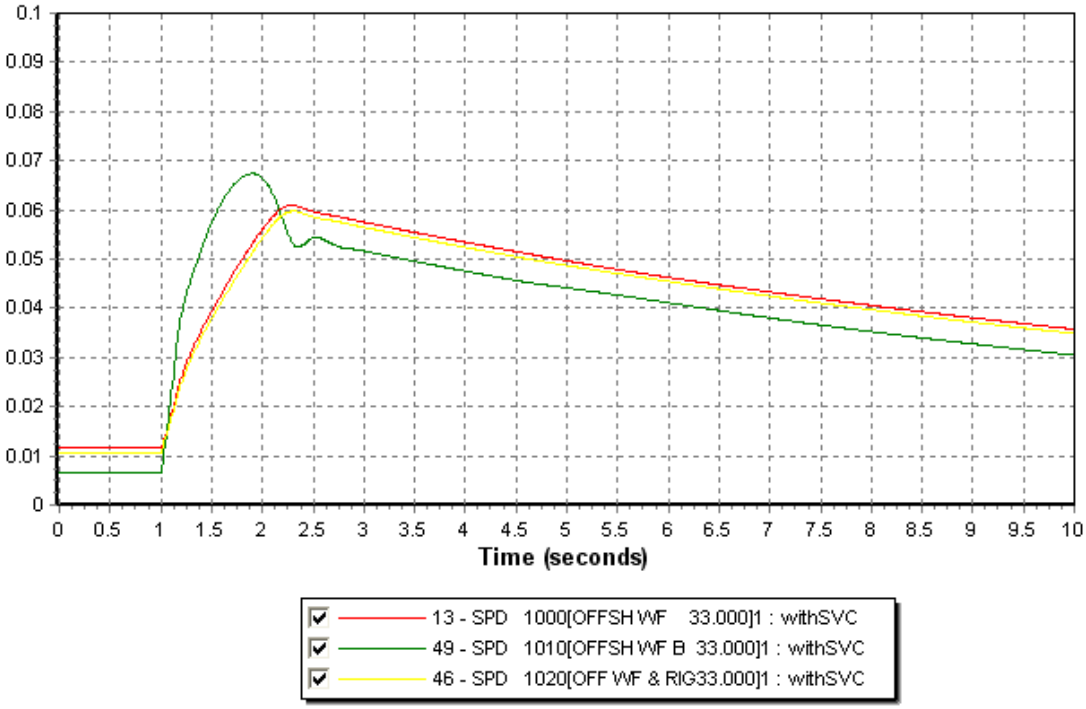

Figure 7-38: Rotor speed for wind turbine generator, fixed speed generator in green

The behaviors of the offshore generators are similar than previously. The rotor speed of the fixed speed generator accelerates more than the 2 others, but goes down quicker. Finally rotor speeds stay under control and go slowly down. See figure above.

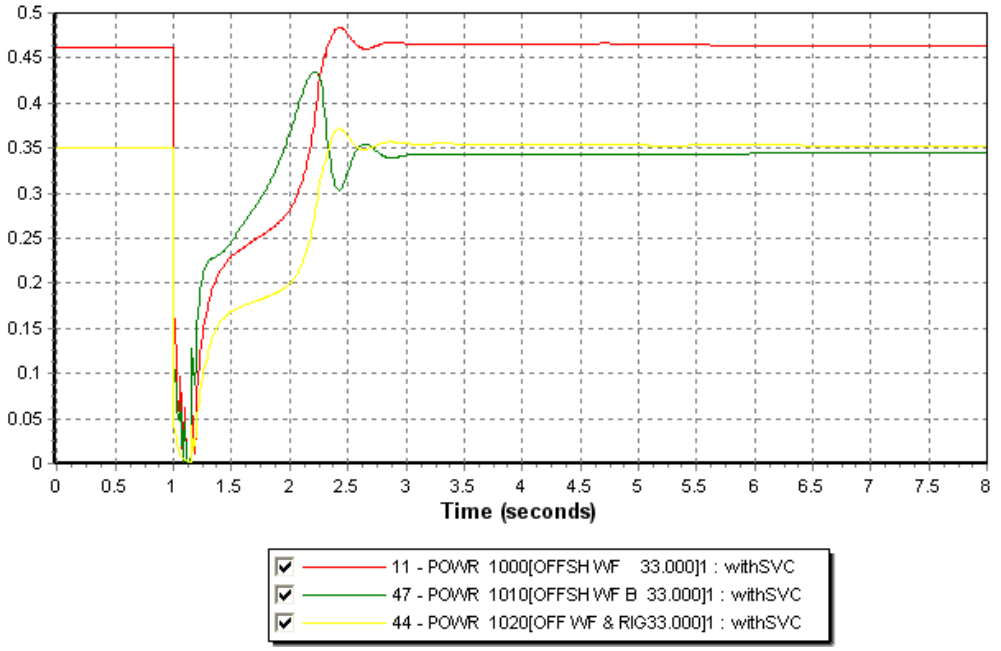

Figure 7-39: Generated power from the wind farms in pu on system base, fixed speed generator in green

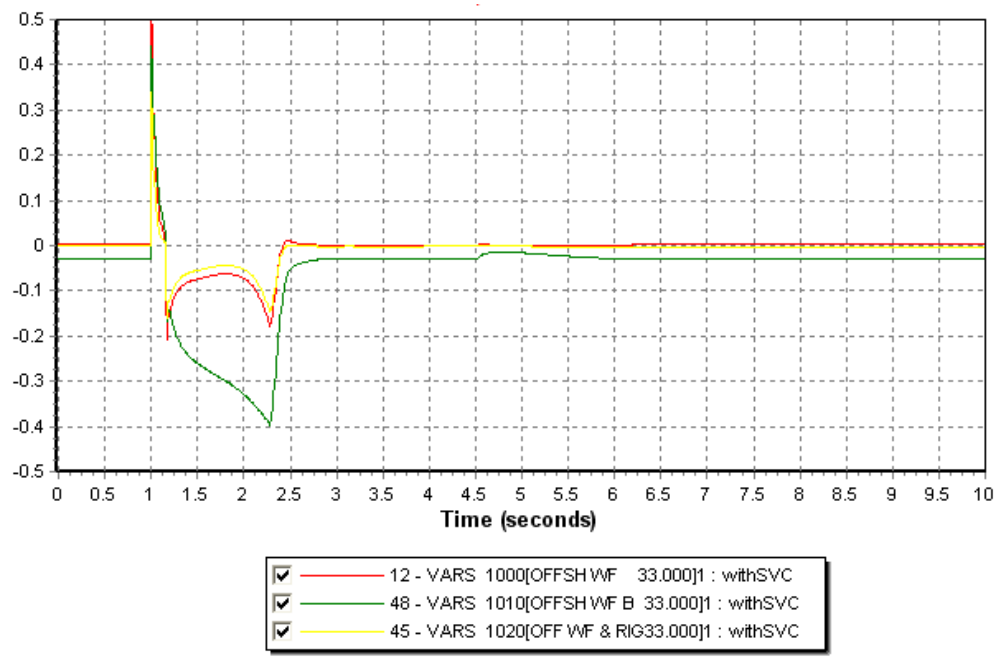

Figure 7-40: Reactive power from the wind farms in pu on system base, fixed speed generator in green

The fixed speed generator reaches a generating state faster than the DFIGs even if it has higher oscillations. See green curve in Figure 7-39. The generators react with similar way as previous.

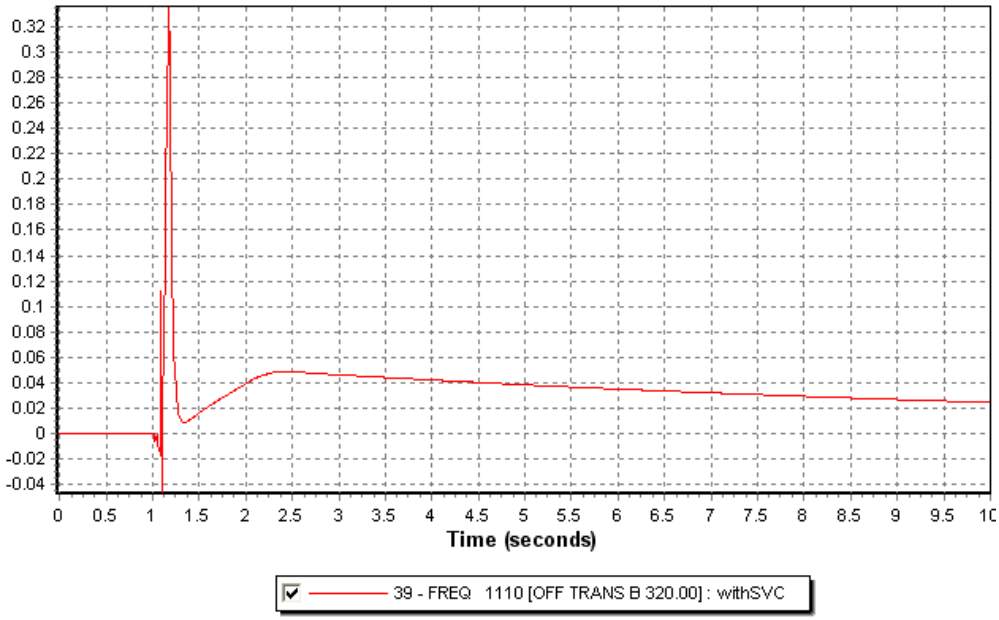

Figure 7-41: Frequency variation at the offshore grid, 0.02pu = 1Hz

The frequency after the fault rises up to 52.5Hz (around 2.5s) by ignoring the peak but then goes slowly down to a higher value 51Hz (from the curve).

7.5.6 DISCUSSION

Using each technology of generator separately is not a problem. However the mix of different types of turbine must be studied in detail. In our case, the replacement of a wind farm equipped with DFIG by a wind farm equipped with fixed speed generator changes the stability of the offshore grid. It becomes unstable because of the different dynamic response of each generator. The need of reactive power to reach a good voltage is different after the fault has been cleared.

Simulations with only FIG have been performed in the wind farm cluster model in order to validate the stability of the model used and to have an idea of the dynamic behaviour of the model. The stability was good and the offshore grid succeeded to ride though fault and disturbance. However, the results of this simulation are not presented in this report.

Due to the capability of the DFIG to run at low voltage, at least the better ride through fault capability than the fixed speed generator, the voltage stays low too longer for the induction machine and then the torque speed curve move to an unstable point for the classical induction machine. In the same time the DFIG doesn't reach this unstable state according to its control. The fact that a part of the grid responds "slower" and so is less subject to low voltage whereas the fixed speed generator reacts faster and then reaches a low voltage earlier and also the breakdown point of stability. In case of a grid equipped only by fixed speed the time with low voltage is shorter and the wind farms are able to recover a stable state. This explains why the same simulation done with only fixed speed turbine stay stable.

This problem could be studied deeper with more detailed wind turbine models and might be a further work.

8 SIMULATION: CONNECTION OF UNIQUE LARGE WIND FARM WITH 2 HVDC TRANSMISSIONS

In this section, a large wind farm is connected to the shore with 2 VSC-HVDC transmissions. THE PCCs are those defined in the chapter 4 (bus 5600 and 600). An offshore fault will be performed at the wind farm and a second simulation will simulate a tripping of the line onshore consequence of a fault. This line links the 2 PCCs. The emphasis will be put on this simulation.

8.1 LOAD FLOW CASE

The load flow is almost unchanged to the shore. The voltage is the same whereas the angles are slightly changed down. The HVDC converters are set with a voltage control on the connection buses. There are supposed to supply half of the reactive power generated or absorbed. The converter connected to bus 5600 reach its nominal reactive power limit, so in order to ensure a reactive power reserve, the converter supply only a quarter of the reactive power needed at bus 5600. The rest is given by the generator.

Bus number	Name	Voltage [pu]	Angle [°]	Pgen [MW]	Qgen [Mvar]
3300	SV-SW	1.000	0	4013.2	2324.3
5400	CNTR3 A	1.007	33.1	1637.5	130.4
5401	CNTR4 A	0.998	30.6		
5600	SOUTH 3A	1.010	28.5	2537.6	380.0
5601	SOUTH 4A	0.992	28.7		
5602	SOUTH 4B	0.969	23.1		
5603	SOUTH 3B	0.936	21.1		
6000	WEST 3	1.005	33.4	1064.2	-105.3
6001	WEST 4	1.000	32.4		
6100	NWEST 3	1.000	32.6	2419.2	749.0
1000	OFFSH WF	1.000	0	1003	49.1
1100	OFFSH CONV A	1.000	-8.1		
1200	SHORE CONV A	1.068	35.3		
1300	OFFSH CONV B	1.000	-8.1		
1400	SHORE CONV B	0.994	40.7		

Table 8-1: Load flow in the surrounding of the PCCs and at the offshore wind farm

The detail of all the load flow can be found in the appendices and the next figure show a zoom on the load flow in the HVDC transmissions. Appendix G - 1 shows the bus voltage and the angle. The power exchange and the generation per area is given in Appendix G - 2. The load flow between the area is almost unchanged according to the losses in the second HVDC transmissions.As indicated in the load flow the upper HVDC transmission has higher losses because of the length of the transmission set at 200km for 100km for the other one. Joule losses are around 10MW per 100km.

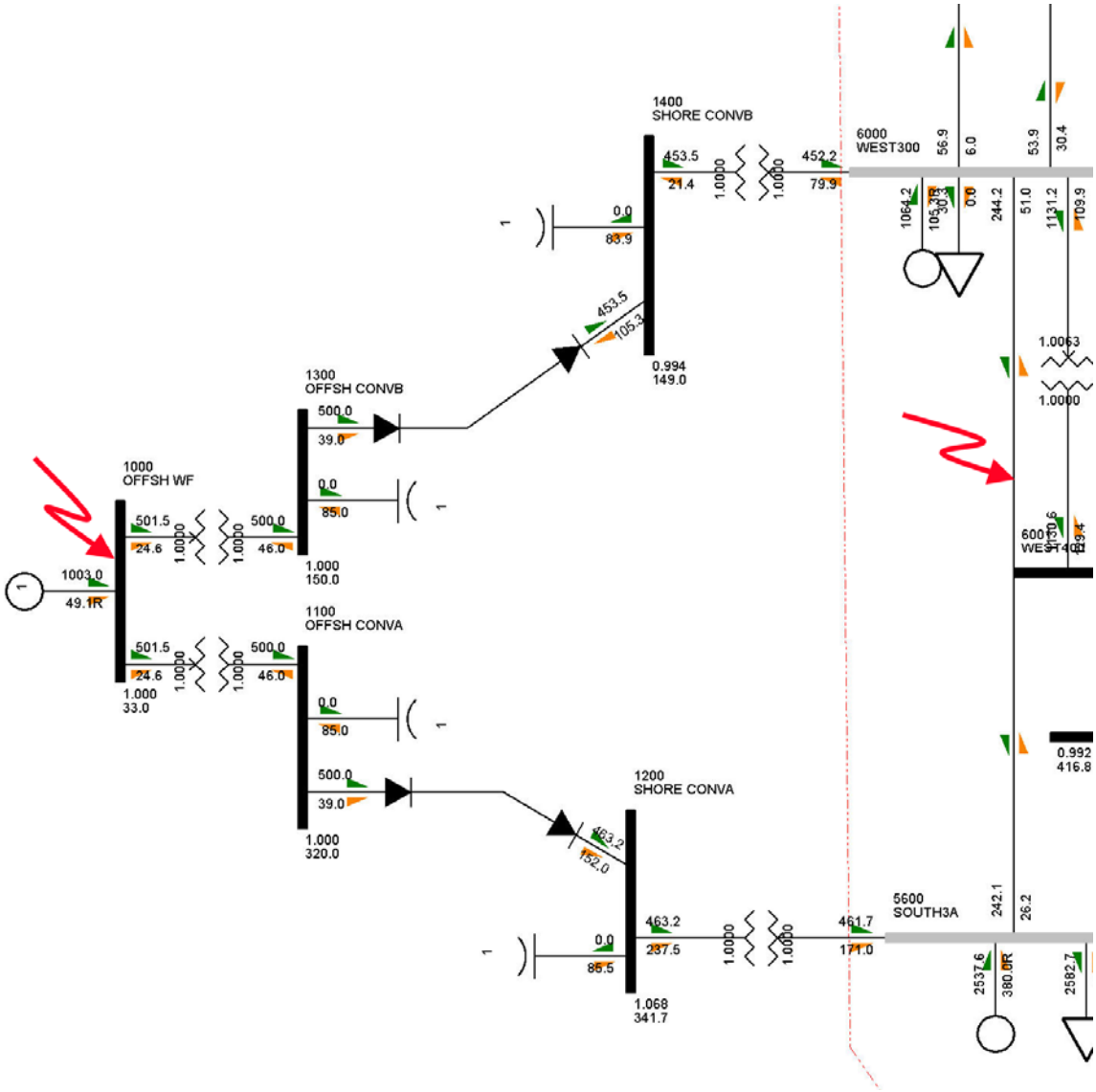

Figure 8-1: Picture of the offshore wind farm and the 2HVDC transmissions.

8.2 OFFSHORE FAULT AT THE WIND FARM

A fault is applied at the bus 1000. The dynamic response of the system is explained below. The voltage recovers 500ms after the fault has been cleared.

At clearing time the voltage recover instantaneously 0.6 pu and then increase progressively during 400 ms to 1 pu. An unexpected peak can be observed during the beginning of the recovery. See Figure 8-2. It can be linked to the peak in the reactive power response of the HVDC converters.

The voltage response of the system is completely different as with one converter. There is here no peak voltage and the difference here can not be explained.

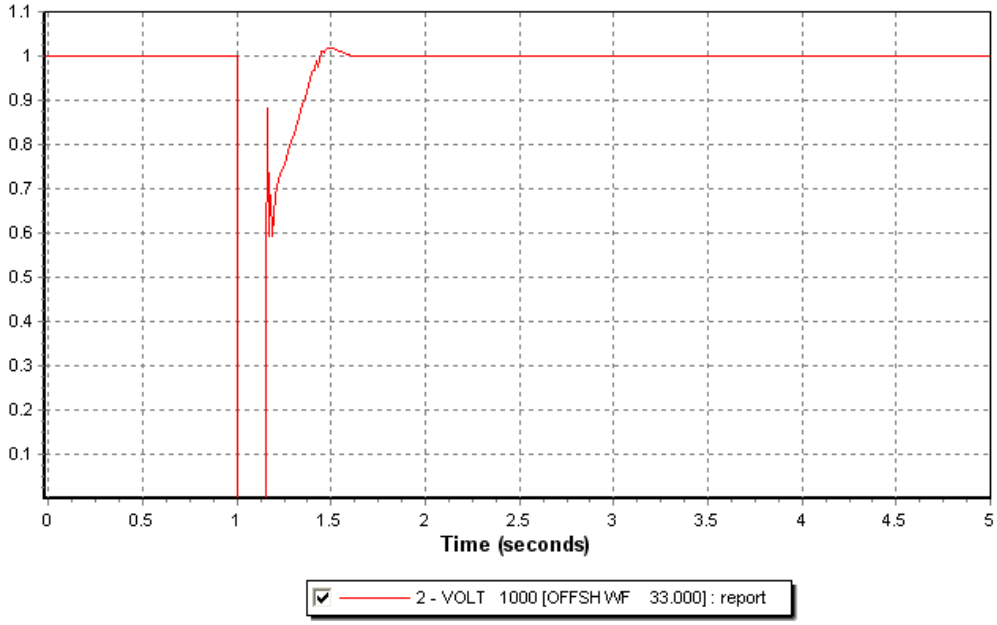

Figure 8-2: voltage at the bus fault in the offshore wind farm in pu.

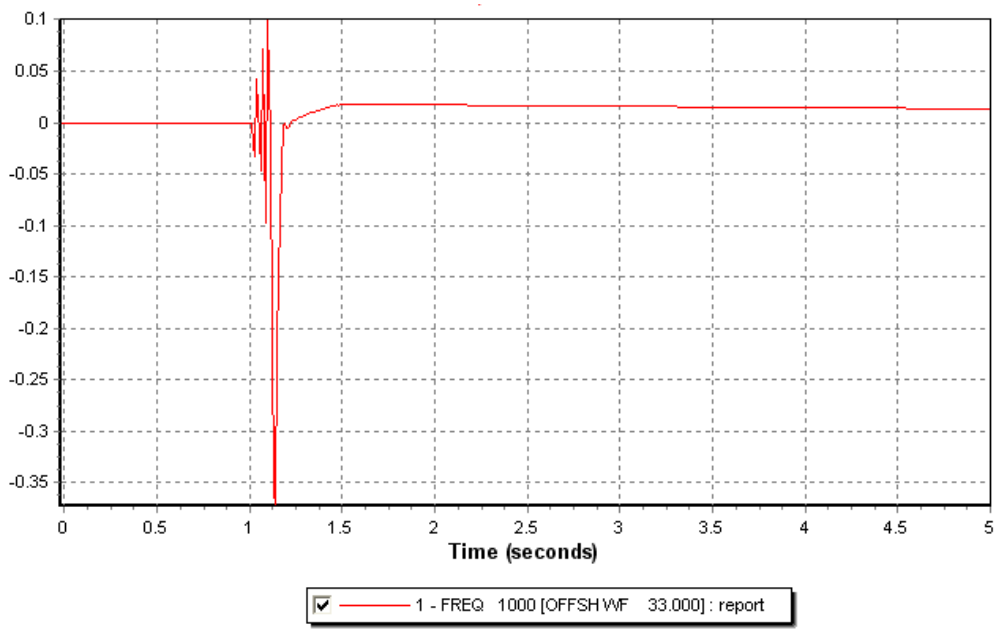

Figure 8-3: Frequency at the bus fault in the offshore wind farm.

The frequency is oscillating during the fault, then a peak down occurs reaching 35Hz and finally frequency rise up to 52 Hz to going slowly to its original value. See Figure 8-3.

Both offshore converters have the same dynamic behaviour according to the symmetry of the system. Absorbing reactive power (39Mvar) in the steady state, they stop during the fault and huge variations during the clearing time occur, then they supply 220Mvar to rise up the voltage. The steady state is recovered slightly after the voltage.

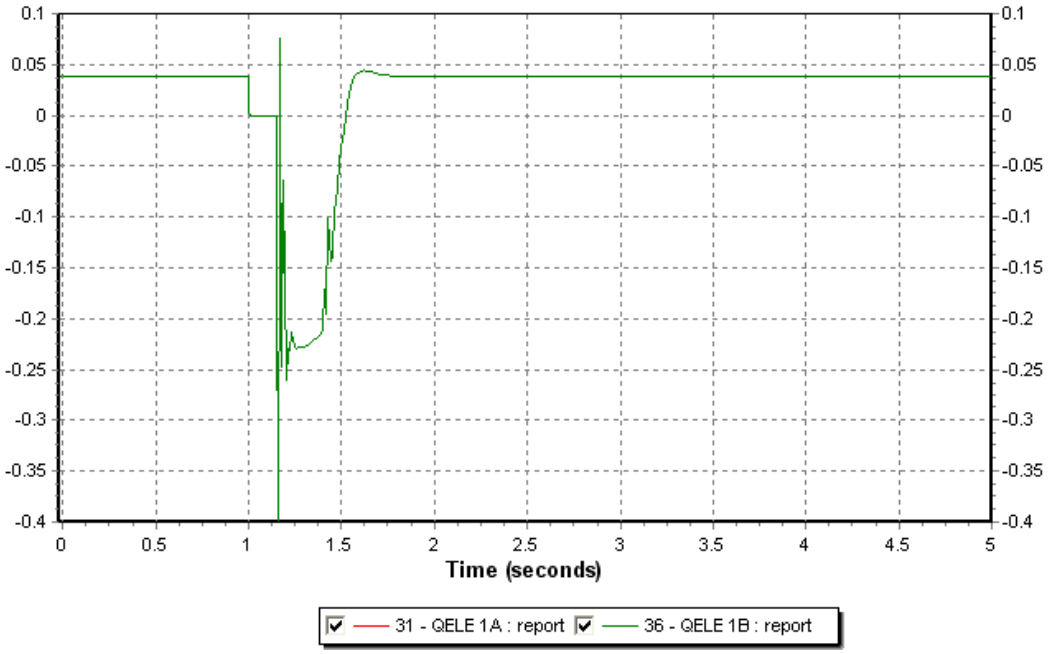

Figure 8-4: Reactive power from the offshore HVDC converters in pu on system base, reversed axis

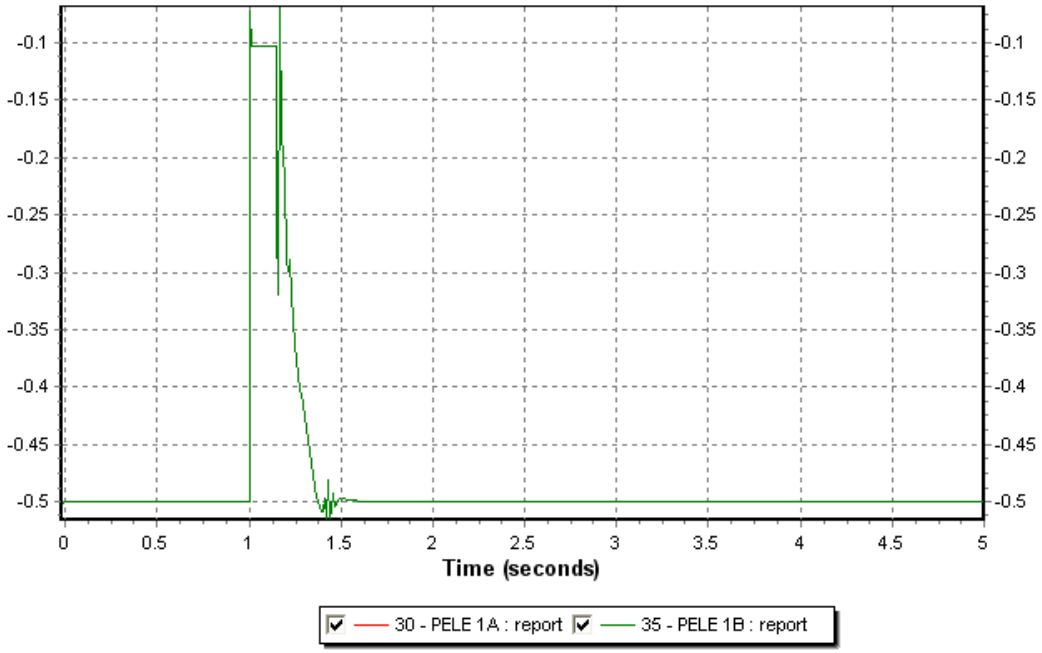

Figure 8-5: Active power from the offshore HVDC converter in pu on system base

The generator absorbs the entire reactive power produced by the converter to regain the original voltage and the nominal active power produced. See Figure 8-6. The speed of the wind turbine generator will increase during all the duration of the fault and then decrease slowly after clearing to its original value. See Figure 8-7 next page.

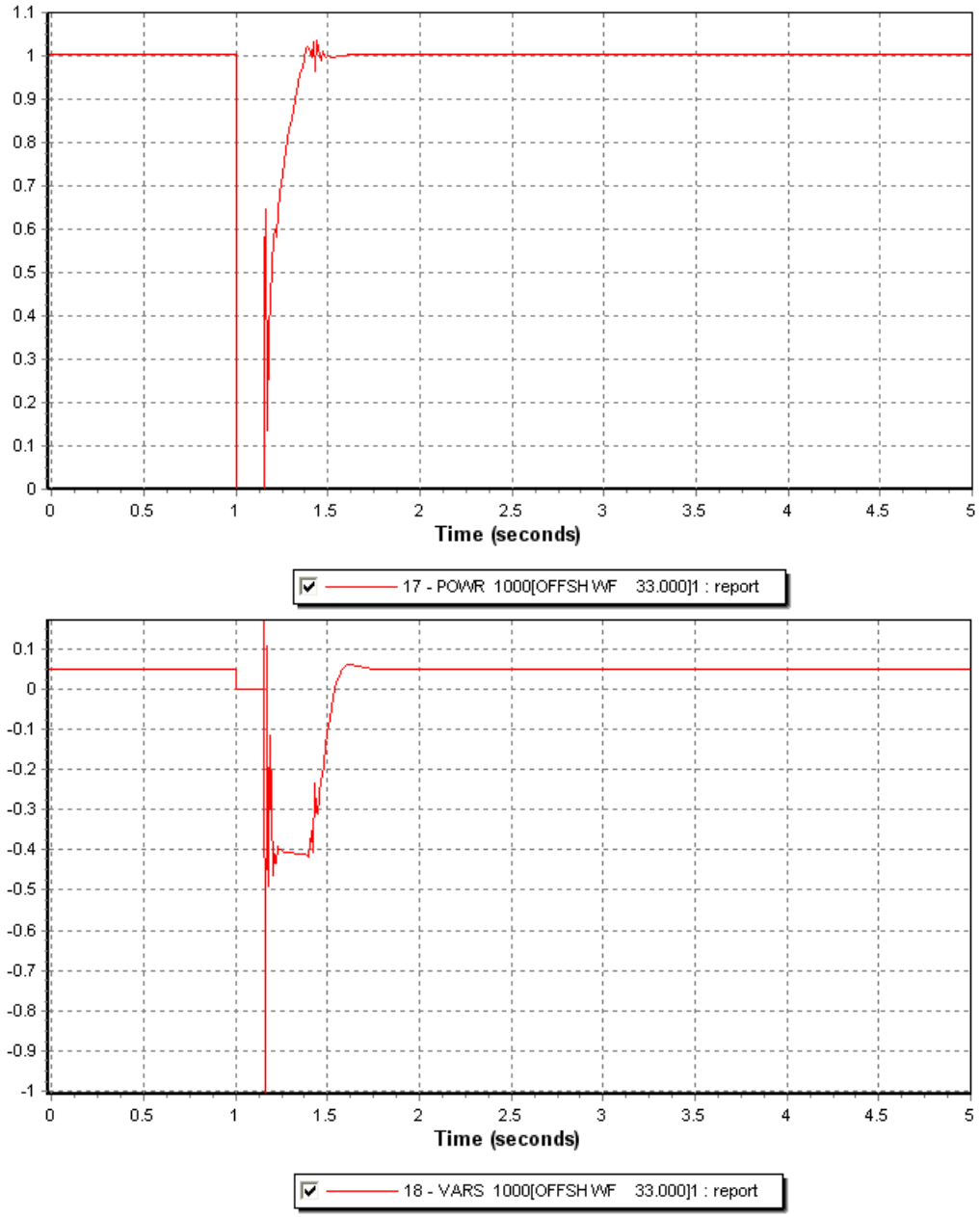

Figure 8-6: Active and reactive power produced by the wind farm, in pu on system base

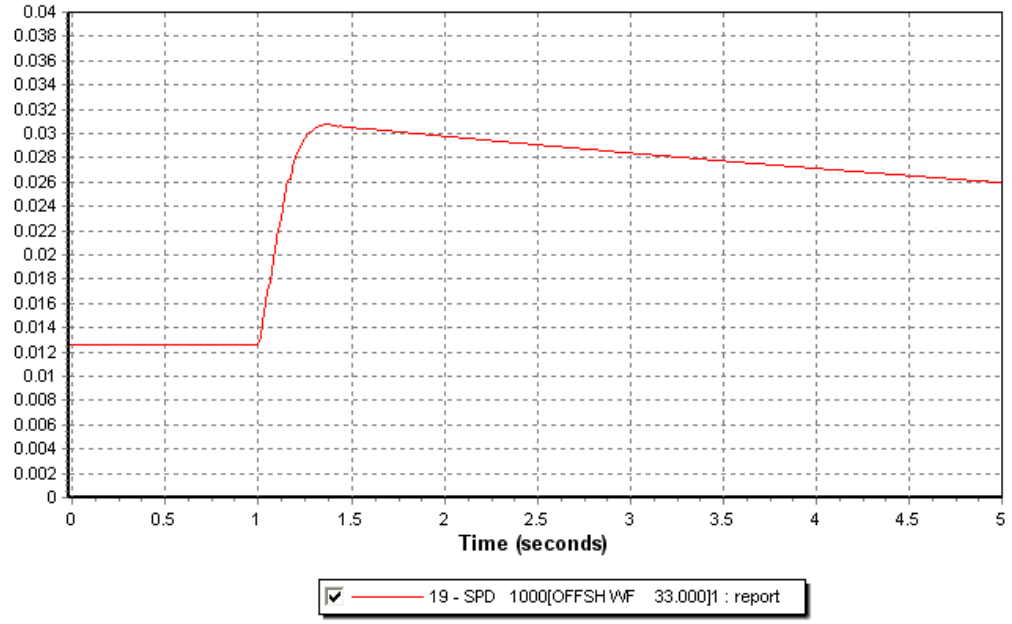

Figure 8-7: Rotor speed of the generator at the wind farm in pu

The fault is almost invisible onshore; few small variations occur for the voltage and the frequency at the connection points (buses 5600 and 6000). But they are quickly damped thanks to the control of the SVC and both HVDC controller. The amplitudes of the responses are up to 20Mvar for the HVDC converters and 50 Mvar for the SVC. See Appendix G-5: Response of the onshore HVDC converters and SVC.

The power flow trough the line between the 2 HVDC converter is also modify due to the fault. Some variations occur with 2Mvar amplitude for the reactive power flow and 15MW for the active power. It is a consequence of the small variation in the generation unit at the connection buses. The active and reactive powers vary slightly due to the fault but the variations disappear progressively. See Appendix G - 6: Behaviour of the generators at the PCCs (buses 5600 & 6000), reactive and active power

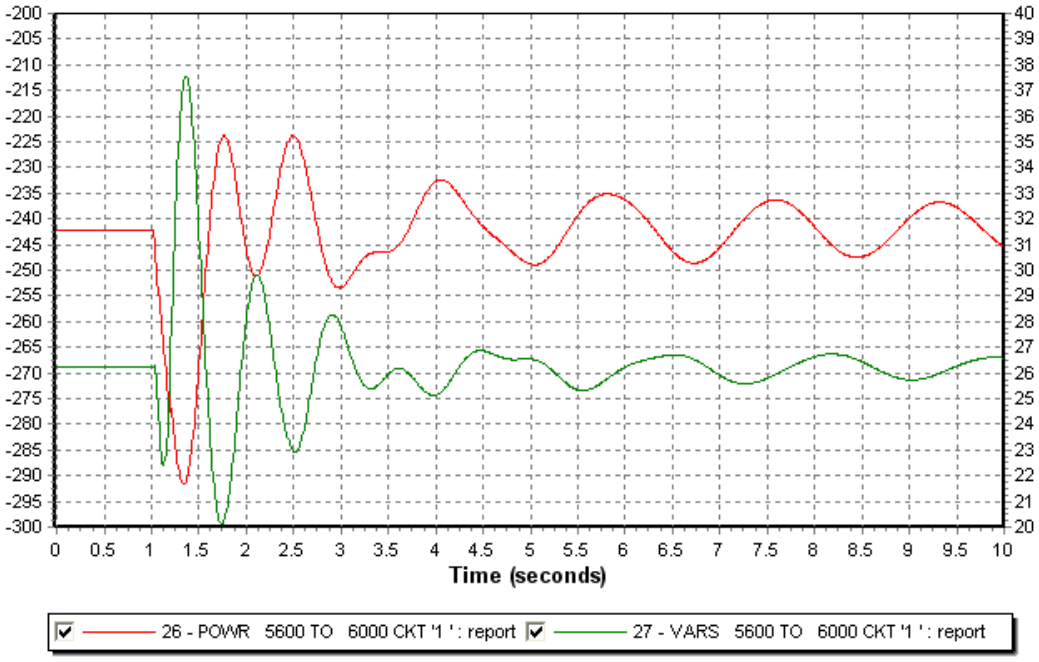

Figure 8-8: Active and reactive power flowing in the line between the HVDC converters in MW and Mvar

8.2.1 DISCUSSION

There is unexplained variation during few ms when the fault is cleared in the response of the HVDC converter.

The voltage recovery is also completely different than with a single converter. As the converters supply together the same amount of reactive power than a single one, the difference of behaviour can only be explained by the dynamic PSS/E model which is slightly different from the model given by ABB. It might be possible that some dynamic parameters are inexact or inaccurate.

8.3 FAULT OFFSHORE AND TRIPPING OF THE LINE

A fault has been performed on the line between the two shore HVDC converters. The fault is a three phase short circuit with an impedance set at 0 and its duration set at 100ms. Then, the fault is cleared and the line disconnected. As the response onshore is longer than offshore due to the dynamic behaviour of the onshore grid; the dynamic simulations last at least 20sec to give a good overview and see the reestablishment of the system.

8.3.1 SIMULATION RESULTS AND PLOTS

A quick overview of the consequence offshore is shown below. The voltage at the offshore buses undergoes very small and short variation, 0.5s after the fault regain its original value. See Figure 8-9. The frequencies change also slightly (0.1Hz). The wind turbine generator is also shortly affected. See Appendix G - 7: Behaviour of the offshore wind turbine generator and Appendix G - 8: Frequencies at the offshore buses

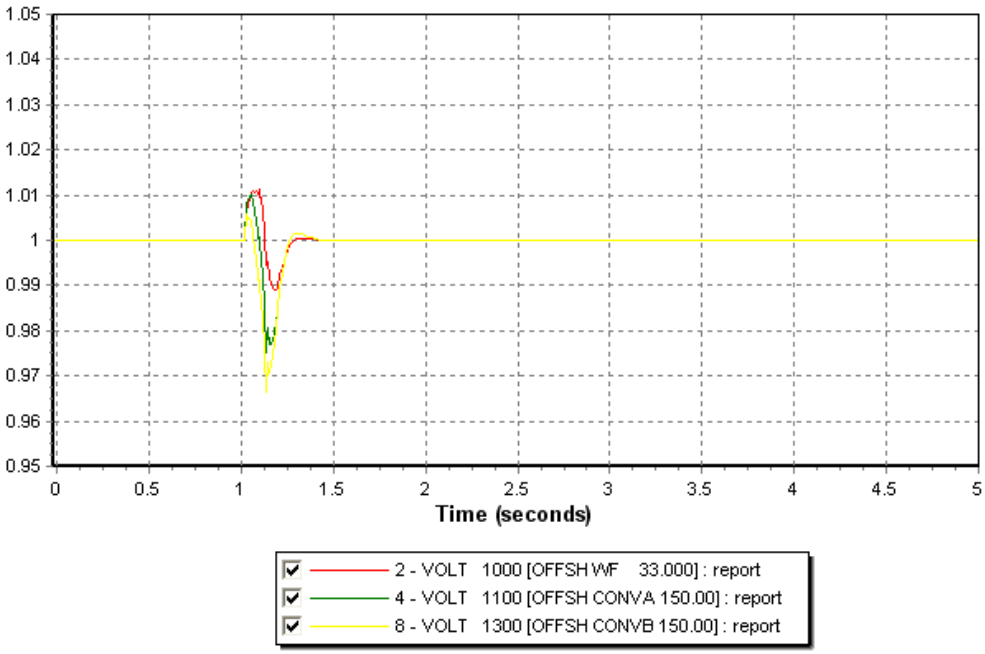

Figure 8-9: Voltage at the offshore buses in pu

The bus 5600 is more affected by the fault because during the pre-fault state the active power on the line flew from the bus 6000 to 5600. Its voltage goes down to 0 whereas the voltage at bus 6000 only goes to 0.6 pu. Then, both voltages recover quickly (300ms). Almost 10s after the fault has been cleared and the line tripped the voltage becomes stable around 1 pu. See Figure 8-10.

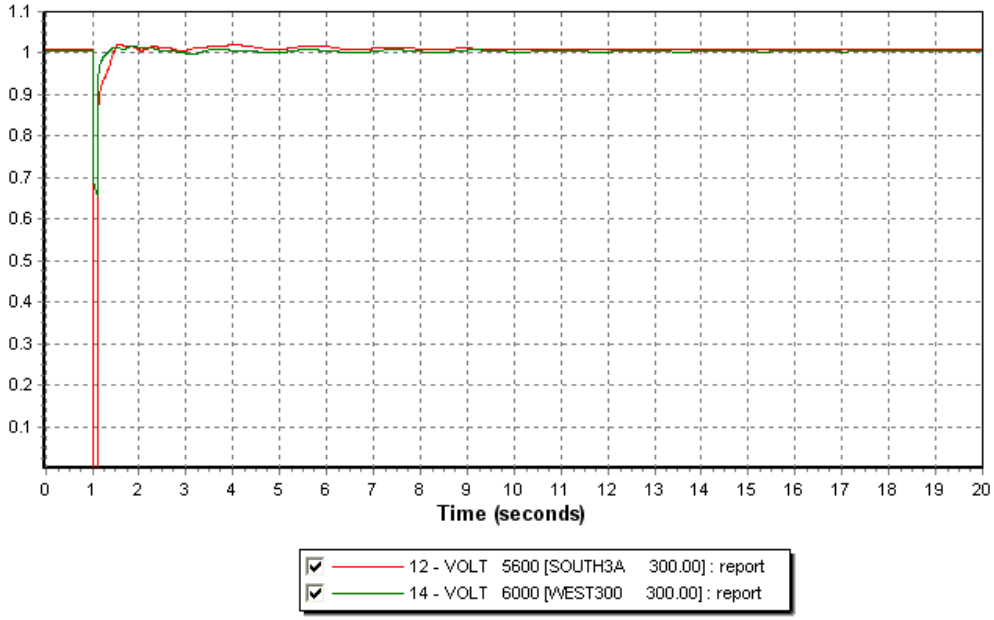

Figure 8-10: Voltage at PCC and at ends of the tripped line in pu

The active power flowing in both HVDC transmissions is also affected. During the fault it almost stops in transmission A (to bus 5600) because of the voltage close to 0 but continues to flow in the transmission B (voltage still "high"). See Appendix G - 9: Active power flowing into the HVDC transmission

As expected the converter responses are different according to the power balance before the fault. During the fault both converters supply in reactive power at the upper limit of their possibilities. After the fault had been cleared and the line tripped, they regulate down the reactive power by absorbing it, the HVDC converter at bus 5600 reach its down limit (-280Mvar). Then, they recover progressively a new state close to the original one. It takes more time for the converter at bus 5600, more than 40s compared to 25s for bus 6000. See the figure below.

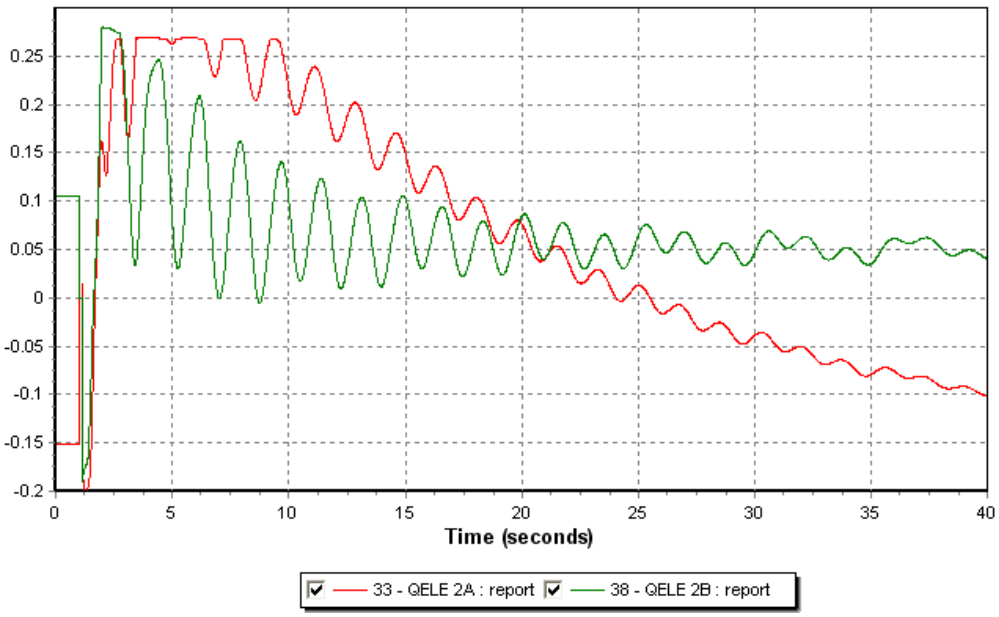

Figure 8-11: Reactive power from the onshore HVDC converters, inverted axis, in pu on system base

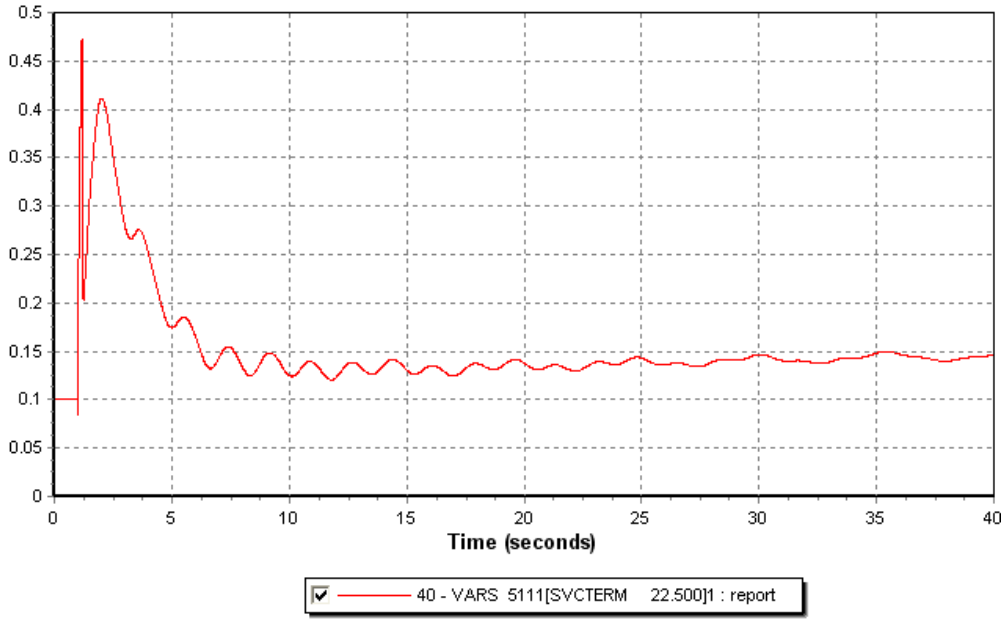

Figure 8-12: Reactive response of the SVC in pu on system base

The SVC regains also another state because of the tripping of the line which leads to a new stable system. It supplies 50Mvar more than previous the fault. The SVC gives approximately 400Mvar when the line is tripped.

It seems that there is a transfer of reactive power from the SVC to the HVDC converters.

By looking at the frequency, on several buses onshore, it can be observed that a stable system is installing after the fault and the tripping of the line. See Figure 8-13. The deviation speed from the synchronous speed from the generator shows also that a new steady state is installing after the disturbance. See Appendix G - 11: Speed deviation from synchronous speed for generator at buses 5600 and 6000.

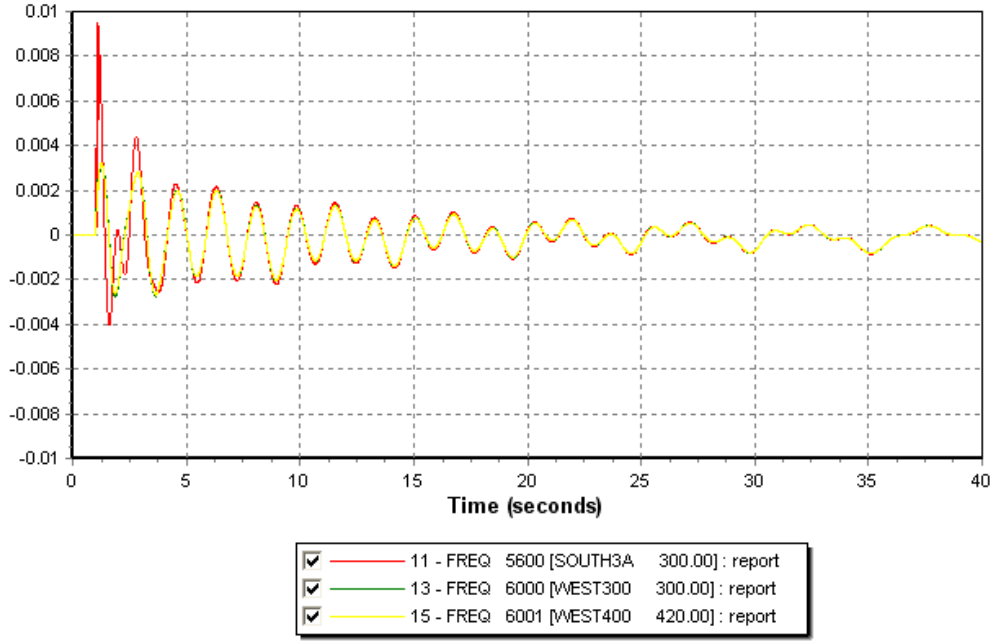

Figure 8-13: Frequency on several onshore buses (5600, 6000 and 6001)

The behaviour of the generator at the point of connection may explain the different responses of the regulating systems (SVC and HVDC controller). The active power produced stops during the fault for generator at bus 5600, then huge decreasing peaks occur the 5 first second follow by damped oscillations. The power generation then swings to the pre-fault value. The generator at bus 6000 has the same behaviour. The amplitude of the first peak is 30% higher than the normal value for both generators. See Figure 8-14.

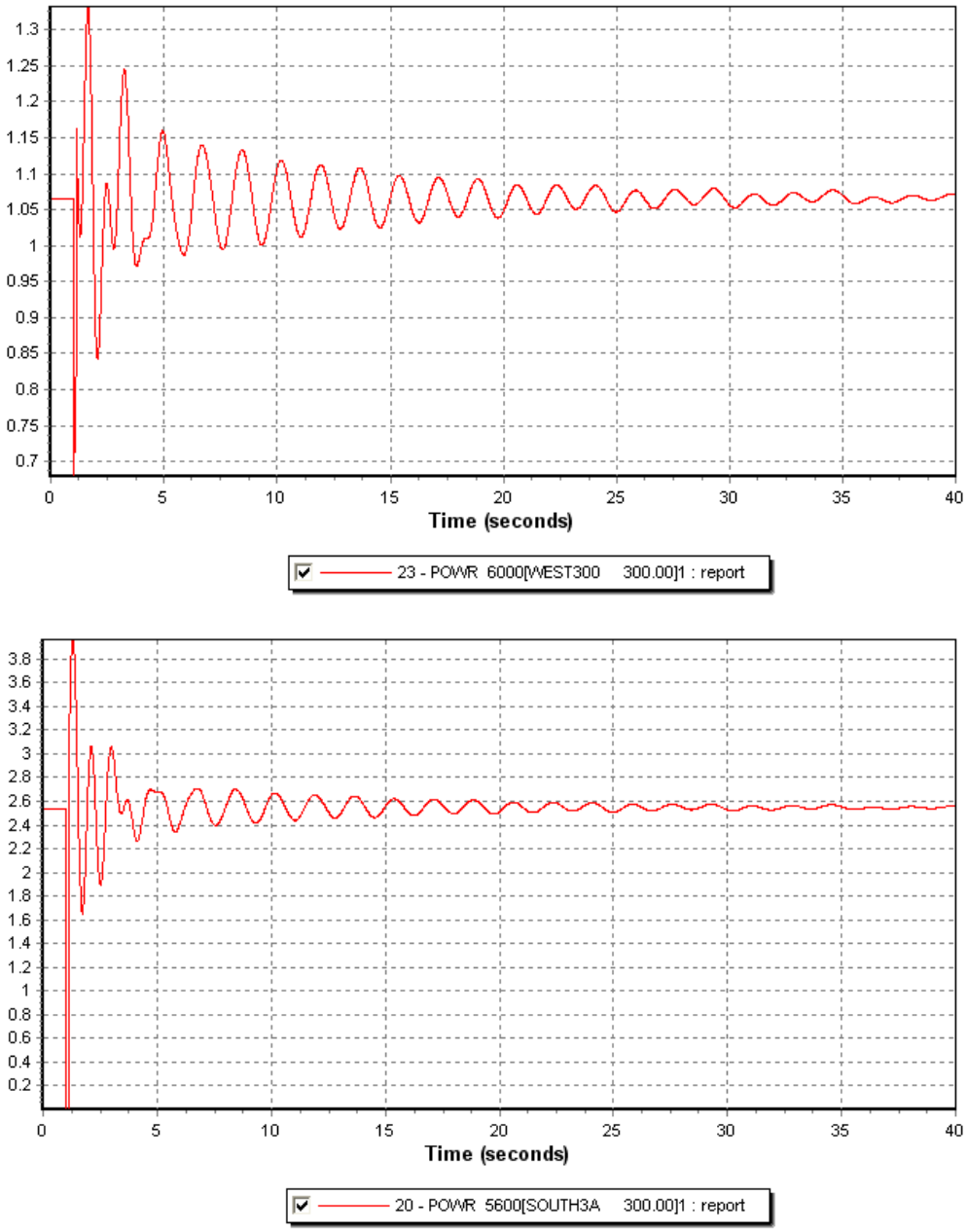

Figure 8-14: Power generated at buses 6000 and 5600

Regarding the reactive power, it falls down to 0 during the fault at bus 5600 and then the generator produces large amount of reactive power (almost the double than during steady state) which is progressively regulated down to a value close to the original, slightly superior. See Figure 8-16.

The case at bus 6000 is different, the generator was absorbing reactive power (100Mvar). By zooming at the fault time, it can be observed that the generator produces a huge peak of reactive power (900Mvar), normally impossible in the reality. As soon as the fault is cleared and the line tripped, the reactive power starts from its original value to absorb few reactive to regain a state close to its original one. See Figure 8-15 below. The zoom on the peak can be observed at Appendix G - 10: Zoom during fault time on the reactive power from generator at bus 6000.

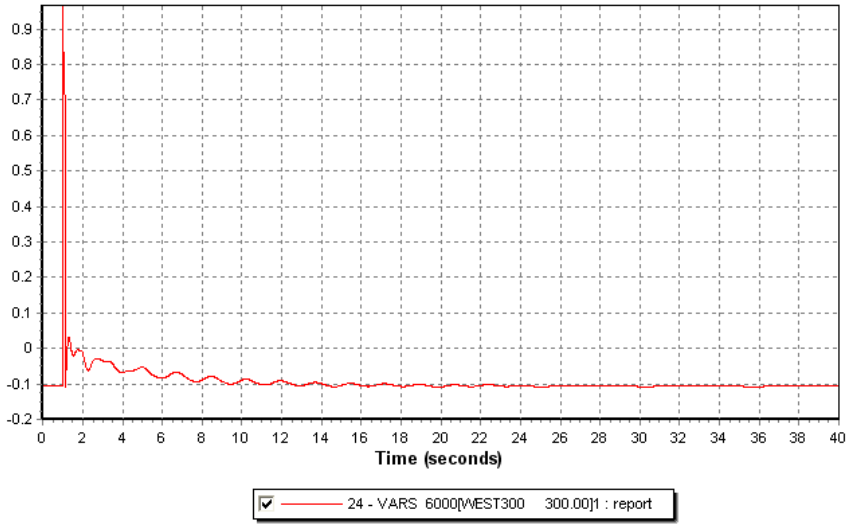

Figure 8-15: Reactive power from the generator at bus 6000

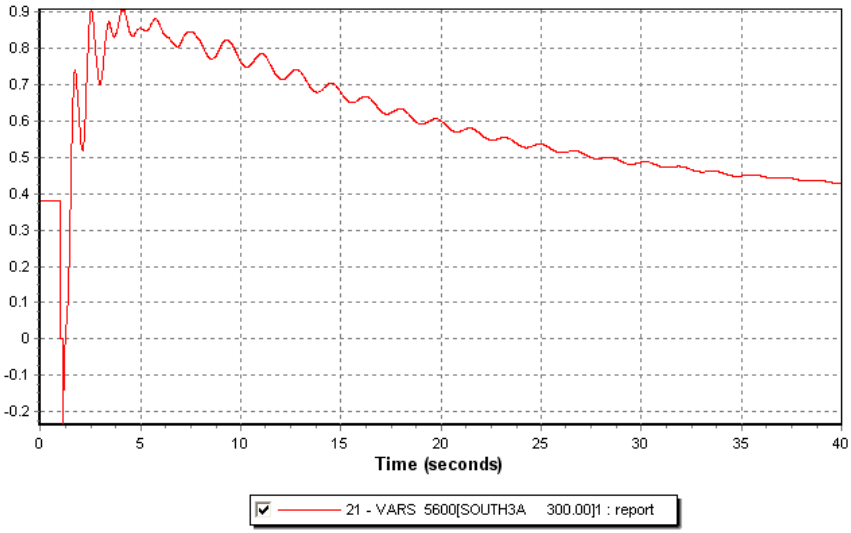

Figure 8-16: Reactive power from the generator at bus 5600

8.3.2 DISCUSSION

Both HVDC converters have a significant role in the stability of the onshore grid. They are able to regulate the voltage and supply reactive power during the fault. Such VSC converter will be helpful to stabilize the main grid after a disturbance. An offshore DC grid in the North Sea equipped with the VSC technology will improve the reliability and the stability of the network in all the countries around.

9 SIMULATION: CONNECTION OF WIND FARM CLUSTER WITH 2 HVDC TRANSMISSIONS

The same wind farm cluster as previous is connected to two VSC-HVDC transmission from the main wind farm (bus 1100) and the halfway wind farm at bus 1300. The emphasis will be but in this section on the stability offshore. First, a fault close to the oil rig will be performed at bus 1320 (ex-1120), then the DFIG generator representing the middle wind farm will be replaced by a fixed speed generator, in the same way as previous, and a fault will be performed at bus 1320. Finally, a fault will be performed on the submarine cable between the 2 HVDC converters leading to a tripping of the line and thus to 2 offshore grids in "island" operation. The simulations are presented below. See in Figure 9-1, the faults are represented by a red lightning and the replacement a red arrowed circle.

9.1 LOAD FLOW

The load flow is almost unchanged to the shore. The voltage is the same whereas the angles are slightly changed down. As previous the HVDC converters are set with a voltage control on the connection buses. There are supposed to supply half of the reactive power generated or absorbed. The converter connected to bus 5600 reach its nominal reactive power limit, so in order to ensure a reactive power reserve, the converter supply only a quarter of the reactive power needed at bus 5600. The rest is given by the generator. The voltage and the angle of the buses in the surrounding of the PCCs and in the offshore grid are given in the table.

Bus number	Name	Voltage [pu]	Angle [°]	Pgen [MW]	Qgen [Mvar]
3300	SV-SW	1.000	0	4013.2	2324.3
5400	CNTR3 A	1.007	33.1	1637.5	130.4
5401	CNTR4 A	0.998	30.6		
5600	SOUTH 3A	1.010	28.5	2537.6	380.0
5601	SOUTH 4A	0.992	28.7		
5602	SOUTH 4B	0.969	23.1		
5603	SOUTH 3B	0.936	21.1		
6000	WEST 3	1.005	33.4	1064.2	-105.3
6001	WEST 4	1.000	32.4		
6100	NWEST 3	1.000	32.6	2419.2	749.0
1000	OFFSH WF1	1.000	0	458.3	7.3
1010	OFFSH WF2	1.000	-1.1	350	1.8
1020	OFFSH WF & RIG	1.000	0.2	350	-21.2
1100	OFFSH CONV A	1.000	-5.3		
1200	SHORE CONV A	1.068	34.1		
1300	OFFSH CONV B	1.000	-5.1		
1320	TRANSFO RIG	1.014	-2		
1400	SHORE CONV B	0.995	40.0		

Table 9-1: Load flow in the surrounding of the PCCs and in wind farm cluster.

The detail of all the load flow can be found in the appendices and the next figure show a zoom on the load flow in the HVDC transmissions. Appendix H - 1 shows the bus voltage and the angle. The power exchange and the generation per area are given in Appendix H - 2.

There is no need to put shunt reactor at the wind farm to draw the reactive power from the capacitive effect of the cable because it is supply by the HVDC converter and the rest are given by the wind farms themselves to reach 1pu.

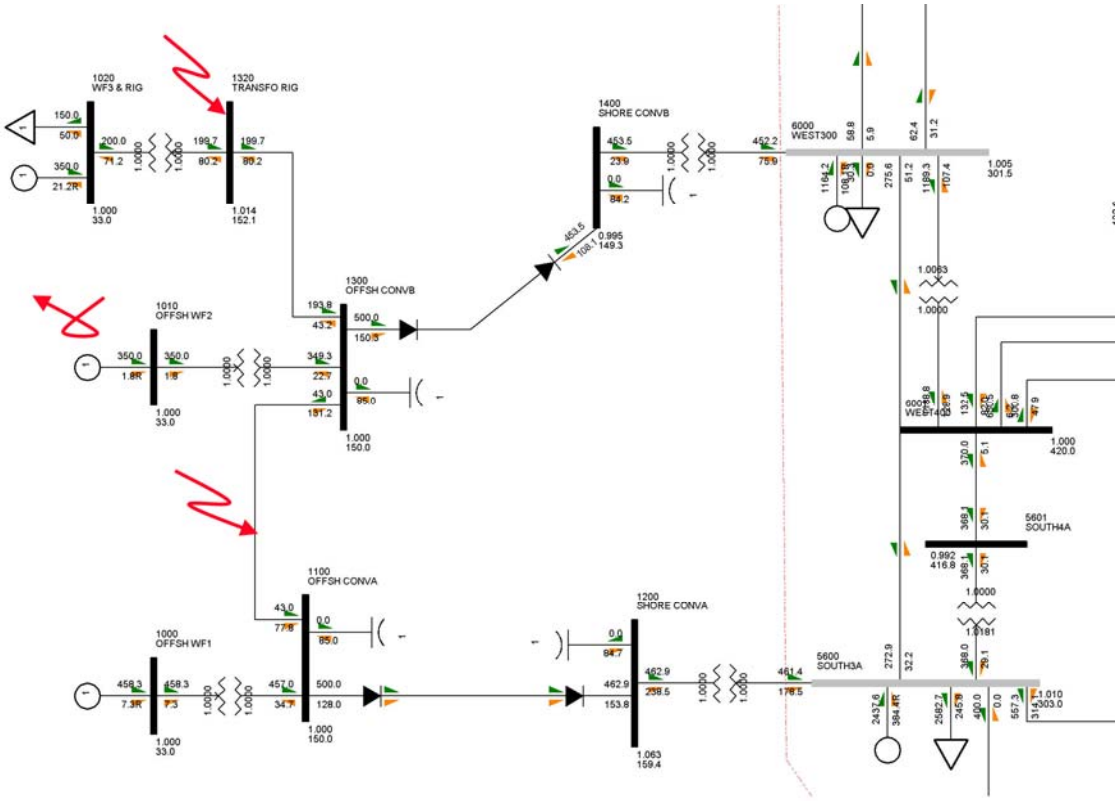

Figure 9-1: Load flow on the cluster wind farm.

9.2 FAULT CLOSE TO THE OIL RIG AT BUS 1320

A 150ms fault has been performed at the transmission bus of the oil rig (1320).It corresponds in the previous simulation to the bus 1120. The results and the plots of the simulation are presented below.

As can be seen from the simulation plots, the voltage is reduced to 0.1 pu during the fault. The voltage is recovered 700ms after the fault is cleared. See the voltage below and in Appendix H - 3.

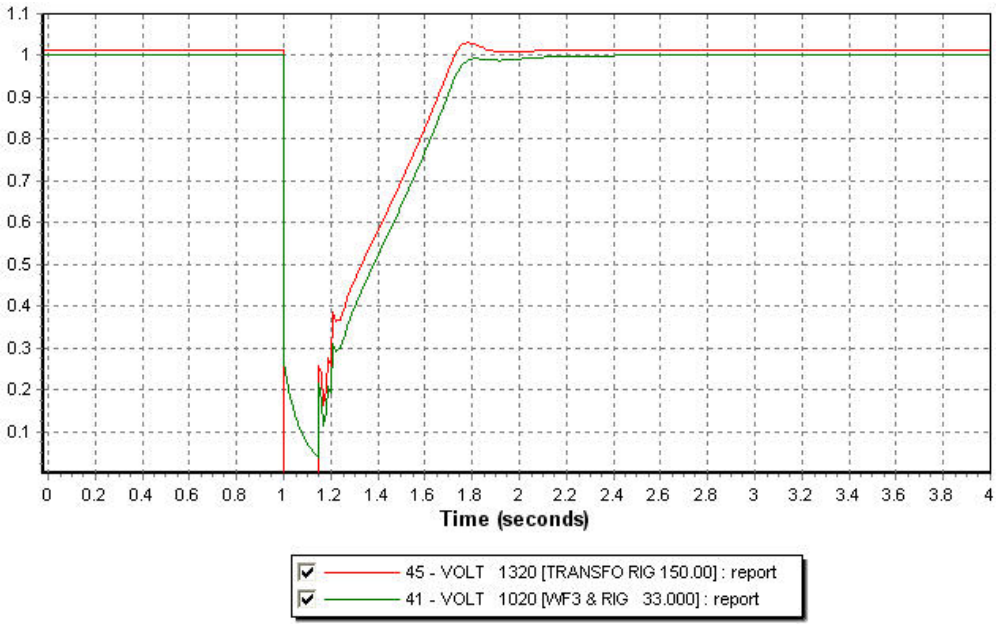

Figure 9-2: Voltage at the oil rig/ wind farm bus (1020) and the transmission bus 1320 in pu

As expected the frequencies oscillates during the fault and then increases during the recovery time until 51Hz. See next figure. As soon as the voltage is recovered the frequency goes slowly down. Frequencies at different buses are shown in the next figure and in Appendix H - 4

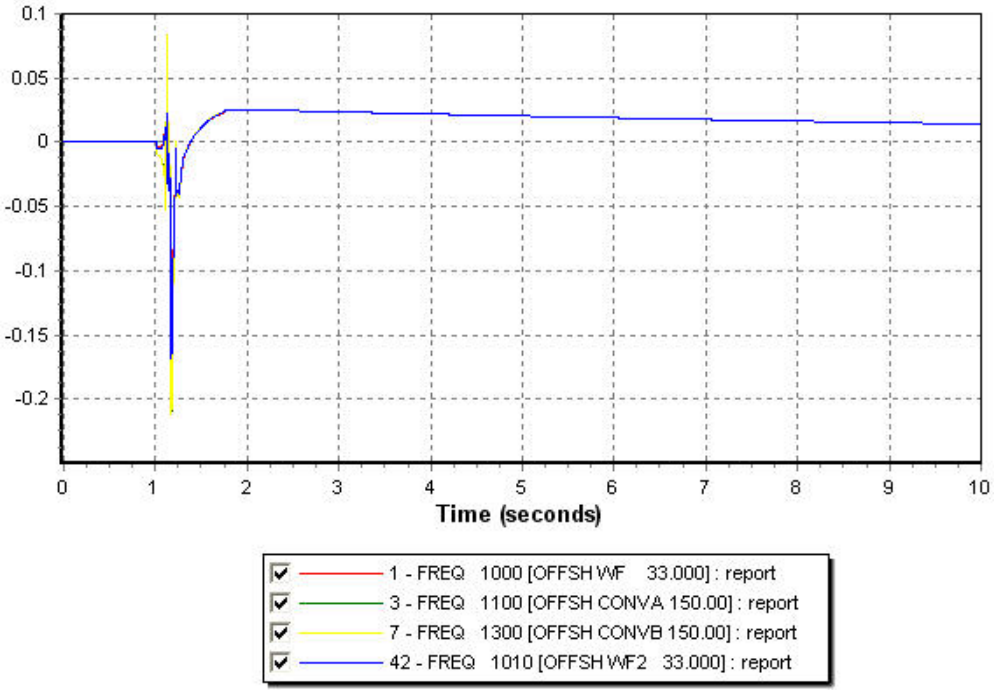

Figure 9-3: Frequency at different buses in pu, 0.02pu = 1Hz

The responses to the fault of the HVDC converters are very similar. They stop during the fault to supply or absorb reactive power. When the fault is cleared, the supply as much as reactive they can supply and then they regulated down when voltage is recovered. The flow of active power almost stops into the HVDC transmissions and stay low 300ms after the fault is cleared. The converters regain the pre-fault state 2s after the fault. See the 2 next figures.

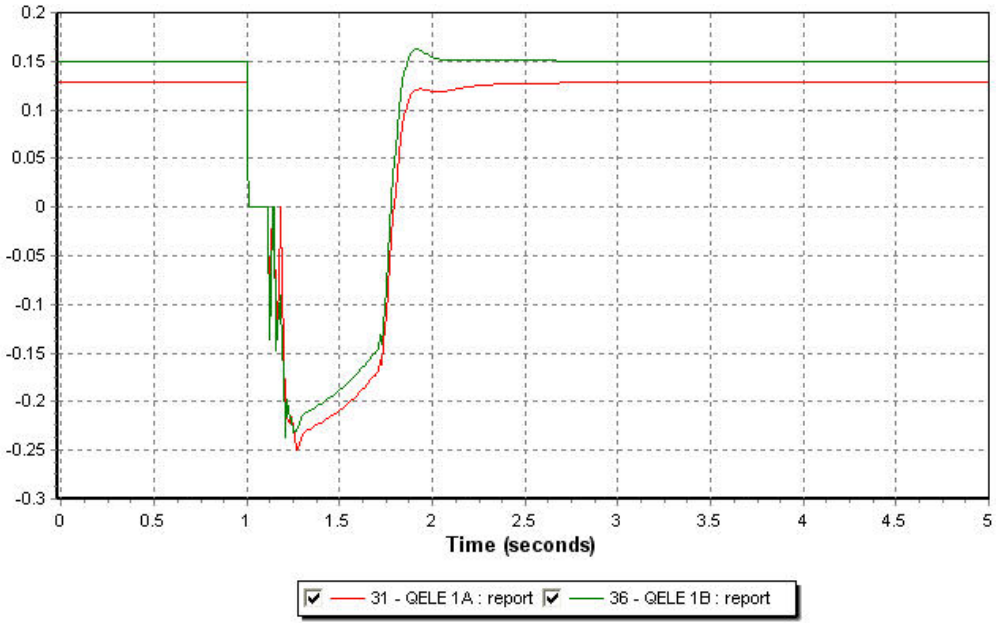

Figure 9-4: Reactive power from the HVDC converters, in pu on system base, reverse axis

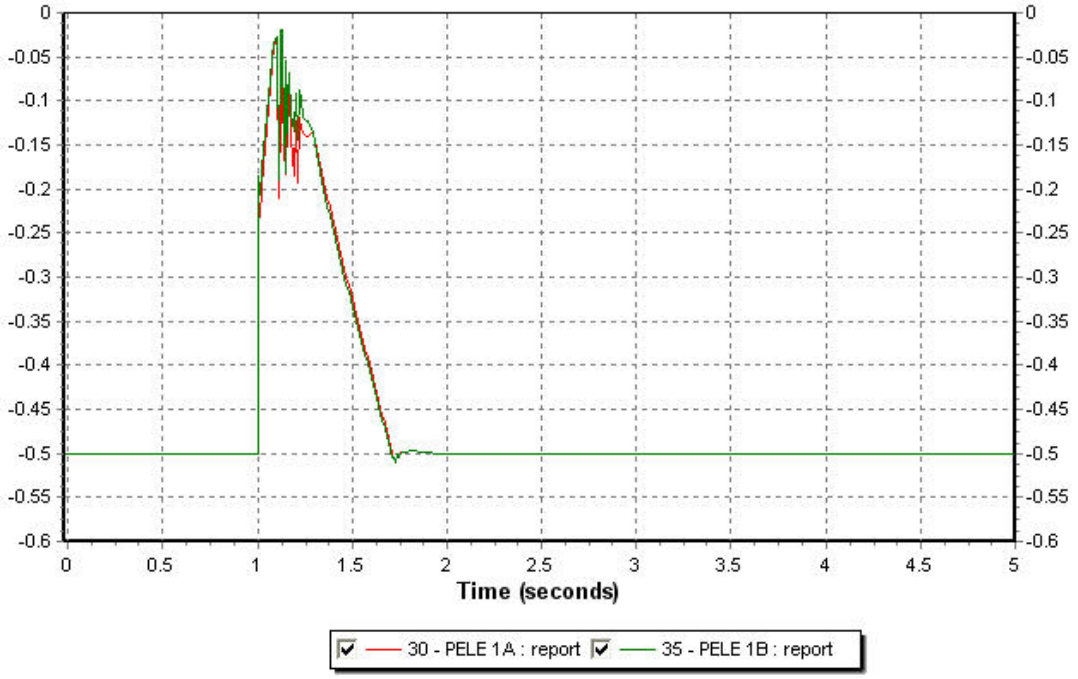

Figure 9-5: Flow of active power into the offshore converter, in pu on system base.

The behaviour of the generator are very similar than in the other simulations. The generator representing the wind farm close to the oil rig is more affected by the fault because closest. The generation of active power stops during the fault whereas it is maintained at a low value for the 2 other (100MW). The generators produce a peak of reactive power during the fault and then absorb lot of reactive power to come back at the original state. 1.5s after the fault all the generator have regained their pre-fault states. See Appendix H - 5, Figure 9-6 and Figure 9-7 .

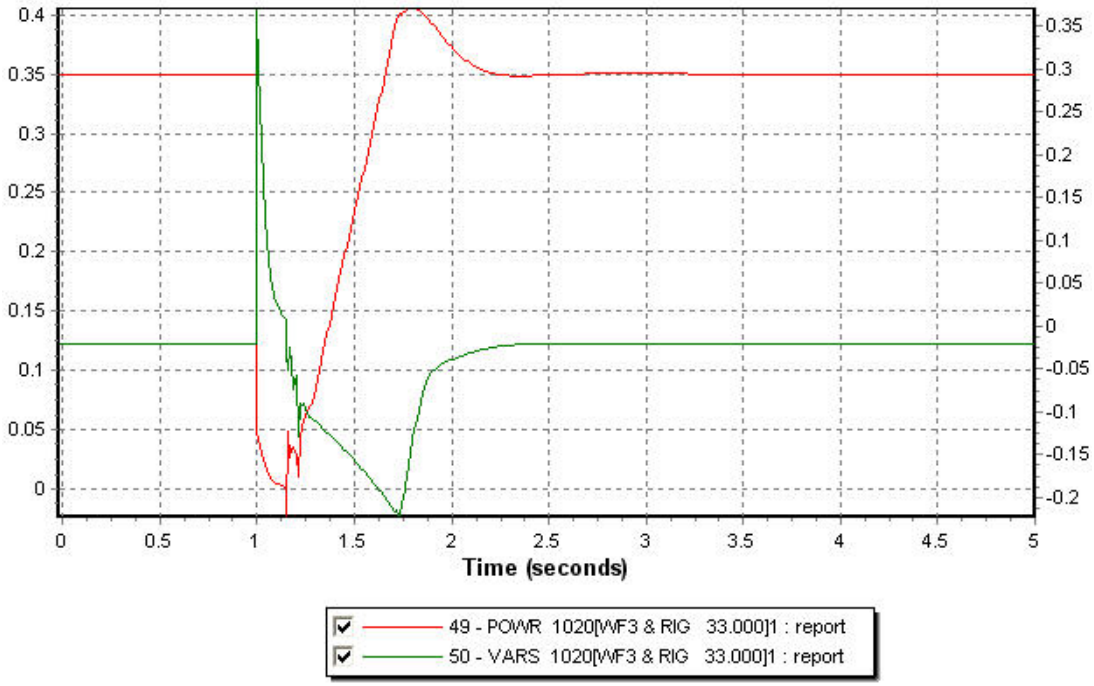

Figure 9-6: Active and reactive power generated by the wind farm at the oil rig, in pu on system base

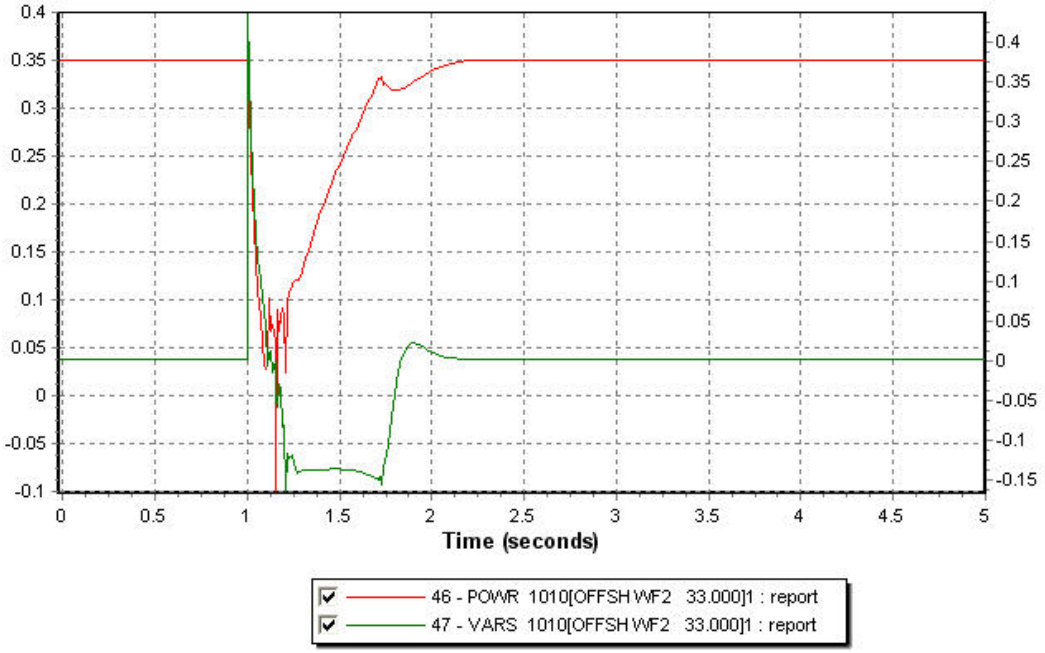

Figure 9-7: Active and reactive power generated at the central wind farm, in pu on system base

By looking at the power flowing into the submarine cables, it can be observed the reactive power coming from the HVDC converter A to the generators at buses 1010 and 1020. See the large peak in green in Figure 9-8 and Figure 9-9.

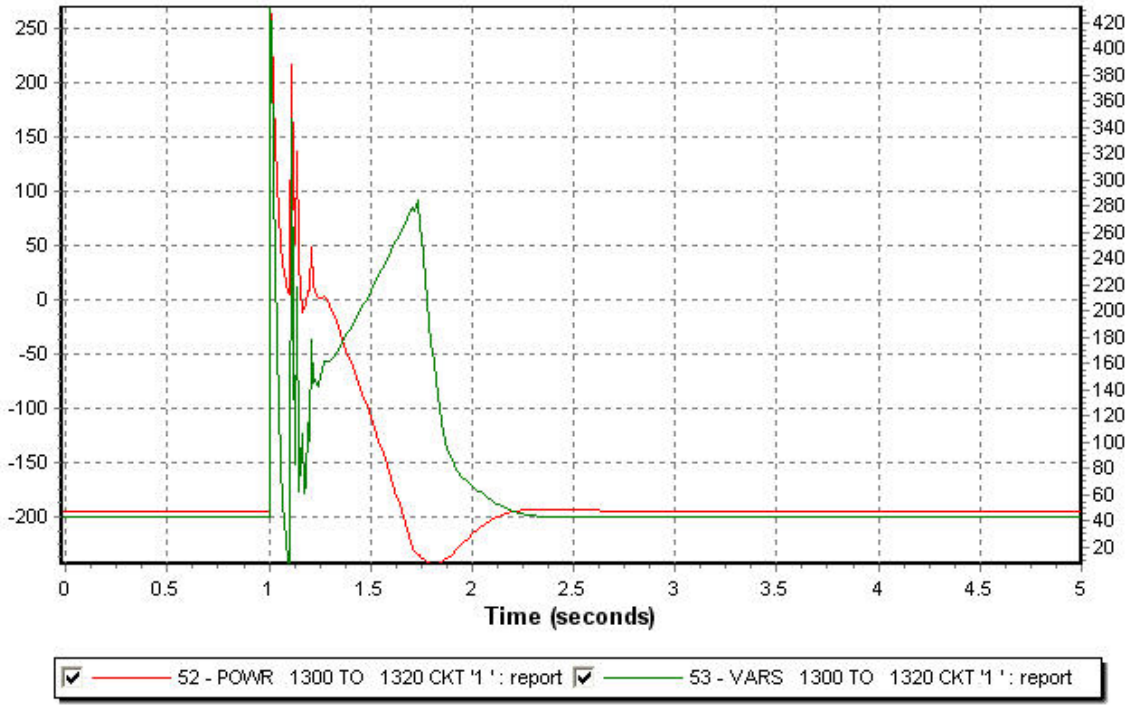

Figure 9-8: Active and reactive power flowing from bus 1300 to 1320 in MW and Mvar

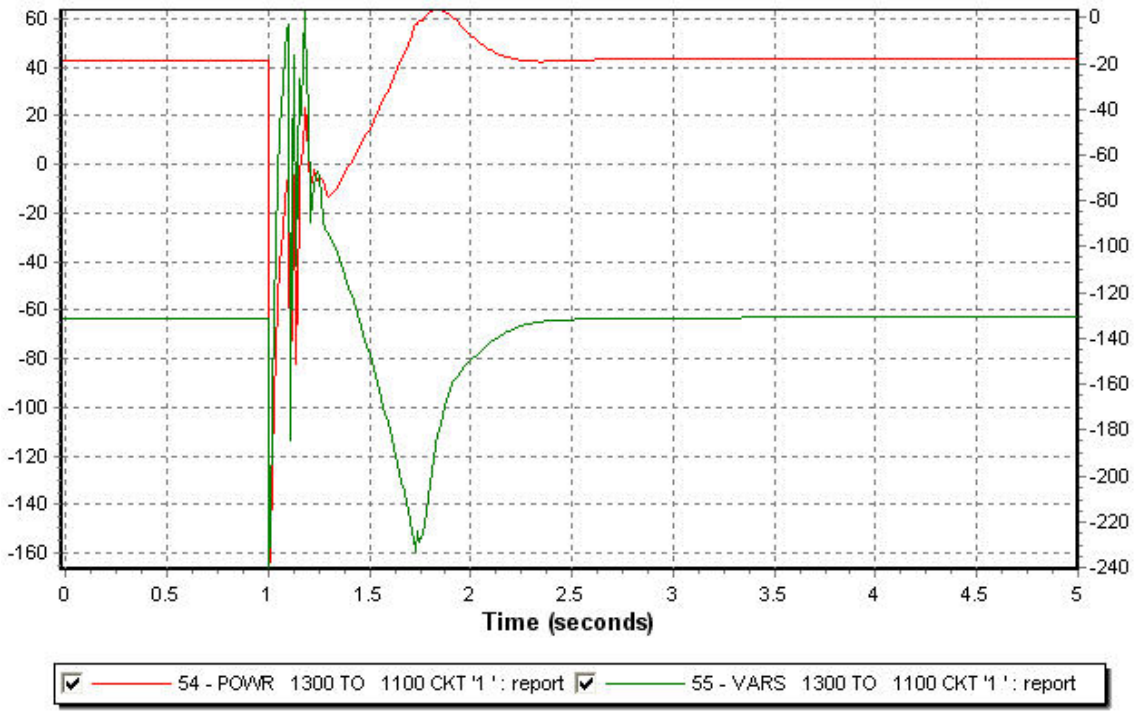

Figure 9-9: Active and reactive power flowing from bus 1300 to bus 1100 in MW and Mvar

The consequences at the PCCs onshore at bus 5600 and 6000 are very small. Small variation less than 0.01 pu occur for the voltage whereas the variation for the frequency are under 0.2 Hz. Voltage and frequency variations can be observed in Appendix H - 6: Voltage onshore at PCCs in pu and Appendix H - 7: Frequency variation offshore at PCCs in pu

Based on the fault ride trough requirement, the wind farms can stay connected during the fault.

9.3 REPLACEMENT OF A DFIG BY A FIG AT BUS 1010

As done in the previous cluster wind farm simulation, the middle wind farm represented by a DFIG generator at bus 1010 is replaced by a fixed speed generator (Bonus parameters). The dynamic behaviour in case of a fault at the transmission bus (1320) close to the oil rig is studied in the following.

9.3.1 SIMULATION RESULTS AND PLOTS

The voltage is reduced to 0.1pu at the offshore wind farms, and less for those at the oil rig bus around 0.08pu. The voltage is recovered 500ms after the fault is cleared. To look at the small overvoltage when the voltage is recovered is important for the following. The overvoltage is more important close to the transmission A than for the rest of the grid. The voltage at the wind farms is presented in Figure 9-10 and in Appendix H - 8: Voltage at each offshore bus in pu.

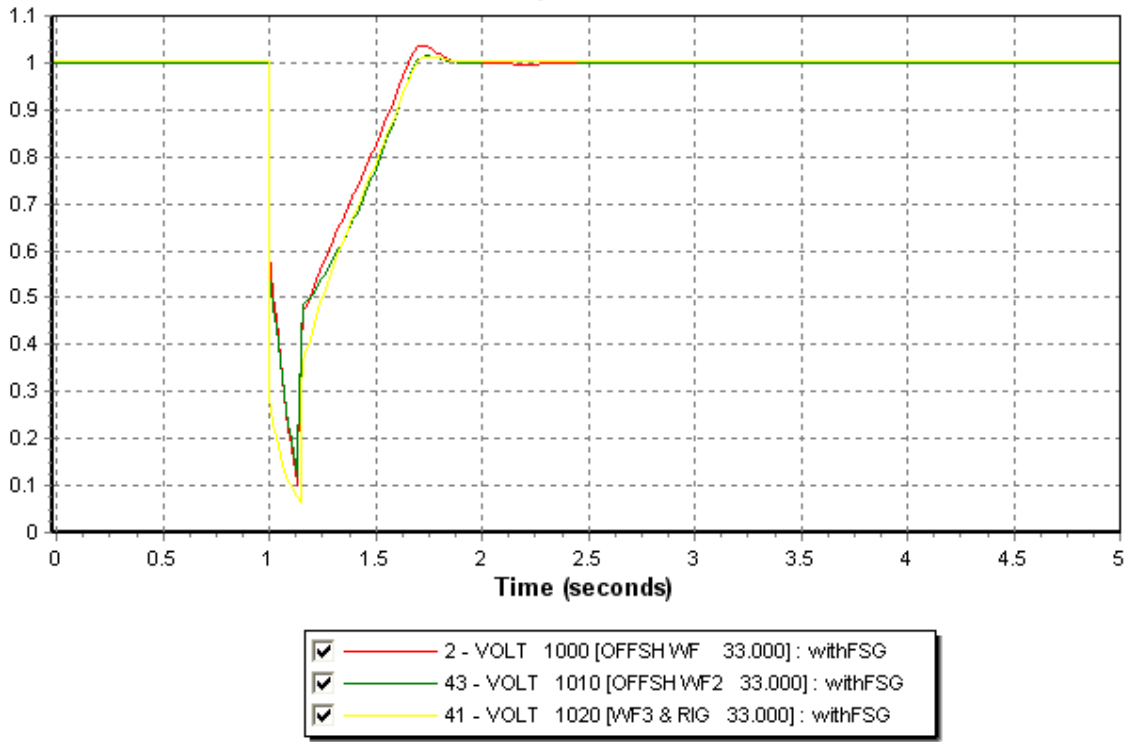

Figure 9-10: Voltage at the offshore wind farm in pu

The response of the HVDC converter is similar on a certain way. Absorbing reactive power in steady state, both converters stop to do it during the fault and then produce as much as possible reactive power for the voltage recovery. However when they regulate down, from 1.7 to 3.5s, their responses are completely different. The farthest HVDC converter (transmission A) has to absorb reactive power to prevent overvoltage at the bus 1000 and 1100, whereas the second converter (transmission B) must still supply reactive power to keep the voltage up at the buses close to the fixed speed generator.

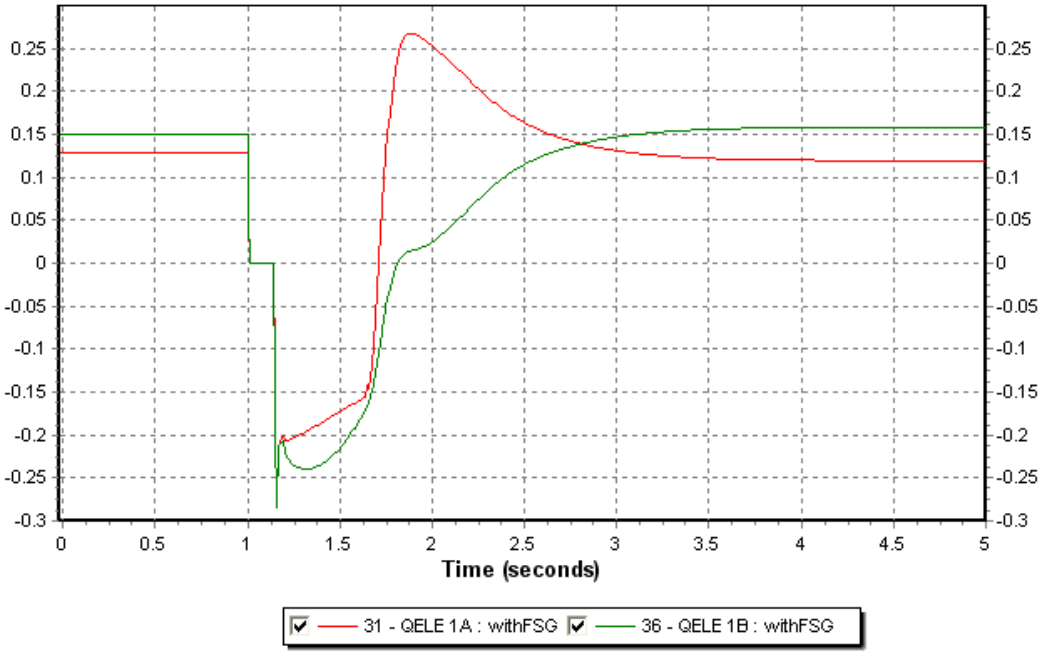

Figure 9-11: Reactive power from the VSC-HVDC converters, in pu on system base

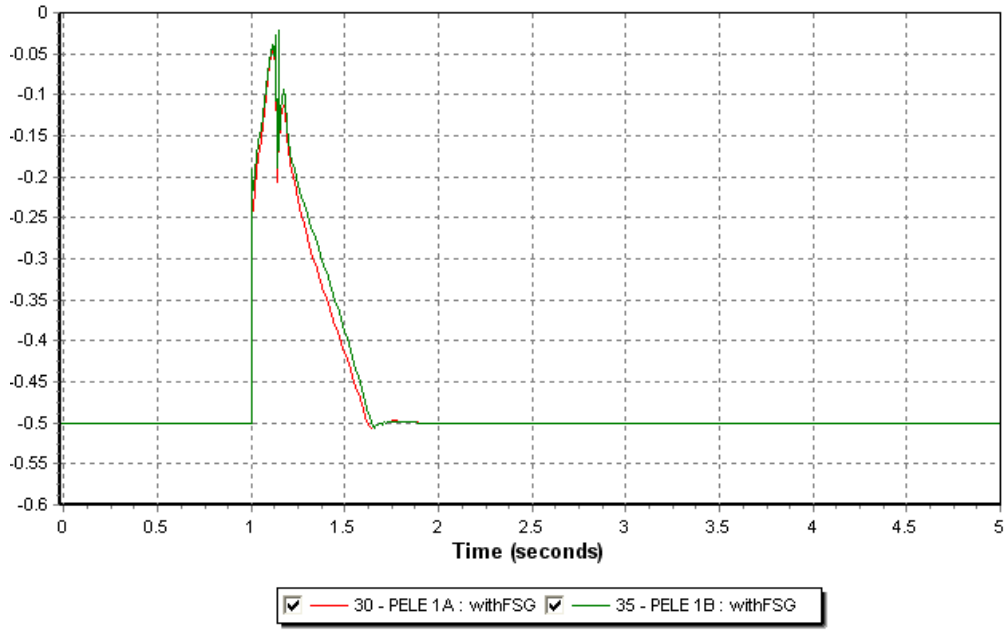

Figure 9-12: Active power flowing into the HVDC transmissions, in pu on system base

As expected the transmission of active power almost stops during the fault. It can be noticed that the transmission A, the farthest, is able to transmit more power during the recovery time.

When the system regains its pre-fault state the frequency has increased of 1.2 Hz, then the frequency decrease slowly to regain a stable state. It might be possible that the final frequency will be up to 50Hz because of the steepness of the frequency curves. See Figure 9-13.

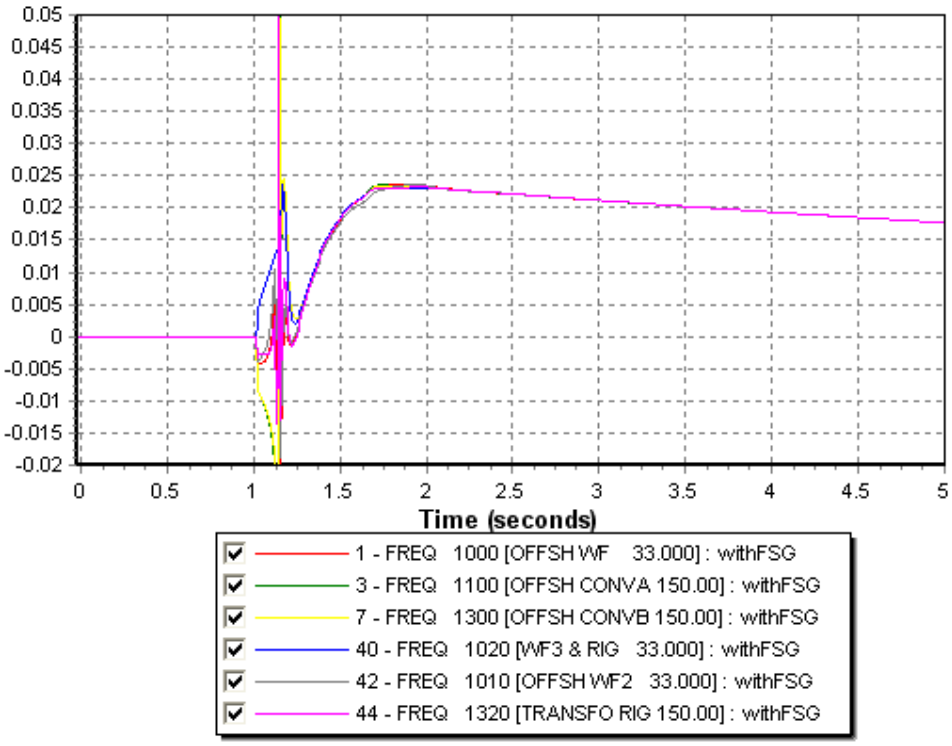

Figure 9-13: Offshore frequency variation at different buses, in pu, 0.02=1Hz

Now the behaviour of the generators representing the wind farms is shown below.
The rotor speed of the fixed speed generator (green curve) increases faster, but it stops earlier to accelerate than the two others. The generator close to the fault gets the highest rotor speed at the recovery time. See Figure 9-14

The fixed speed generator is able to generate quickly its pre-fault active power generation; almost 200ms after the fault is cleared. Some variations occur for the generators close the fault during the recovery of generation. Around 2.3s the generator representing the 500MW wind farm has to slightly increase its production to compensate a lack from the 2 others. See Figure 9-15.

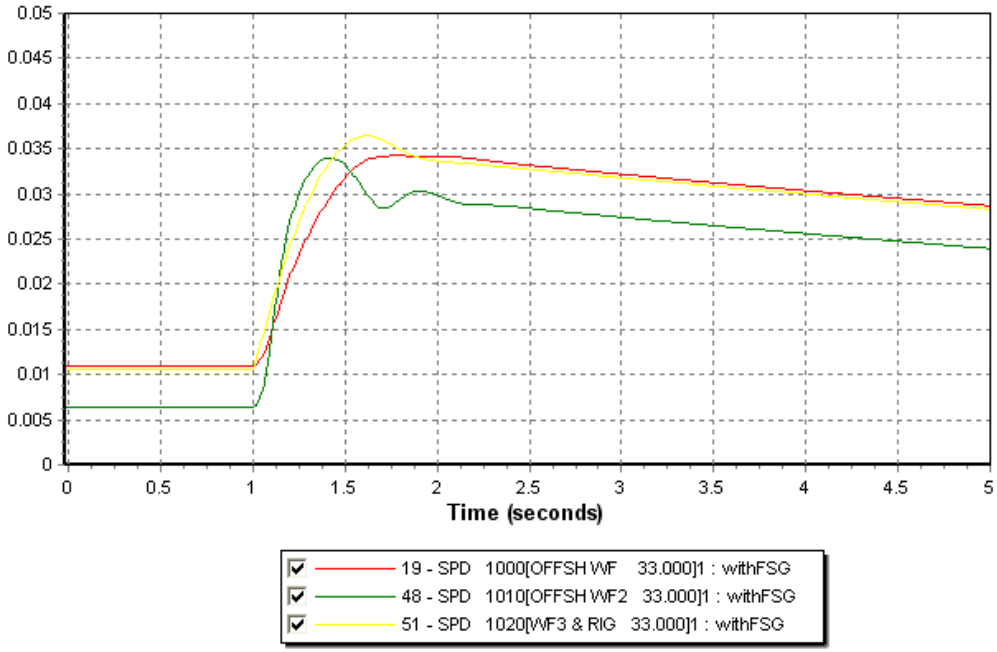

Figure 9-14: Rotor speed from the generator representing the wind farm, green fixed speed, in pu

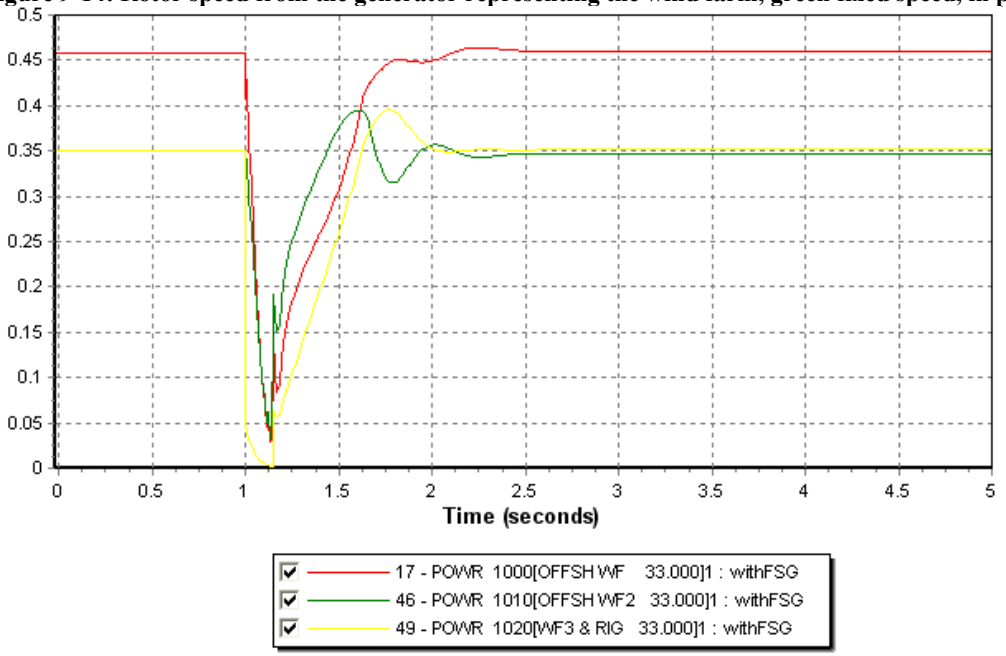

Figure 9-15: Active power generated by the generator representing the wind farms, in pu on system base

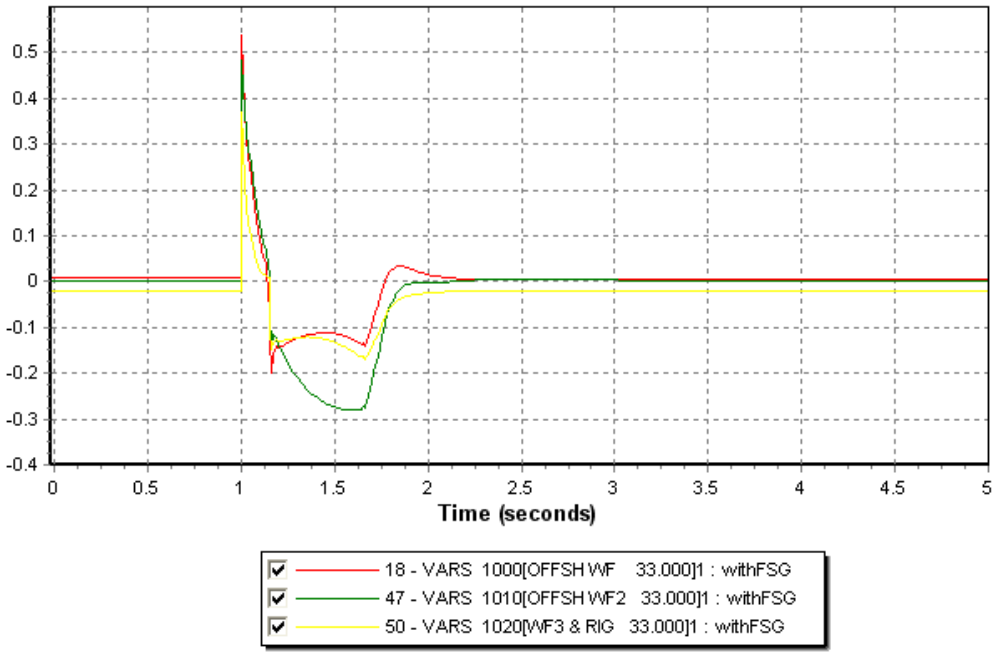

Figure 9-16: Reactive power from the generator representing the wind farms, in pu on system base

The generator contributions of reactive power are similar to the previous simulation but the fixed speed generator absorb less reactive power in this configuration than in the other (270Mvar).See Figure 9-16.

The active and reactive power flowing into the submarine cables show also the transfer of active and reactive power during and after the fault. The 270 MW peak inside the cable from bus 1300 to 1320 shows the contribution of the system to the short circuit current. In a similar way, the down peak of power show the contribution to the short circuit current from the main wind farm, approximately 170MW. Then, we can deduce that the middle wind farm contribute to approximately 100MW.
Similar thinking could be done on the reactive power. See Figure 9-17 and Figure 9-18.

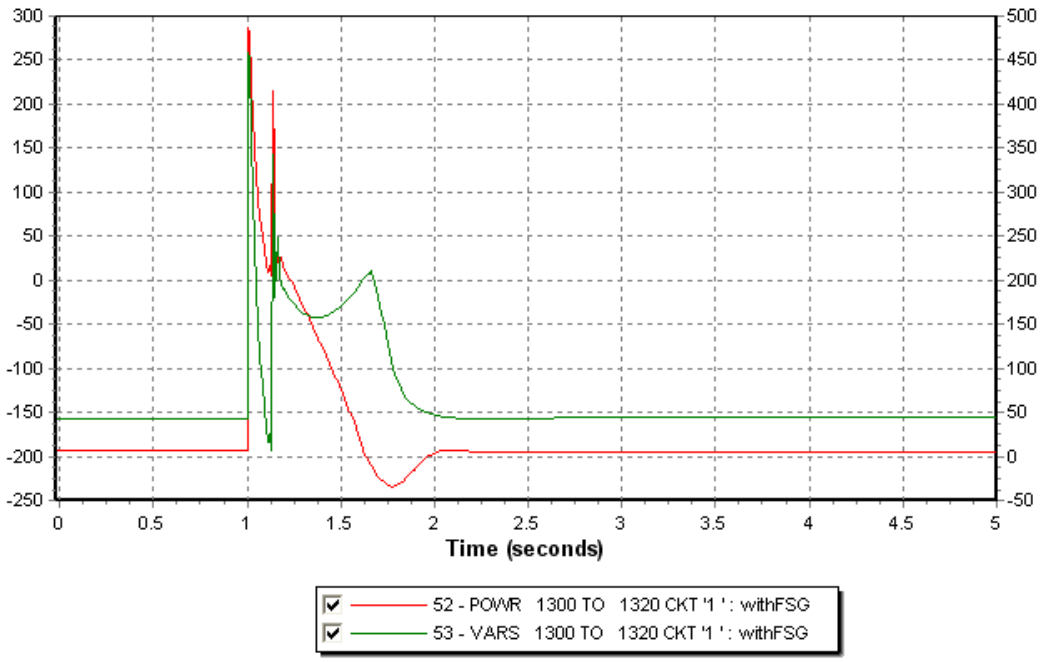

Figure 9-17: Active and reactive power flowing from bus 1300 to 1320, in MW and Mvar

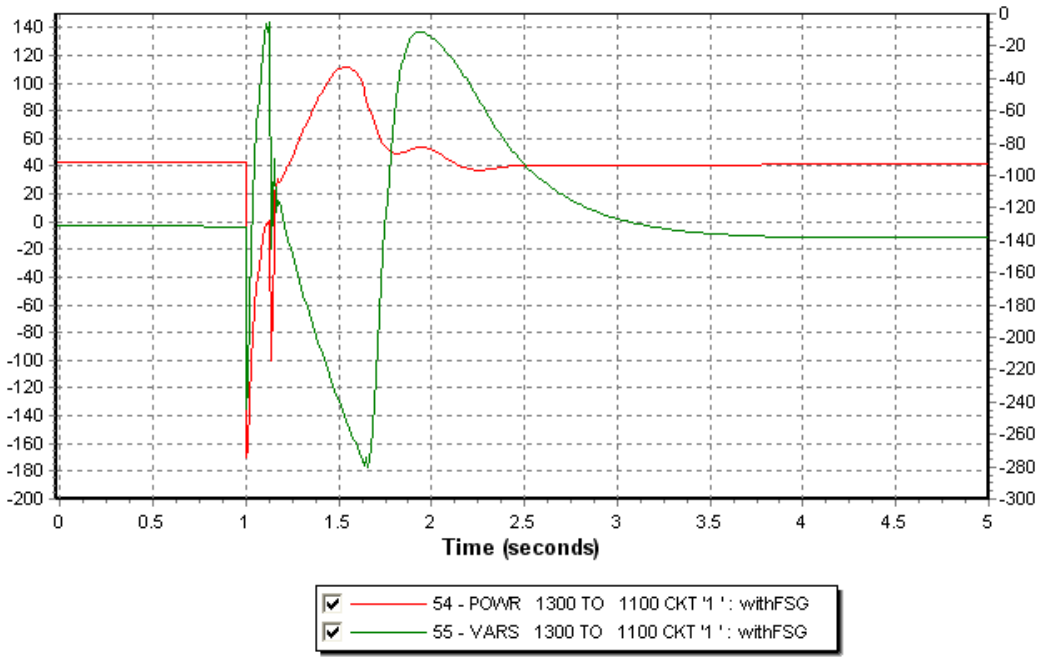

Figure 9-18: Active and reactive power flowing from bus 1300 to 1100, in MW and Mvar

The consequences of this fault are negligible onshore, small variation less than 0.005pu for the voltage and 0.1Hz for the frequency occur in the Norwegian grid. See Appendix H-9: Voltage and frequency variation in the Norwegian grid, both in pu.

9.3.2 BENEFIT OF 2 VSC-HVDC TRANSMISSIONS FOR A CLUSTER

The benefit of having 2 HVDC transmission is clearly shown here. In a configuration with only one HVDC transmission with same amount of reactive power reserve, the system is not able to ride through this fault at bus 1320. By dispatching this reserve thanks this 2 HVDC converters the system become more stable and the voltage control done by the VSC-converter act as SVC with voltage control.

By comparison with the configuration with an SVC set at the same bus as the wind farm equipped with fixed speed generator. The system recovers faster with 2 HVDC converters than equipped with a SVC. The main reason is because the SVC has the inconvenient at low voltage to not be able to supply the maximum reactive power it would which is not the case with the VSC-converter.

Finally thank to this voltage control, the fixed speed generator during the recovery time need less reactive power than with a control on the bus by SVC or alone.

This configuration will be preferred, from the point of view of the control and the regulation of the offshore grid, but without regarding cost of construction or economic view.

9.4 FAULT OFFSHORE AND TRIPPING OF THE LINE BETWEEN THE OFFSHORE HVDC CONVERTERS

Now, a 100ms fault has been performed on the submarine cable between the VSC-HVDC converters and leads to the destruction of the cable, at least after the fault the line is out of service. This could be the consequence of damages on the cable from ship anchors or fishing trawl. The consequence of this fault is that the offshore grid will be divided into 2 parts: one only with the main 500MW wind farm and the second with the oil rig and the 2 400MW wind farms. The result of this simulation will be now presented below.

9.4.1 SIMULATION RESULTS AND PLOTS

The small grid with only the main wind farm and the transmission A will be call the grid A and the second system the grid B.

In the grid A, the voltage at the converter station becomes very low and even reaches 0. After the fault is cleared and the line is tripped, the voltage is recovered very quickly, approximately 300ms after. The voltage in this grid fulfills the ride fault through requirement for the voltage. See Figure 9-19.

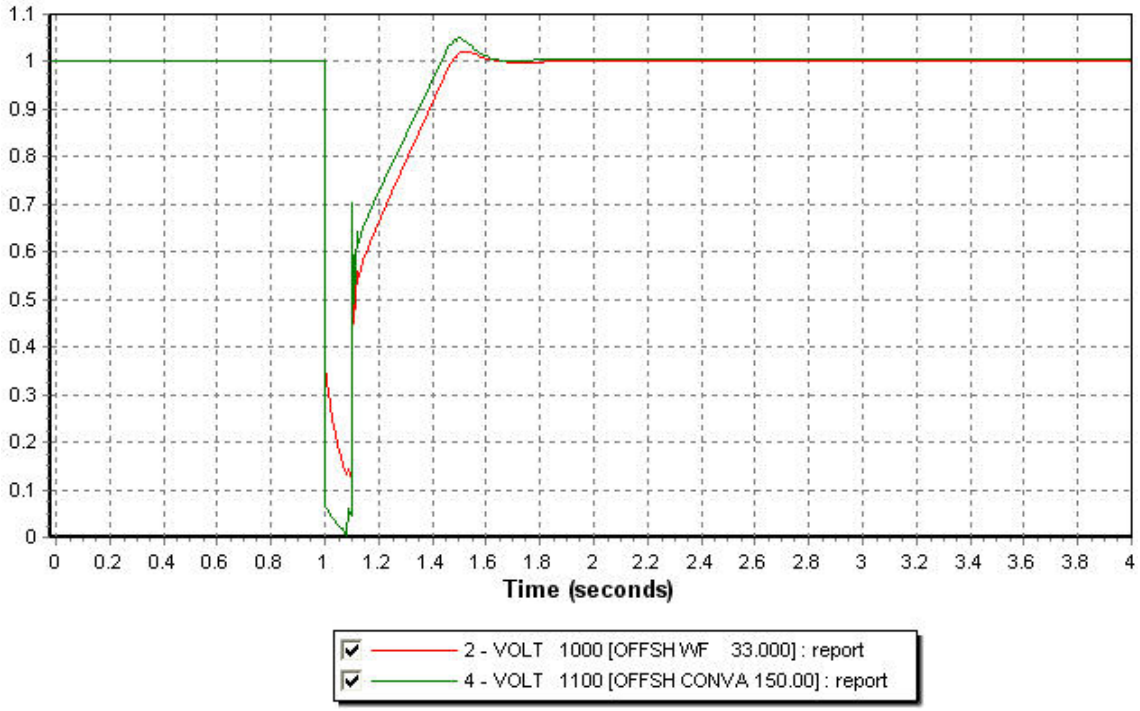

Figure 9-19: Voltage in the grid A in pu

The voltage is longer to be recovered in the grid B. Almost 900ms are necessary before the voltage is recovered. The voltage still success to regain its pre-fault level. The wind farm can also stay connected according the ride fault through requirements. See Figure 9-20.

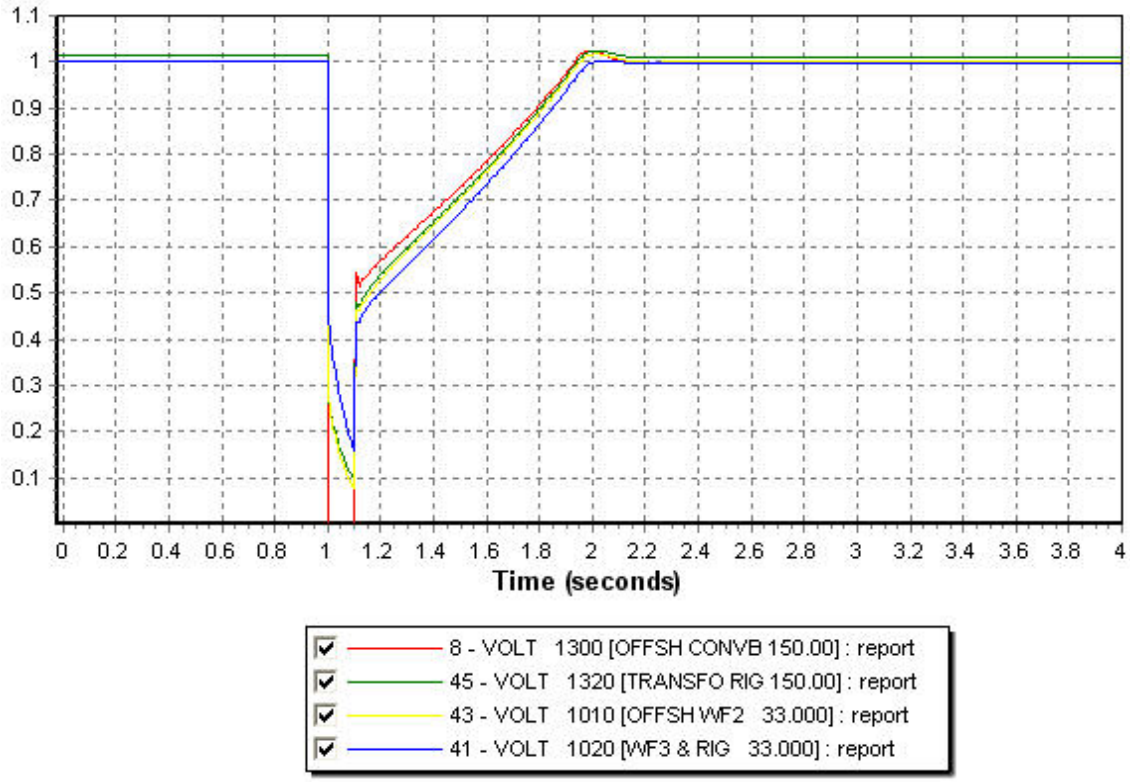

Figure 9-20: Voltage in the grid B in pu

The response of the VSC-converter is now presented. They have similar behaviour. Absorbing reactive power at the pre-fault state, they supply as much as reactive power they can in order to rise up the voltage in both grids, but the VSC-converter in grid B do it longer. Then they regulate down and stabilize at new state, still absorbing reactive power but less than at the pre-fault state. The transmission is also affected by the same way. The pre-fault transmission state is recovered later for the HVDC transmission B. However it has to be notice that the same amount of active power is sent to the Norwegian grid. So, it implies that the wind farm was able to generate more power in the grid A and less in the grid B. difficult to achieve in the reality because the output generated active power is directly connected to the wind speed. The response of the offshore converter A is presented in Figure 9-21 whereas the response of the converter B is shown in Figure 9-22.

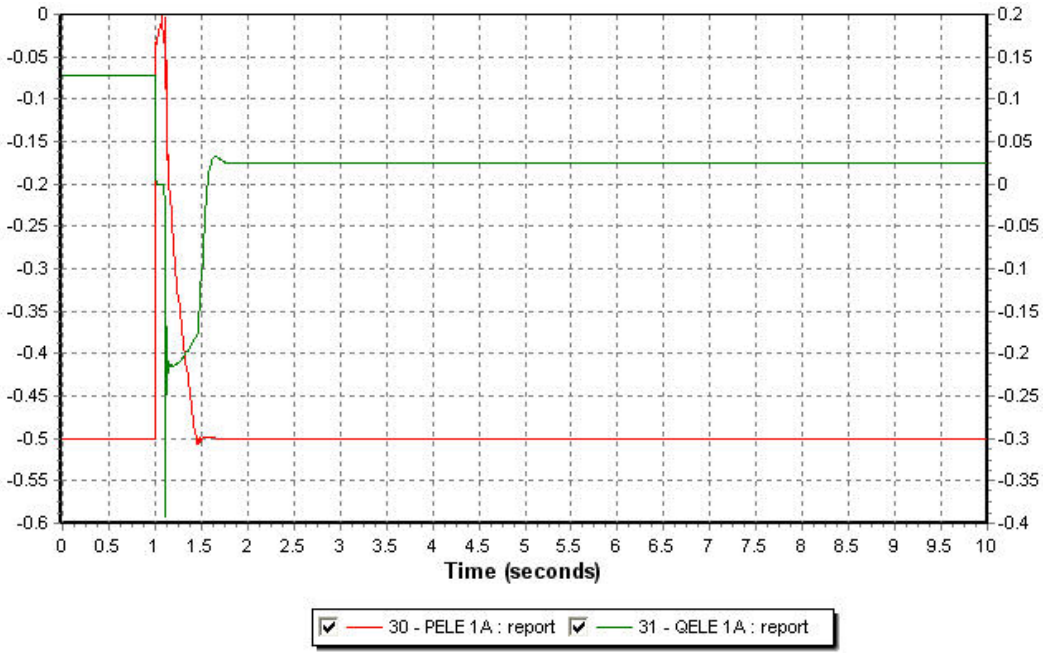

Figure 9-21: Response of the VSC converter from the offshore grid A, in pu on system base

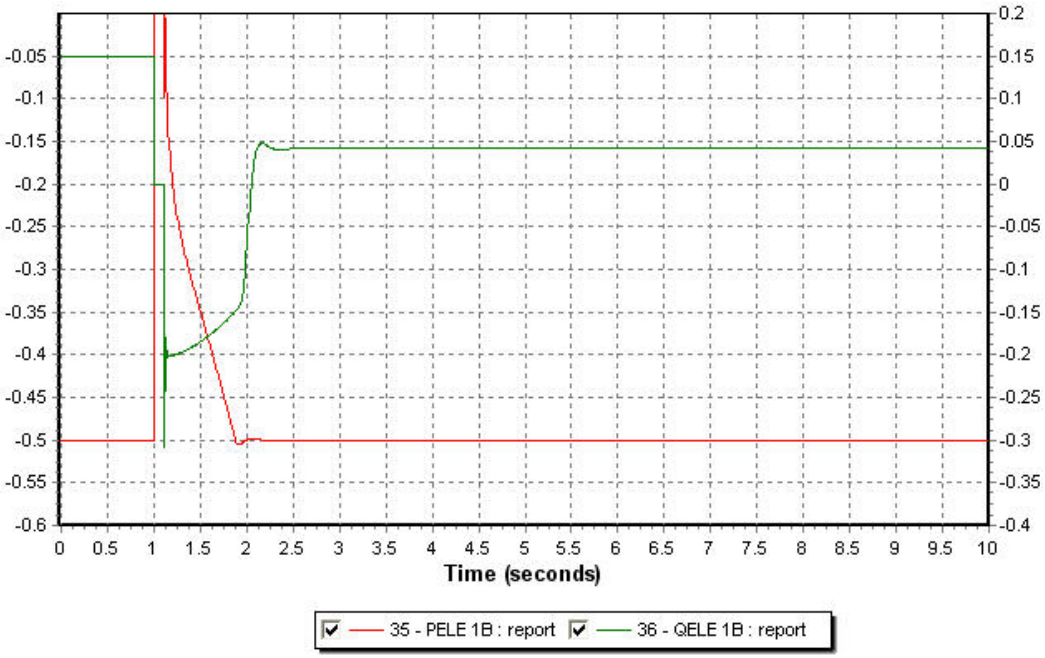

Figure 9-22: Response of the VSC converter from the offshore grid B, in pu on system base

As said previously the generators representing the wind farm have to change their production of active and reactive power according to the new state. They have similar behaviour as describe in the previous simulation during the fault and the recovery time. But a new generation scheme set in. The wind farm A increases its production whereas the wind farms from the grid B decrease their production. The reactive power generated is also slightly changed. This point is discussed in the next part.
The active and reactive powers of the offshore wind farms are given in Figure 9-23, Figure 9-24 and Figure 9-25.
This is also observed in the power flowing into the submarine cable from the oil rig to the HVDC converter B. See Appendix H - 10: Active and reactive power flowing into the cable from the converter to the rig, in MW and Mvar.

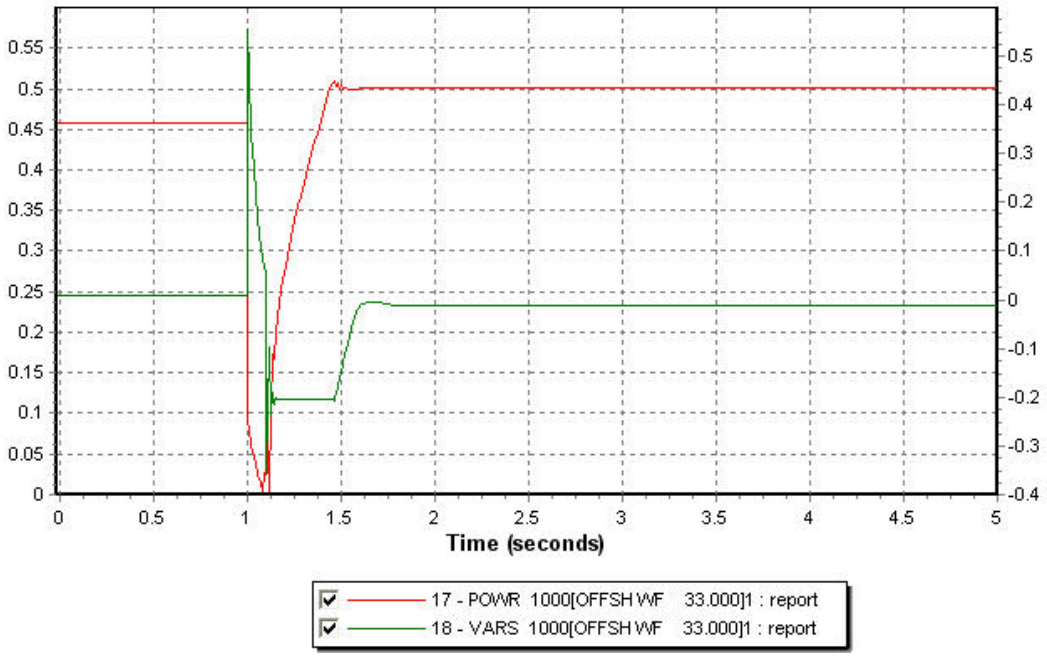

Figure 9-23: Active and reactive power generated by the wind farm from grid A, in pu on system base

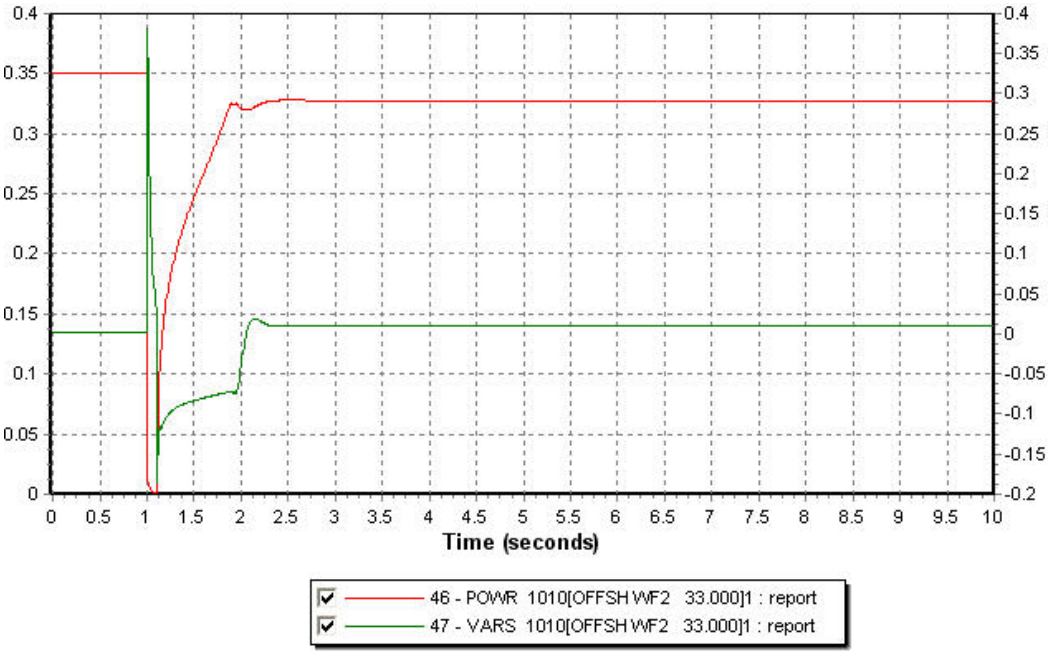

Figure 9-24: Active and reactive power generated by the middle wind farm from grid B, in pu on system base

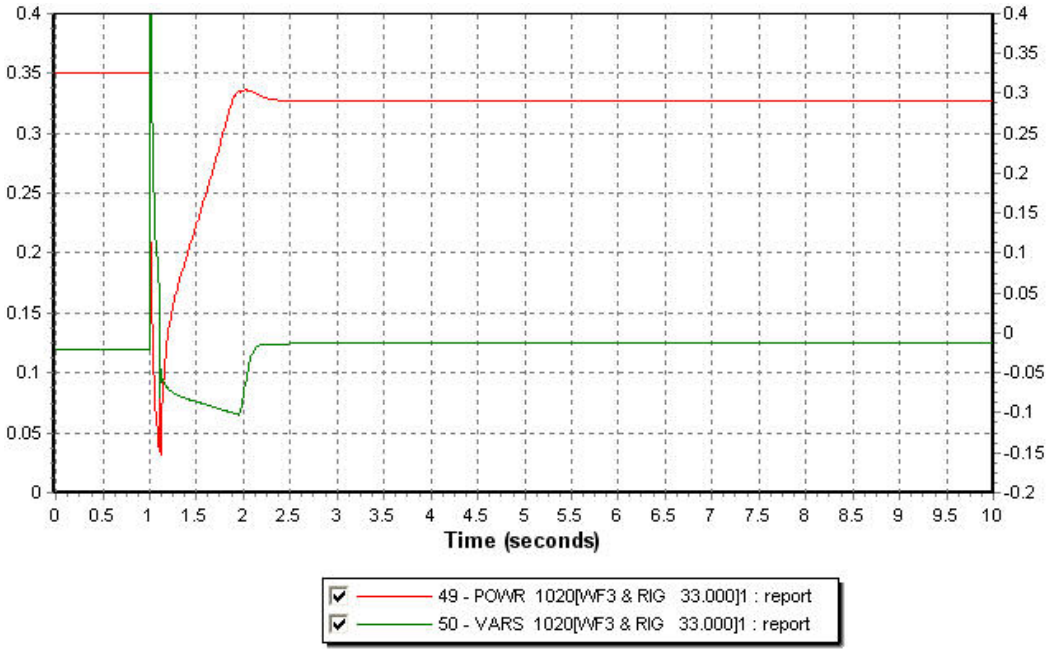

Figure 9-25: Active and reactive power generated by the wind farm at the oil rig in offshore grid B, in pu on system base

From the previous plots, it can be deduced that a new stable state set in inside both new grid. This can be confirmed by looking at the rotor speed and the frequency variation. The rotor speed for all the generators representing the offshore wind farm increases during the fault, but after the recovery time the speed decreases at the generator from the grid A (-0.07 pu from synchronous speed) whereas the generators in the grid B increase their rotor speed to 0.08 pu from synchronous speed). Then a steady set in. See Figure 9-26.

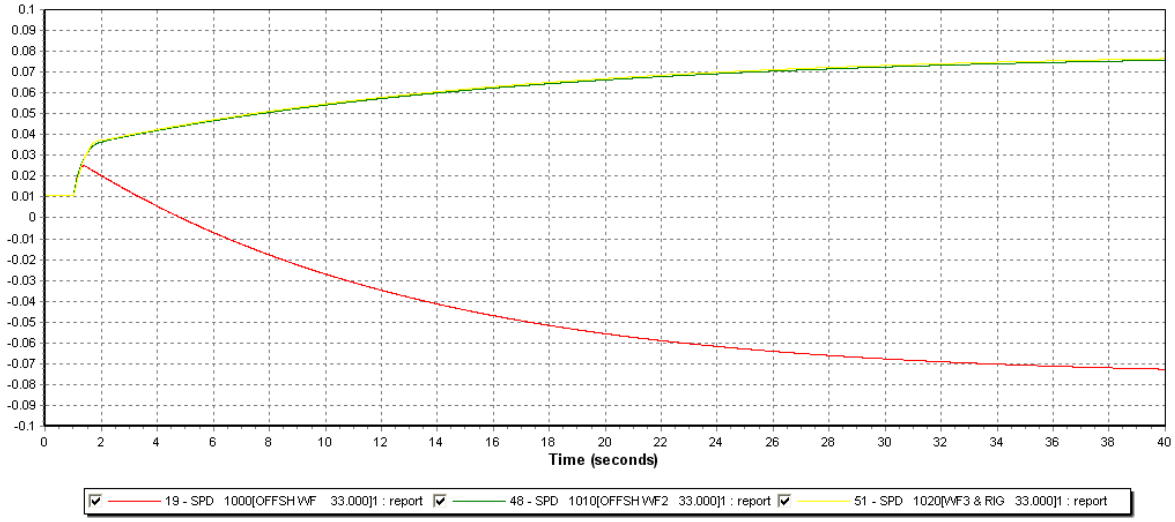

Figure 9-26: Deviation from synchronous rotor speed from generators in pu, red grid A and green and yellow grid B

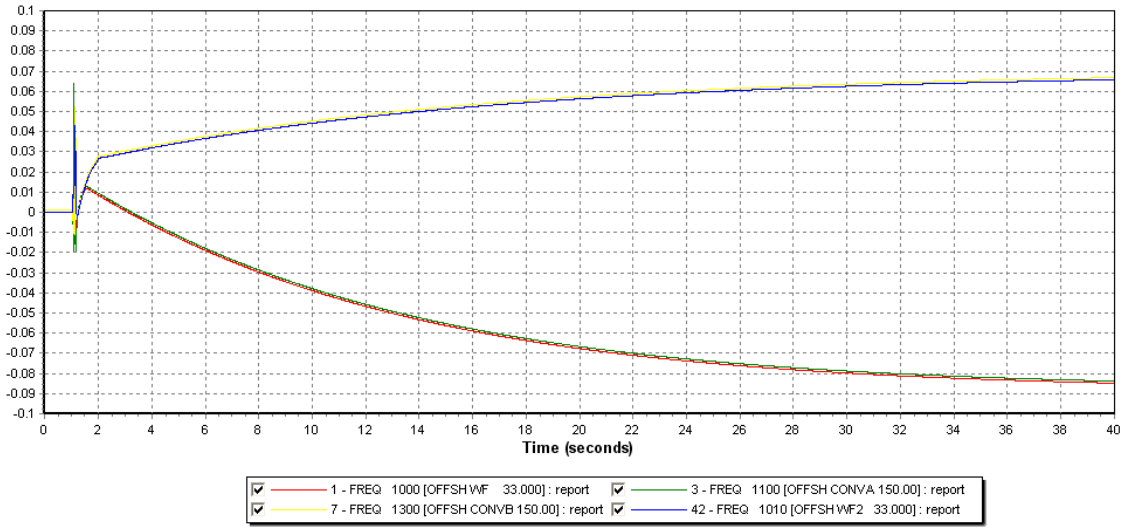

Figure 9-27: Frequency variation in offshore grid A (red & green) and grid B (blue & yellow) 0.02pu=1Hz

The frequency directly linked to the rotor speed has the same behaviour in increase in the grid B until 53.5Hz whereas it goes down to 46Hz in the grid A. So, in this case the frequency is just at the limit of the grid requirement in the grid B but out for the grid A. The wind farm has to be disconnected in grid A according to grid requirement which say that a plant cannot be connected more than 20s below 47.5 Hz. This will be discussed later because no grid requirements are available in Norway for offshore wind power linked to HVDC to the main grid.

The consequences on the main grid are now analyzed.

As presented below the voltage and the frequency are slightly modified with damped oscillations. They swing around the same value as the pre-fault state with amplitude less than 0.005pu for the voltage and less than 0.1Hz for the frequency. See Figure 9-28 and Figure 9-29.

The SVC in the main grid reacts to these changes and supply little reactive power to stabilize the voltage. See Appendix H - 11: Response of the SVC in the grid offshore, in pu on system base.

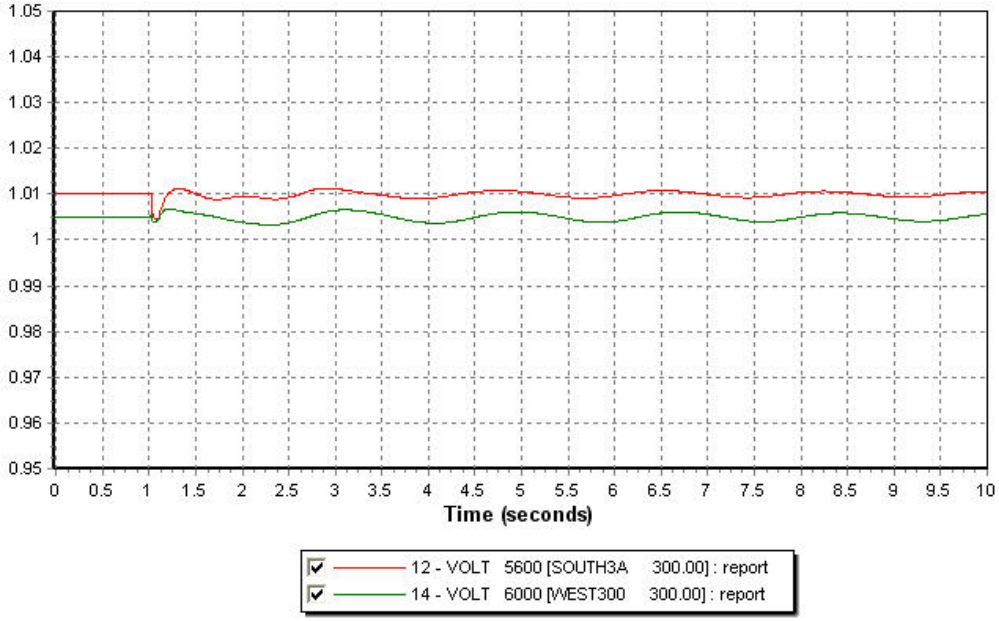

Figure 9-28: Voltage at the main grid in pu

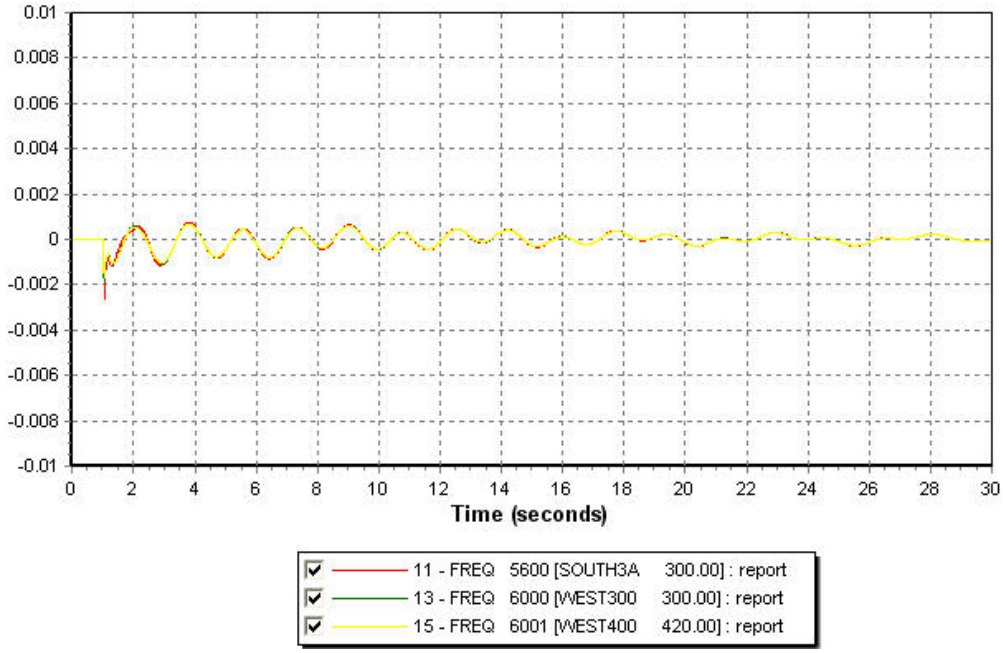

Figure 9-29: Frequency variation in the main grid in pu, 0.02pu= 1Hz

9.4.2 DISCUSSION

The aim of the simulation was to check if the VSC converter was able to control a new small island grid and to establishe a new stable steady state. Any results were expected before this simulation.

Both VSC converters are able to stabilize the system to a new state, but frequency problem occur because too low or too high. One system generates too much active and the frequency goes up and the contrary for grid A. Solutions exist to solve the problem by controlling the HVDC transmission or the wind turbine generator representing the wind farms

After the fault, as the HVDC transmissions keep the transfer of active power at the pre-fault level, it becomes a problem. So, it implies that the wind farm is able to generate more power in the grid A and less in the grid B. To generate more active power for a wind farm is difficult to achieve in the reality because the generated active power is directly connected to the wind speed. The solution is either to have a sufficient reserve of active power in the wind farm by regulating mechanically the blade (stall or pitch angle) or to reduce the active power sent to the shore and to increase production of hydro plant on shore in the same time. This is the easiest solution because having a reserve of active power for wind power is economically a non sense.

During the simulation, the power flowing into the DC transmission could not been changed by the user and it was hard to control the generated power only with the electrical model of the wind turbine generator (CIMTR3). So, in this case, it will have been useful to have a complete wind turbine model to control the pitch angle or some mechanical control on the machine. Furthermore some restrictions on the control of the frequency exits on this model when place in island situation [39].

Anyway, the rise or the drop of frequency inside an offshore wind farm connected by VSC-HVDC is not a problem for the main grid because “isolated” with HVDC transmission. It has been demonstrated in this simulation after the fault, three grids are connected with different frequencies. So, in the actual case of the grid requirement, the wind farm would have been disconnected. However in the future new grid requirements will be established to take into account the new flexibility offered by the VSC-HVDC transmission, i.e. a variable frequency offshore.

10 DISCUSSION

Some points have already been discussed above in the previous sections. An overall discussion is made in this chapter.

For some simulations, it have been noticed the limit of the CIMTR3 model to simulate an entire wind farm. Furthermore, only the electrical model has been used while the control of the wind turbine is also done by mechanical controls such as the control of the pitch angle of the blade or the active/passive stall. In several simulations, the acceleration of the rotor is very important and in the reality this mechanical control of the turbine will have limited this acceleration. In the same way, the representation of a DFIG turbine with a classical induction generator with a large inertia to represent the control on the rotor is also source of uncertainties and inaccuracy in the response of the turbine to a disturbance.

As said in the chapter on the VSC-HVDC representation, the library model from PSS/E has been used to model the HVDC Light transmission. This model has the inconvenient to not respond exactly as the model given by ABB according to the studies made by the University of KTH. The plots with the reactive power from the HVDC converters should be subject of some inaccuracies. For example, some unexplainable peaks may appear during the response or the huge step at the instant the fault is cleared do not seem to be realistic. Simulations should be compared with the HVDC Light mode given by ABB or better with a real measurements of an existing HVDC Light system.

In the case with a 1 GW wind farm connected with a single HVDC transmission the response of the system to an offshore fault at the wind farm buses must be confirmed by other simulations with more accurate model because the high voltage peak during the recovery is very huge and is not acceptable in the reality. Although this simulation has been done several times while changing some parameters, the same result has been obtained. So, in this case, the model of a real wind farm should be used.

Some aspects have been put forward during the simulations.

First, VSC-HVDC converter has the capacity to stabilize alone a small grid. It has been demonstrated when the line has been tripped in the case of a wind farm cluster connected with two HVDC links.

Secondly, it has been observed the property of the HVDC transmission based on VSC technology to “isolate” a fault. The voltage and the frequency in the offshore grid are practically unaffected by a disturbance on the onshore grid and vice versa.

Then, it may be some interactions between the types of generator used inside a wind farm cluster. The replacement of a generator by another type of generator for one of the wind farm may change completely the dynamic behaviour after a disturbance. A wind farm cluster comprising only one type of generator and able to stabilize itself after a disturbance, may become unstable; if the wind farm cluster comprises a mix of generator type (DFIG and FIG). The system is not able to ride through the fault and collapses. The wind farms have to be disconnected. This phenomenon must be studied more into details.

Finally, as expected it as been demonstrate that the multiplication of the VSC-HVDC converter in a grid improve the stability of the system. This skill is particularly important, the reliability and the stability of the main grid will be improved by the different converters of the future offshore DC grid if the VSC technology is widely employed.

11 CONCLUSION

Europe and Norway will benefit from a huge development of the offshore wind power in the North Sea in many aspects. First, it will reduce the dependency to the fossil fuel in the electricity production, except for Norway, where the power production comes mainly from hydro power. Then, this offshore development will reduce the CO_2 emission in respect of the international engagements face to the climate changes. This offshore development in the North Sea will also include a development of the interconnection between the neighbouring countries of the North Sea with the creation of an offshore HVDC grid. In this context, Norway will have a great role with its capacity to balance wind power with hydropower and the high wind resource along the coast The offshore experience of the petroleum sector industries and the recent development of the floating turbine not yet available on the market but in few years will also be an asset. Finally, the petroleum installations will benefit of an green electrification thanks to the HVDC grid. It will also open up new possibilities in the trade of electricity between the NORDEL, the UCTE and the UKTSOA systems.However, this offshore wind power development creates new challenges; not only in the wind turbine construction or in the wind power technologies in general, but also for the electrical power transmission, for the grid regulation and for the power generation.

In this report, the grid integration of different offshore wind farm configurations (single or in cluster) with HVDC transmissions based VSC technology has been studied. Four configurations has been modeled and their electrical stabilities studied regarding the voltage and the frequency: a single 1 GW wind farm with a single HVDC transmission, a cluster of three wind farms connected to an oil rig with a single HVDC transmission and the same configurations as previous but with two HVDC transmissions. The wind farms have not been modeled in detail but represented either equipped with DFIG generators or fixed speed generator. The HVDC transmission based on the VSC technology is well suitable for the offshore transmission because of the small size of the converter which can easily be installed on an offshore platform. Furthermore, this technology offers a significant advantage with voltage control and the control of the reactive power independently of the active power. In addition, with no length restriction as the AC transmission, HVDC can connected wind farms located far from the coast. Finally, with a rating up to 1000MW, it was very suitable for the transmission of such large farms.

First, load flows have been performed to establish the initial conditions of the dynamic simulation. Then, different faults have been applied on buses and the dynamic response analyzed. The VSC-converter reacts always with the same way. When the fault is cleared, the converter supplies as much as possible reactive power in order to increase the low voltage following the fault. The reactive power produced by the converter allows supporting the voltage into the grid. It is finally regulated down to maintain the voltage at approximately 1pu. So, the HVDC converter based on VSC technology contributes to the voltage recovery so that the fault ride trough requirements requires the wind farm to stay connected.

The emphasis has been put on some aspects. First, it may have some interactions between the types of generator used inside a wind farm cluster. A wind farm cluster comprising only one type of generator and able to stabilize itself after a disturbance may become unstable if the wind farm cluster comprises a mix of generator type (DFIG and FIG). The system is not able to ride through the fault and collapses. The wind farms have to be disconnected.

Secondly, a VSC-HVDC converter has the capacity to alone stabilize a small grid. Then, the VSC-HVDC transmission has the capacity to “isolate” a disturbance. The voltage and the frequency offshore are practically unaffected by a fault offshore and vice versa.

Finally, as expected, it as been demonstrated that the multiplication of the VSC-HVDC converter in a grid improves the stability of the system. The HVDC transmission based on VSC technology will be well suitable in the future HVDC grid in the North Sea and will contribute to improve the stability of the main grid in the neighbouring countries of the North Sea.

12 FURTHER WORK

Some suggestions for further work are presented in this chapter. They could be used as input or idea to formulating new projects for master thesis.

Following this thesis, some aspects have to be studied and investigated more into detail. The interaction and the impact of different wind turbine generators could be studied. For one year, Siemens has now updated its library PSS/E with a wind power package which comprises model of the four main types of generator, fixed speed generator, improved variable speed generator, DFIG and full scale frequency converter.

Another interesting case to investigate is the future HVDC grid that is planned. Inside this large idea some aspects could be studied such as the multiterminal HVDC technology. There is no model of multiterminal HVDC with the VSC technology available in the library, but a model is planned to be added very soon. Now, only a model based on the LCC technology is available.
The creation of a reduced PSS/E model of this HVDC grid and the national grids of Scandinavia, Great Britan and Germany could be a base of work to investigate different problem such as the repartition of the wind farms and the impact on the onshore generation system and the stability of some parts of the system. This offshore HVDC grid model could be based on the NORDEL 32 that has been used in this thesis or done in a similar way.

REFERENCES

[1]Delivering offshore wind power in Europe – European Wind Energy Association – December 2007
[2] Global wind energy outlook 2008 - GWEC
[3] HVDC connection of offshore wind farms to the transmission system – P. Bresetti, W.L.Kling, R.L. Hendriks – IEEE – March 2007
[4] http://www.trade-wind.eu/
[5] http://www.norsewind.eu/public/index.html
[6] http://www.nve.no/
[7] Large scale integration of wind energy in the european power supply – Table 3: Overview of wind turbine concepts – EWEA – 2007
[8] http://www.actu-environnement.com/ae/news/produciton_eolienne_espagne_6282.php4
[9] A north sea electricity grid [r]evolution – Report from 3E (Belgium) for Greenpeace – July 2008
[10] Floating windmills – HYDRO Oil & energy - 2008
[11] http://sway.no/
[12] Integration of offshore windpower in Northern Europe – European coordinator's report – Mr Georg Wilhelm Adamowitsch – Malmö 2008
[13] The ABCs of HVDC transmission technology – 1540-7977 IEEE – M.P. Bahrman, B.K. Johnson – April 2007
[14] HVDC Transmission Proven Technology for power exchange – Siemens document
[15] Power electronics Converters, applications and design – Chapter 16 Line frequency phase controlled rectifiers and inverters – Mohans, Undeland and Robbins - 2003
[16] It's time to connect Technical Description of HVDCLight technology – ABB - 2008
[17] HVDC Plus Principle of operation and basis – SIEMENS - 2008
[18] HVDC Classic ABB document – Reference List – Elanders – 2006
[19] International research and development trends and problems of HVDC cables with polymeric insulation – table II – Salah Khalil – IEE Electrical insulation magazine -November/December 1997
[20] http://www.abb.com/cawp/gad02181/8b7855aed33f6befc1256d8800401fa0.aspx
[21] Connecting offshore wind farms to (VSC-) HVDC interconnectors – R. L. Hendriks, G.C. Paap, W.L. Kling - Nordic wind power conference - 2006
[22] Realisierung ein offshore Vindpark: Anbildung mit selbstgefurther HGÜ – ABB – Gunter Stark – April 2008
[23] Advanced power electronics for cable connection of offshore wind farm – Comparison HVDC technology – Bo Normark E. K. Nielsen – Copenhagen Offshore Wind 2005
[24] SwePol Link sets new environmental standard for HVDC transmission - Leif Söderberg, Bernt Abrahamsson- ABB review 4 - 2001
[25] Advanced power electronics for cable connection of offshore wind – B. Normark &E. Koldby Nielsen - 2005
[26] http://www.abb.com/cawp/gad02181/306c726f332f36d3c1257353003b91f0.aspx - November 2007
[27] FISK Funksjonkrav i kraftsystemet – Veileder - Statnett
[28] Definition and classification of power system stability – IEEE/CIGRE – May 2004
[29] IEEE Guide for Planning DC Links Terminating at AC Locations Having Low Short-Circuit Capacities-1997
[30] Connection of large offshore wind farm to the Norwegian grid – Knut Sommerfelt - 2008
[31] User's manual for PSS/E – Program application guide: volume II – 14.4.4 Generator rotor speed damping
[32] Modelling of the power system of Gotland in PSS/E with a focus on HVDC Light – Martin Brask – June 2008
[33] Presentation ABB "HVDC studies and applications" – Don MARTIN – October 2008
[34] User's manual for PSS/E – Program application guide: volume II – 23.9.4 VSC DC Power Flow representation
[35] User's manual for PSS/E – Program operation manual: volume II – L.11 VSCDCT
[36] Comparison of the response of Double Fed and fixed speed induction generator for wind turbine to changes in the network frequency – Nick Jenkins, Janaka etanayake – IEEE –December 2004
[37] Model building manual wind generation – Midwest reliability organization – October 2007
[38]XLPE submarine cables – User's guide - ABB
[39] User's manual for PSS/E – Program application guide volume II – L26 Modes of extended term simulation

APPENDIX

A PRESENTATION

Appendix A - 1: Global cumulative installed capacity of wind power in the period of 1996-2007

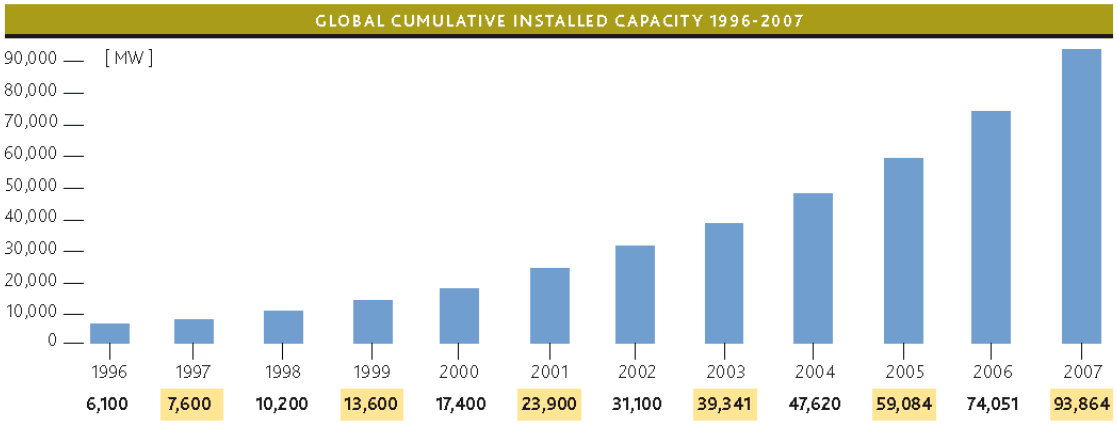

B HVDC TECHNOLOGY

Appendix B - 1: Summing up table to compare different cable technologies.
The table compares different technologies of HVDC submarine cable.[3]

	Cables \ Features	Light land	Light submarine	MIND	LPOF	IRC
Corrosion protection	**Conductor**	Aluminum	Copper	Copper	Copper	copper
	Insulating	Polymeric	Polymeric	Paper	paper	Mass impregnated / Polymeric
	Galvanization	No	Steel wires	Steel wires	Steel wires	Steel wires
	Interior corrosion protection	Aluminum laminate	Lead alloy	Lead sheath	Lead sheath	Lead sheath
	Wet exterior protection	No	Yes	Yes	Yes	Yes
	Outer cover	polyethylene or PVC	PP yarn	PP yarn	PP yarn	PP yarn
Mechanical protection	**Double armouring**	No	Yes	available	reinforcement	Yes*
	Bending radius during installation	15 De	>15De	Bad	Bad	Bad
	Bending radius after installation	10 De	>15De	Bad	Bad	Bad
	Tensile armour	copper wires	steel wires	steel wires	steel wires	steel wires / return conductor
	Resistance torsion	good	good	not bad	bad	free
	Resistance tensile	good	good	bad	bad	good
	Laying depth cable [m]		1500	1000	500	350**
	Laying depth joint [m]		>1000	500	No data found	500
	Power range per cable [MW]	500	250	600	1000	250*
	Voltage range [kV]	150	300	500	600	250
	Temperature max [ºC]	90	90	70	85	70
	Operating experience	<10 years	NC	>20years	>20years	<10 years
	Limitation	Voltage and power	Voltage and power	Temperature	Length - Oil restriction	Weight

* return conductor is part of the armouring **only one cable built, without doubt more De=outer radius PP=polypropylene

[3] The table is extracted from a previous work done in the pre-master thesis: HVDC submarine cables

C HVDC TRANSMISSION & OFFSHORE WIND FARM

Appendix C - 1: Short circuit power for buses 5600 and 6000

```
                                  <-SCMVA-> <-Sym I''k rms--> <-ip(B)-> <-ip(C)-> <-DC Ib-> <Sym Ib-> <Asym Ib>
                                              /I/    AN(I)       /I/       /I/       /I/       /I/       /I/
X---------- BUS ----------X          P.U.      P.U.     DEG       P.U.      P.U.      P.U.      P.U.      P.U.
  5600 [SOUTH3A     300.00] 3PH      18.15    18.1490   -88.28   49.1618   49.2011   12.6136  213.8027  213.6021

THEVENIN IMPEDANCE (PU), X/R
Z+: 0.001823+j0.060582, 33.228485

-------------------------------------------------------------------------------------------------------------
       *** FAULTED BUS IS:   5600 [SOUTH3A     300.00] ***   0 LEVELS AWAY ***
AT BUS   5600 [SOUTH3A     300.00] AREA   56
    (PU) VA:   0.0000+J 0.0000     VB:   0.0000+J 0.0000     VC:   0.0000+J 0.0000

                                          X-------------------------THREE PHASE FAULT-------------------------X
X--------- FROM ----------X AREA CKT    I     RE(IA)   IM(IA)   RE(IB)   IM(IB)   RE(IC)   IM(IC)
MACHINE 1                               PU    6.5561  -8.8883 -10.9756  -1.2336   4.4195  10.1219
  5601 [SOUTH4A     420.00]   56 1      PU    0.2505  -5.9255  -5.2568   2.7458   5.0064   3.1796
  5603 [SOUTH3B     300.00]   56 1      PU    0.1626  -2.2223  -2.0059   0.9704   1.8433   1.2520
  6000 [WEST300     300.00]   60 1      PU    0.1966  -2.2372  -2.0358   0.9483   1.8392   1.2889
INITIAL SYM. S.C. CURRENT(I''k)(RMS)   P.U.   0.5459 -18.1408 -15.9834   8.5976  15.4374   9.5432
                     I''k (MAG/ANG)    P.U.  18.1490   -88.28  18.1490   151.72  18.1490    31.72

-------------------------------------------------------------------------------------------------------------


                                  <-SCMVA-> <-Sym I''k rms--> <-ip(B)-> <-ip(C)-> <-DC Ib-> <Sym Ib-> <Asym Ib>
                                              /I/    AN(I)       /I/       /I/       /I/       /I/       /I/
X---------- BUS ----------X          P.U.      P.U.     DEG       P.U.      P.U.      P.U.      P.U.      P.U.
  6000 [WEST300     300.00] 3PH      26.82    26.8212   -87.72   71.6820   71.7209    9.8282  218.4014  218.3041

THEVENIN IMPEDANCE (PU), X/R
Z+: 0.001629+j0.040980, 25.149437

-------------------------------------------------------------------------------------------------------------|
       *** FAULTED BUS IS:   6000 [WEST300     300.00] ***   0 LEVELS AWAY ***
AT BUS   6000 [WEST300     300.00] AREA   60
    (PU) VA:   0.0000+J 0.0000     VB:   0.0000+J 0.0000     VC:   0.0000+J 0.0000

                                          X-------------------------THREE PHASE FAULT-------------------------X
X--------- FROM ----------X AREA CKT    I     RE(IA)   IM(IA)   RE(IB)   IM(IB)   RE(IC)   IM(IC)
MACHINE 1                               PU    3.3401  -3.6561  -4.8364  -1.0645   1.4963   4.7207
  5400 [CNTR3-A     300.00]   54 1      PU    0.3873  -5.1315  -4.6377   2.2303   4.2504   2.9012
  5600 [SOUTH3A     300.00]   56 1      PU    0.1294  -1.8210  -1.6418   0.7984   1.5123   1.0226
  6001 [WEST400     420.00]   60 1      PU    0.3476 -12.0207 -10.5840   5.7093  10.2364   6.3114
  6100 [NWEST3      300.00]   61 1      PU    0.2129  -3.2636  -2.9328   1.4474   2.7199   1.8162
INITIAL SYM. S.C. CURRENT(I''k)(RMS)   P.U.   1.0656 -26.8000 -23.7423  12.4772  22.6767  14.3229
                     I''k (MAG/ANG)    P.U.  26.8212   -87.72  26.8212   152.28  26.8212    32.28

-------------------------------------------------------------------------------------------------------------
```

D PSS/E MODEL

D.1 CONVERSION OF LOAD

Appendix D - 1: Load conversion

For all the simulations, the parameters of a normal load conversion have been used.

Load representation	Normal load		Industrial load	
	P %	Q%	P%	Q%
Constant power	40	30	0	0
Constant current	40	20	100	0
Constant admittance	20	50	0	100

D.2 NORDEL GRID USED

Appendix D - 2: Nordel grid used after changes.

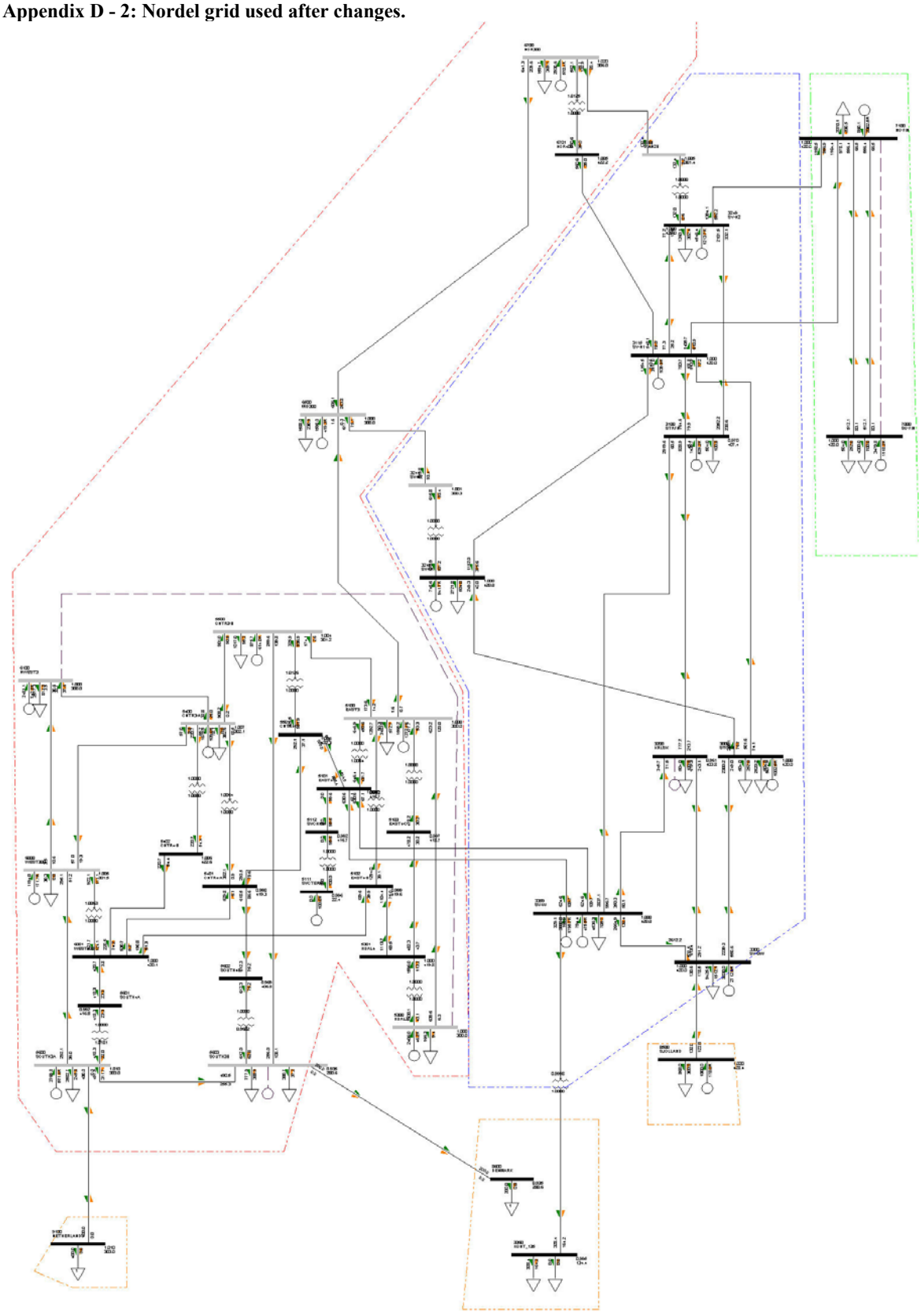

D.3 ORIGINAL LOAD FLOW CASE

Appendix D - 3: Buses data voltage in pu and angle in degree.

```
------------------------------------------------------------------------------

    PTI INTERACTIVE POWER SYSTEM SIMULATOR--PSS(tm)E    THU, APR 09 2009  18:24
 REDUCED NORDEL POWER SYSTEM MODEL                                    BUS DATA
 V 3.2, 12.08.97
                                      S H U N T S
   BUS# X-- NAME --X BASKV CODE LOADS FIXED SWITCHED  VOLT   ANGLE AREA ZONE OWNER
   3000 STCKH       420.00   2    2     0       0    1.00000   22.4   40    2    1
   3100 STRFN       420.00   2    1     0       0    0.97000   34.3   40    2    1
   3115 SV-N1       420.00   2    0     0       0    1.00000   53.8   40    2    1
   3200 KRLSK       420.00   1    1     0       0    0.96430    5.8   40    2    1
   3244 SV-M2       300.00   1    0     0       0    1.00110   20.4   40    2    1
   3245 SV-M1       420.00   2    1     0       0    1.00000   19.7   40    2    1
   3249 SV-N2       420.00   2    1     0       0    1.00000   52.8   40    2    1
   3300 SV-SW       420.00   3    1     0       0    1.00000    0.0   40    2    1
   3359 SV-W        420.00   2    1     0       0    1.00000   12.9   40    2    1
   3360 KONT_135    135.00   1    2     0       0    0.99523   12.6   40    3    1
   3701 SV-N2B      300.00   1    0     0       0    1.00439   56.6   40    2    1
   5100 EAST3       300.00   2    1     0       0    1.00000   21.2   51    1    1
   5101 EAST4-A     420.00   1    0     0       0    0.99217   20.1   51    1    1
   5102 EAST4-B     420.00   1    0     0       0    0.99906   23.5   51    1    1
   5103 EAST4-C     420.00   1    0     0       0    0.99701   24.0   51    1    1
   5111 SVCTERM     22.500  -2    0     0       0    0.99585   20.1   51    1    1
   5112 SVCHIGH     420.00   1    0     0       0    0.99217   20.1   51    1    1
   5300 HDAL3       300.00   2    1     0       0    1.00000   36.0   53    1    1
   5301 HDAL4       420.00   1    0     0       0    0.99958   30.4   53    1    1
   5400 CNTR3-A     300.00   2    1     0       0    1.00700   28.4   54    1    1
   5401 CNTR4-A     420.00   1    0     0       0    0.99825   25.8   54    1    1
   5402 CNTR4-B     420.00   1    0     0       0    1.00610   28.2   54    1    1
   5500 CNTR3-B     300.00   2    1     0       0    1.00400   22.7   55    1    1
   5501 CNTR4-C     420.00   1    0     0       0    1.00556   22.4   55    1    1
   5600 SOUTH3A     300.00   2    1     0       0    1.01000   22.2   56    1    1
   5601 SOUTH4A     420.00   1    0     0       0    0.99234   22.4   56    1    1
   5602 SOUTH4B     420.00   1    0     0       0    0.96852   17.1   56    1    1
   5603 SOUTH3B     300.00  -2    2     0       0    0.93517   15.9   56    1    1
   6000 WEST300     300.00   2    1     0       0    1.00500   28.1   60    1    1
   6001 WEST400     420.00   1    0     0       0    1.00015   27.3   60    1    1
   6100 NWEST3      300.00   2    1     0       0    1.00000   28.1   61    1    1
   6500 MID300      300.00   2    1     0       0    1.00000   22.1   65    1    1
   6700 NOR300      300.00   2    1     0       0    1.02000   64.2   67    1    1
   6701 NOR400      420.00   1    0     0       0    1.00524   63.5   67    1    1
   7000 SO-FIN      420.00   2    2     0       0    1.00000  -45.9   70    2    1
   7100 NO-FIN      420.00   2    1     0       0    1.00000  -12.9   71    2    1
   8500 SJOLLAND    420.00   2    1     0       0    1.02000    2.1   90    3    1
   8600 DENMARK     300.00   1    1     0       0    0.93517   15.9   90    3    1
   9100 NETHERLANDS 300.00   1    1     0       0    1.01000   22.2   91    3    1
```

Appendix D - 4: Exchange flow and production of each zone.

```
------------------------------------------------------------------------------

    PTI INTERACTIVE POWER SYSTEM SIMULATOR--PSS(tm)E    THU, APR 09 2009  18:20
 REDUCED NORDEL POWER SYSTEM MODEL                                    ZONE
 V 3.2, 12.08.97                                                   INTERCHANGE

       TO ZONE:     1     2     3
 FROM ZONE    *------------------
         1    *        2567   600
 NORWAY       *        -265     0
              *------------------
         2    * -2567         199
 SWE & FIN    *   265          -12
              *------------------
         3    *  -600  -199
 DEN & NETH   *     0    12
              *------------------



------------------------------------------------------------------------------

    PTI INTERACTIVE POWER SYSTEM SIMULATOR--PSS(tm)E    THU, APR 09 2009  18:23
 REDUCED NORDEL POWER SYSTEM MODEL                                 ZONE TOTALS
 V 3.2, 12.08.97                                                    IN MW/MVAR

                 FROM      TO    TO BUS  TO LINE     FROM      TO
 X-- ZONE --X GENERATION  LOAD    SHUNT    SHUNT CHARGING  NET INT   LOSSES
```

1	17500.0	14217.0	0.0	0.6	0.0	3166.5	115.8
NORWAY	3041.0	2760.1	0.0	-26.3	1101.5	-265.4	1674.2
2	27164.4	28550.2	0.0	0.0	0.0	-2368.0	982.1
SWE & FIN	12510.3	5134.4	0.0	0.0	2049.2	253.9	9171.2
3	1000.0	1796.4	0.0	0.0	0.0	-798.5	2.1
DEN & NETH	178.0	464.2	0.0	0.0	306.1	11.6	8.3
TOTALS	45664.4	44563.7	0.0	0.6	0.0	0.0	1100.1
	15729.2	8358.7	0.0	-26.3	3456.8	0.0	10853.7

Appendix D - 5: Generator data.

PTI INTERACTIVE POWER SYSTEM SIMULATOR--PSS(tm)E THU, APR 09 2009 18:24
REDUCED NORDEL POWER SYSTEM MODEL GENERATOR
V 3.2, 12.08.97 UNIT DATA

BUS#	NAME	BASKV	CD	ID	ST	PGEN	QGEN	QMAX	QMIN	PMAX	PMIN	MBASE
	Z S O	R C E										
3000	STCKH	420	2	1	1	5072.9	979.5	49995	*******	49995	*******	6500
	0	0.225										
3100	STRFN	420	2	1	1	1435.7	539.5	49995	*******	49995	*******	2500
	0	0.1169										
3115	SV-N1	420	2	1	1	3417	931.1	49995	*******	49995	*******	4000
	0	0.23										
3200	KRLSK	420	1	1	0	0	0	49995	*******	49995	*******	500
	0	1										
3245	SV-M1	420	2	1	1	746.6	931.8	49995	*******	49995	*******	1500
	0	0.1539										
3249	SV-N2	420	2	1	1	4546.4	1218.5	49995	*******	49995	*******	5500
	0	0.21										
3300	SV-SW	420	3	1	1	4255.9	2558.3	49995	*******	49995	*******	5000
	0	0.16										
3359	SV-W	420	2	1	1	2555.6	1701.7	49995	*******	49995	*******	4000
	0	0.1937										
3359	SV-W	420	2	2	1	794.4	529	9999	-9999	9999	-9999	1200
	0	0.1937										
5100	EAST3	300	2	1	1	1565.2	1273.8	49995	*******	49995	*******	2100
	0	0.1514										
5111	SVCTERM	22.5	-2	1	1	0	100	100	-100	0	0	600
	0	1										
5300	HDAL3	300	2	1	1	2406	46.1	49995	*******	49995	*******	2750
	0	0.26										
5400	CNTR3-A	300	2	1	1	1679.5	109	49995	*******	49995	*******	1900
	0	0.16										
5500	CNTR3-B	300	2	1	1	875.7	-613.7	49995	*******	49995	*******	1200
	0	0.2282										
5600	SOUTH3A	300	2	1	1	2769.8	571.6	49995	*******	49995	*******	2850
	0	0.28										
5603	SOUTH3B	300	-2	1	0	100	0	9999	-9999	9999	-9999	1000
	0	1										
6000	WEST300	300	2	1	1	1194	-171.1	1000	-1000	49995	*******	1400
	0	0.28										
6100	NWEST3	300	2	1	1	2481.1	742.8	49995	*******	49995	*******	2900
	0	0.18										
6500	MID300	300	2	1	1	1598	415.3	49995	*******	49995	*******	1900
	0	0.158										
6700	NOR300	300	2	1	1	2930.6	567.1	49995	*******	49995	*******	3400
	0	0.1706										
7000	SO-FIN	420	2	1	1	3479.8	1118.2	49995	*******	49995	*******	6500
	0	0.225										
7100	NO-FIN	420	2	1	1	860.1	2002.6	49995	*******	49995	*******	2200
	0	0.1539										
8500	SJOLLAND	420	2	1	1	1000	178	49995	*******	49995	*******	2000
	0	0.1706										

D.4 ORIGINAL MODEL

Appendix D - 6: Parameter for the SVC at bus 5111 to control the grid.

Static Var Compensator at bus 5111 to control the voltage of the model: library CSVGN5

	Original configuration	Selected configuration
TS1	0	0
VE MAX	0.15	0.1
TS2	0	0.1
TS3 (>0)	0.025	5
TS4	0	0
TS5	0.7	0.7
KSVS	100	200
KSD	0	0
BMAX	1	0.8
B'MAX	1	0.8
B'MIN	-1.1	-0.5
B MIN	-1.1	-0.5
TS6 (>0)	0.03	0.02
DV	0.25	0.05
Remote controlled bus	5111	5401

A fault has been performed at bus 5600 and the response has been analyzed with different SVC parameter and addition of damping coefficient for all the generators. The parameters which have given the better response (low damped oscillations and quick voltage recovery) have been selected for the rest of the simulation as reference model.

Appendix D - 7: Selected configuration, voltage & frequency bus 5600 & 6000

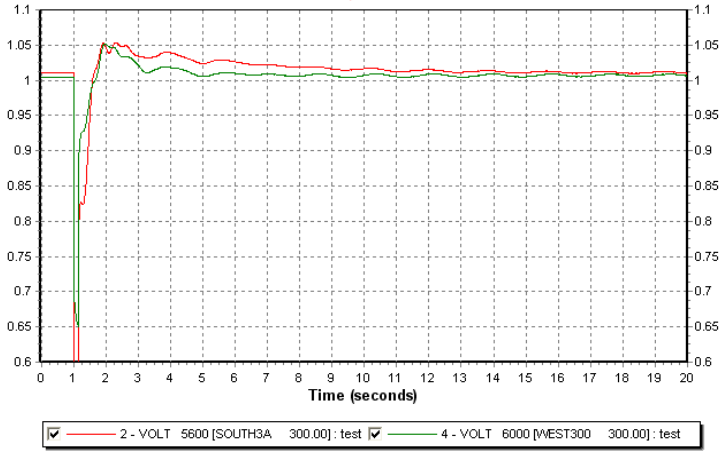

Voltage at bus 5600 and 6000: At 20s voltage oscillation amplitude less than 0.01pu

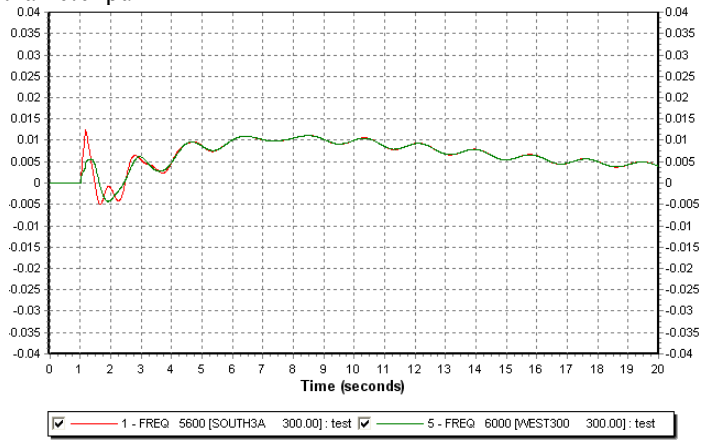

Frequency deviation at bus 5600 and 6000: max deviation 0.5Hz and amplitude oscillation 0.1 Hz

Appendix D - 8: Original configuration, voltage & frequency bus 5600 & 6000

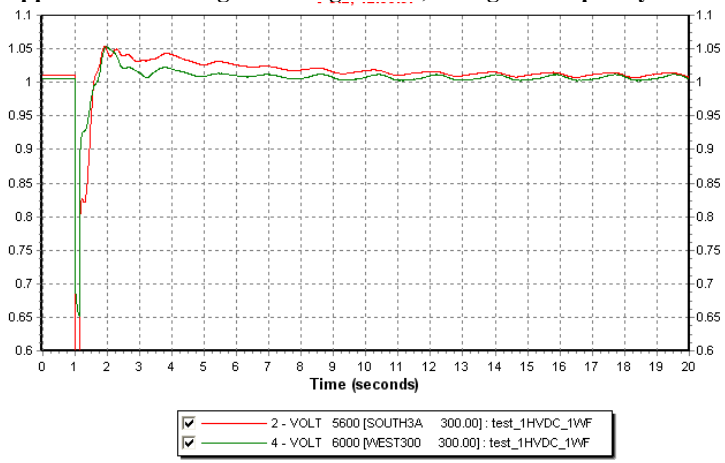

Voltage at bus 5600 and 6000: At 20s voltage oscillation amplitude up to 0.03pu

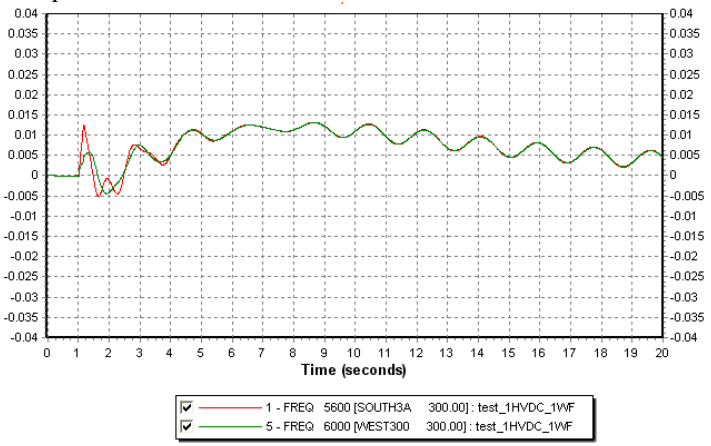

Frequency variation at bus 5600 and 6000: maximum deviation 0.7Hz and amplitude oscillation 0.3Hz

Appendix D - 9: Selected configuration, active and reactive power at bus 5600

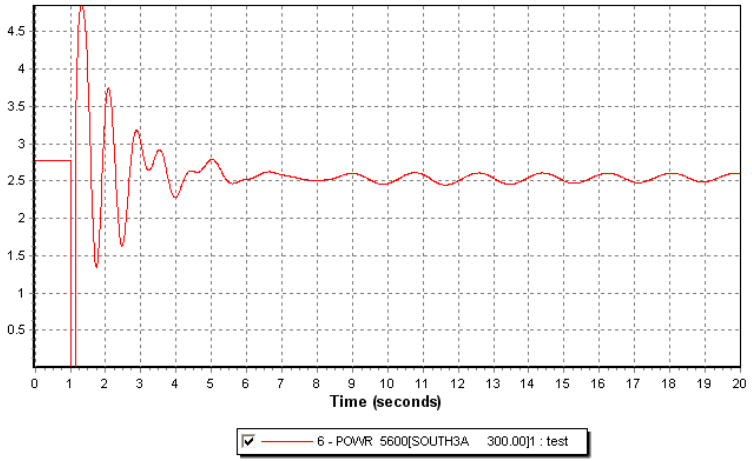

Active power at bus 5600 in pu on system base

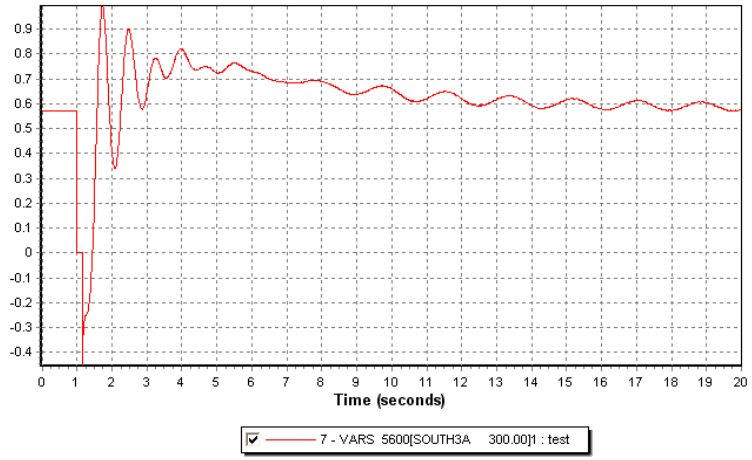

Reactive power at bus 5600 in pu on system base

Appendix D - 10: Original configuration, active and reactive power at bus 5600

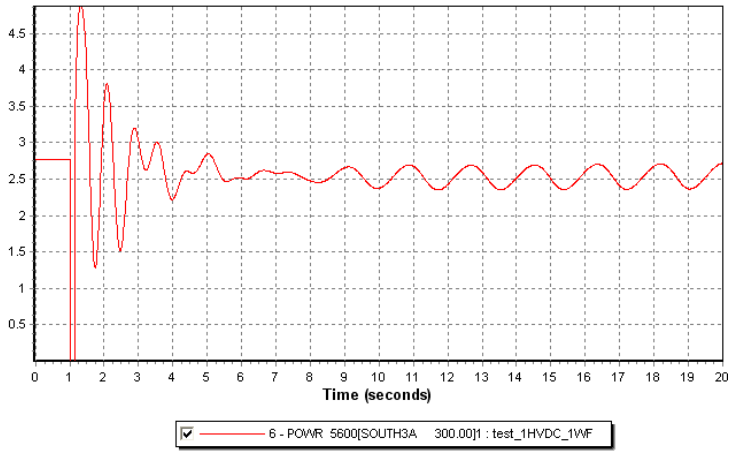

Active power at bus 5600 in pu on system base

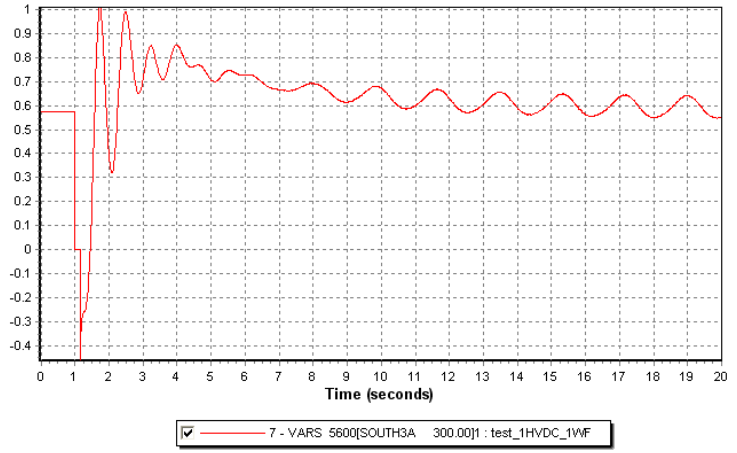

Reactive power at bus 5600 in pu on system base

Appendix D - 11: Response of the selected SVC and the original SVC.

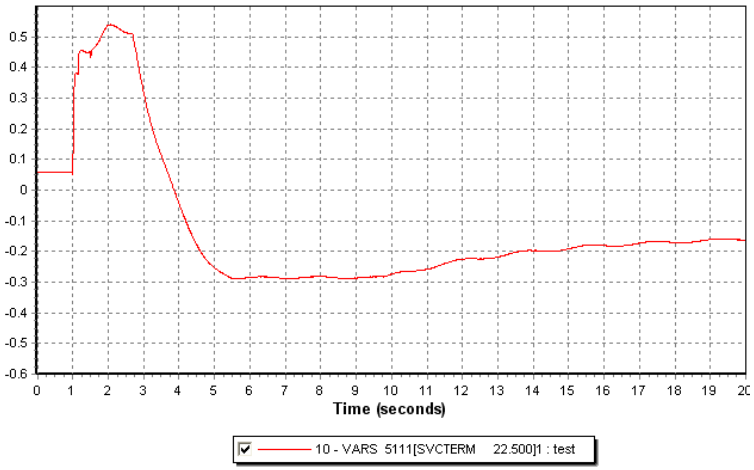

Response of the selected SVC: supply 540 Mvar maximum.

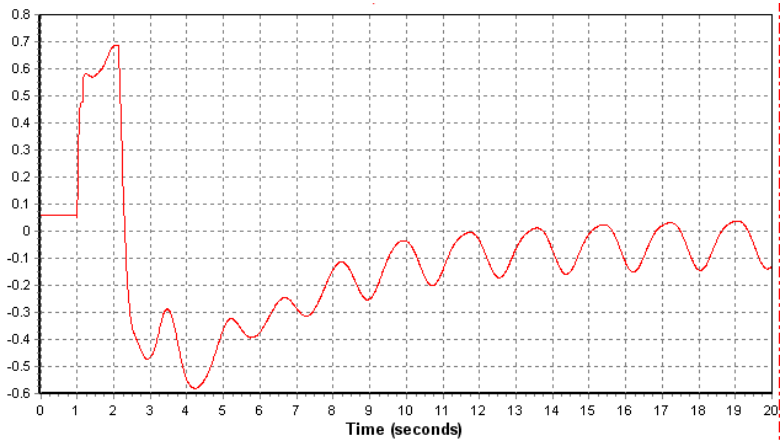

Response of the original SVC: supply 680 Mvar maximum

D.5 DYNAMIC FOR THE VSC-HVDC MODEL FROM PSS/E LIBRARY

Appendix D - 12: Dynamic data used for the dynamic simulation of the VSC-HVDC

Parameters that have been changed from the original model in library are in yellow.

Module		M9 1140MVA	M6 570MVA
VSC 1	Tpo	0.07	0.07
	aclim	0	0
	Ac volt contr gain	1.5	1.5
	T cst AC PI int	0.01	0.01
	T cst AC trans	0.01	0.01
	Imax	1	1
	AC volt drop contr	0	0
	V max	1.1	1.1
	Xreact	0.2	0.2
	Qmax	400	200
	Qmin	-570	-285
	reactive power limiter	1.2	1.2
	current order limiter	1	1
VSC2	Tpo	0.07	0.07
	aclim	0	0
	Ac volt contr gain	1.5	1.5
	T cst AC PI int	0.01	0.01
	T cst AC trans	0.01	0.01
	Imax	1	1
	AC volt drop contr	0	0
	V max	1.1	1.1
	Xreact	0.2	0.2
	Qmax	400	200
	Qmin	-570	-285
	reactive power limiter	1.2	1.2
	current order limiter	1	1
DC line	time cst power control	0.05	0.05
	time cst power limiter	0.05	0.05

D.6 GENERATOR CIMTR3

Appendix D - 13: Generator parameter for CIMTR3

This induction generator type has been used to simulate the dynamic behaviour of the entire wind farm.

CIMTR3 Program manual operation Volume II E3
Induction generator

CONs	Description	Bonus 2.3MW FIG	Vestas V 82 DFIG
j	**T'**	1.44459	1.073
j+1	**T''**	0	0
j+2	**Inertia, H**	2	5.26
j+3	**X**	3.38487	4.18
j+4	**X'**	0.19927	0.22
j+5	**X''**	0	0.178
j+6	**Xl**	0.14816	0.143
j+7	**E1**	1	1
j+8	**S(E1)**	0.2093	0.17
j+9	**E2**	1.1	1.2
j+10	**S(E2)**	0.46938	0.44
1+11	**Switch**	0	0
j+12	**Syn-pow**	0.1	0.01

E SIMULATION: UNIQUE HVDC TRANSMISSION & LARGE OFFSHORE WIND FARM

E.1 LOAD FLOW CASE

Appendix E - 1: Buses voltages in pu and angle in degrees

```
--------------------------------------------------------------------------------

     PTI INTERACTIVE POWER SYSTEM SIMULATOR--PSS(tm)E    SUN, APR 12 2009  17:51
 REDUCED NORDEL POWER SYSTEM MODEL                                    BUS DATA
 V 3.2, 12.08.97
                                      S H U N T S
   BUS# X-- NAME --X BASKV CODE LOADS FIXED SWITCHED  VOLT   ANGLE AREA ZONE OWNER
   1000 OFFSH WF    33.000   2    0     0       0    1.00000    0.0   10    4     1
   1100 OFFSH CONV  320.00   1    0     1       0    1.00000   -8.1   20    4     1
   1200 SHORE CONV  320.00   1    0     1       0    1.04794   37.0   20    4     1
   3000 STCKH       420.00   2    2     0       0    1.00000   22.3   40    2     1
   3100 STRFN       420.00   2    1     0       0    0.97000   34.9   40    2     1
   3115 SV-N1       420.00   2    0     0       0    1.00000   53.8   40    2     1
   3200 KRLSK       420.00   1    1     0       0    0.96296    6.2   40    2     1
   3244 SV-M2       300.00   1    0     0       0    1.00109   20.2   40    2     1
   3245 SV-M1       420.00   2    1     0       0    1.00000   19.5   40    2     1
   3249 SV-N2       420.00   2    1     0       0    1.00000   53.1   40    2     1
   3300 SV-SW       420.00   2    1     0       0    1.00000    0.0   40    2     1
   3359 SV-W        420.00   2    1     0       0    1.00000   14.1   40    2     1
   3360 KONT_135    135.00   1    2     0       0    0.99653   13.7   40    3     1
   3701 SV-N2B      300.00   1    0     0       0    1.00514   56.5   40    2     1
   5100 EAST3       300.00   2    1     0       0    1.00000   24.3   51    1     1
   5101 EAST4-A     420.00   1    0     0       0    0.99110   23.0   51    1     1
   5102 EAST4-B     420.00   1    0     0       0    0.99891   26.7   51    1     1
   5103 EAST4-C     420.00   1    0     0       0    0.99719   27.0   51    1     1
   5111 SVCTERM     22.500   2    0     0       0    0.99479   23.0   51    1     1
   5112 SVCHIGH     420.00   1    0     0       0    0.99110   23.0   51    1     1
   5300 HDAL3       300.00   2    1     0       0    1.00000   38.8   53    1     1
   5301 HDAL4       420.00   1    0     0       0    0.99983   33.3   53    1     1
   5400 CNTR3-A     300.00   2    1     0       0    1.00700   33.3   54    1     1
   5401 CNTR4-A     420.00   1    0     0       0    0.99832   30.9   54    1     1
   5402 CNTR4-B     420.00   1    0     0       0    1.00607   33.2   54    1     1
   5500 CNTR3-B     300.00   2    1     0       0    1.00400   26.6   55    1     1
   5501 CNTR4-C     420.00   1    0     0       0    1.00526   26.2   55    1     1
   5600 SOUTH3A     300.00   2    1     0       0    1.01000   30.9   56    1     1
   5601 SOUTH4A     420.00   1    0     0       0    0.99255   31.0   56    1     1
   5602 SOUTH4B     420.00   1    0     0       0    0.96866   23.3   56    1     1
   5603 SOUTH3B     300.00   2    2     0       0    0.93484   22.3   56    1     1
   6000 WEST300     300.00   2    1     0       0    1.00500   33.5   60    1     1
   6001 WEST400     420.00   1    0     0       0    1.00020   32.7   60    1     1
   6100 NWEST3      300.00   2    1     0       0    1.00000   32.8   61    1     1
   6500 MID300      300.00   2    1     0       0    1.00000   21.9   65    1     1
   6700 NOR300      300.00   2    1     0       0    1.02000   63.3   67    1     1
   6701 NOR400      420.00   1    0     0       0    1.00551   62.7   67    1     1
   7000 SO-FIN      420.00   2    2     0       0    1.00000  -45.7   70    2     1
   7100 NO-FIN      420.00   2    1     0       0    1.00000  -12.7   71    2     1
   8500 SJOLLAND    420.00   2    1     0       0    1.02000    2.9   90    3     1
   8600 DENMARK     300.00   1    1     0       0    0.93484   22.3   90    3     1
   9100 NETHERLANDS 300.00   1    1     0       0    1.01000   30.9   91    3     1
```

Appendix E - 2: Exchange flow and production per area.

```
     PTI INTERACTIVE POWER SYSTEM SIMULATOR--PSS(tm)E    SUN, APR 12 2009  17:50
 REDUCED NORDEL POWER SYSTEM MODEL                                  ZONE TOTALS
 V 3.2, 12.08.97                                                     IN MW/MVAR

                  FROM       TO     TO BUS  TO LINE     FROM       TO
 X-- ZONE --X GENERATION   LOAD     SHUNT    SHUNT CHARGING  NET INT   LOSSES

    1          16800.0  14217.0       0.0      0.6      0.0   2459.2    123.2
 NORWAY         2807.3   2760.1       0.0    -27.8   1101.1   -663.0   1839.2

    2          26897.0  28550.2       0.0      0.0      0.0  -2639.0    985.8
 SWE & FIN     11879.1   4471.2       0.0      0.0   2048.8    237.2   9219.4

    3           1038.6   1796.4       0.0      0.0      0.0   -760.7      2.9
 DEN & NETH      169.8    400.0       0.0      0.0    306.1     64.6     11.3

    4           1002.5      0.0       0.0      0.0      0.0    940.5     62.0
 OFFSHORE         52.7      0.0    -340.2      0.0      0.0    361.2     31.7

 TOTALS         45738.2  44563.7       0.0      0.6      0.0      0.0   1173.9
                14908.8   7631.3    -340.2    -27.8   3456.0      0.0  11101.5
```

```
     PTI INTERACTIVE POWER SYSTEM SIMULATOR--PSS(tm)E    SUN, APR 12 2009  17:50
 REDUCED NORDEL POWER SYSTEM MODEL                                      ZONE
 V 3.2, 12.08.97                                                     INTERCHANGE

       TO ZONE:      1      2      3      4
 FROM ZONE     *-------------------------
         1     *          2800    600   -941
 NORWAY        *          -302      0   -361
               *-------------------------
         2     *  -2800           161
 SWE & FIN     *    302           -65
               *-------------------------
         3     *   -600   -161
 DEN & NETH    *      0     65
               *-------------------------
         4     *    941
 OFFSHORE      *    361
               *-------------------------
```

E.2 ONSHORE FAULT AT PCC WITH POWER FLOW CONTROL

Appendix E - 3: Voltage onshore in pu.

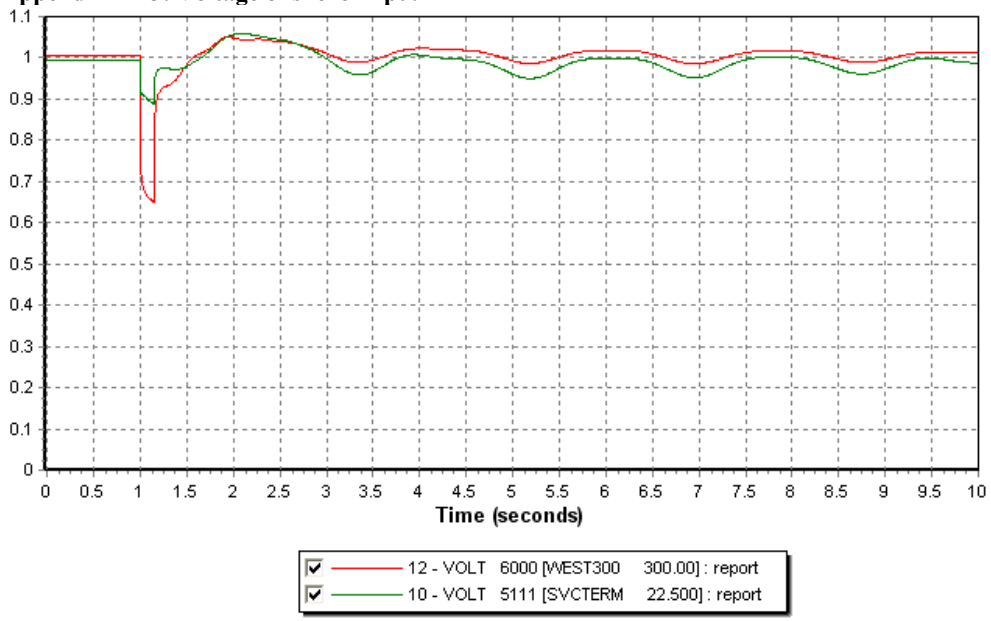

E.3 ONSHORE FAULT AT PCC WITH POWER FLOW CONTROL

Appendix E - 4: Generator behaviour at bus 5600: speed variation at synchronous speed, reactive and active power.

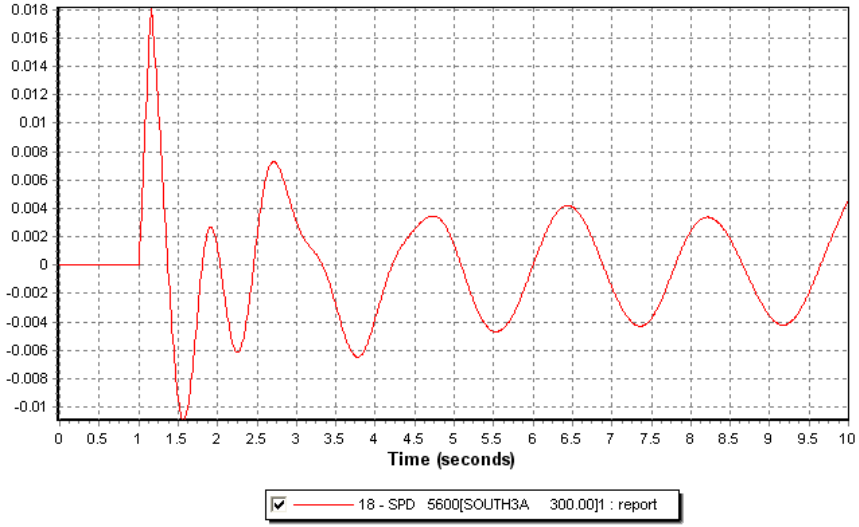

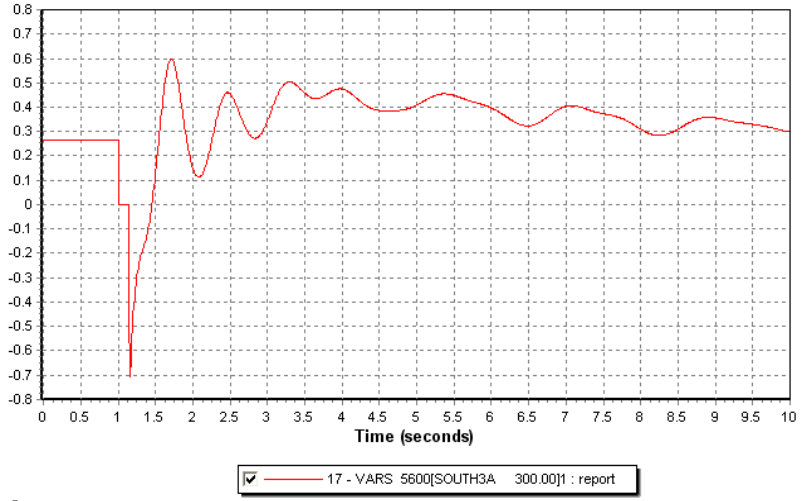

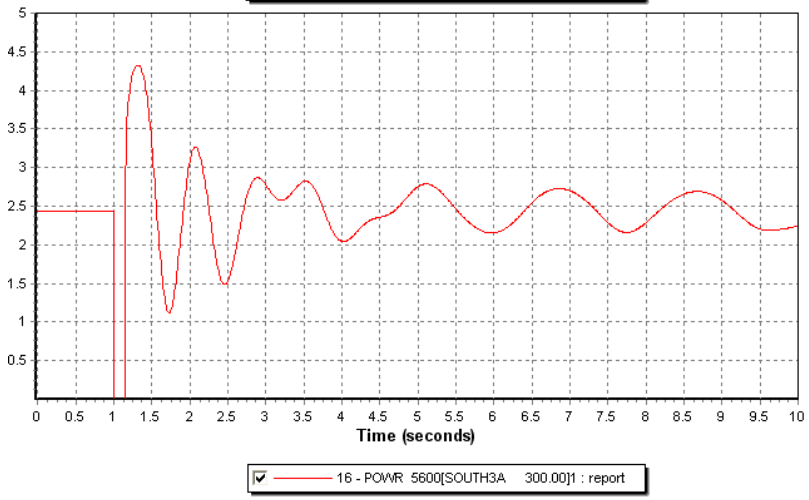

E.4 ONSHORE FAULT AND CONVERTER WITH VOLTAGE CONTROL

Appendix E - 5: Voltage onshore at bus 1200 (shore converter)

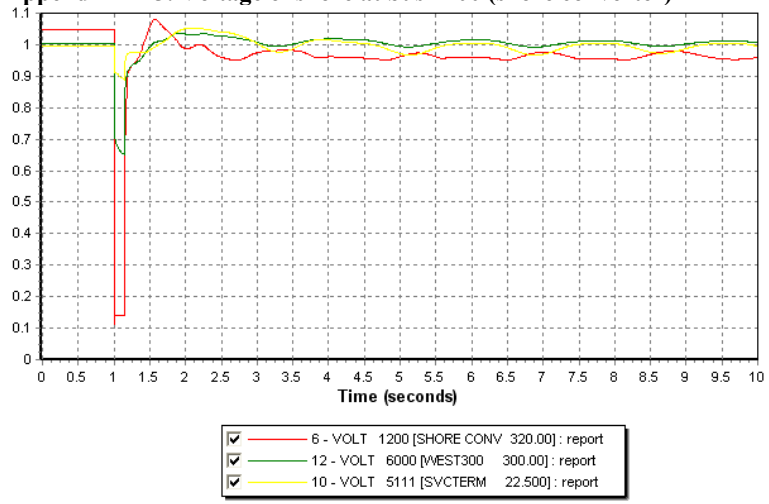

Appendix E - 6: Behaviour of the generator at the PCC, reactive power, variation at synchronous speed and active power.

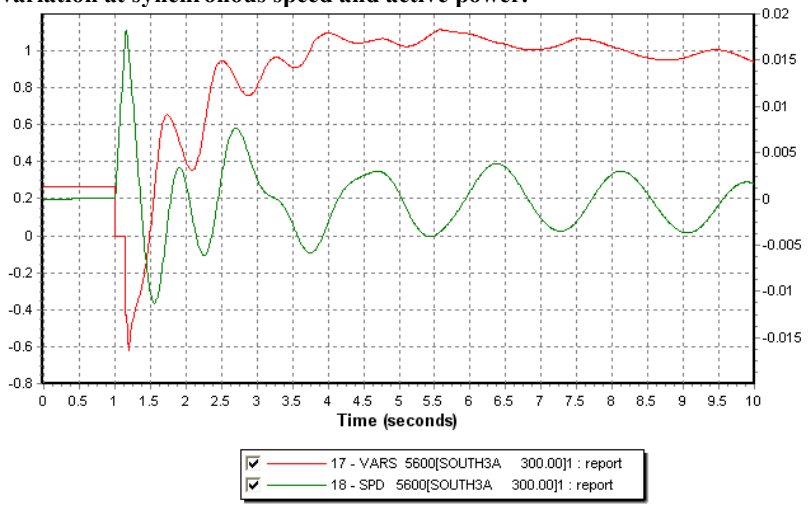

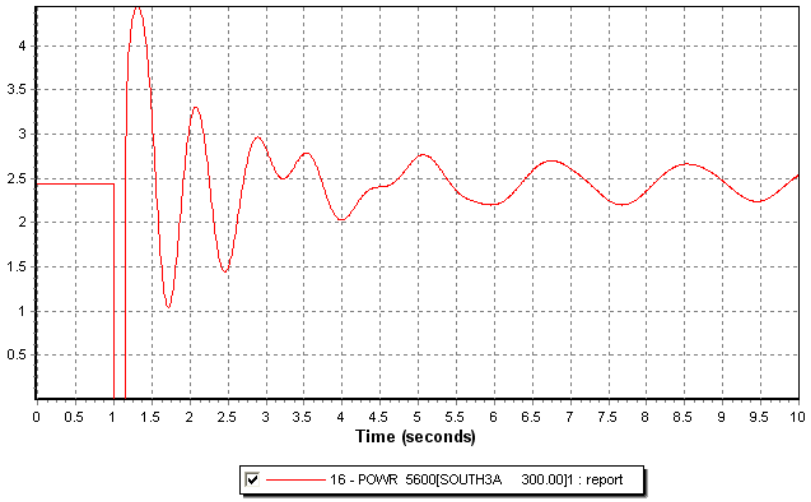

Appendix E - 7: Behaviour of the generator at buses 5600 and 6000, active and reactive power in pu on system base

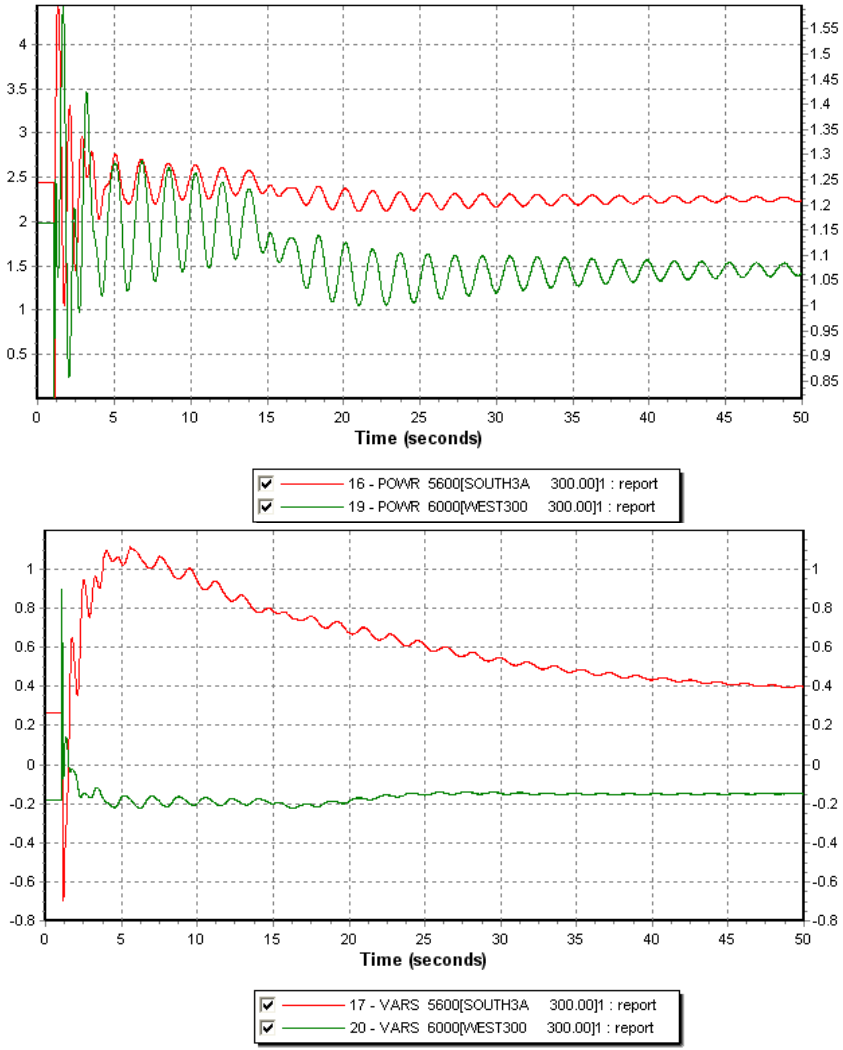

F SIMULATION: CONNECTION OF A WIND FARM CLUSTER AT BUS 5600

F.1 LOAD FLOW CASE

Appendix F - 1: Bus voltage in pu and angle in degree

```
--------------------------------------------------------------------------------

    PTI INTERACTIVE POWER SYSTEM SIMULATOR--PSS(tm)E    WED, APR 15 2009  10:17
 REDUCED NORDEL POWER SYSTEM MODEL                                    BUS DATA
 V 3.2, 12.08.97
                                      S H U N T S
   BUS# X-- NAME --X BASKV CODE LOADS FIXED SWITCHED  VOLT   ANGLE AREA ZONE OWNER
   1000 OFFSH WF    33.000   3    0     0       0    1.00000    0.0   10    4     1
   1010 OFFSH WF B  33.000   2    0     1       0    1.00000   -0.8   10    4     1
   1020 OFF WF & RIG33.000   2    1     1       0    1.00000   -1.7   10    4     1
   1100 OFFSH CONV  320.00   2    0     1       0    1.00000   -5.3   20    4     1
   1110 OFF TRANS B 320.00   1    0     0       0    1.01430   -4.1   10    4     1
   1120 OFF TRANS C 320.00   1    0     0       0    1.01783   -3.6   10    4     1
   1200 SHORE CONV  320.00   2    0     1       0    1.05430   37.2   20    4     1
   3000 STCKH       420.00   2    2     0       0    1.00000   22.3   40    2     1
   3100 STRFN       420.00   2    1     0       0    0.97000   34.9   40    2     1
   3115 SV-N1       420.00   2    0     0       0    1.00000   53.8   40    2     1
   3200 KRLSK       420.00   1    1     0       0    0.96296    6.2   40    2     1
   3244 SV-M2       300.00   1    0     0       0    1.00109   20.2   40    2     1
   3245 SV-M1       420.00   2    1     0       0    1.00000   19.5   40    2     1
   3249 SV-N2       420.00   2    1     0       0    1.00000   53.1   40    2     1
   3300 SV-SW       420.00   3    1     0       0    1.00000    0.0   40    2     1
   3359 SV-W        420.00   2    1     0       0    1.00000   14.1   40    2     1
   3360 KONT_135    135.00   1    2     0       0    0.99653   13.7   40    3     1
   3701 SV-N2B      300.00   1    0     0       0    1.00514   56.5   40    2     1
   5100 EAST3       300.00   2    1     0       0    1.00000   24.3   51    1     1
   5101 EAST4-A     420.00   1    0     0       0    0.99110   23.0   51    1     1
   5102 EAST4-B     420.00   1    0     0       0    0.99891   26.7   51    1     1
   5103 EAST4-C     420.00   1    0     0       0    0.99719   27.0   51    1     1
   5111 SVCTERM     22.500  -2    0     0       0    0.99479   23.0   51    1     1
   5112 SVCHIGH     420.00   1    0     0       0    0.99110   23.0   51    1     1
   5300 HDAL3       300.00   2    1     0       0    1.00000   38.8   53    1     1
   5301 HDAL4       420.00   1    0     0       0    0.99983   33.3   53    1     1
   5400 CNTR3-A     300.00   2    1     0       0    1.00700   33.3   54    1     1
   5401 CNTR4-A     420.00   1    0     0       0    0.99832   30.9   54    1     1
   5402 CNTR4-B     420.00   1    0     0       0    1.00607   33.2   54    1     1
   5500 CNTR3-B     300.00   2    1     0       0    1.00400   26.6   55    1     1
   5501 CNTR4-C     420.00   1    0     0       0    1.00526   26.2   55    1     1
   5600 SOUTH3A     300.00   2    1     0       0    1.01000   30.9   56    1     1
   5601 SOUTH4A     420.00   1    0     0       0    0.99255   31.0   56    1     1
   5602 SOUTH4B     420.00   1    0     0       0    0.96866   23.3   56    1     1
   5603 SOUTH3B     300.00  -2    2     0       0    0.93484   22.3   56    1     1
   6000 WEST300     300.00   2    1     0       0    1.00500   33.5   60    1     1
   6001 WEST400     420.00   1    0     0       0    1.00020   32.7   60    1     1
   6100 NWEST3      300.00   2    1     0       0    1.00000   32.8   61    1     1
   6500 MID300      300.00   2    1     0       0    1.00000   21.9   65    1     1
   6700 NOR300      300.00   2    1     0       0    1.02000   63.3   67    1     1
   6701 NOR400      420.00   1    0     0       0    1.00551   62.7   67    1     1
   7000 SO-FIN      420.00   2    2     0       0    1.00000  -45.7   70    2     1
   7100 NO-FIN      420.00   2    1     0       0    1.00000  -12.7   71    2     1
   8500 SJOLLAND    420.00   2    1     0       0    1.02000    2.9   90    3     1
   8600 DENMARK     300.00   1    1     0       0    0.93484   22.3   90    3     1
   9100 NETHERLANDS 300.00   1    1     0       0    1.01000   30.9   91    3     1
```

Appendix F - 2: Exchange flow and production per area

```
--------------------------------------------------------------------------------

     PTI INTERACTIVE POWER SYSTEM SIMULATOR--PSS(tm)E    WED, APR 15 2009  10:16
 REDUCED NORDEL POWER SYSTEM MODEL                                   ZONE TOTALS
 V 3.2, 12.08.97                                                      IN MW/MVAR

                 FROM      TO    TO BUS  TO LINE     FROM      TO
 X-- ZONE --X GENERATION  LOAD    SHUNT    SHUNT CHARGING  NET INT   LOSSES

    1         16800.0  14217.0      0.0      0.6      0.0   2459.1    123.3
 NORWAY        2769.5   2760.1      0.0    -27.8   1101.1   -707.9   1846.2

    2         26897.1  28550.2      0.0      0.0      0.0  -2638.9    985.8
 SWE & FIN    11879.0   4471.2      0.0      0.0   2048.8    237.2   9219.4

    3          1038.6   1796.4      0.0      0.0      0.0   -760.7      2.9
 DEN & NETH     169.8    400.0      0.0      0.0    306.1     64.6     11.3

    4          1161.2    150.0      0.0      0.0      0.0    940.5     70.7
 OFFSHORE       -28.2     50.0   -227.8      0.0    342.4    406.1     86.0

 TOTALS        45896.9  44713.7      0.0      0.6      0.0      0.0   1182.6
               14790.2   7681.3   -227.8    -27.8   3798.4      0.0  11162.9


--------------------------------------------------------------------------------

     PTI INTERACTIVE POWER SYSTEM SIMULATOR--PSS(tm)E    WED, APR 15 2009  10:17
 REDUCED NORDEL POWER SYSTEM MODEL                                       ZONE
 V 3.2, 12.08.97                                                     INTERCHANGE

       TO ZONE:     1     2     3     4
 FROM ZONE     *------------------------
         1     *         2800   600  -941
 NORWAY        *         -302     0  -406
               *------------------------
          2    * -2800          161
 SWE & FIN     *   302          -65
               *------------------------
          3    *  -600  -161
 DEN & NETH    *     0    65
               *------------------------
          4    *   941
 OFFSHORE      *   406
               *------------------------
```

F.2 OFFSHORE FAULT AT MAIN WIND FARM

Appendix F - 3: Voltage at the other buses of the offshore grid

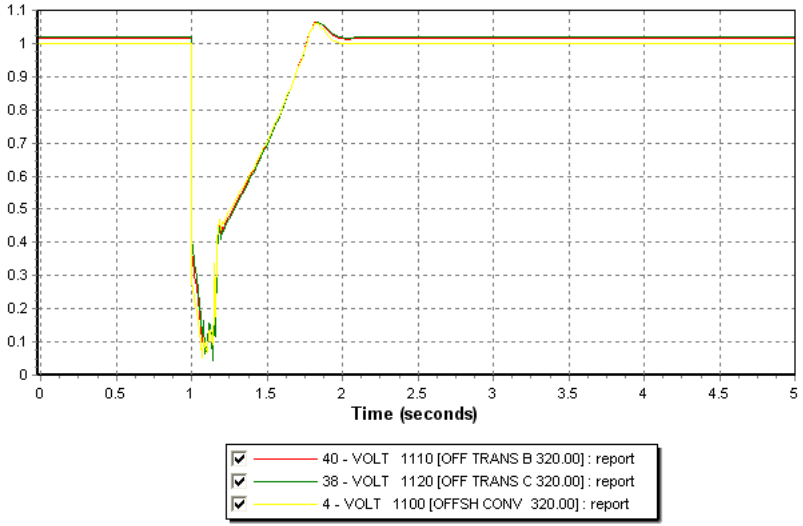

Appendix F - 4: Synchronous speed of the generator in the main wind farm.

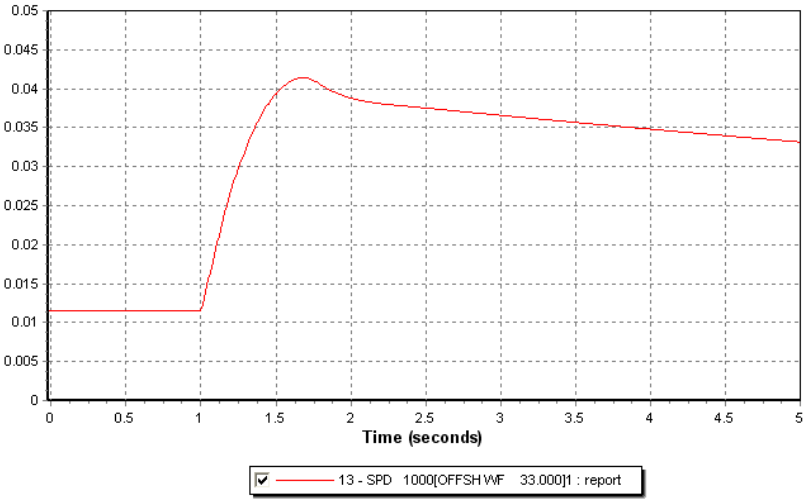

Appendix F - 5: Behaviour of the generator in the other wind farm, reactive power and active power

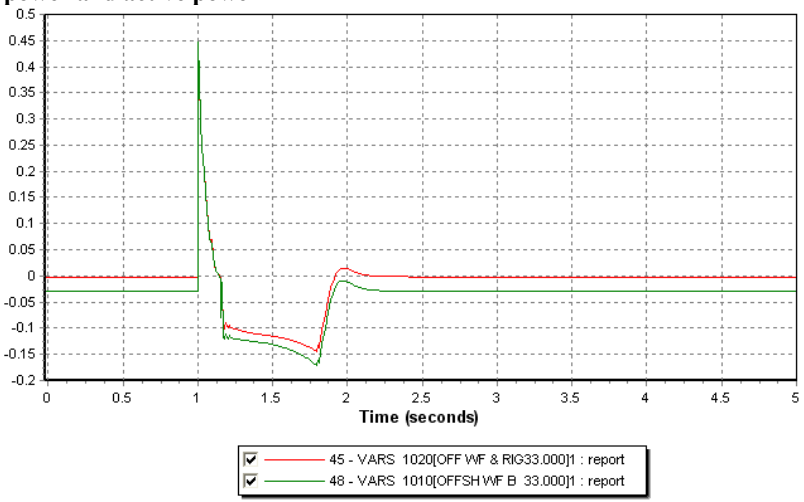

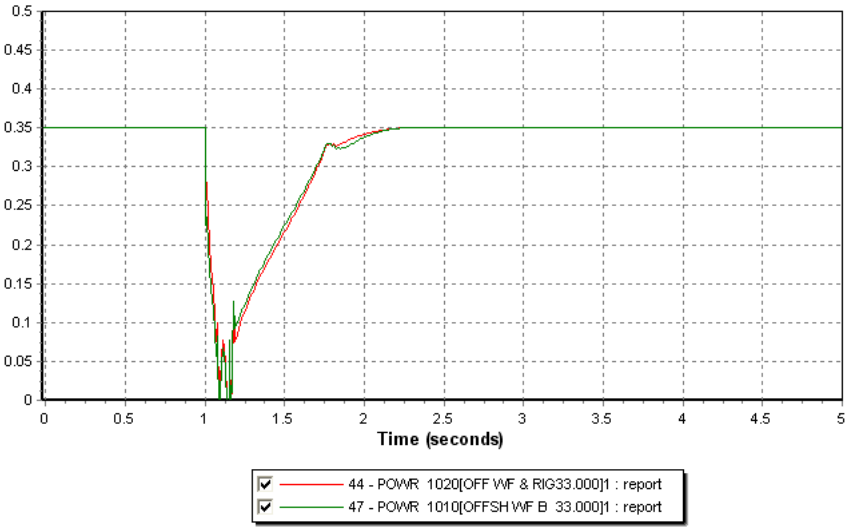

Appendix F - 6: Response of the SVC due to fault at the main wind farm

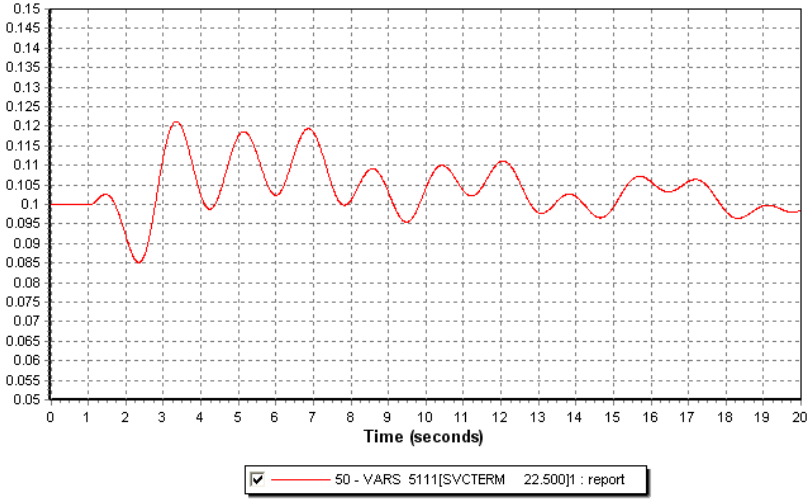

Appendix F - 7: Frequency variation at the buses 5600 and 6000 due to fault at the main wind farm.

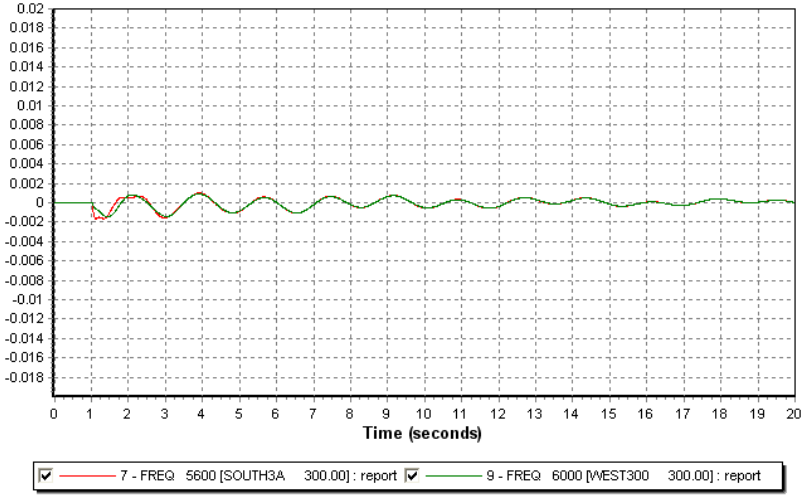

F.3 OFFSHORE FAULT CLOSE TO THE OIL RIG AT BUS 1120

Appendix F - 8: Voltage at the wind farm 2 (bus 1010) and the transmission (bus 1110)

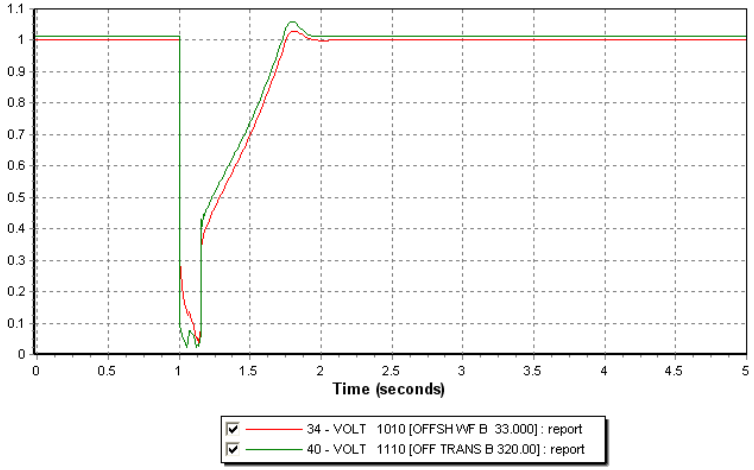

Appendix F - 9: Frequency variation at the wind farm 2 (bus 1010) and the transmission (bus 1110)

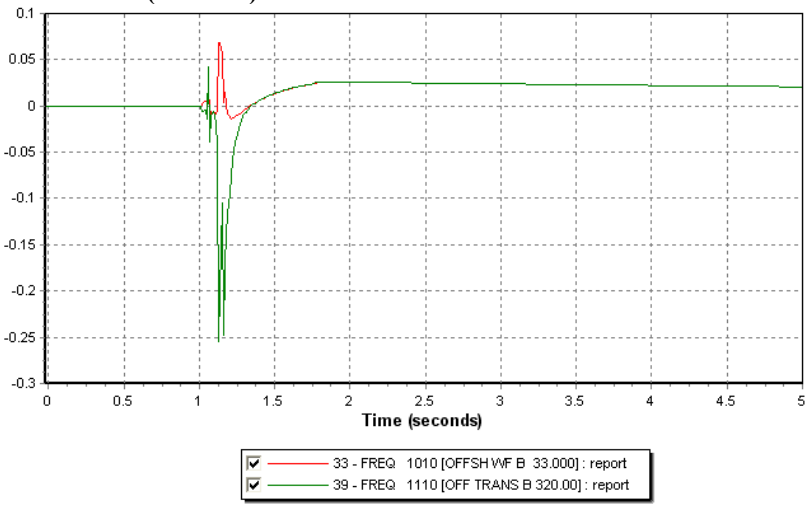

Appendix F - 10: Detailed behaviour of the generator in wind farm close to the fault

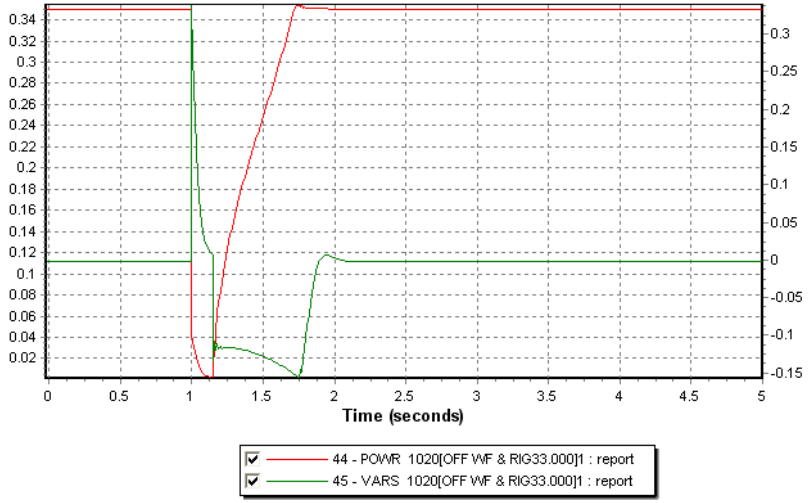

Appendix F - 11: Frequency variation and voltage at the PCC in pu

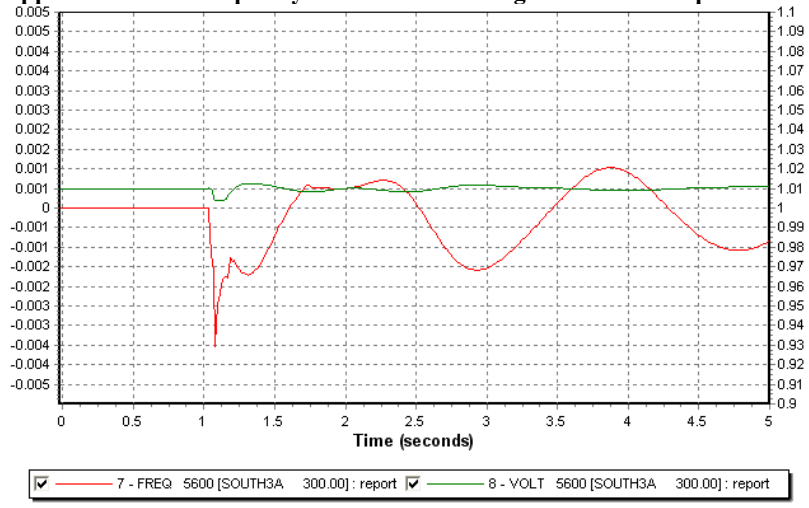

F.4 REPLACEMENT DFIG BY FIXED SPEED GENERATOR AT BUS 1010

Appendix F - 12:On shore voltage at bus 5600 and 6000 in pu

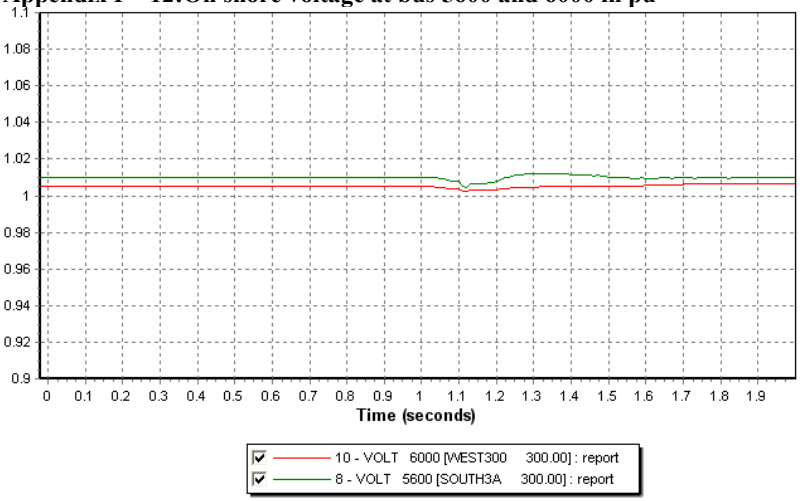

Appendix F - 13: Frequency variation at buses 5600 and 6000 in pu on system base

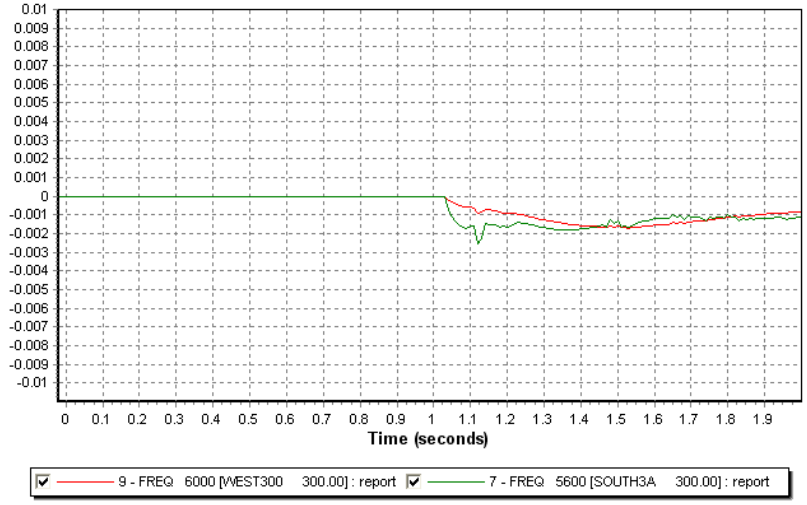

G SIMULATION: CONNECTION OF A UNIQUE WIND FARM WITH 2 HVDC TRANSMISSIONS

G.1 LOAD FLOW CASE

Appendix G - 1: Bus voltage in pu and angle in degree

```
--------------------------------------------------------------------------------

     PTI INTERACTIVE POWER SYSTEM SIMULATOR--PSS(tm)E    FRI, APR 17 2009  12:22
 REDUCED NORDEL POWER SYSTEM MODEL                                    BUS DATA
 V 3.2, 12.08.97
                                        S H U N T S
   BUS# X-- NAME --X BASKV CODE LOADS FIXED SWITCHED  VOLT   ANGLE AREA ZONE OWNER
   1000 OFFSH WF    33.000    3     0     0       0    1.00000    0.0   10    4     1
   1100 OFFSH CONVA 150.00    2     0     1       0    1.00000   -8.1   20    4     1
   1200 SHORE CONVA 150.00    2     0     1       0    1.06772   35.3   20    4     1
   1300 OFFSH CONVB 150.00    2     0     1       0    1.00000   -8.1   10    4     1
   1400 SHORE CONVB 150.00    2     0     1       0    0.99352   40.7   10    4     1
   3000 STCKH       420.00    2     2     0       0    1.00000   22.3   40    2     1
   3100 STRFN       420.00    2     1     0       0    0.97000   34.8   40    2     1
   3115 SV-N1       420.00    2     0     0       0    1.00000   53.8   40    2     1
   3200 KRLSK       420.00    1     1     0       0    0.96313    6.1   40    2     1
   3244 SV-M2       300.00    1     0     0       0    1.00108   20.2   40    2     1
   3245 SV-M1       420.00    2     1     0       0    1.00000   19.5   40    2     1
   3249 SV-N2       420.00    2     1     0       0    1.00000   53.0   40    2     1
   3300 SV-SW       420.00    3     1     0       0    1.00000    0.0   40    2     1
   3359 SV-W        420.00    2     1     0       0    1.00000   14.0   40    2     1
   3360 KONT_135    135.00    1     2     0       0    0.99653   13.6   40    3     1
   3701 SV-N2B      300.00    1     0     0       0    1.00514   56.4   40    2     1
   5100 EAST3       300.00    2     1     0       0    1.00000   24.0   51    1     1
   5101 EAST4-A     420.00    1     0     0       0    0.99119   22.8   51    1     1
   5102 EAST4-B     420.00    1     0     0       0    0.99891   26.4   51    1     1
   5103 EAST4-C     420.00    1     0     0       0    0.99719   26.7   51    1     1
   5111 SVCTERM     22.500   -2     0     0       0    0.99488   22.8   51    1     1
   5112 SVCHIGH     420.00    1     0     0       0    0.99119   22.8   51    1     1
   5300 HDAL3       300.00    2     1     0       0    1.00000   38.5   53    1     1
   5301 HDAL4       420.00    1     0     0       0    0.99983   33.1   53    1     1
   5400 CNTR3-A     300.00    2     1     0       0    1.00700   33.1   54    1     1
   5401 CNTR4-A     420.00    1     0     0       0    0.99803   30.6   54    1     1
   5402 CNTR4-B     420.00    1     0     0       0    1.00606   33.0   54    1     1
   5500 CNTR3-B     300.00    2     1     0       0    1.00400   26.3   55    1     1
   5501 CNTR4-C     420.00    1     0     0       0    1.00526   25.9   55    1     1
   5600 SOUTH3A     300.00    2     1     0       0    1.01000   28.5   56    1     1
   5601 SOUTH4A     420.00    1     0     0       0    0.99243   28.7   56    1     1
   5602 SOUTH4B     420.00    1     0     0       0    0.96849   22.2   56    1     1
   5603 SOUTH3B     300.00   -2     2     0       0    0.93502   21.1   56    1     1
   6000 WEST300     300.00    2     1     0       0    1.00500   33.4   60    1     1
   6001 WEST400     420.00    1     0     0       0    1.00010   32.4   60    1     1
   6100 NWEST3      300.00    2     1     0       0    1.00000   32.6   61    1     1
   6500 MID300      300.00    2     1     0       0    1.00000   21.9   65    1     1
   6700 NOR300      300.00    2     1     0       0    1.02000   63.2   67    1     1
   6701 NOR400      420.00    1     0     0       0    1.00551   62.6   67    1     1
   7000 SO-FIN      420.00    2     2     0       0    1.00000  -45.8   70    2     1
   7100 NO-FIN      420.00    2     1     0       0    1.00000  -12.8   71    2     1
   8500 SJOLLAND    420.00    2     1     0       0    1.02000    2.9   90    3     1
   8600 DENMARK     300.00    1     1     0       0    0.93502   21.1   90    3     1
   9100 NETHERLANDS 300.00    1     1     0       0    1.01000   28.5   91    3     1
```

Appendix G - 2: Power flow exchange and generation per area.

```
--------------------------------------------------------------------------------

     PTI INTERACTIVE POWER SYSTEM SIMULATOR--PSS(tm)E    FRI, APR 17 2009  12:24
 REDUCED NORDEL POWER SYSTEM MODEL                                      ZONE
 V 3.2, 12.08.97                                                    INTERCHANGE

       TO ZONE:     1     2     3     4
 FROM ZONE     *------------------------
         1     *         2774   600  -915
 NORWAY        *         -299     0  -158
               *------------------------
         2     * -2774          161
 SWE & FIN     *   299          -65
               *------------------------
         3     *  -600  -161
 DEN & NETH    *     0    65
               *------------------------
         4     *   915
 OFFSHORE      *   158
               *------------------------



--------------------------------------------------------------------------------

     PTI INTERACTIVE POWER SYSTEM SIMULATOR--PSS(tm)E    FRI, APR 17 2009  12:24
 REDUCED NORDEL POWER SYSTEM MODEL                                  ZONE TOTALS
 V 3.2, 12.08.97                                                     IN MW/MVAR

                 FROM      TO     TO BUS  TO LINE     FROM      TO
 X-- ZONE --X GENERATION  LOAD     SHUNT    SHUNT CHARGING  NET INT   LOSSES

    1         16800.0  14217.0      0.0      0.6      0.0   2458.2    124.2
 NORWAY        3004.7   2760.1      0.0    -27.6   1101.1   -456.5   1829.7

    2         26921.7  28550.2      0.0      0.0      0.0  -2612.9    984.4
 SWE & FIN    11858.9   4471.2      0.0      0.0   2048.9    234.3   9202.3

    3          1038.6   1796.4      0.0      0.0      0.0   -760.7      2.9
 DEN & NETH     169.8    400.0      0.0      0.0    306.1     64.6     11.3

    4          1003.0      0.0      0.0      0.0      0.0    915.4     87.6
 OFFSHORE        49.1      0.0   -339.4      0.0      0.0    157.6    230.9

 TOTALS       45763.4  44563.7      0.0      0.6      0.0      0.0   1199.1
              15082.5   7631.3   -339.4    -27.6   3456.0      0.0  11274.2
```

G.2 OFFSHORE FAULT AT THE WIND FARM

Appendix G - 3: Offshore voltage at the converters.

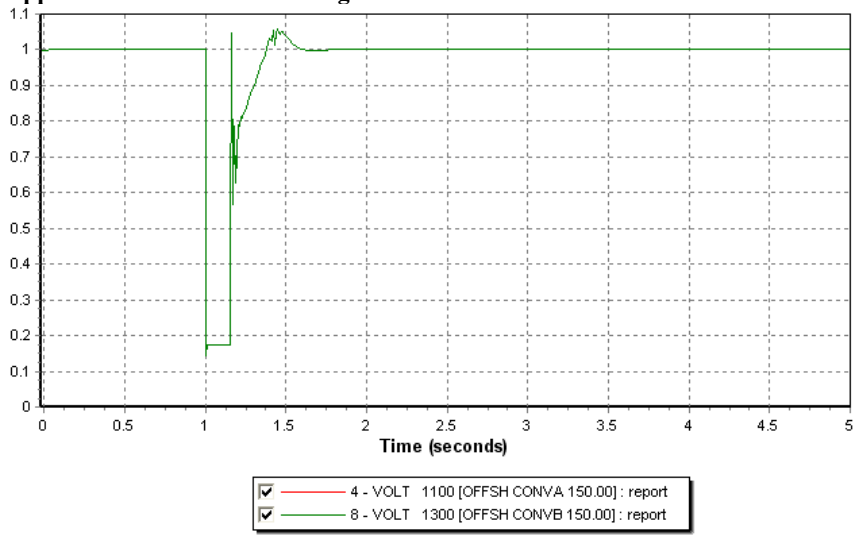

Appendix G - 4: Voltage and frequency on shore, see left column

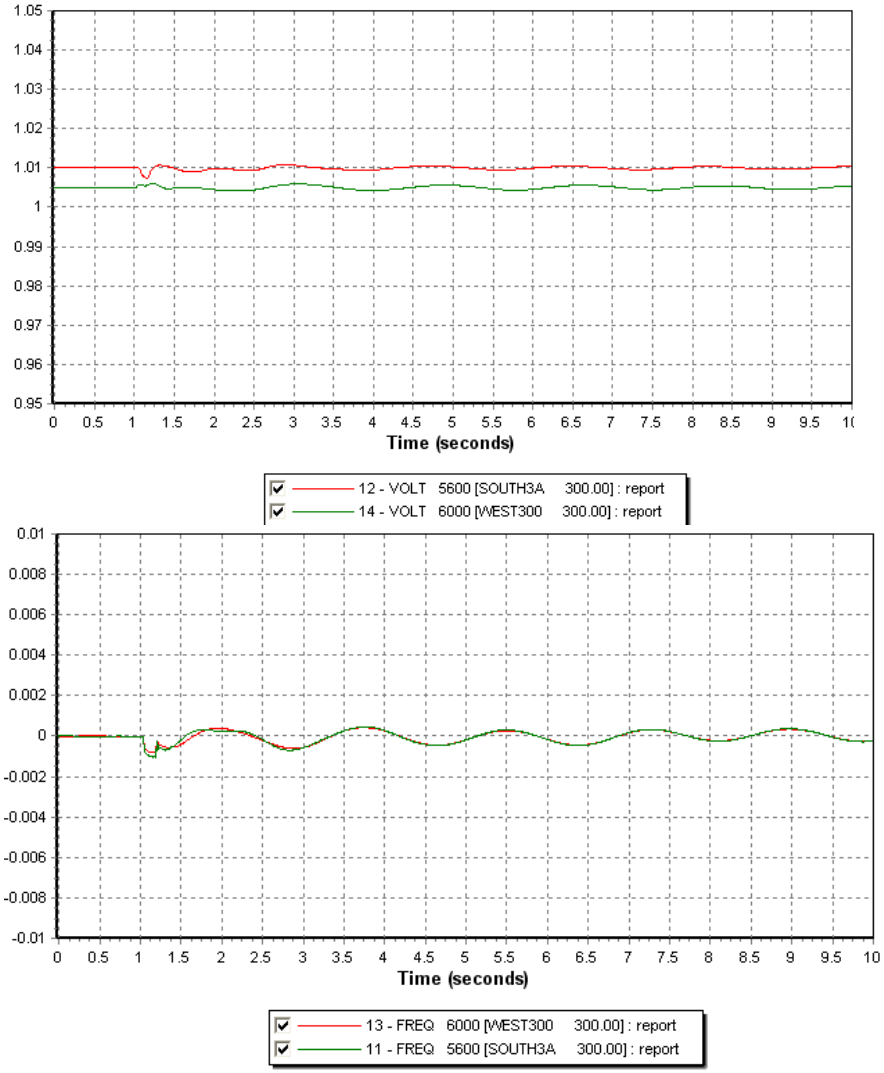

Appendix G - 5: Response of the onshore HVDC converters and SVC.

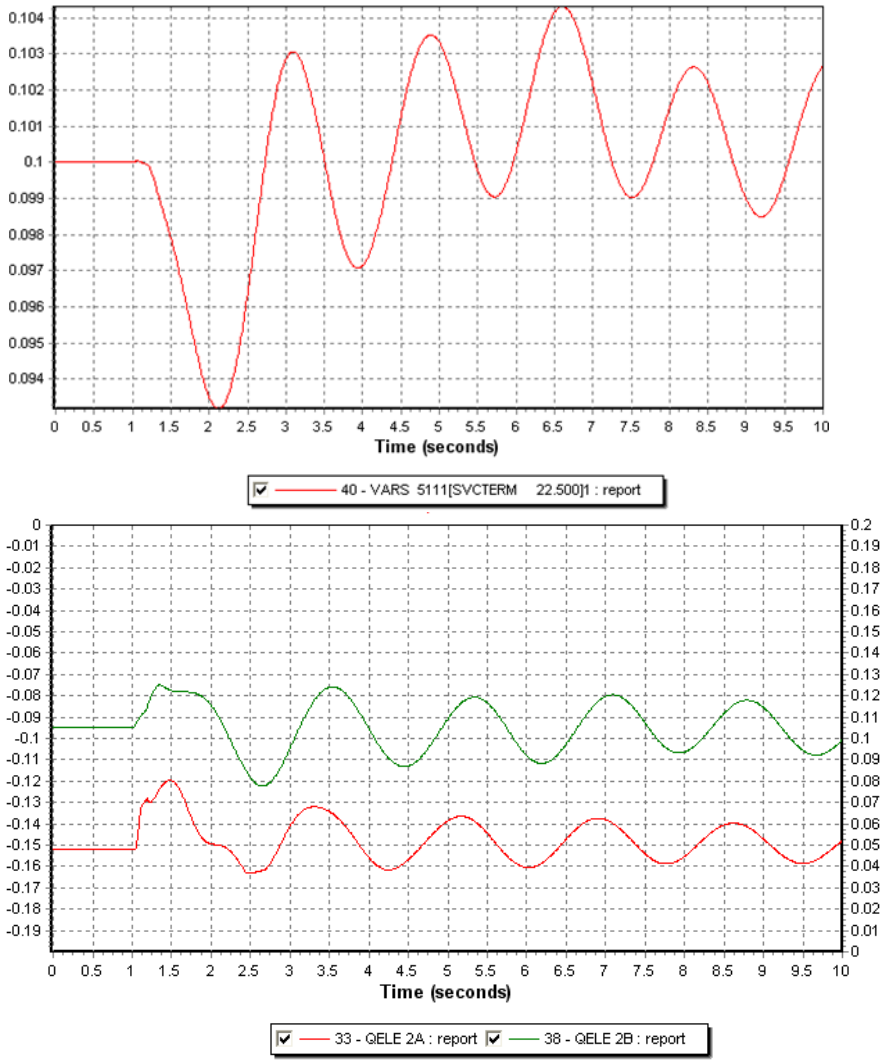

Appendix G - 6: Behaviour of the generators at the PCCs (buses 5600 & 6000), reactive and active power

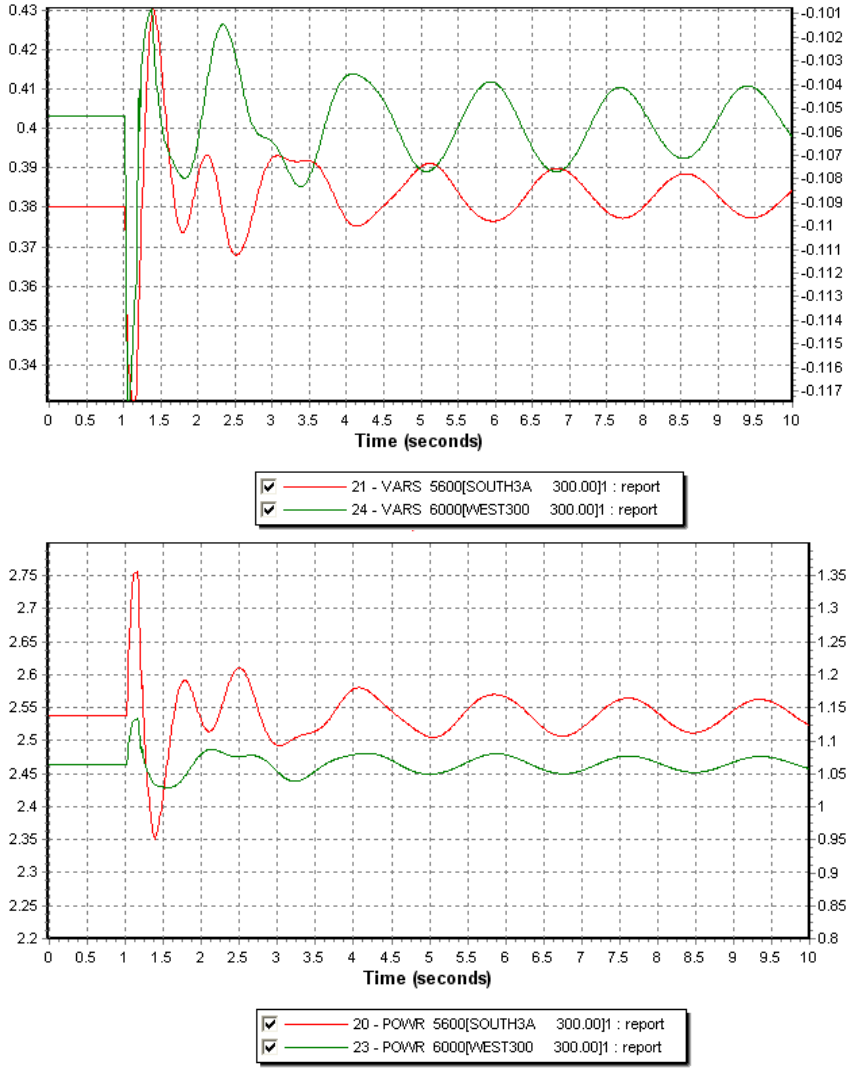

G.3 FAULT ONSHORE AND TRIPPING OF THE LINE

Appendix G - 7: Behaviour of the offshore wind turbine generator

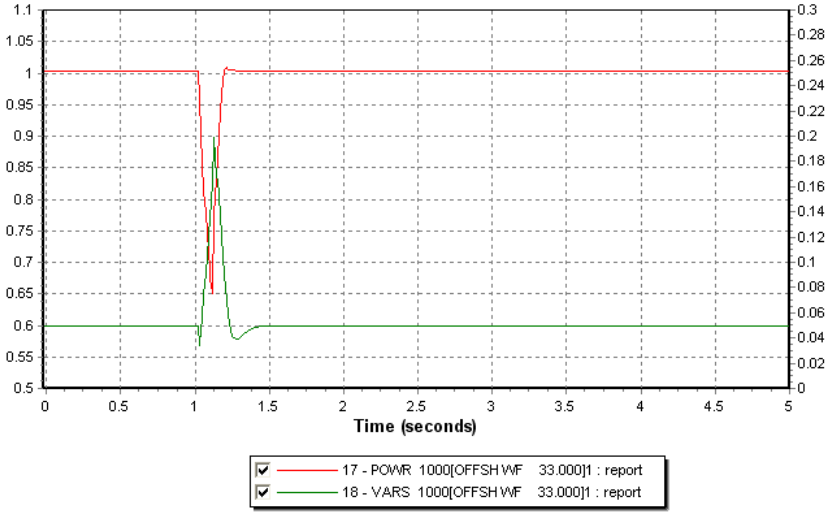

Appendix G - 8: Frequencies at the offshore buses

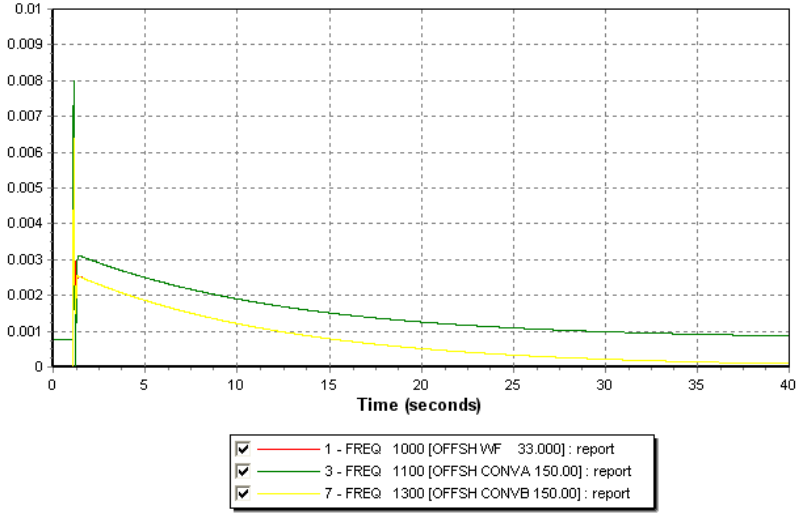

Appendix G - 9: Active power flowing into the HVDC transmissions (A red and B green).

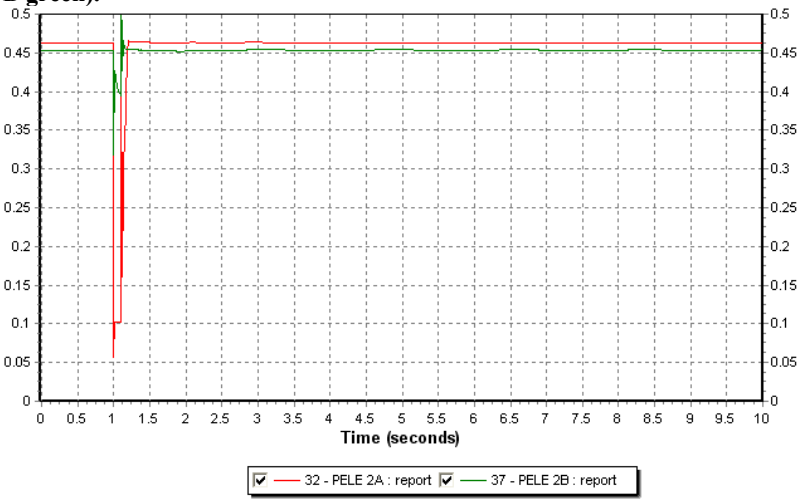

Appendix G - 10: Zoom during fault time on the reactive power from generator at bus 6000

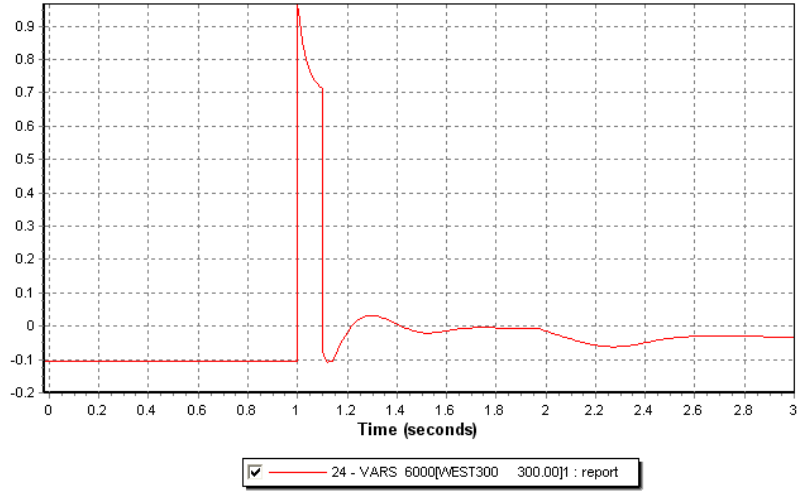

Appendix G - 11: Speed deviation from synchronous speed for generator at buses 5600 and 6000

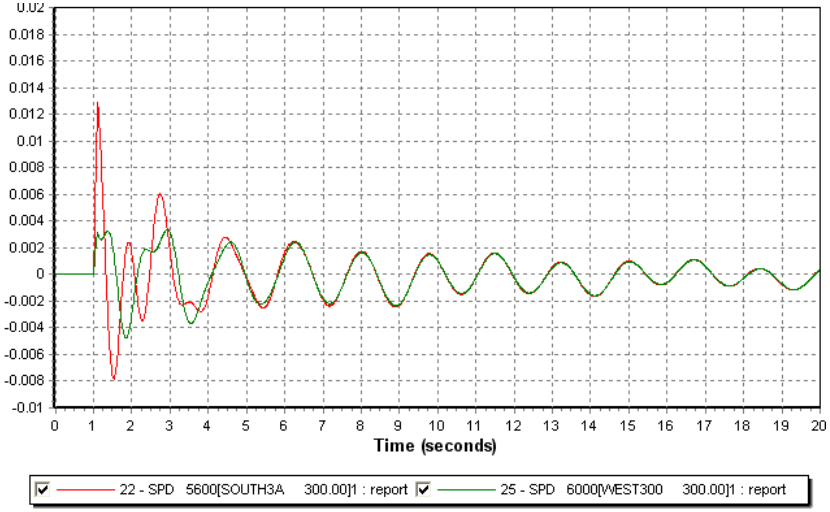

H SIMULATION: CONNECTION OF A WIND FARM CLUSTER WITH 2 HVDC TRANSMISSIONS

H.1 LOAD FLOW CASE

Appendix H - 1: Bus voltage and angle

```
------------------------------------------------------------------------------

    PTI INTERACTIVE POWER SYSTEM SIMULATOR--PSS(tm)E    MON, APR 20 2009  10:34
 REDUCED NORDEL POWER SYSTEM MODEL                                   BUS DATA
 V 3.2, 12.08.97
                                    S H U N T S
   BUS# X-- NAME --X BASKV CODE LOADS FIXED SWITCHED  VOLT   ANGLE AREA ZONE OWNER
   1000 OFFSH WF1   33.000   3    0     0       0    1.00000    0.0   10    4     1
   1010 OFFSH WF2   33.000   2    0     0       0    1.00000   -1.1   10    4     1
   1020 WF3 & RIG   33.000   2    1     0       0    1.00000    0.2   10    4     1
   1100 OFFSH CONVA 150.00   2    0     1       0    1.00000   -5.3   20    4     1
   1200 SHORE CONVA 150.00   2    0     1       0    1.06297   34.1   20    4     1
   1300 OFFSH CONVB 150.00   2    0     1       0    1.00000   -5.1   20    4     1
   1320 TRANSFO RIG 150.00   1    0     0       0    1.01384   -2.0   10    4     1
   1400 SHORE CONVB 150.00   2    0     1       0    0.99525   40.0   20    4     1
   3000 STCKH       420.00   2    2     0       0    1.00000   22.3   40    2     1
   3100 STRFN       420.00   2    1     0       0    0.97000   34.8   40    2     1
   3115 SV-N1       420.00   2    0     0       0    1.00000   53.8   40    2     1
   3200 KRLSK       420.00   1    1     0       0    0.96314    6.1   40    2     1
   3244 SV-M2       300.00   1    0     0       0    1.00108   20.2   40    2     1
   3245 SV-M1       420.00   2    1     0       0    1.00000   19.5   40    2     1
   3249 SV-N2       420.00   2    1     0       0    1.00000   53.0   40    2     1
   3300 SV-SW       420.00   3    1     0       0    1.00000    0.0   40    2     1
   3359 SV-W        420.00   2    1     0       0    1.00000   14.0   40    2     1
   3360 KONT_135    135.00   1    2     0       0    0.99653   13.6   40    3     1
   3701 SV-N2B      300.00   1    0     0       0    1.00514   56.4   40    2     1
   5100 EAST3       300.00   2    1     0       0    1.00000   24.0   51    1     1
   5101 EAST4-A     420.00   1    0     0       0    0.99119   22.7   51    1     1
   5102 EAST4-B     420.00   1    0     0       0    0.99890   26.4   51    1     1
   5103 EAST4-C     420.00   1    0     0       0    0.99719   26.7   51    1     1
   5111 SVCTERM     22.500  -2    0     0       0    0.99488   22.7   51    1     1
   5112 SVCHIGH     420.00   1    0     0       0    0.99119   22.7   51    1     1
   5300 HDAL3       300.00   2    1     0       0    1.00000   38.5   53    1     1
   5301 HDAL4       420.00   1    0     0       0    0.99983   33.1   53    1     1
   5400 CNTR3-A     300.00   2    1     0       0    1.00700   33.1   54    1     1
   5401 CNTR4-A     420.00   1    0     0       0    0.99792   30.6   54    1     1
   5402 CNTR4-B     420.00   1    0     0       0    1.00605   33.0   54    1     1
   5500 CNTR3-B     300.00   2    1     0       0    1.00400   26.3   55    1     1
   5501 CNTR4-C     420.00   1    0     0       0    1.00525   25.9   55    1     1
   5600 SOUTH3A     300.00   2    1     0       0    1.01000   28.0   56    1     1
   5601 SOUTH4A     420.00   1    0     0       0    0.99238   28.1   56    1     1
   5602 SOUTH4B     420.00   1    0     0       0    0.96838   22.0   56    1     1
   5603 SOUTH3B     300.00  -2    2     0       0    0.93500   20.9   56    1     1
   6000 WEST300     300.00   2    1     0       0    1.00500   33.5   60    1     1
   6001 WEST400     420.00   1    0     0       0    1.00005   32.4   60    1     1
   6100 NWEST3      300.00   2    1     0       0    1.00000   32.7   61    1     1
   6500 MID300      300.00   2    1     0       0    1.00000   21.9   65    1     1
   6700 NOR300      300.00   2    1     0       0    1.02000   63.2   67    1     1
   6701 NOR400      420.00   1    0     0       0    1.00551   62.6   67    1     1
   7000 SO-FIN      420.00   2    2     0       0    1.00000  -45.8   70    2     1
   7100 NO-FIN      420.00   2    1     0       0    1.00000  -12.8   71    2     1
   8500 SJOLLAND    420.00   2    1     0       0    1.02000    2.9   90    3     1
   8600 DENMARK     300.00   1    1     0       0    0.93500   20.9   90    3     1
   9100 NETHERLANDS 300.00   1    1     0       0    1.01000   28.0   91    3     1
```

Appendix H - 2: Power flow exchange and generation per area

```
    PTI INTERACTIVE POWER SYSTEM SIMULATOR--PSS(tm)E    MON, APR 20 2009  10:33
 REDUCED NORDEL POWER SYSTEM MODEL                                   ZONE TOTALS
 V 3.2, 12.08.97                                                      IN MW/MVAR

                 FROM      TO    TO BUS  TO LINE     FROM      TO
 X-- ZONE --X GENERATION  LOAD    SHUNT    SHUNT CHARGING  NET INT   LOSSES

    1         16800.0  14217.0      0.0      0.6      0.0   2457.1    125.3
 NORWAY        3010.9   2760.1      0.0    -27.6   1101.0   -461.3   1840.8

    2         26923.1  28550.2      0.0      0.0      0.0  -2611.5    984.3
 SWE & FIN    11857.8   4471.2      0.0      0.0   2048.9    234.1   9201.4

    3          1038.6   1796.4      0.0      0.0      0.0   -760.7      2.9
 DEN & NETH     169.8    400.0      0.0      0.0    306.1     64.6     11.3

    4          1158.3    150.0      0.0      0.0      0.0    915.1     93.2
 OFFSHORE       -12.1     50.0   -338.9      0.0    255.7    162.6    369.9

 TOTALS        45920.0  44713.7      0.0      0.6      0.0      0.0   1205.7
               15026.4   7681.3   -338.9    -27.6   3711.6      0.0  11423.3



    PTI INTERACTIVE POWER SYSTEM SIMULATOR--PSS(tm)E    MON, APR 20 2009  10:33
 REDUCED NORDEL POWER SYSTEM MODEL                                      ZONE
 V 3.2, 12.08.97                                                     INTERCHANGE

       TO ZONE:     1     2     3     4
 FROM ZONE    *------------------------
         1    *        2772   600  -915
 NORWAY       *        -299     0  -163
              *------------------------
         2    * -2772         161
 SWE & FIN    *   299         -65
              *------------------------
         3    *  -600  -161
 DEN & NETH   *     0    65
              *------------------------
         4    *   915
 OFFSHORE     *   163
              *------------------------
```

H.2 FAULT OFFSHORE AT THE TRANSMISSION BUS 1320

Appendix H - 3: Offshore voltage at different buses in pu

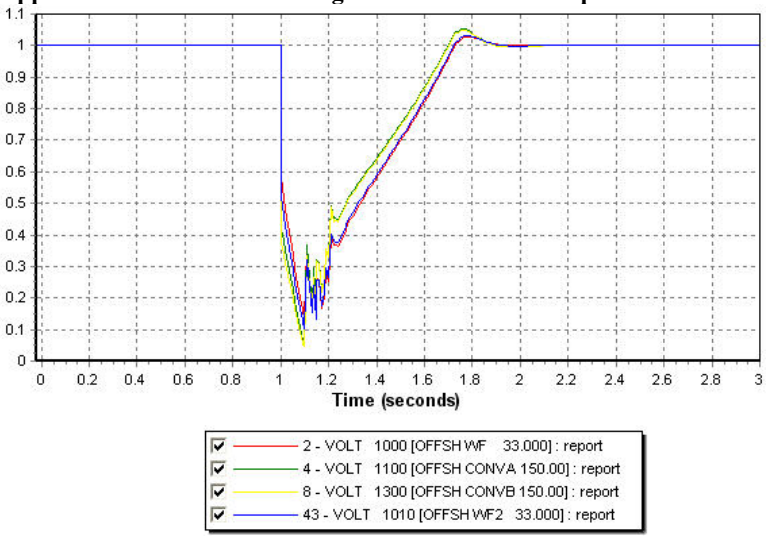

Appendix H - 4: Frequency at buses 1320 and 1020, 0.02pu=1Hz

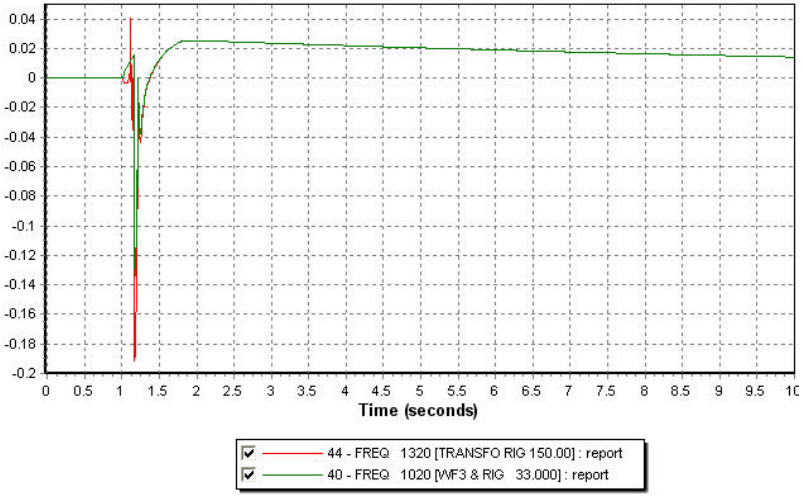

Appendix H - 5: Active and reactive power generated by the main wind farm, in pu on system base.

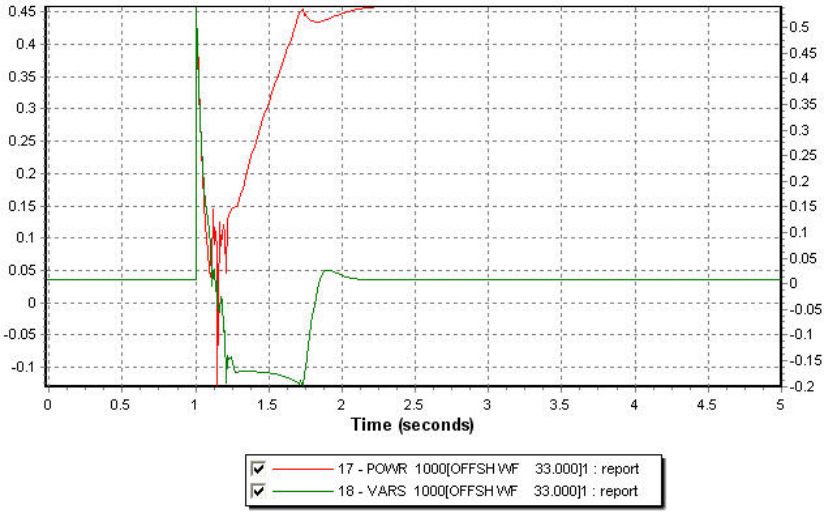

Appendix H - 6: Voltage onshore at PCCs in pu

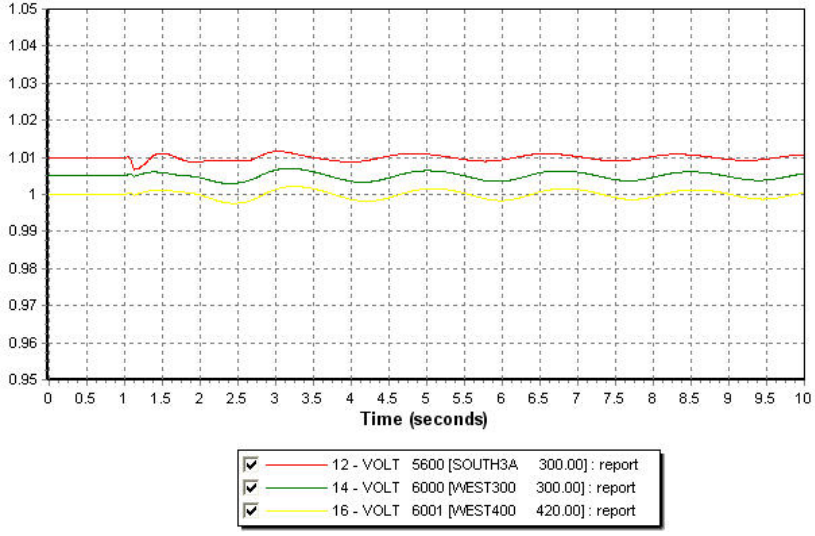

Appendix H - 7: Frequency variation offshore at PCCs in pu

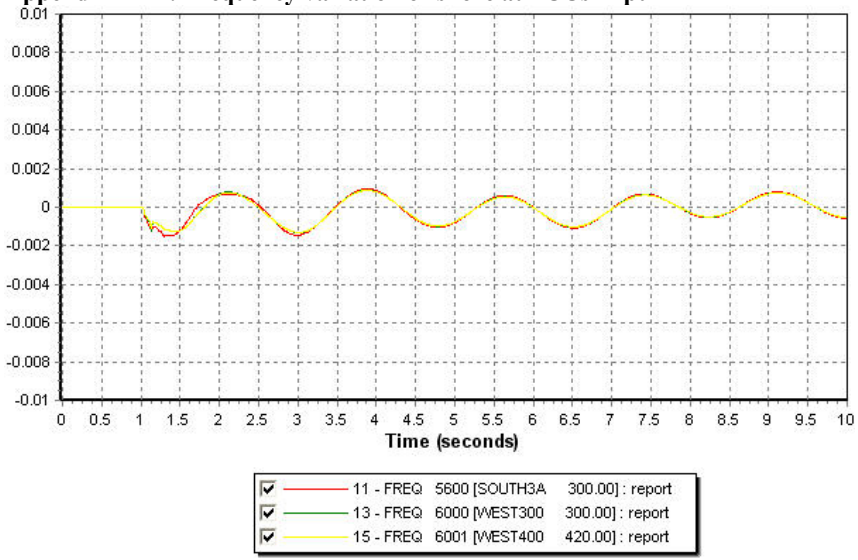

H.3 REPLACEMENT OF DFIG GENERATOR BY FIXED SPEED GENERATOR AND FAULT AT BUS 1320

Appendix H - 8: Voltage at each offshore bus in pu

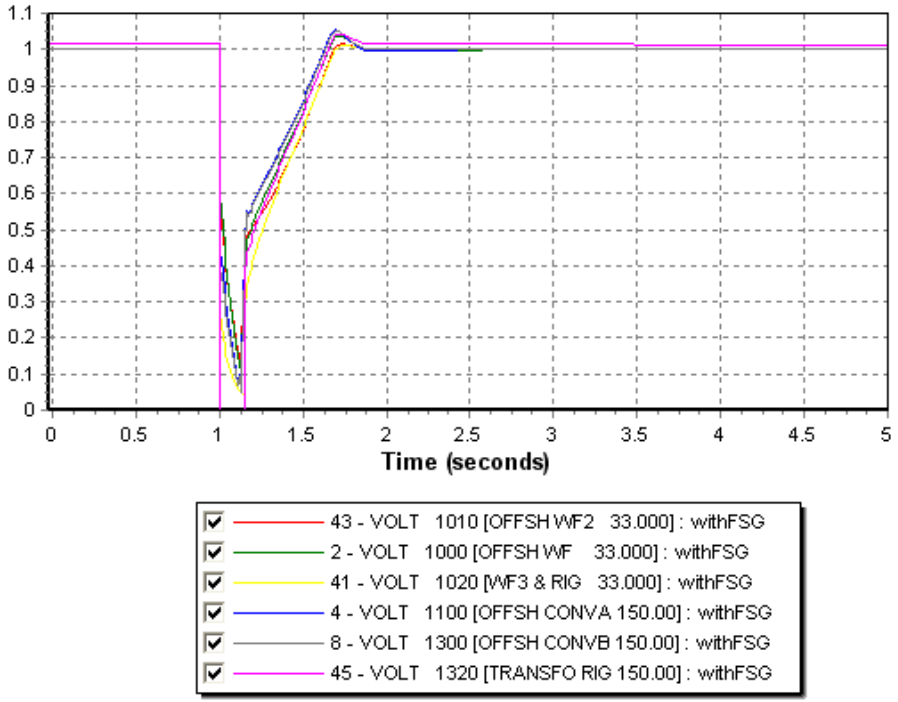

Appendix H - 9: Voltage and frequency variation in the Norwegian grid, both in pu

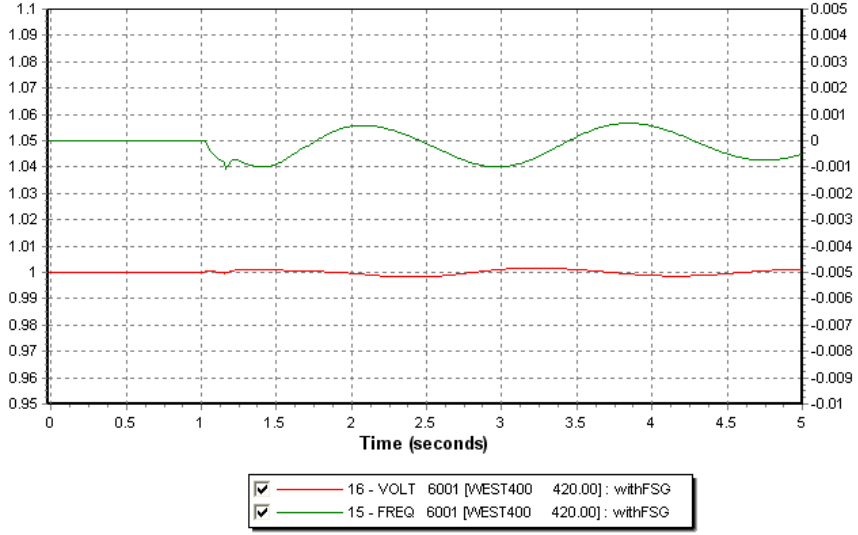

H.4 OFFSHORE FAULT ON CABLE AND TRIPPING OF THE LINE BETWEEN THE VSC CONVERTERS

Appendix H - 10: Active and reactive power flowing into the cable from the converter to the rig, in MW and Mvar

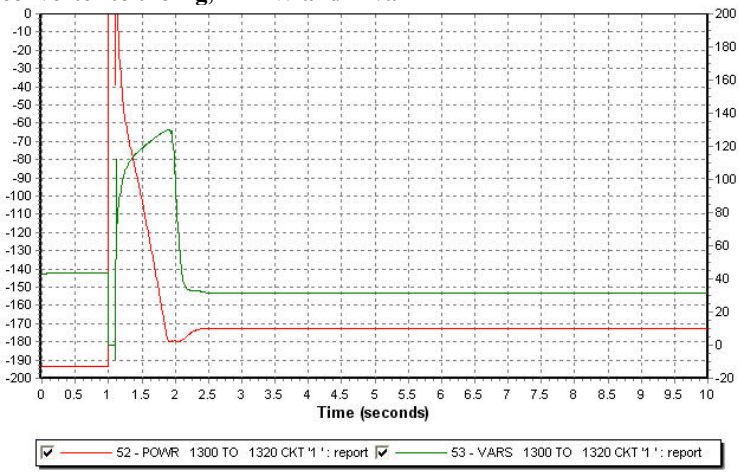

Appendix H - 11: Response of the SVC in the grid offshore, in pu on system base